Mathematical Modelling of Nanofluid Thermophysical Properties Using Copulas

by

Vishal Ramnath

Submitted in partial fulfilment of the requirements for the degree

Master of Engineering (Mechanical Engineering)

in the Department of Mechanical and Aeronautical Engineering,
Faculty of Engineering, Built Environment and Information Technology

University of Pretoria

July 2018

Abstract

Title: Mathematical Modelling of Nanofluid Thermophysical Properties
Using Copulas
Supervisor: Prof. Mohsen Sharifpur and Prof. Josua Petrus Meyer
Department: Mechanical and Aeronautical Engineering
Degree: Master of Engineering (Mechanical Engineering)

In this dissertation, mathematical research is performed to model nanofluid thermophysical properties in terms of multivariate probability density functions utilizing copulas from known verified and validated experimental data for water/alumina nanofluid mixtures.

A comprehensive review of the available data from the open scientific literature is undertaken to first understand the accuracy limits of the combination of available experimental and theoretical data for nanofluids. The nanofluid data is then processed using multivariate statistical analysis techniques in order to mathematically incorporate the input process parameter's intrinsic measurement uncertainties. Having analysed the verified data, optimal functional expressions for the effective thermal conductivity are then determined. This mathematical analysis is inclusive of estimates of the process parameter's respective experimental statistical uncertainties through stochastic based Monte Carlo simulations by incorporating information of the nanoparticle morphology such as the nanoparticle size and volume fraction, and the nanofluid temperature.

Numerical simulations are performed for the resulting copula-based PDF's with custom developed multivariate sampling strategies which are derived and tested. These model predictions were verified and validated by comparing them to a MLP-NN scheme to check for consistency. Quantitative results from these simulations indicate that the copula mathematical model is able to achieve an $AARD = 3.0953\%$ accuracy for predicted behaviours of the developed thermal conductivity database compared to an $AARD = 4.2376\%$ accuracy for a conventional MLP neural network. The proposed mathematical modelling approach is a new novel original research technique that has been developed which is able to incorporate physical experimental measurement uncertainties such that the model is able to adaptively refine the predicted nanofluid model quantitative uncertainties in sub-domains of the input meta-parameters which is not presently mathematically possible with existing neural network modelling approaches.

Keywords: *Mathematical modelling, nanofluid, Monte Carlo, multivariate copulas, thermophysical properties*

Acknowledgements

Declaration

I, Vishal Ramnath, hereby declare that the research embodied in this dissertation, *Mathematical Modelling of Nanofluid Thermophysical Properties Using Copulas*, is the result of research investigations carried out under the supervision of Prof M Sharifpur and Prof JP Meyer in the Department of Mechanical and Aeronautical Engineering, University of Pretoria, South Africa, towards the awarding of the degree *Master of Engineering*, and that this dissertation has not been submitted elsewhere for any degree or diploma.

Vishal Ramnath
25 July 2018

Publications

From the research work performed in the course of this master's dissertation the following publications were produced:

<u>**Articles for International Journals:**</u>

    • V. Ramnath, M. Sharifpur and J. P. Meyer, "*Mathematical Quantification of Predicted Nanofluid Thermophysical Uncertainties Utilizing Algebraic Models with PDF's of Parameters*" (submitted to International Journal of Heat and Mass Transfer, based on material from Chapter 2 & Chapter 3)

    • V. Ramnath, M. Sharifpur and J. P. Meyer, "*Mathematical Analysis of Nanofluid Thermophysical Statistical Models Utilizing Multivariate Copulas*" (submitted to Computers and Fluids, based on material from Chapter 3 and Chapter 4)

Contents

List of Tables

List of Figures

Nomenclature

Symbol	Description
$\mathbf{q}/[\mathrm{W\ m^{-2}}]$	Heat flux vector for thermal conduction in Fourier's law
$k/[\mathrm{W\ m^{-1}\ K^{-1}}]$	Thermal conductivity
k_B	Boltzmann constant
$h_c/[\mathrm{W\ m^{-2}\ K^{-1}}]$	Convective heat transfer coefficient for a fluid
$q_s/[\mathrm{W\ m^{-2}}]$	Convective heat flux across a solid surface for Newton's cooling law
$k_f/[\mathrm{W\ m^{-1}\ K^{-1}}]$	Thermal conductivity of a fluid
$\mathbf{V}/[\mathrm{m\ s^{-1}}]$	Fluid velocity vector
$p/[\mathrm{Pa}]$	Absolute fluid pressure
$T/[\mathrm{K}]$	Absolute thermodynamic temperature
$\rho(p,T)/[\mathrm{kg\ m^{-3}}]$	Mass density of a fluid as auxiliary thermodynamic fluid property
$h(p,T)/[\mathrm{J\ kg^{-1}}]$	Specific enthalpy of a fluid as an auxiliary thermodynamic property
$\mu(p,T)/[\mathrm{Pa\ s^{-1}}]$	Dynamic viscosity of a fluid as an auxiliary thermodynamic property
$\mathbf{f}/[\mathrm{N}]$	Body force vector exerted on a volume of fluid
$e/[\mathrm{J\ kg^{-1}}]$	Specific internal energy per unit mass for a fluid
$E_t/[\mathrm{J\ m^{-3}}\ ]$	Total energy per unit volume
$\mathbf{\Pi}_{ij}/[\mathrm{Pa}]$	Stress tensor for a fluid
$\tau_{ij}/[\mathrm{Pa}]$	Shear stress for a fluid
$\mathrm{Al_2O_3}$	Alumina oxide
$\mathrm{H_2O}$	Water
ϕ or φ	Dimensionless volume fraction of nanofluid
DSMC	Direct Simulation Monte Carlo (computational technique)
CFD	Computational Fluid Dynamics
HPC	High Performance Computing
$d/[\mathrm{m}]$	Particle size
$k_{eff}/[\mathrm{W\ m^{-1}\ K^{-1}}]$	Effective thermal conductivity of a nanofluid
$\mu_{eff}/[\mathrm{Pa\ s^{-1}}]$	Effective viscosity of a nanofluid
VEROS	Vacuum Evaporation onto a Running Oil Substrate
EG	Ethylene glycol
$k_b/[\mathrm{W\ m^{-1}\ K^{-1}}]$	Base fluid thermal conductivity
$t/[\mathrm{^{\circ}C}]$	Fluid temperature
Re	Reynolds number
Pr	Prandtl number
$k_p/[\mathrm{W\ m^{-1}\ K^{-1}}]$	Thermal conductivity of a nanoparticle
ψ	Particle sphericity
$\rho_{eff}/[\mathrm{kg\ m^{-3}}]$	Effective mass density of a nanofluid
$c_{p,eff}/[\mathrm{J\ kg^{-3}K^{-1}}]$	Effective specific heat capacity of a nanofluid
ω or w	Dimensionless weight fraction of a nanofluid
$W_{bf}/[\mathrm{kg}]$	Weight (mass) of a quantity of a base fluid
$W_p/[\mathrm{kg}]$	Weight (mass) of a quantity of a nanoparticle matter
$\alpha - \mathrm{Al_2O_3}$	A particular type of chemical composition of alumina oxide matter

$\gamma - \mathrm{Al_2O_3}$	A particular type of chemical composition of alumina oxide matter
SSA	Specific Surface Area
t_v/[m]	Nanolayer thickness
d_p/[m]	Nanoparticle diameter
$\mathbb{R}$	Set of real numbers
$\varnothing$	Mathematical empty set
Nu	Nusselt number
L_c/[m]	Characteristic length of a system
MAE	Mean Absolute Error
MRE	Mean Relative Error
RMSE	Root Mean Square Error
AARD%	Absolute Average Relative Deviation (in percent)
GMD-NN	Group Methof of Data handling Neural Network
$\pi_1,\ \pi_2,\dots$	Dimensionless parameters
β_{eff}/[K^{-1}]	Effective thermal expansion coefficient
k	Statistical converage factor for specified confidence level
μ_r	Relative viscosity referred to a base fluid viscosity
D_B	Brownian diffusion coefficient
D_T	Thermophoretic diffusion coefficient
T_{fr}/[K]	Freezing temperature point of a fluid
u_p/[m s^{-1}]	Nanoparticle Brownian velocity
d_f/[m]	Equivalent diamater of a base fluid molecule, c.f. Eq(2.55)
S_m	Source term for momentum transport in Navier-Stokes equations
S_e	Source term for energy transport in Navier-Stokes equations
$[\mu]$	Intrinsic viscosity equal to 2.5 for spherical nanoparticles
GUM	Guide to the Uncertainty of Measurement (statistical UQ)
UQ	Uncertainty Quantification
MP	Meta-Parameter (representative random variable for a model)
GA	Genetic Algorithm
ANN	Artifical Neural Network
LSSVM	Least Squares Supprt Vector Machine
SVM	Support Vector Machine
RBF	Radial Basis Function
pH	Scale of acidity level
ΔP/[Pa]	Pressure gradient
V_B/[m s^{-1}]	Brownian velocity
η_r	Relative viscosity
EDL	Electrical Double Layer
γ/[s^{-1}]	Shear rate within a fluid
ζ/[V]	Zeta-potential, electrokinetic potential in colloidal dispersions
$u_c(y)$	Combined standard uncertainty for measurand y using the GUM
$c_i = \frac{\partial f}{\partial x_i}$	Sensitivity coefficient using the GUM
$U = k_p u_c$	Expanded uncertainty (Accuracy for 95% confidence)
CLT	Central Limit Theory
v_{eff}	Effective degrees of freedom (shape of Gaussian PDF using GUM)

OFAT	One Factor At a Time
DOE	Design of Experiments
RSM	Response Surface Methodology
GLM	Generalized Linear Model
MLP	Multiple Level Perceptron (a type of Neural Network topology)
$F = F(T, V)$	Helmholtz free energy (a type of thermodynamic function for matter)
G	Gibbs free energy (a type of thermodynamic function for matter)
CIPM	International Committee for Weights and Measures (scientific body)
IAPWS	International Association for the Properties of Water & Steam
ITS-90	International Temperature Scale of 1990
PDE	Partial Differntial Equation
LCS	Largest Consistent Subset (statistical concept for consistency)
SEM	Scanning Electron Microscope
TEM	Transmission Electron Microscope
DLS	Dynamic Light Scattering
$X_k(\mathbf{x})$	Basis function for measurand $\mathbf{x} = [x_1, \dots, x_M]^{\mathrm{T}} \in \mathbb{R}^N$
χ^2	Chi-squared merit function (statistical quantity for goodness of fit)
$Q(\rho)$	Quantile function
ELD	Extended Lambda Distribution (special type of quantile function)
$g(\eta)$	Probability density function for random variable η
$G(\eta)$	Distribution function for random variable η
σ^2	Variance equal to square of standard deviation
$\mathbf{C}$	Covariance matrix (off-diagonals covariances, diagonals variances)
$\mathbf{D}_k$	Dataset of nanofluid thermal conductivity information, c.f. Eq(3.26)
$\mathbf{D}_\mu$	Dataset of nanofluid viscosity information, c.f. Eq(3.27)
R_{hyd}	Hydrodynamic size of nanoparticles, c.f. Eq(3.41)
$\langle \cdot \rangle$	Ensemble average (statistical mechanics technique)
$\mathscr{A}$/[nm]	Agglomeration size (approimation of size of group of nanoparticles)
E_n	Normalized error, statistical consistency, c.f. Eq(3.54)
Kn	Knudsen number, indication of type of flow regime
ℓ	Mean free path, c.f. Eq(3.62)
LJ	Lennard-Jones, a semi-empirical molecular interaction potential
NEMD	Non-Equilibrium Molecular Dynamics
MCMC	Markov Chain Monte Carlo (statistical analysis using a prior PDF's)
KL	Kullback-Leibler, a type of statistical quality of statistical error
MC	Monte Carlo
C	Copula, a mathematical multivariate mapping $C: \mathbb{I}^n \to \mathbb{I}$, c.f Eq(3.84)
u	Cumulative distribution, c.f. Eq(3.85)
$f(x, y)$	Bivariate joint PDF constructed with a copula, c.f. Eq(3.87)
$\mathbb{C}_n(\mathbf{u})$	Empirical copula, a copula defined entirely by data, c.f. Eq(3.103)
CDF	Cumulative Distribution Function, defined as $F(\xi) = \int_{-\infty}^{\xi} f(\eta) \ \mathrm{d}\eta$
GS1	GUM Supplement 1, technique for Monte Carlo based univariate UQ
GS2	GUM Supplement 2, technique for monte Carlo based multivariate UQ
$F(x\|\mathbf{v})$	Conditional distribution function, c.f. Eq(3.124)
AI	Artificial Intelligence
C-vine	Parameters based model of 'star-shaped' multivariate copulas

1 Introduction

1.1 Research Context

In the field of mechanical engineering, the three conventional modes of heat transfer are conduction, convection and thermal radiation for a variety of instruments, equipment, machinery and systems encountered in practice and which are usually analysed using the principles of conservation of mass, momentum and energy along with relevant mathematical models of constituent material properties. The underlying heat transfer rate equations are usually derived using an energy balance equation of the form $\dot{E}_{\text{in}} + \dot{E}_g - \dot{E}_{\text{out}} = \dot{E}_{st}$ where $\dot{E}_{\text{in}}/[\text{J s}^{-1}]$ is the rate of energy entering a physically appropriate control volume $\mathcal{V}/[\text{m}^3]$, $\dot{E}_g$ is the rate of energy generated within $\mathcal{V}$, $\dot{E}_{\text{out}}$ is the rate of energy leaving $\mathcal{V}$, and $\dot{E}_{st}$ is the rate of energy stored within $\mathcal{V}$ as discussed by Incropera & DeWitt [1].

Theories for heat transfer through conduction in solid materials are usually formulated in terms of Fourier's law of the form $\mathbf{q} = -k\nabla T$ where $\mathbf{q}/[\text{W m}^{-2}]$ is the heat flux, $T/[\text{K}]$ is the solid temperature and $k/[\text{W m}^{-1} \text{ K}^{-1}]$ is the thermal conductivity which may in principle be calculated using either the kinetic transportation theory or condensed matter theory as discussed by Ashcroft & Mermin [2]. On the other hand, radiative heat transfer effects underpinned at a fundamental physics level by the Maxwell electromagnetic equations are usually modelled using Planck's law where the spectral emissive power $e_{\lambda b}(\lambda_0, T)/[\text{W m}^{-3}\text{sr}^{-1}]$ is of the form $e_{\lambda b}(\lambda_0, T) = 2\pi C_1/[\lambda_0^5(e^{C_2/\lambda_0 T} - 1)]$ for radiative heat transfer in vacuum where $C_1 = hc_0^2$ and $C_2 = hc_0/k_B$ are the first and second radiation constants where c_0 is the speed of light, h is Planck's constant, and k_B is the Boltzmann constant as discussed by Siegel & Howell [3] with appropriate modifications in terms of the generalized radiation transport equation as discussed by Castor [4] for radiative heat transfer through optically dense fluid mediums such as air, water and oil. Usually, radiative heat transfer calculations for many engineering problems are performed with the simplified blackbody radiation model where the thermal radiative emissive power integrated over all wavelengths is simply $E = \sigma T^4$ where $E/[\text{W m}^{-2}]$ is the radiative flux and σ is the Stefan-Boltzmann constant, and as a result thermal radiation effects are completely specified by existing electromagnetic theories. Consequently of the three heat transfer modes, it is usually convective heat transfer that receives the most attention in mechanical engineering studies since it is this mode of heat transfer that is the least well understood in terms of existing physical theories.

By convention convective heat transfer is defined as the heat transfer that takes place from a solid surface to a moving fluid such as the inside surface of a pipe to the working fluid flowing through the pipe. As a result the convective heat transfer coefficient $h_c/[\text{W m}^{-2} \text{ K}^{-1}]$ defined in terms of the equation $q_s = h_c\Delta T$ which is usually referred to a Newton's law of cooling where $q_s/[\text{W m}^{-2}]$ is the convective heat flux across the solid surface, T_s is the solid surface temperature, T_e is the working fluid free stream temperature and $\Delta T = T_s - T_e$ is a temperature gradient, is then usually a complicated function of the surface geometry/temperature, the fluid temperature/velocity and the fluid thermophysical properties as discussed by Mills [5]. By considering the velocity boundary layer and thermal boundary at the interface between the working fluid and the solid surface Incropera & DeWitt [1] derived a formula for h_c in the case of

Newton's law of cooling where x is a localized spatial coordinate tangential to the solid surface in the direction of the fluid flow and y is a localized spatial normal to the solid surface of the form

$$h_c \stackrel{\text{def}}{=} \frac{-k_f \times \left[\frac{\partial T}{\partial y} \Big|_{y=0} \right]}{T_s - T_e} \tag{1.1}$$

Referring to the above formula, it may be observed that the convective heat transfer coefficient is dependent on both the fluid thermal conductivity as well as the normal temperature gradient at the interface of the fluid and surface. Although fluid properties for many engineering working fluids such as water and various type of machinery oils and lubricants are available in tables and charts in general temperature gradients have to be either experimentally measured with thermocouples or resistance-temperature-devices (RTD's) or alternately estimated through numerical simulations performed with Computational Fluid Dynamics (CFD) software codes. Since the laws of mass, momentum and energy conservation which are implemented with CFD codes through for example the solution of the Navier-Stokes equations under a continuum modelling assumption and which solve for the fluid's velocity $\mathbf{V} = [u, v, w]^{\mathrm{T}}$, pressure p and temperature T are in turn dependant on the fluid's auxiliary thermodynamic properties of density $\rho(p, T)$, enthalpy $h(p, T)$, viscosity $\mu(p, T)$ and thermal conductivity $k(p, T)$ it is seen that convective heat transfer estimates and calculations are critically reliant on accurate knowledge and predictions of the particular working fluid's thermal conductivity and viscosity respectively. Considering the general form of the convective heat transfer coefficient h_c it is observed that if statistical models for the working fluid's thermal conductivity and viscosity are known then the corresponding uncertainty of h_c may in principle be readily computed through stochastic based Monte Carlo simulations of the corresponding mathematical models of the relevant fluid/solid behaviour for any physical system such as for example heat exchangers which may utilize a nanofluid as a working fluid. Knowledge of the statistical properties and behaviour of the convective heat transfer coefficient h_c may then be utilized in reliability engineering and technical feasibility studies of mechanical systems that incorporate machinery, equipment or instruments that are reliant on nanofluids.

In general, most engineering working fluids such as water and oil tend to exhibit poor thermal conductivities, while most engineering solid materials in various components and sub-systems using metals such as aluminium and copper have by contrast excellent thermal conductivities. Motivated in part by this observation Stephen Choi [6] through a set of a combination of microfluidic/nanofluidic experiments conducted at the Argonne National Laboratory, USA developed and introduced the modern concept of nanofluids by combining solid materials such as aluminium-oxide and copper-oxide nanoparticles with diameters d_p such that $d_p/[\text{nm}] \leq 100$ suspended in a base liquid such as water or glycerol so that the new mixture exhibited markedly superior thermophysical properties.

Since the introduction of the concept of nanofluids there has been a worldwide research undertaking to further study, understand, model and apply nanofluids to a diverse range of engineering applications. Apart from the application of nanofluids as more efficient convective heat transfer working fluids in traditional heat exchangers which has potential implications of massive water savings for power stations and manufacturing plants in South Africa which is a water scarce country, nanofluids also have potential further applications in electronic cooling

systems, vehicle engine lubricant systems, nuclear reactor cooling systems, and biomedical drug delivery systems, all of which are potentially attractive technology applications of nanofluids to enhance the competitiveness of the South African engineering sector in line with the country's industrial policy action plan commonly known and abbreviated as IPAP2017 [7].

From a review of the technical literature of nanofluids a research gap of an absence of the incorporation of aleatory uncertainties i.e. natural statistical based variations of experimental measurement data in nanofluid model constructions has been identified and which presents a potential novel research avenue of investigation for mathematically modelling and predicting a nanofluid's effective thermal conductivity and effective viscosity directly in terms of multivariate statistical data that incorporates the intrinsic experimental uncertainty data.

1.2 Research Aims

In this dissertation, mathematical modelling research is performed in order to investigate the optimal approach for modelling and incorporating intrinsic aleatoric thermophysical data uncertainties so that the resultant nanofluid thermophysical properties predicted by derived analytical mathematical expressions for the effective thermal conductivity and effective viscosity exhibits behaviour, properties and characteristics in terms of multivariate probability density functions which are mathematically modelled with copulas that are consistent with the known uncertainties.

1.3 Research Objectives

   • Develop a database of nanofluid thermophysical properties that contains uncertainties of both the effective thermal conductivity and effective viscosity for a water/alumina nanofluid as well as the uncertainties of the intrinsic meta-parameters of the nanoparticle size, concentration and temperature

   • Perform full Monte Carlo based stochastic simulations to generate probability density function multivariate statistical data for constructing models for the effective thermal conductivity and effective viscosity

   • Investigate the mathematical modelling with multivariate copulas for constructing and building mathematical expressions for the effective thermal conductivity and effective viscosity from the Monte Carlo multivariate data

1.4 Research Scope

Research studies in the field of mechanical engineering have historically been categorized as either experimental research or as theoretical research, however, a new third category of computational research has emerged in the last decade that is neither distinctly experimental nor distinctly

theoretical. This third research category of Computational Science & Engineering (CSE) as it is nowadays known which is distinct from the more traditional mathematical field of numerical analysis as it incorporates a mixture of other domain disciplines such as theoretical physics and scientific computing is more accurately categorized as an interdisciplinary and in some cases a multidisciplinary research paradigm of which the research category of Modelling and Simulation (M&S) has now been firmly established as a more accurate descriptor for this field of research work.

More formal rigorous abstract definitions of modelling techniques with roots in the disciplines of computer science incorporating concepts such as Data Flow Modelling (DFM) and from systems engineering incorporating concepts such as Entity Relationship Modelling (ERM) are possible however in this research investigation a set of informal definitions is considered adequate. In the field of M&S research the descriptor of modelling is conventionally taken to encompass the use of models as conceptual abstractions of systems which in this investigation may then be informally categorized as simply the conceptualization and construction of appropriate mathematical equations for nanofluid thermophysical properties of varying levels of complexity. Although the term simulation is sometimes ambiguous as it may encompass both numerical analysis, scientific computing and computational engineering as distinct but overlapping research scopes in this dissertation the descriptor of simulations is limited as being the practical implementation of developed mathematical models i.e. the analytical/numerical solution of the mathematical equations developed from the modelling process for predicting the nanofluid thermophysical properties as opposed to more general computational fluid dynamics based simulations with open source or commercial computer codes for particular mechanical engineering machinery, equipment or instruments that utilize nanofluids as the working fluid.

For the particular research investigation in this dissertation, the research scope of the study is limited to exploratory investigations of physical and mathematical equations which is logically inclusive of statistics as a branch of mathematics to model the thermophysical properties of a water/alumina nanofluid. In the course of the investigation, the focus is concentrated on the application of copulas for the mathematical and statistical modelling of water/alumina nanofluid using existing reported experimental data sourced from the open scientific literature for the nanoparticle sizes/concentrations and the base fluid temperature as natural meta-parameters. Although the related concepts of modelling and simulation are nominally independent in many practical M&S studies they are inter-related so as part of the study a computational application of the mathematical model for the utilization and implementation of the developed mathematical models for predicting the effective thermal conductivity and effective viscosity of the nanofluid as a convenient means to validate and verify (V&V) our constructed mathematical model is included.

1.5 Research Organization

To perform the research study, the research investigation is structured as follows:

    • *Chapter 1* – In this chapter, the context and relevance of nanofluid thermophysical properties is presented with an explanation of the identified current research gap of the absence of the incorporation of aleatory uncertainties of experimental measurement data in model constructions

with an associated absence of model parameter uncertainties necessary for a more rigorous mathematical uncertainty analysis of the property predictions, and how this identified research gap is addressed

• *Chapter 2* – In this chapter, an investigation is performed of nanofluid thermophysical property experimental and theoretical data reported in the open scientific literature in order to construct a database of nanofluid thermophysical properties verified multivariate statistical data that is inclusive of aleatory physical experimental uncertainties

• *Chapter 3* – In this chapter, different fluid physical theories and aspects which must be accounted for in nanofluid studies are investigated and analysis techniques of how to utilize higher dimensional multivariate copulas to mathematically model nanofluid thermophysical properties from verified multivariate statistical data are considered

• *Chapter 4* – In this chapter, the developed mathematical copula model from the research investigation is implemented to predict the effective thermal conductivity and effective viscosity of the water/alumina nanofluid and comparisons of the predictions with known property values is undertaken in order to validate the copula mathematical model for a range of nanofluid properties and characteristics

• *Chapter 5* – In this chapter, the main outcomes of the research objectives are summarized for each of the chapters, with explanations of how the specific research sub-objectives and overall research objective were met, and some potential future areas of a research study that emanate from this dissertation are proposed

2 Literature Review

2.1 Classical Fluid Physical Theories

In the field of mechanical engineering constituent matter in single-phase and multi-phase states in machinery, equipment and devices of various types is conventionally classified as either occupying one of three classical macroscopic physical phase states such as liquids, solids or gases, or alternately combinations of the three classical states of matter such as gas and liquid states in for example a water steam/liquid mixture. A partial exception to this classification scheme in which a constituent volume of matter cannot be decomposed into either one of three classical states or equivalently a mixture of the three classical states of matter is that of plasmas which are sometimes informally considered as a special fourth type of state of matter. This is usually undertaken particularly for plasma physics studies and radiative hydrodynamics problems in which the classical states of matter such as liquids and gases for fluids problems are not able to fully capture the underlying physical processes as discussed by Mihalas & Weibel-Mihalas [8]. Typical applications of plasmas occur and are present in very high temperature applications usually but not always above $3000\ \text{K}$ where de-ionization of the fluid starts to take place necessitating more complex generalized energy modelling terms. Examples of such problems are in for example very high Mach number flows, atmospheric re-entry vehicles, laser processes in manufacturing, and stellar atmosphere dynamics problems amongst other physical scenarios for which specialist modelling techniques are available. As a result in the vast majority of practical macroscopic scale mechanical engineering problems encountered which utilize the modelling of matter properties, characteristics and behaviour for the design, analysis or operation of machinery, equipment and devices the modelling of the applicable constituent matter properties then usually reverts back to formulations of pure liquids, solids or gases, or alternatively mixtures of these known classical phase states of matter.

At the present time of writing the fundamental physics of modelling matter for characterizations and predictions in engineering problems is loosely grouped into '*solid-like*' matter states such as for various pure metals and alloys, and to '*fluid-like*' matter states such as for gas and liquid mixture categories since there does not exist any formal mathematical or physical definitions to rigorously delineate the distinction between these two categories. This lack of delineation between solid-like and fluid-like matter states is due to the physically observed phenomena whereby the same state of matter may, in fact, behave differently for different particular combinations of length and time scales such as in certain grades of glasses which behave as a 'solid' for small length scales but which in turn and contrastingly exhibit 'fluid' characteristics over long timescales. This particular observation then necessitates the implicit assumption of physical validity limits for any particular mathematical model of a fluid such as constraints imposed on the transport properties for specified temperature and pressure operating conditions of the machinery, equipment or devices, whereby these physical validity limits impact on the accuracy of numerical predictions which utilize the underlying respective model. Examples of such implicit physical validity limits to mathematical models of fluids include for example accuracy specifications and limit ranges of thermal conductivities and viscosities of pure gases such as nitrogen as discussed by Lemmon & Jacobsen [9] when these fluid transport properties are determined through combinations of experimental measurements with explicit/implicit experimental uncertainties and theoretical

predictions with their own explicit/implicit limitations, assumptions and/or approximations. Such physical validity limits are an unavoidable part of the fluid mathematical modelling process based on intrinsic limitations in the underlying data for varying reasons and are an essential practical constraint to take into account in order to avoid or at least mitigate against unrealistic and physically implausible predictions of machinery, equipment and devices for real engineering applications numerical based studies.

With regards to mainly crystalline types of solids such as metallic compounds and ceramics which resist deformation and retain their shape in such a way that their stress is a function of the strain it is known that these types of solids are generally well characterized and understood in terms of classical solid state physics as a mature area of research as discussed by Ashcroft [2] to the extent that their intrinsic mechanical physical properties may be predicted. An example of such a case is the prediction of a material's Young's modulus of elasticity E and Poisson's ratio ν for arbitrary compositions and mixtures using disparate base components such as for example a tungsten matrix embedded with carbide particles which may be accurately predicted using density functional theory (DFT) simulation codes from physics based *ab initio* first principles simulations. The use of solid state physics may also if necessary also be used to model and predict the shapes and sizes of molecules of various crystalline substances as well as the structure and characteristics of both metallic and non-metallic molecules of solids. As a result, solid state physics may in principle be used to predict at an *ab initio* level the properties of nanoparticles which are used in the manufacture of nanofluids by combining the nanoparticles with a suitable base fluid such as water or oil.

For fluids in the form of both single and multiple component gas species mixtures the physical properties are modelled in terms of the kinetic theory of gases which is formally underpinned by statistical mechanics as outlined by Reif [10] and which has historically been studied utilizing earlier implementations pioneered by Chapman & Cowling [11] and as result gas material property studies are also considered to be a relatively mature and complete area of research. The study of fluid properties for liquids is by contrast not considered a mature field of research since there is no corresponding comprehensive body of theory for liquid properties as there is for solids and gases.

Fluids for the purposes of classification schemes are loosely defined as constituent matter which do not retain their shape when exposed to applied forces in such a way that the fluid internal stress is a function of the strain rate as discussed by Reddy [12] from a continuum mechanics modelling assumption although this assumption is not necessarily always physically valid in for example certain non-continuum flows such as rarefied gas dynamics problems under hard vacuum pressures. These types of '*classical*' fluids adhering to the conventional notions of fluid classification schemes are usually understood and modelled in terms of approximations using phenomenological models such as the Navier-Stokes equations which is a first-order approximation of the Boltzmann equation as discussed by García-Colín *et al.*[13] utilizing the continuum fluid hypothesis as discussed by White [14] due to the absence of computationally tractable *ab initio* schemes for high particle number density values N of the Boltzmann equation. The phenomenological modelling process is realized through an appropriate choice of the fluid stress tensor $\mathbf{\Pi}_{ij}$ for the coupled system of differential equations for the conservation of mass, momentum and energy such that

$$\frac{\partial \rho}{\partial t} + \nabla \cdot (\rho \mathbf{V}) = 0 \tag{2.1}$$

$$\frac{\partial}{\partial t}(\rho \mathbf{V}) + \nabla \cdot \rho \mathbf{V} \mathbf{V} = \rho \mathbf{f} + \nabla \cdot \mathbf{\Pi}_{ij} \tag{2.2}$$

$$\frac{\partial E_t}{\partial t} + \nabla \cdot E_t \mathbf{V} = \frac{\partial Q}{\partial t} - \nabla \cdot \mathbf{q} + \rho \mathbf{f} \cdot \mathbf{V} + \nabla \cdot \left(\mathbf{\Pi}_{ij} \cdot \mathbf{V}\right) \tag{2.3}$$

as per the discussion by Tannehill *et al.* [15] where $\mathbf{V} = [u_1, u_2, u_3]^{\mathrm{T}}$ is the fluid velocity, $\mathbf{f}$ is a term to account for the body forces which is usually just set to $\mathbf{f} = \rho \mathbf{g}$ if $\mathbf{g}$ is the gravitational acceleration vector and which we will ignore unless otherwise specified, $\dot{Q} = \partial Q / \partial t$ is the rate of heat produced per unit volume by external heat sources, e is the internal energy per unit mass, and E_t and $\mathbf{q}$ are the total energy per unit volume and heat transfer through conduction respectively under the assumption of Fourier's law of heat conduction of the form

$$E_t = \rho \left(e + \frac{1}{2} \parallel \mathbf{V} \parallel^2 + \text{potentialenergy}\right) \tag{2.5}$$

$$\mathbf{q} = -k \nabla T \tag{2.4}$$

In the above system the stress tensor $\mathbf{\Pi}_{ij}$ is completely general and the system of equations for the conservation of mass, momentum and energy is mathematically valid for both continuum as well as non-continuum flows when coupled with appropriate auxiliary relations for the thermal conductivity k, viscosity μ, enthalpy h and density ρ respectively. For the particular case of a Newtonian fluid, the stress tensor phenomenological model is approximated using Stokes hypothesis $\lambda + \frac{2}{3}\mu = 0$ where λ is the second viscosity coefficient using the Einstein summation convention where δ_{ij} is the Dirac-delta function as

$$\mathbf{\Pi}_{ij} = -p\delta_{ij} + \tau_{ij} \tag{2.6}$$

$$\tau_{ij} = \mu \left[\left(\frac{\partial u_i}{\partial x_j} + \frac{\partial u_j}{\partial x_i}\right) - \frac{2}{3}\delta_{ij}\frac{\partial u_k}{\partial x_k}\right] \tag{2.7}$$

Although the Boltzmann equation as a fundamental equation of statistical mechanics is theoretically valid for any physical state of matter in the observable universe be it gas, liquid, solid or plasma and whether these states of matter are continuum or non-continuum fluids, and is thus applicable for completely arbitrary particle number densities N and whilst it is able to fully capture the underlying physics for microscopic and even for macroscopic liquid systems exhibiting arbitrary length, time, and constituent molecular species components such as fluid H_2O molecules and nanoparticle Al_2O_3 molecules if appropriate collision integral terms are present it is not currently physically possible to solve the full Boltzmann equation with present computer technologies due to the extreme challenges with directly evaluating the collision integral source terms.

Part of the difficulty with theoretically modelling nanofluids is that the presence of the nanoparticles destroys the short-range order of the classical base fluid medium since the motion of the nanoparticles in the surrounding carrier medium induces unpredictable stochastic i.e. non-deterministic micro-fluctuations in the density field $\rho(\mathbf{x}, t)$ and velocity field $\mathbf{V}(\mathbf{x}, t)$ of the

carrier medium molecules surrounding the nanoparticles which is presently thought to be one of the underlying physical causes to explain the thermo-physical characteristics of nano-fluids. Whilst it is theoretically possible to model at an *ab initio* level the inter-action and induced micro-fluctuation effects between the molecules of the carrier fluid and the molecules of the nanoparticles either with the full Boltzmann equation, a full molecular dynamics simulation, or a stratified sampling scheme of a full molecular dynamics simulation using the direct simulation Monte Carlo (DSMC) method these respective approaches are not considered computationally feasible for full macroscopic systems. As a result at a conceptual mathematical modelling level there is a similar analogy with the modelling of turbulence effects of classical fluids in the sense that whilst there are known theoretical models that are available that may in principle fully capture the underlying physical processes such a direct numerical simulation (DNS) of the Navier-Stokes equations with various numerical discretization and solution techniques that these *ab initio* theoretical approaches are in most cases simply computationally infeasible with existing local and distributed computer systems, and that the more complex macroscopic physical properties and processes have to be modelled with various simplifications and approximations in order to realize results and predictions for applied engineering problems.

Consequently the theoretical approach of utilizing the Boltzmann equation is therefore only applicable and computationally feasible with existing local and distributed computing system for systems exhibiting smaller number density values N or equivalently smaller closed systems such as for example mainly gas mixtures with nanoparticle suspensions using the kinetic theory of gases as discussed in the review paper by Ya Rudyak [16]. Based on this review paper it has been reported that the viscosity of gas nanosuspensions significantly differs from classical fluids i.e. gas mixtures without nanoparticles and in addition that predictions are not possible using the classical Einstein theory of gas mixtures with Brownian motion which is a simplification of the kinetic theory where the viscosity η of a fluid with dispersed particles takes the form $\eta = \eta_0(1 + 2.5\phi)$ where ϕ is the volume fraction of the dispersed particles. In the original Einstein model, the dependence of the viscosity is only a function of the volume fraction ϕ and does not depend on either the temperature t or the shape of the doped nanoparticles amongst other physical parameters and quantities which may influence the final bulk fluid density. On the other hand on a practical level additional complexities arise when attempting to model liquids using classical kinetic theories since the liquid molecules are significantly more closely packed to each other when compared to molecules in gas mixtures with and without the presence of nanoparticles and as a result the mechanism of momentum transfer becomes significantly more complicated and less amenable to statistical mechanics simplifications as is the case with the kinetic theory of gases. For liquids when the molecules collide the momentum is typically re-distributed on a local scale as opposed to a global scale for gases, and as a result the viscosity of a liquid which is a measure of the fluid momentum transfer mechanism is significantly affected by the molecular structure of the fluid i.e. the inter-action between the base fluid molecule such as a H_2O molecule and its inter-action with surrounding and nearby nanoparticles such as Al_2O_3 molecules. This phenomena and complexity of molecular structure effects in the absence of a comprehensive physical theory for liquids amenable to accurate predictions has in the past been incorporated through the modelling of various non-Newtonian viscosity fluid models in an attempt to incorporate the influence of varying mass fractions, volume fractions, concentrations and temperature effects as input parameters which influence the transport properties of nano-fluids which when produced with nanoparticle raw materials are known to have significant variations of nanoparticle shapes and

sizes. Based on various experimental and theoretical studies one particular current approach in many reported nanofluid studies for the modelling of viscosity is to adopt a quadratic dependence on the volume fraction ϕ for particular nanoparticle sizes d such that the nanofluid viscosity takes the form $\eta = \eta_0[1 + k_1(d)\phi + k_2(d)\phi^2]$ where $k_1(d)$ and $k_2(d)$ are unknown functions which must be determined to optimally model a nanofluid in terms of the carrier fluid and nanoparticle doping material.

Due to the complexity of the above system of equations, one particular approach is usually known as the single-phase modelling approach simply utilizes the stress tensor for a Newtonian fluid where refinements for non-classical fluids are implemented for an '*effective thermal conductivity*' k_{eff} and an '*effective viscosity*' μ_{eff} since it is generally more convenient to adapt and refine the auxiliary relations for k and μ which may be modified without the need to develop a new solver, instead of simultaneously refining Π_{ij}, k and μ with the possible need to develop a new solver. Alternative single-phase phenomenological models to the Navier-Stokes equations which is a first order $\mathcal{O}(Kn)$ Knudsen number approximation of the Boltzmann equation are also technically possible and include the second order $\mathcal{O}(Kn^2)$ Burnett and third order super-Burnett $\mathcal{O}(Kn^3)$ hydrodynamic equations which are numerically unstable, or the linearized G13 and R13 13-moment equations which are numerically stable but which are substantially more mathematically complex as discussed by Young [17]. Occasionally in some studies a multi-phase modelling approach which simultaneously considers both the liquid base fluid as well as the solid nanoparticles is adopted over a single-phase modelling approach, however whilst a multi-phase modelling may in some instances offer superior predictive capabilities this functionality comes at the expense of substantial increased model complexity. One particular example of such complexity is in terms of the appropriate fluid boundary conditions of a fluid/solid mixture which impinges on a solid surface and how to adequately incorporate conservation of momentum at the interface of the mixed-phase fluid/solid mixture, which by contrast is not a major issue with single-phase fluids under the assumption of a mathematical continuum since first-order Maxwell velocity-slip and Smoluchowski temperature-jump boundary conditions may be readily incorporated into conventional commercial CFD codes.

As a result whilst a research strategy to directly utilize the Boltzmann equation is theoretically valid from a fundamental physics point of view and it is known that it will completely capture the underlying physics of nanofluid systems this is presently computationally infeasible even on massively parallel supercomputing systems that are currently available within South Africa for simulations at typical operating pressure and temperature values for engineering equipment such a heat exchangers, and the associated pumping and piping systems. The remaining numerical simulation strategy and option is to model nanofluid systems either with modifications of simplifications to the Boltzmann equation (such as a 0th order Euler equations, 1st order Navier-Stokes equations, or 2nd order Burnett hydrodynamic equations) such as optimized thermo-physical functional forms for the thermal conductivity and viscosity to match verified experimental data results. Alternatives to optimized modifications of the auxiliary relations for the Navier-Stokes equations are mathematically equivalent asymptotic approximations of the Boltzmann equation such as the mesoscopic lattice Boltzmann method (LBM) which is computationally feasible and has found relative success in numerically capturing certain nanofluid physical behaviour, however the length scale of typical LBM simulations is usually in the range from 100 nm to about 1000 nm i.e. from a length of a very large nanoparticle up to the lower length

scale of a few fractions of a micron that is typically resolved with conventional CFD codes near the continuum hypothesis limit. As a result mesoscopic simulations as a branch of condensed matter physics loosely defined as an intermediate field of study between microscopic and macroscopic length scales whilst offering the ability to slightly extend the validity limits of conventional macroscopic CFD type simulations also suffers from the same limitations since it cannot accurately extend predictions down to length scales of 1 nm to 10 nm which is where much of the unique physics of nanofluids is currently thought to emanate from such as the effects of the nanolayer that surrounds the nanoparticles and in the random interactions effects between the nanoparticles and the base fluid molecules. The challenge of this limitation is that in general there are a range of nanoparticle sizes that are physically present in any nanofluid and that the different sizes of nanoparticles will interact both with each other as well as the surrounding base fluid molecules in a manner which cannot be easily studied if the underlying spatial resolution that is possible with the mesoscopic model is larger than the length scale at which the nanofluid physical phenomena is manifested. As a result whilst LBM simulations may yield qualitatively reasonable results from numerical simulations for various nanofluid systems the accuracy of such solutions is constrained by the validity limits of the particular mesoscopic modelling approach such as for example how the Boltzmann collision integral terms are approximated, how the interaction effects between the nanoparticle and base fluid molecules are approximated, and how the boundary conditions such as the interactions between the nanofluid and solid surfaces are modelled either for single-phase or multi-phase schemes for nanofluids as discussed by Yan *et al.* [18] or in applied studies such as the estimation of convective heat transfer coefficients in nanofluid systems as discussed by Sheikholeslami *et al.* [19]. Alternatives to mesoscopic simulation approaches are stratified sampling particle based schemes to the Boltzmann equation such as the direct simulation Monte Carlo (DSMC) method which is not constrained by any particular length scale but which does unfortunately suffer from the presence of 'statistical noise' for high number densities typically encountered in liquids but which may in the future be mitigated through more modern DSMC codes such as that developed by Scanlon *et al.*[20] which improves on the earlier historical DSMC codes by Bird [21] and which may potentially be amenable to numerical simulations implemented on massively parallel supercomputing systems. Although both LBM, as well as DSMC implementations of nanofluid simulations, have been reported in the literature, these results are at present of writing considered preliminary numerical results to verify and validate (V&V) both experimental measurements and traditional finite volume CFD type of simulations. Part of the caution that is necessary with predictions with LBM and DSMC simulations is that as per the discussion by Karniadakis *et al.*[22] who investigated numerical methods for atomistic simulations it was determined that the continuum assumption for liquids breaks down for length scales of 10 molecules or smaller regardless of the type of fluid molecules i.e. a continuum modelling hypothesis is not considered physically realistic for clusters of molecules which is the physical case for any nanofluid. Due to this physical reality whilst continuum fluid models may be refined through for example modifications of velocity slip models these refinements may be considered approximations since at the present of writing only molecular dynamics simulations are known to be able to yield physically realistic results for liquids at an *ab initio* physics first-principles level. A potential future research strategy for nanofluid computational modelling is to perform *ab initio* molecular dynamics studies and use these validated & verified results which do not utilize any simplifications to "*calibrate*" an intermolecular potential function for the nanoparticle and base fluid molecules i.e. to construct an approximation of the actual intermolecular potential function from the actual molecular dynamics

based potential function for small clusters and agglomerations of 10 to 1000 nanoparticle and base fluid molecules i.e. for length scales from a fraction of 1 nm to about 10 nm, and to then utilize this approximate potential as an input into further DSMC simulations for length scales made of more than 1000 nanoparticle/liquid molecules i.e. for length scales from around 10 nm to about 100 nm since techniques have now been developed and presently exist to perform DSMC simulations with generalized interaction potential functions as discussed by Sharipov & Strapasson [23], so that the DSMC simulations may then in turn be used to "*calibrate*" continuum model based results such as CFD simulations with modified velocity slip models at length scales larger than 100 nm. As a result this sequential "*calibration*" scheme may be used to verify & validate various nanofluid models from the microscopic to mesoscopic to macroscopic length scales with the associated stress-strain characteristics of the nanofluid within the various modelling assumptions and numerical accuracies achievable from the respective mathematical and computational nanofluid modelling schemes, however this potential future research strategy for nanofluids is crucially and critically dependent on the future availability of high performance computing (HPC) resources to initiate the initial *ab initio* molecular dynamics computational simulations for the nanofluid.

Whilst the the stress-strain state characteristics of gases may be conveniently modelled in terms of the compressible Navier-Stokes equations utilizing either experimental or theoretical thermodynamic properties data as outlined by Canuto *et al.* [24], the modelling of liquids by contrast in the absence of a comprehensive physical theory that is easily implementable for common liquids in engineering problems as previously discussed is inevitably undertaken particularly for single-phase models through experimental measurements. These experimental measurements for classical or Newtonian fluids include that for the particular fluid's mass density $\rho/[\text{kg m}^{-3}] = \rho(p,T)$, viscosity $\mu/[\text{Pa} \cdot \text{s}] = \mu(p,T)$, specific enthalpy $h/[\text{J kg}^{-1}]$, and thermal conductivity $k/[\text{W m}^{-1} \text{ K}^{-1}]$ which are considered as auxiliary relations to close the conservation equations of mass, momentum, and energy respectively in terms of the primary variables of the pressure $p/[\text{Pa}]$ and temperature $T/[\text{K}]$ based on particular modelling assumptions of the fluid's stress-strain relationship. If these four auxiliary relations are known then the conservation equations of mass, momentum and energy are formally mathematically closed and they may then be numerically solved in order to determine the fluid's velocity field $\mathbf{V}(\mathbf{x},t) = [u,v,w]^{\text{T}}$, pressure distribution and heat transfer behaviour such as convective heat transfer coefficients amongst other characteristics for spatial positions as a function of time t for a specified three dimensional domain Ω so that this information may be used for designing, testing, commissioning and verifying various machinery, equipment and devices in engineering applications.

Although this general simulation approach for fluids using either custom developed research codes, open source software packages such as OpenFOAM or commercial software packages such as Ansys Fluent is in principle applicable to any *classical* fluid amenable to a continuum modelling hypothesis such as various grades of machine oils, lubricants, water and air for mechanical engineering applications, various modelling difficulties are generally encountered in nanofluids which are classified as *non-classical* fluids. In this dissertation a working definition to define nano-fluids as classical fluids such as water or oil, usually referred to as the carrying medium, which when doped with various metallic/non-metallic nanoparticles typically with particle sizes d usually less than $d \sim 50$ nm to avoid sedimentation and suspension issues of the nanoparticles

then exhibit vastly superior overall thermal transport properties when compared to traditional classical engineering fluids is considered as per standard nanofluid research studies as reported by Wang & Mujumdar [25]. As a result even though nano-fluids are ostensibly utilized in conventional macroscopic fluid systems due to the vastly different physical interaction effects which occur at intrinsically nano-scale length scales systems utilizing nanofluids such as high efficiency heat exchangers are comprehensively more difficult to mathematically model and numerically simulate from well known physical principles and theories when compared to classical fluids for both macroscopic and microscopic engineering applications as discussed by Bruus [6].

In the event that the conventional Navier-Stokes mass, momentum and energy conservation equations for classical continuum fluids as implemented in many CFD codes are retained then the phenomenological single-phase modelling of nanofluids may be to a large extent be adequately encompassed through appropriate choices of models for the auxiliary relations. As a result, the focus in this dissertation is on studying and modelling numerical models of nano-fluids systems using single-phase models for the effective thermal conductivity k_{eff} and effective viscosity μ_{eff} respectively which incorporate knowledge of the base fluid thermo-physical and transport properties along with the constituent nanoparticle physical and chemical properties and specifications for various mixtures such that the resulting numerical models optimize in some sense CFD based thermo-flow simulation results for various applications and configurations with corresponding experimental results.

2.2 Nanofluid Experimental Measurement Considerations

The study of nanofluids as an area of the physics of fluids field of research is now more than 25 years old as originally discussed by Choi [6] although theoretical and experimental studies of the suspensions of solid particles in fluids have been studied for almost a 100 years going back to the time of James Clerk Maxwell. In most cases these studies have been motivated by the fact that the convective heat transfer characteristics of liquids are often restricted by the particular flow geometries and boundary conditions, and as a result are difficult to improve without changing the characteristics of the working fluid. When solid particles are present in a surrounding fluid medium by virtue of the fact that most solids have superior thermal conductivities the resulting mixture of a base fluid with solid particles has been experimentally observed to have substantially superior heat transfer characteristics. Due to the fact that larger solid particles which have higher densities will generally settle out from the surrounding fluid medium for practical reasons smaller size particles usually of the order of nano-meters are necessary as originally observed by Choi [6] who coined the modern expression and meaning of the term nanofluid as is nowadays commonly understood as a base carrier fluid which contains doped nanoparticles. Usually these nanoparticles have nominal equivalent diameter sizes of $d \leq 50$ nm for metallic/non-metallic solid materials and due to their much larger relative surface area when compared to nominal suspended solids in fluid mixtures tend to exhibit superior heat transfer characteristics and suspension stabilities in the base fluid.

Historically the production of nanofluids has been a non-trivial matter as nanoparticles cannot simply be mixed with a base fluid without being prone to settling down, agglomeration or failing to exhibit stable and durable suspension characteristics and have either to be produced by the 'one-

step' method or the 'two-step' method. In the one-step method which is used to produce nanoparticles directly inside a fluid and which is also called the Vacuum Evaporation onto a Running Oil Substrate (VEROS) method the general idea is that a vapour of the constituent solid material such is condensed into nanoparticles when the vapour comes into contact with a flowing low vapour pressure liquid. The VEROS technique and a related technique called the vacuum-SANSS (submerged arc nanoparticle synthesis system) are able to produce Cu and Ni based nano-fluids. The two-step method on the other hand is used to produce the actual nanofluids for other nano-fluids such as water/alumina (H_2O/Al_2O_3) or water copper-oxide (CuO) mixtures since they are relatively common and inexpensive where a first step is to produce the nanoparticles using any convenient technique and then as a second step the nanoparticles are mixed into the base fluid usually through the use of ultra-sonic equipment which tends to avoid agglomeration issues. Additional fluid pH control and active surface agents are then used usually employed as additional measures to enhance the stability of the mixtures and mitigate against sedimentation of the nanoparticles. Different techniques have in the past been used to measure nano-fluids thermal conductivities and include amongst other approaches the traditional transient hot-wire method, the steady state parallel technique method, and the temperature oscillation technique. Amongst these techniques the main issue which arises is that some nano-fluids are electrically conductive and although coating the hot wire in for example the commonly used transient hot-wire method with an epoxy adhesive to provide electrical insulation is possible this approach as the disadvantage that there may be a concentration of ions from the conducting fluid around the hot wire which would affect the physical accuracies of the experiment measurements. For this reason the oscillation method which is a purely thermal based experimental technique is preferred for nanofluid thermal conductivity experimental measurements. An alternative technique for this earlier time period known as the 3ω method has been reported in the literature by Oh *et al.*[27] as an alternative to the more common transient hot wire technique which potentially offers the means to mitigate against agglomeration and sedimentation issues with the more traditional techniques. The 3ω measurement technique has mainly in the past been used to measure the properties of thin films and solid substrates and was adapted and used by Oh *et al.* to characterise a Al_2O_3/water mixture with a volume fraction from 1% to 4% which compared favourably with earlier reported works. According to Oh *et al.* the main proposed advantages of the 3ω method for thermal conductivity experimental testing are that (i) it may be used to determine whether homogeneous mixtures have been achieved since it can test small volumes of nanofluids, (ii) it may be used to test spatial variations of mixtures again because it can test small volumes, and (iii) it may in principle be extended to investigate thermal conductivity changes with variations in temperature and pressure. Later experiments by Turgut *et al.*[28] who calibrated the typical commercially available 3ω measurement apparatus against known thermal conductivities of pure water, methanol, ethanol and ethylene glycol (EG) established that 3ω thermal conductivity measurements have achievable accuracies of $\pm2\%$ in most practical experiment measurement situations using standard laboratory equipment in thermophysical studies.

Earlier experiments with Al_2O_3 particles using more traditional measurement techniques found that the thermal conductivity was enhanced by a difference in the pH of the suspension and the isoelectric point i.e. the pH where a molecule carries no nett electrical charge, was highly dependant on the specific surface area (SSA) of the mixture, but was not affected by the crystalline phase of the nanoparticles. Effects of the variation of temperature T and volume fraction ϕ for 36 nm area weighted diameters of water Al_2O_3 mixtures were studied by Li & Peterson [29]

who determined a correlation of the form

$$\frac{k_{eff} - k_{fluid}}{k_{fluid}} = 0.764481464\phi + 0.018688867t - 0.462147175 \tag{2.8}$$

for volume fractions of 2%, 4%, 6% and 10% for temperatures from 27.5°C to 34.7°C where the benefit of this earlier publication is that it provided specific experimental accuracies for the results. For this experimental data-set the authors determined that their apparatus could experimentally measure thermal accuracies to within an experimental accuracy of ±2.5%. These results were then further analysed by Li & Peterson using a two-factor linear regression analysis which yielded the relation

$$\frac{k_{eff} - k_b}{k_b} = 0.764\phi + 0.0187(T - 273.15) - 0.462 \tag{2.9}$$

This two-factor linear regression was used to model the relationship between the volume fraction ϕ of the nanoparticle and the bulk temperature $t/[°C]$. Additional comparisons by Li & Peterson with thermal conductivity data were subsequently performed from which it was demonstrated that there can be marked differences in nanofluid thermal conductivity results for the same volume fractions ϕ by different investigators and they concluded that the classical Maxwell model is inaccurate for large volume fractions.

Limited natural convective heat transfer h studies were performed in the earlier years and where data was available results were more qualitative in nature such that the convective heat transfer coefficient tended to usually but always increase with an increase in nanoparticles due to discrepancies from various investigators. Many of the earlier studies adopted a single-phase formulation to numerically study heat transfer characteristics of nano-fluids in order to determine Nusselt numbers in terms of the Reynolds and Prandtl numbers for a combination of laminar and turbulent flows mainly because a single-phase model is still amenable to a continuum assumption and may therefore still be used by conventional finite volume based CFD software such as Ansys, and since it was not clear at the time that multi-phase models, i.e. modelling the combination of both the base fluid medium and surrounding solid nanoparticles offered significant benefits over single-phase models. Reasons for some of these discrepancies between the earlier numerical studies and the experimental studies may be partially attributed to that fact that not all earlier numerical studies explicitly included process parameters such as the particle size, particle shape and particle distribution since all of these in combination and not just a single nanofluid parameters have a physical influence on the flow and heat transfer characteristics.

Although there was no general consensus on an appropriate theoretical explanation for the massive increase in heat transfer performance of nanofluids as factors such a Brownian motion, liquid-solid interface layers, ballistic phonon transport effects and surface charge states were considered and debated in the literature semi-empirical relations were nevertheless possible due to their simplicity and practical utility. One of the earliest models was that of Maxwell of the form

$$k_{eff} = \frac{k_p + 2k_b + 2(k_p - k_b)\phi}{k_p + 2k_b - (k_p - k_b)\phi} k_b \tag{2.10}$$

where k_p is the thermal conductivity of the particle, k_b is the thermal conductivity of the base fluid, and ϕ is the particle volume fraction unless otherwise stated (where usually in nanofluid studies volumetric fractions are assumed unless otherwise stated). As previously discussed the Maxwell model is now considered to be inaccurate except for relatively small volume fractions but it still nevertheless provides a convenient bench-mark to compare other predictions. For homogeneous spherical inclusions the Bruggeman model of the form

$$\phi\left(\frac{k_p - k_{eff}}{k_p + 2k_{eff}}\right) + (1 - \phi)\left(\frac{k_b - k_{eff}}{k_b + 2k_{eff}}\right) = 0 \tag{2.11}$$

is commonly employed whilst the Hamilton & Crosser model of the form

$$k_{eff} = \frac{k_p + (n-1)k_b - (n-1)(k_b - k_p)\phi}{k_p + (n-1)k_b + (k_b - k_p)\phi}, \frac{k_p}{k_b} > 100 \tag{2.12}$$

$$n = \frac{3}{\psi} \tag{2.13}$$

$$\psi = \frac{\text{surface area of a sphere with volume equal to that of particle}}{\text{surface area of particle}} \tag{2.14}$$

is used for liquid-solid mixtures with non-spherical particles where ψ is the particle sphericity and n is an empirical shape factor as indicated above. Comparisons of predictions of the Hamilton & Crosser model with that of the Maxwell model reveal that the Maxwell model is simply a special case of the Hamilton & Crosser model when there are perfectly spherical nanoparticles. An extension to the classical Maxwell model to incorporate the effects of the nano-layer was proposed by Yu & Choi as further discussed by Ravisankar & Tara Chand [30] of the form

$$k_{eff} = \frac{k_{pe} + 2k_b + 2(k_{pe} - k_b)(1 + \beta)^3 \phi}{k_{pe} + 2k_b - (k_{pe} - k_b)(1 + \beta)^3 \phi} k_b \tag{2.15}$$

$$k_{pe} = \frac{[2(1-\gamma) + (1+\beta)^3(1+2\gamma)]\gamma}{-(1-\gamma) + (1+\beta)^3(1+2\gamma)} k_p \tag{2.16}$$

$$\gamma = \frac{k_{layer}}{k_p} = \frac{\text{nano-layer thermal conductivity}}{\text{nano-particle thermal conductivity}} \tag{2.17}$$

$$\beta = \frac{h}{r} = \frac{\text{nano-layerthickness}}{\text{nano-particleradius}} \tag{2.18}$$

The above modified Maxwell model with a nano-layer term was found to be able to predict the presence of nano-layers with a thickness less than 10 nm and it also introduced to investigators of the possibility that the addition of nanoparticles smaller than 10 nm could, in fact, be potentially more advantageous for nanofluid thermal conductivity than simply increasing the solid nanoparticle volume fraction ϕ. As a result, these earlier models emphasised the complexity of the underlying physical interactions and processes at the nano-scale level and the need for various researchers to study a combination of process parameters when they constructed various nanofluid

models. It could arguably be claimed that the observance of the various complex physical processes at play laid the later foundation for future researchers to consider more advanced computational intelligence techniques such as neural networks and artificial learning systems in order to make sense of and model the at times inconsistent and contradictory mixture of experimental and theoretical results.

Unless otherwise specified the density ρ and specific heat c_p are usually assumed to be

$$\rho_{eff} = (1 - \phi_p)\rho_b + \phi_b\rho_b \tag{2.19}$$

$$c_{p,eff} = \frac{(1 - \phi_p)(\rho c_p)_b + \phi_p(\rho c_p)_p}{(1 - \phi_p)\rho_b + \phi_p\rho_p} \tag{2.20}$$

as discussed and derived by Wang & Mujumdar [31] where the subscript b denotes the base or carrier fluid such as water whilst the subscript p denotes the nanoparticle such as alumina, copper oxide or titanium oxide particles. The above formula for the density of nanofluids which is sometimes referred to as the Pak & Cho formula was investigated by Vajjha *et al.*[32] who performed experiments on at $60:40$ ethylene glycol/water mixture using aluminium oxide (Al_2O_3), antimony-tin oxide ($Sb_2O_5:SnO_2$) and zinc oxide nanoparticles and verified that the conventional mixture formula for the effective density ρ_{eff} gives good agreement between the experimental results and recommendations from the ASHRAE 2005 handbook when using standard ASTM test methods for density measurements of fluids. These experimental studies therefore verified the validity of the density mixing formula for Al_2O_3 nanoparticles with an average diameter of 44 nm in a $60:40$ EG/W mixture for density mixtures by mass of 1%, 2%, 4%, 6%, 8% and 10% respectively over a temperature of $0 \leq t/[°C] \leq 50$ as graphically summarized in Figure 2.1.
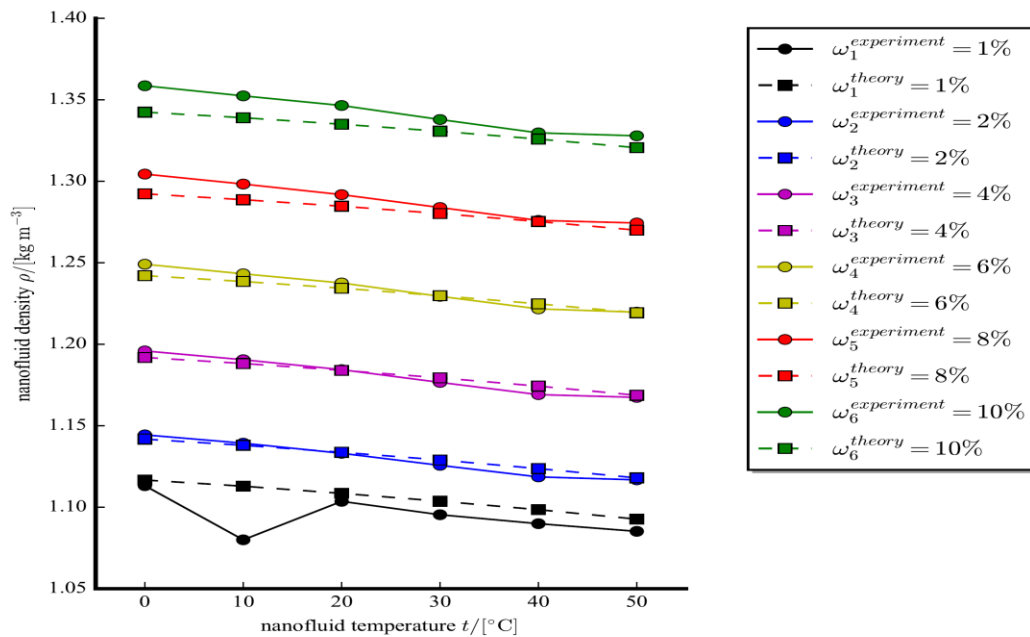
Figure 2-1 Illustration of validation of mixing density formula of Pak & Cho based on experimental data reported by Vajjha et al.[32]

17

When this data set was analysed by Vajjha *et al.*they concluded that for Al_2O_3 nanoparticles in the EG/W base fluid showed agreement to the Pak & Cho formula with an absolute average deviation of 0.39% with a maximum deviation of 1.2%. The one issue in this experimental study was that the Pak & Cho formula performed poorly for Sb_2O_5:SnO_2 nanoparticles in the EG/W base fluid and tended give to results only accurate to about 8%, however, the overall conclusion of Vajjha *et al.*was that the Pak & Cho formula is in fact suitable for estimating the density of alumina/water nano-fluids.

Similar experiments by Teng & Hung [33] for the density and specific heat of alumina/water nanofluids were also performed in 2012 but only reported a few years later in the 2014 literature where they came to a similar conclusion as Vajjha *et al.* that the mixed density formula generally gives reasonable results within the expected accuracy levels of about 1.5%. These experiments used a differential scanning calorimeter for the specific heat measurements and a dynamic light scattering analyser to investigate the particle size distribution. In this study, Teng & Hung developed two alternative sets of equations for the nanofluid density and specific heat as

$$\rho_{nf} = (1 - \phi)\rho_{bf} + \phi\rho_p \qquad \text{: Option 1} \qquad (2.21)$$

$$\rho_{nf} = \frac{(1 - \phi)\rho_{bf}\rho_{bf} + \phi\rho_p\rho_p}{(1 - \phi)\rho_{bf} + \phi\rho_p} \qquad \text{: Option 2} \qquad (2.22)$$

$$\rho_{nf} = (1 - \omega)\rho_{bf} + \omega\rho_p \qquad \text{: Option 2 (equivalent form)} \qquad (2.23)$$

and

$$c_{p,nf} = (1 - \phi)c_{p,bf} + \phi c_{p,p} \qquad \text{: Option 1} \qquad (2.24)$$

$$c_{p,nf} = \frac{(1 - \phi)(\rho_{bf}c_{p,bf})}{(1 - \phi)(\rho_{bf}) + \phi(\rho_p)} \qquad \text{: Option 2} \qquad (2.25)$$

$$c_{p,nf} = (1 - \omega)c_{p,bf} + \omega c_{p,p} \qquad \text{: Option 2 (equivalent form)} \qquad (2.26)$$

where ω is the weight function. The weight function is used to convert a weight fraction to a volume fraction by using the equation

$$\phi = \frac{\left(\frac{W_p}{\rho_p}\right)}{\left(\frac{W_{nf}}{\rho_{nf}}\right)} \qquad (2.27)$$

$$\phi = \omega\left(\frac{\rho_{nf}}{\rho_p}\right) \qquad (2.28)$$

where W_{bf} is the weight i.e. mass of the base fluid, W_p is the mass of the nanoparticle and W_{nf} is the mass of the nanofluid mixture. This set of experiments for the densities by Teng & Hung were performed over a temperature range of $10 \leq t/[°C] \leq 40$ and when they analysed the data they concluded that when predicting densities that Option 1 yielded results with deviations of densities in the range from -1.50% to 0.06% and that Option 2 yielded results with deviations of densities in the range from 0.25% to 2.53% where in general their investigation showed a greater deviation with an increased concentration in the nano-fluid, where they speculated that interface layer between the nanoparticles and the surrounding water may tend to play an increasing

role in explaining why there are higher deviations in predictions between the theoretical formulae and the experimental results at higher nanoparticle concentrations.

With regards to the specific heat experimental results which were performed over a temperature range of $25 \leq t/[°C] \leq 65$ they concluded that when using Option 1 that this formula tends to over-estimate the specific heat that were experimentally measured, and that the difference between the experimental results and the predictions with the Option 1 formula tended to decrease with a decrease in the nanoparticle concentration, however they were not able to discern how the temperature affects changes in the specific heat the Al_2O_3/mixture with any confidence.

A similar pattern was observed with the use of the Option 2 formula for the specific heat predictions and when both the Option 1 and Option 2 formula were compared to the experimental results they found that the deviations between the theoretical prediction and experimental measurements ranged from -0.07% to 5.88% with the Option 1 formula and ranged from -0.35% to 4.94% with the Option 2 specific heat formula. As a result, they concluded that the Option 2 formula for specific heat predictions tends to offer superior results for predicting the specific heat for when the nanofluid concentration is low. It is therefore concluded that the predictions of effective density and effective specific heat using the conventional mixing modelling approach which indirectly draws from mixing theory concepts from ideal gas mixtures using classical statistical mechanics ideas are generally reasonably accurate in most practical cases when taking into account their associated accuracy prediction levels. The one main experimental observation from the Teng & Hung study to note is that of the observed variation in nanoparticle sizes that are present in any practical nanofluid mixture. Regardless of nanoparticle size, the specific heat for the alumina/water nanofluid mixtures was observed to increase with temperature for both $\alpha - Al_2O_3$ and $\gamma - Al_2O_3$ nanoparticles however this effect was much more pronounced for smaller size nanoparticles. Teng & Hung speculated five main physical reasons for this phenomena involving *inter alia* effects of larger specific surface area (SSA), larger porosities for the same amount of nanoparticle matter in the base fluid, an increase in the number of interface layers between the smaller nanoparticles and the surrounding base fluid for the same amount of nanoparticle matter, increased associated energies for fine-grained i.e. smaller than course-grained i.e. larger nanoparticles, and finally the phenomena whereby the heat capacity tends to increase with increments of the nanoparticles excess volume i.e. there is an increase in heat capacity based on the changes in nanoparticle grain sizes.

For the particular experimental study, Teng & Hung reported an increase of 16.37% when smaller 20 nm $\gamma - Al_2O_3$ particles were present for the temperature range of $25 \leq t/[°C] \leq 65$ they studied and this affect is generally consistent with similar reported observations in studies as discussed in an earlier paper by Teng *et al.*[34] who performed a regression analysis of the experimental data with 20 nm, 50 nm and 100 nm Al_2O_3 nanoparticles in water to model the enhanced thermal conductivity k_{nf}/k_{bf} as a function of the temperature $T/[K]$, weight fraction $\omega/[\%]$ and particle size $d_p/[nm]$ such that

$$
\begin{aligned}
\frac{k_{nf}}{k_{bf}} = {} & C_0 + C_1(100\omega) + C_2(T - 273.15) + C_3 d_p + C_4(100\omega)^2 \\
& + C_5(T - 273.15)^2 + C_6 d_p^2 + C_7(100\omega)^3 + C_8(T - 273.15)^3
\end{aligned}
\tag{2.29}
$$

where $C_0 = 0.991$, $C_1 = 0.253$, $C_2 = -0.001$, $C_3 = -0.002$, $C_4 = -0.189$, $C_5 = 6.190 \times 10^{-5}$, $C_6 = 1.317 \times 10^{-5}$, $C_7 = 0.049$ and $C_8 = -7.66 \times 10^{-7}$ respectively according to their regression analysis with a regression fit of $R^2 = 0.90$.

A more recent result for the nanofluid density has recently been reported by Sharifpur *et al.*[35] that incorporates the nanolayer volume surrounding the nanoparticle such that the actual nanofluid density is $\rho_{nf}^{(new)} = (m_p + m_f)/(V_p + V_f + V_v)$ where m_p is the mass of the nanoparticle, m_f is the mass of the base fluid, V_p is the conventional volume of the nanoparticle, V_f is the conventional volume of the base fluid, and V_v is an estimate of the volume of the nanolayer. The modelling approach used in the new density formula is based on approximating V_v using an equivalent nanolayer thickness term such that the total nanoparticle volume is $(V_p + V_v) = n \times \frac{4}{3}\pi(r_p + t_v)^3$ where n is the total number of nanoparticles. Under these assumptions, the new formulae for the density and volume fraction then take the forms

$$\varphi^{(old)} = \frac{V_p}{V_p + V_f} \tag{2.30}$$

$$\varphi^{(new)} = \frac{\frac{m_p}{\rho_p}}{\left(\frac{m_f}{\rho_f} + \left(\frac{m_p}{\rho_p}\frac{(r_p + t_v)^3}{r_p^3}\right)\right)} \tag{2.31}$$

$$\varphi^{(new)} = \frac{1}{\frac{1}{\varphi^{(old)}} - 1 + \frac{(r_p + t_v)^3}{r_p^3}} \tag{2.32}$$

and

$$\rho_{nf}^{(new)} = \frac{\rho_{nf}^{(old)}}{(1 - \varphi^{(old)}) + \varphi^{(old)}\frac{(r_p + t_v)^3}{r_p^3}} \tag{2.33}$$

The above new forms for the estimate of the nanofluid density and volume fraction are expected to become more widely utilized as additional experimental data values and associated uncertainties for the nanolayer thickness t_v becomes available, so that higher accuracy correlations between the nanolayer thickness t_v and nanoparticle diameter d_p can be constructed.

The uncertainty effects of nanofluid thermophysical properties of thermal conductivity and viscosity were originally identified by Sharifpur & Meyer [36] who studied how different mathematical models for k_{eff} and μ_{eff} influenced estimates on the Nusselt number for convective heat transfer systems. In this study Sharifpur & Meyer concluded that various inconsistencies in effective thermal conductivity model predictions were present that negatively impacted on the resultant uncertainties in convective heat transfer results and that the earlier nanofluid viscosity models were inadequate as not all viscosity models took into account physical parameters such as *inter alia* volume fractions, base fluid temperature, packing fractions, nanolayer thickness, nanoparticle shape & aspect ratios, nanoparticle diameters, spacing and capping layer effects.

Motivated by the earlier observations by Sharifpur & Meyer [36] later work by Mehrabi *et al.* [37]

investigated the influence of the Reynolds number Re, Prandtl number Pr, nanoparticle volume fraction ϕ and nanoparticle diameter d_p as parameters on the nanofluid Nusselt number Nu_{nf} and nanofluid pressure drop ΔP_{nf} using a multi-objective approach where the functional relations $Nu_{nf} = f_1(Re, Pr, \phi, d_p)$ and $\Delta P_{nf} = f_2(Re, \phi, d_p)$ were determined using a genetic algorithm (GA) based polynomial neural network (PNN) where the GA-PNN was used to solve for the Pareto optimality condition for the nanofluid Nusselt number and pressure drop. The Pareto frontier $P(\mathbf{Y})$ may for our purposes be mathematically specified by considering a mapping $\mathbf{f}: \mathbb{R}^n \to \mathbb{R}^m$ for $n, m \in \mathbb{Z}$ such that $\mathbf{Y} = \{\mathbf{y} \in \mathbb{R}^m : \mathbf{y} = \mathbf{f}(\mathbf{x}), \mathbf{x} \in \mathbf{X} \subset \mathbb{R}^n\}$, so that $P(\mathbf{Y}) = \{\mathbf{y}' : \{\mathbf{y}'' \in \mathbf{Y} : \mathbf{y}'' > \mathbf{y}' \wedge \mathbf{y}'' \neq \mathbf{y}'\} = \emptyset\}$. Although the design space for Nu_{nf} is $\mathbb{R}^4$ and that for ΔP_{nf} is $\mathbb{R}^3$ respectively based on the cardinalities of the parameters, say $\mathbf{a} = [Re, Pr, \phi, d_p]^{\mathrm{T}}$ for Nu_{nf} and $\mathbf{b} = [Re, \phi, d_p]^{\mathrm{T}}$ for ΔP_{nf}, of each of the associated optimizations the general idea of the Pareto optimality is the same. For the present context, this is simply the selection of parameters $\mathbf{a}$ such that no further Pareto improvements are possible i.e. the value of $\mathbf{a}$ is selected such that Nu_{nf} is a maximum and ΔP_{nf} is a minimum since in a convective heat transfer system it is desired to maximize the Nusselt number $Nu_{nf} = \frac{h_{nf}L_c}{k_{nf}}$ where h_{nf} is the equivalent convective heat transfer coefficient for the particular nanofluid system, L_c is a characteristic length of the system and k_{nf} is the effective thermal conductivity of the nanofluid, and simultaneously minimize the pressure drop ΔP_{nf} for the mechanical system.

In this study, the multi-objective optimization was to maximise the Nusselt number and minimize the pressure drop where a combination of experimental data points from the literature and semi-empirical relations for the nanofluid Nusselt number were used to specify the values used in the optimization exercise, where the mean absolute error $MAE = \frac{1}{n}\sum_{i=1}^{n} |X_p - X_a|$, mean relative error $MRE(\%) = \frac{100}{n}\sum_{i=1}^{n} \left(\frac{|X_p - X_a|}{X_a}\right)$, and root mean square error $RMSE = \sqrt{\frac{1}{n}\sum_{i=1}^{n} (X_p - X_a)^2}$ were used as statistical criteria to determine the optimality of the results where X_p were the predicted values and X_a were the actual values. Later investigations by Mehrabi $et\ al.$[38] then focused on building models for the nanofluid viscosity using an artificial intelligence (AI) approach where it was concluded that the particle size d_p, volume concentration ϕ and temperature t were in fact the main variables that effected the results from the model construction and predictions that resulted from the model using experimental data for a water/Al_2O_3 from Nguyen $et\ al.$[39], Tavman $et\ al.$[40], Lee $et\ al.$[41], Annop $et\ al.$[42], Pastoriza-Gallego $et\ al.$[43] and Kwek $et\ al.$[44] respectively. Further experimental studies by Adio $et\ al.$[45] were then performed to understand the interaction between the viscosity, electrical conductivity and pH of nanofluids in the Einstein concentration regime which is by convention specified as nanoparticle volume concentrations below 2% where it was determined that the classical mathematical models under-predicted the viscosity and that the electrical conductivity and pH values for the nanofluid were significantly affected by both the temperature as well as the volume fraction. More recent experimental research was reported by Sharifpur $et\ al.$[46] for a glycerol/Al_2O_3 mixture where the refined the nanofluid viscosity models by using a dimensional analysis approach. In this study Sharifpur $et\ al.$developed an empirical correlation for the viscosity using a Group Method of Data handling Neural Network (GMD-NN) where the dimensionless parameters were $\pi_1 = \frac{\mu_{nf}}{\mu_{bf}}$, $\pi_2 =$

$\frac{T}{T_0}$, $\pi_3 = \phi$, $\pi_4 = \frac{d}{h}$ and $\pi_5 = \frac{\rho_{nf}}{\rho_{bf}}$ respectively where $h = 1$ nm is an assumed value for the nanoparticle capping layer thickness. When the analysis was performed it was determined that the viscosity tended to increase as the volume fraction increased but decreased as the temperature increased, and that the smallest nanoparticle mixtures exhibit the highest shear resistance.

In most cases the above discussed modelling approach for single phase models is adequate for the majority of nano-fluids which use mixtures of a single base fluid and single type of nanoparticle however it is necessary to make appropriate natural modifications in the special case of so-called '*hybrid*' nano-fluids which incorporate mixtures of different types of nanoparticles for example a nanofluid composed of water as the base fluid and a Al_2O_3/CuO mixture of nanoparticles in an attempt to combine different characteristics of conventional water/alumina and water/copper oxide nano-fluids as discussed by Ranga Babu *et al.* [145] which is a relatively new development in the research area of nano-fluids. When the above modelling assumptions are used the nanofluid enthalpy may then using standard CFD modelling approaches as discussed in White [194] be approximated under the single-phase continuum modelling assumption using the Maxwell thermodynamic relations such that

$$dH = c_p dT + V(1 - \alpha T)dp \tag{2.34}$$

$$\alpha = \frac{1}{V}\left(\frac{\partial V}{\partial T}\right)_p \tag{2.35}$$

where V is the fluid volume, $h = H/m$ is the specific enthalpy, H is the total enthalpy and α is the coefficient of cubic thermal expansion of the fluid. In many literature sources, the thermal expansion coefficient is usually also sometimes written as β_{eff} for a nano-fluid. The practical consequence of this relation is that it allows one to simply determine the enthalpy if $c_p(p,T)$ and $V(p,T)$ are known in terms of the pressure p and temperature T. Results between experimental measured specific heat c_p values and predictions with the Option 1 and Option 2 formulae as reported by Teng & Hung [33]. Referring to these results it may be concluded that the standard mixing formulae for specific heats of nano-fluids give reasonably consistent results within their reported accuracy levels for moderate nanofluid temperature ranges and low concentrations, and as a result the energy equation for single-phase models of nano-fluids using the Navier-Stokes equations are adequately modelled in terms of the appropriate auxiliary thermodynamic relations. In the general case where the variation in specific heat capacity with temperature may be significant then the energy equation for a nanofluid may be approximated using a thermal dispersion model of the form

$$\frac{\partial T}{\partial t} + \nabla \cdot (\mathbf{V}T) = \nabla \cdot \left(\frac{k_{nf}}{(\rho c_p)_{nf}} \nabla T\right) \tag{2.36}$$

as discussed by Kumar *et al.*[48] where the above equation for a single-phase nanofluid model is technically valid only under the two assumptions that (i) a no-slip velocity condition holds between the nanoparticles and the surrounding base fluid, and (ii) that there is a local thermodynamic equilibrium at the interfaces between the nanoparticles and the base fluid. For steady state conditions, the single-phase CFD equations following Moraveji & Ardehali [49] take the form

$$\nabla \cdot (\rho_{nf} \mathbf{V}_m) = 0 \qquad\qquad\qquad\text{: Continuity} \tag{2.37}$$
$$\nabla \cdot (\rho_{nf} \mathbf{V}_m \mathbf{V}_m) = -\nabla P + \nabla \cdot (\mu_{nf} \nabla \mathbf{V}_m) \quad\text{: Momentum} \tag{2.38}$$
$$\nabla \cdot (\rho_{nf} C_{nf} \mathbf{V}_m T) = \nabla \cdot (k_{nf} \nabla T) \qquad\text{: Energy} \tag{2.39}$$

where C_{nf} is the equivalent specific heat capacity of the nano-fluid. A similar single-phase CFD approach was later applied by Davarnejad *et al.*[50] using the Yu & Choi correlation as previously discussed for the effective thermal conductivity with a ratio of nanolayer thickness to the nanoparticle radius of $\beta = (h/r) = 0.1$ for a Al_2O_3/water nanofluid dispersed with 20 nm and 50 nm nanoparticles for volume concentrations of 0.2%, 1.0%, 1.5%, 2.0% and 2.5% respectively and which yielded good results under the assumption that the thermo-physical properties were temperature independent.

Common mixing models for β_{eff} following a similar line of reasoning as for the effective density and effective specific heat capacity functions usually take the form

$$\beta_{eff} = \frac{(1-\phi_p)(\rho\beta)_f + \phi_p(\rho\beta)_p}{\rho_{eff}} \qquad\text{: Option 1} \tag{2.40}$$
$$\beta_{eff} = (1 - \phi_p)\beta_f + \phi_p\beta_p \qquad\text{: Option 2} \tag{2.41}$$

However investigations by Khanafer & Vafai [51] reveal that both of these models exhibit inaccuracies for a range of volume fractions. Based on this shortcoming Khanafer & Vafai re-analysed earlier data and developed an improved estimate for the nanofluid volumetric expansion coefficient as

$$\beta_{eff} = \left(-0.479\phi_p + 9.3158 \times 10^{-3}T - \frac{4.7211}{T^2}\right) \times 10^{-3},$$
$$0 \le \phi_p \le 0.04 \quad \& \quad 10 \le T/[°C] \le 40 \tag{2.42}$$

When using the thermodynamic relation $h = e + \frac{p}{\rho}$ these equations can then be used to form the equivalent conservation of energy equation

$$\rho \frac{\mathrm{D}h}{\mathrm{D}t} = \frac{\mathrm{D}p}{\mathrm{D}t} + \nabla \cdot (k\nabla T) + \Phi \tag{2.43}$$

$$\Phi = \mu\left[2\left(\frac{\partial u}{\partial x}\right)^2 + 2\left(\frac{\partial v}{\partial y}\right)^2 + 2\left(\frac{\partial w}{\partial z}\right)^2 + \left(\frac{\partial v}{\partial x} + \frac{\partial u}{\partial y}\right)^2 \right.$$
$$\left. + \left(\frac{\partial w}{\partial y} + \frac{\partial v}{\partial z}\right)^2 + \left(\frac{\partial u}{\partial z} + \frac{\partial w}{\partial x}\right)^2\right] + \lambda\left(\frac{\partial u}{\partial x} + \frac{\partial v}{\partial y} + \frac{\partial w}{\partial z}\right)^2 \tag{2.44}$$

In the above system of equations $\frac{\mathrm{D}}{\mathrm{D}t} \equiv \frac{\partial}{\partial t} + \mathbf{V} \cdot \nabla$ is the particle derivative operator, λ is the second viscosity coefficient usually just calculated under the assumption of Stoke's 1845 hypothesis $\lambda + \frac{2}{3}\mu = 0$, and Φ is the viscous dissipation function. As a result, when characterizing nanofluids, we only need to focus on developing mathematical functional forms for the effective thermal conductivity k_{eff} and effective viscosity μ_{eff}.

While there have been many earlier quantitative studies on nanofluid thermal conductivities the state of knowledge for nanofluid viscosities has by contrast been relatively sparse although the general trend of an increase in relative viscosity with increasing solid volume fractions has been a general observable qualitative trend. The effects of temperature and particle volume concentration have however been experimentally studied using a commercial ViscoLab450 viscometer model from Cambridge Applied Systems (USA) which is based on a 'piston-type' viscometer measurement technique for alumina-water mixtures over a restricted range of temperatures and moderate volume concentrations by Nguyen *et al.* [52].

The basic measurement principle of the piston-type viscometer referring to Figure 2.2 is that a Couette flow inside a cylindrical chamber is established by electrically powering two magnetic coils inside a stainless steel body. First, the piston is placed within the cylinder, and Coil A is powered which induces an electromagnetic force that is exerted on the piston in one direction based on the direction of the electric current within the coil from the voltage source V_1 and then using the same principle with another Coil B powered by a different voltage source V_2 an opposite force is similarly generated.

(a) Electromagnetic system   (b) Fluid system
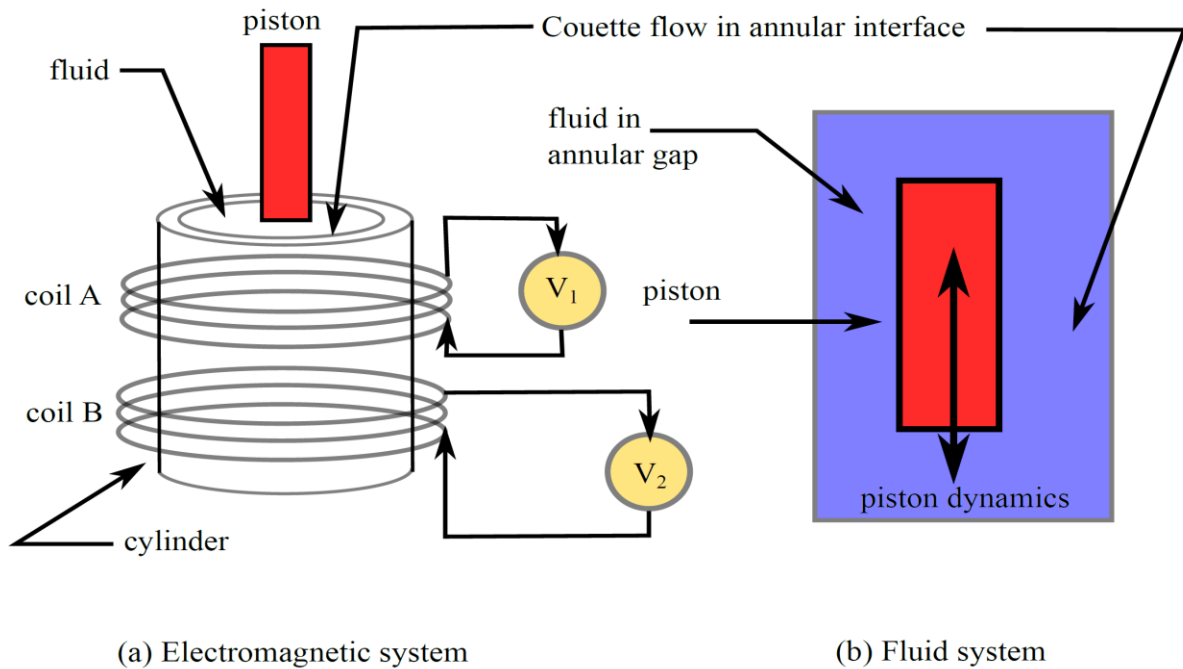
Figure 2-2 Illustration of experimental viscosity measuring equipment operating principle for a piston-type viscometer

As a result, when the coils are electrically powered an induced electro-magnetic force is created when then moves the piston back and forth over a small distance of about 5 mm inside the cylindrical chamber. The measurement time of the piston movement is then correlated in terms of

the fluid viscosity, the geometrical properties of the piston/cylinder arrangement and the thermometers of the viscometer system. Final experimental viscosity measurements for alumina/water mixtures have an accuracy of $\pm1\%$ with a repeatability of $\pm0.8\%$. In this dissertation unless otherwise specified we will always assume that the engineering term "*accuracy*" corresponds to the metrological (measurement theory) term of "*expanded uncertainty*" with a coverage factor of $k = 2$ for a confidence level of 95.45% since very few of the data sources in the open literature explicitly state measurement results in accordance with the GUM [53]. When Nguyen *et al.* analysed their experimental viscosity data for 36 nm and 47 nm average diameter nanoparticles purchased from Nanophase Technologies (USA) they concluded that none of the conventional classical viscosity formulae such as those by Einstein, Brinkman and Batchelor were actually able to accurately predict the nanofluid viscosity values for the range of operating conditions they investigated. The reasoning behind this shortcoming were speculated as being that the classical solid in a fluid formulae such as the Einstein formula is actually based on a single nanoparticle in a surrounding liquid which is not the case in an actual nanofluid due to the presence of numerous nanoparticles which cause a more complex interaction affect in the nanofluid medium. For this reason, the authors proposed correlations for low volume fractions for a low 1% and a medium 4% mixtures of the relative viscosities $\mu_r = \mu/\mu_0$ as

$$\mu_r = 1.125 - 0.0007t \qquad\qquad : \phi = 1\% \tag{2.45}$$
$$\mu_r = 2.1275 - 0.0215t + 0.0002t^2 \quad : \phi = 4\% \tag{2.46}$$

where $t/[°\text{C}]$ is the fluid temperature and the low and medium correlations exhibit average errors of 0.06% and 1.28% respectively with corresponding standard deviations of 3.75% and 11.39% respectively. Due to the complexity of the data at higher volume fractions closer to 10% they were unable to take into account the combined influence of temperature, nanoparticle size and volume particle concentrations.

Earlier viscosity results by Chandrasekar et al. [54] and Hosseini & Ghader [55] were subsequently utilized in later studies and for the period prior to 2007 to 2012 a representative set of effective thermal conductivity and effective viscosity results for alumina/water nanofluid mixtures by Khanafer & Vafai [51] is first defined in terms of the base fluid density of the form

$$\mu_f(T) = (2.414 \times 10^{-5}) \times \left(10^{\frac{247.8}{(T-140)}}\right)s \tag{2.47}$$

The above base fluid density expression may then be used so that the effective viscosity is then calculated as

$$\mu_{eff} = -0.4491 + \frac{28.837}{T} + 0.574\phi_p - 0.1634\phi_p^2 + 23.053\frac{\phi_p^2}{T^2} + 0.0132\phi_p^3$$
$$\qquad - 2354.735\frac{\phi_p}{T^3} + 23.498\frac{\phi_p^2}{d_p^2} - 3.0185\frac{\phi_p^3}{d_p^2}, \tag{2.48}$$
$$\text{for } 1 \leq \phi_p/[\%] \leq 9, 20 \leq T/[°\text{C}] \leq 70, 13 \leq d_p/[\text{nm}] \leq 131$$

$$\frac{k_{eff}}{k_f} = 0.9843 + 0.398\phi_p^{0.7383}\left(\frac{1}{d_p/[\text{nm}]}\right)^{0.2246}\left(\frac{\mu_{eff}(T)}{\mu_f(T)}\right)^{0.0235} \tag{2.49}$$

$$- \ 3.9517 \frac{\phi_p}{T} + 34.034 \frac{\phi_p^2}{T^3} + 32.509 \frac{\phi_p}{T^2},$$

$$\text{for} \quad 0 \leq \phi_p/[\%] \leq 10, 11 \leq d/[\text{nm}] \leq 150, 20 \leq T/[^\circ\text{C}] \leq 70$$

Investigations in the subsequent period from around 2013 and later started to make further use of multi-phase models where an early and well-known study was that of Corcione *et al.* [56]. In this study, Corcione *et al.* made the modelling assumption of local thermodynamic equilibrium as per the single-phase nanofluid model but also allowed for the possibility of slip velocities where this phenomenon was considered to be caused by a combination of the Brownian motion of the nanoparticles and thermophoresis i.e. Ludwig-Soret thermo-diffusion where for example H_2O and Al_2O_3 molecules are allowed to exhibit two different particle molecular responses to the same localized temperature gradient. When a nanoparticle mass fraction term m was considered a mass diffusion equation of the form

$$\frac{\partial(\rho_n m)}{\partial t} + \nabla \cdot (\rho_n \mathbf{V} m) = -\nabla \cdot \mathbf{J}_p \tag{2.50}$$

$$\mathbf{J}_p = -\rho_n \left(D_B \nabla m + D_T \frac{\nabla T}{T} \right) \tag{2.51}$$

was then considered to be present in a nanofluid system. This equation was then a fourth governing equation that was coupled to the existing mass, momentum and energy conservation equations to model the flow characteristics of a nanofluid system. The mass diffusion equation inputs are D_B which is a Brownian diffusion coefficient, D_T which is an analogous thermophoretic diffusion coefficient, and these two diffusion coefficients are used to model the flux changes where $\mathbf{J}_p/[\text{kg m}^{-2}\text{ s}^{-1}]$ is the nanoparticle diffusion mass flux where ρ_n is the nanofluid density as previously discussed. Corcione *et al.*used this equation system of four coupled differential equations to study convective heat transfer effects in various nanofluid systems with a mixed-phase modelling approach. For this study newer correlations for the nanofluid thermal conductivity k_n to base fluid thermal conductivity were used in terms of nanoparticle Reynolds number Re_p, Prandtl number of the base fluid Pr_f and surprisingly the freezing point T_{fr} of the base liquid of the form

$$\frac{k_n}{k_f} = 1 + 4.4 Re_p^{0.4} Pr_f^{0.66} \left(\frac{T}{T_{fr}} \right)^{10} \left(\frac{k_s}{k_f} \right)^{0.03} \varphi^{0.66} \tag{2.52}$$

According to this study the nanoparticle Reynolds is calculated as

$$Re_p = \frac{2\rho_f k_b T}{\pi \mu_f^2 d_p} \tag{2.53}$$

where ρ_f is the base fluid density, $k_b = 1.638066 \times 10^{-23}$ J K^{-1} is the Boltzmann constant, μ_f is the base fluid viscosity, d_p is the nanoparticle diameter, and T is the bulk temperature. This formulation is based on the assumption that $Re_p = (\rho_f u_p d_p)/\mu_f$ where u_p is the nanoparticle Brownian velocity which is calculated as $u_p = d_p/t_D$ where t_D is a corresponding time period associated with the Brownian motion such that $t_D = (d_p^2)/(6D_B)$ where the Brownian diffusion coefficient is calculated using the Einstein-Stoke's equation such that $D_B = (k_b T)/(3\pi \mu_f d_p)$. A corresponding thermophoretic diffusion coefficient of the dispersed molecules takes the form

$D_T = 0.26 \frac{k_f}{k_f + k_s} \frac{\mu_f}{\rho_f} m$ where as previously stated m is the nanoparticle mass fraction. The ratio of nanofluid viscosity to base fluid viscosity in this study took the form

$$\frac{\mu_n}{\mu_f} = \frac{1}{1 - 34.87 \left(\frac{d_p}{d_f}\right)^{-0.3} \varphi^{1.03}} \tag{2.54}$$

where d_f is an equivalent diameter of the base fluid molecule. The calculation to estimate d_f took the form

$$d_f = 0.1 \left[\frac{6M}{N\pi\rho_{f0}}\right]^{\frac{1}{3}} \tag{2.55}$$

where M is the base fluid molar mass, ρ_{f0} is the base fluid mass density, V_m is the base fluid molecular volume all evaluated at a reference temperature of $T_0 = 293$ K, $N = 6.022 \times 10^{23}$ mol^{-1} is the Avogadro number, and the quantities are related to other according to the formula $M = \rho_{f0} V_m N$. At the same time studies such as that of Albadr *et al.*[57] furthered the state of knowledge of convective heat transfer coefficients for horizontal shell and tube heat exchangers for lower volume fractions in the range 0.01% to 0.3% for alumina/water mixtures using the standard mixing formulae for densities and specific heats, the Yu & Choi formula for thermal conductivity and the classical Einstein formula $\mu_{nf} = (1 + 2.5\phi)\mu_w$ for the viscosity which provided an earlier perspective that the viscosity of nano-fluids was not a well understand research area at the time. A more detailed comparison between the single-phase and multi-phase modelling approaches was performed by Moraveji *et al.*[49] who concluded that whilst mixed-phase models tend to give superior performance when compared to single-phase models that one of the issues with multi-phase models is their relatively high computational costs and their high central processor units (CPU) demands i.e. high CPU clock speeds which are necessary when solving the matrix equations using conventional finite volume solvers for industrial problems. This issue of high computational cost for two-phase models was still considered a serious impediment by Safaei *et al.*[58] of two-phase models when compared to single-phase models where two-phase models reported in the literature used both finite volume schemes with commercial codes as well as custom written finite difference schemes implemented in Fortran for higher computational performance. In the case of two-phase models the two predominant approaches are those of a Lagrangian-Eulerian and a Eulerian-Eulerian formulations. In the Lagrangian-Eulerian modelling approach the base fluid is considered as a normal continuum fluid however the Navier-Stokes equations have to be considered in a time averaged form whilst the dispersed phase which represents the nanoparticles moving through the continuum of the base fluid are considered by tracking their trajectories within the Lagrangian frame of reference by determining their motions and behaviours relative to the frame of reference. In this approach the conservation of mass, momentum and energy take the steady state form

$$\nabla \cdot (\rho \mathbf{u}) = 0 \tag{2.56}$$
$$\nabla \cdot (\rho \mathbf{u}\mathbf{u}) = -\nabla P + \nabla \cdot (\mu \nabla \mathbf{u}) + S_m \tag{2.57}$$
$$\nabla \cdot (\rho c_p \mathbf{u}T) = \nabla \cdot (k \nabla T) + S_e \tag{2.58}$$

where the symbols have their usual meaning where $\mathbf{u} = [u, v, w]^{\mathrm{T}}$ is now the velocity vector and

S_m and S_e are equivalent source terms for the momentum and energy equations in a conventional finite volume discretization scheme as discussed by Versteeg & Malalasekera [50]. The source terms S_m and S_e are considered necessary as they are used to model the exchange of momentum and energy between the liquid and solid phases in the nano-fluid. According to this scheme within the Lagrangian reference frame the nanoparticle motion and energy are then modelled according to the equations

$$m_p \frac{\mathrm{d}\mathbf{u}_p}{\mathrm{d}t} = \mathbf{F}_g + \mathbf{F}_D + \mathbf{F}_L + \mathbf{F}_{Br} + \mathbf{F}_b \tag{2.59}$$

$$m_p c_p \frac{\mathrm{d}T_p}{\mathrm{d}t} = Nu_p \pi d_p k_f (T_f - T_p) \tag{2.60}$$

where

$$Nu_p = 2 + 0.6 Re_p^{0.5} Pr^{0.333} \tag{2.61}$$

is an equivalent Nusselt number for the particle using, for example, a Ranz correlation between the particle Reynolds number and the Prandtl number, and the force terms account for gravity, drag, Saffman's lift i.e. inertia shear lift, Brownian and buoyancy force components respectively.

With regards to Eulerian-Eulerian models at present of writing there are three main schemes known as the mixture, Eulerian and Volume-of-Fluid (VOF) approaches. The basic idea for the VOF model is that a mass conservation equation for each phase of the form $\nabla \cdot (\varphi_z \rho_z \mathbf{u}_z) = 0, z = 1, ..., n$ is present where n is the number of phases, say $n = 2$ for a single base fluid and a single nanoparticle but in principle, n could be larger in for example the case of the hybrid nano-fluids previously discussed, and respective properties are computed through a weighted sum $N = \sum_{z=1}^{n} \varphi_z N_z$ where N_z is a particular property when the system of continuity equations are jointly solved with a single set of spatial momentum equations and a single energy equation. With regards to the mixture model the main features are that (i) all the phases are assumed to share a single pressure, (ii) the interactions between the different dispersed phases are assumed to be negligible, (iii) the nanoparticles are usually but not always assumed to be spherical shaped with a uniform size, and that (iv) the concentration of the secondary phase i.e. the nanoparticle distribution within the base fluid is solved by a scalar equation which incorporates the corrections caused the velocity slip between the solid and liquid phases, where one particular observation is that the viscosity of the mixture is usually but not always calculated as $\mu_m = \sum_{z=1}^{n} \varphi_z \mu_z$ in various mixing model formulations. Finally, in the Eulerian model, there is again the assumption that the pressure is assumed to be equal for all of the phases present and based on this assumption the mass, momentum energy equations are solved separately for the primary base fluid and secondary nanoparticle solid phases.

Different types of two-phase modelling schemes with various refinements and approximations are possible and have been reported in the literature however the main observation is that whilst two-phase models for nano-fluids do offer the potential of superior performance that this is almost inevitably at the cost of increased computational costs for many problems. Nevertheless even with the limitations imposed on single-phase models which when contrasted with two-phase models may exhibit under-estimation of Nusselt numbers Safaei *et al.* concluded that single-phase nanofluid models can still offer good results under certain modifications. They recommended that

the main shortcoming in single-phase models could be mitigated by specifically considering variable temperature thermophysical properties and through the inclusion of the chaotic movement of the nanoparticles within the base fluid. At the present time of writing the Eulerian-Lagrangian approach appears to be the most promising multi-phase mathematical modelling approach for nano-fluids in terms of modelling the nanofluid thermo-physical properties and behaviour according to Sidik *et al.* [60].

Recognizing the importance of the relative absence of nanofluid viscosity correlations in many studies Ghanbarpour *et al.* [61] conducted experimental studies for thermal conductivities as summarized in Figure 2.3 as well as for viscosities as summarized in Figure 2.4 where the mass weight fraction of $\omega = 0\%$ corresponds to the state of deionized water with no nanoparticles.

Referring to their results for mass fractions in the range 3% to 50% and temperatures in the range 293 K to 323 K where the conversion between mass fraction w and volume fraction ϕ is

$$\frac{1-w}{w} \cdot \frac{\rho_p}{\rho_f} = \frac{1-\phi}{\phi} \tag{2.62}$$

they concluded that the Prasher modified Maxwell model for the nanofluid thermal conductivity of the form

$$k_{nf} = (1 + A \cdot Re^m Pr^{0.333}\phi) \left[\frac{[k_p(1+2\alpha) + k_m] + 2\phi[k_p(1-\alpha) - k_m]}{[k_p(1+2\alpha) + 2k_m] - \phi[k_p(1-\alpha) - k_m]} \right] k_f \tag{2.63}$$

where A and m are experimental fitting parameters to determine based on the data gives relatively good results.
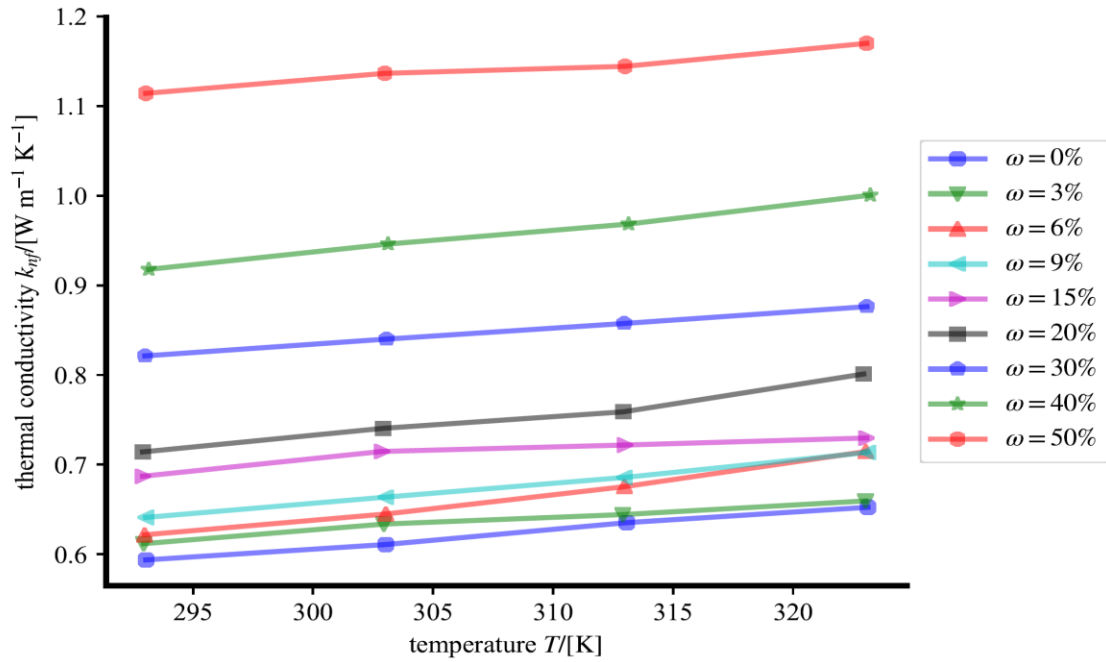
Figure 2-3 Temperature-dependent thermal conductivity results for alumina/water mixtures with a nanoparticle diameter of d=235nm and an expanded uncertainty of U(k_nf)=±2% from experimental data from Ghanbarpour et al.[61]
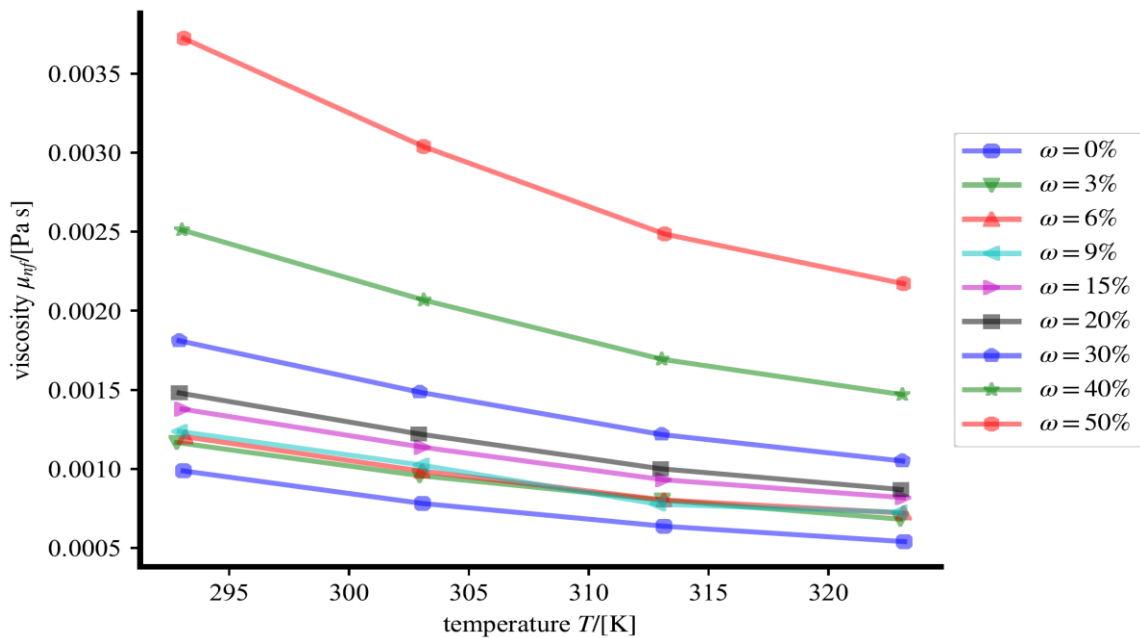
Figure 2-4 Temperature dependent viscosity results for alumina/water mixtures with a nanoparticle diameter of d=235nm from experimental data with an expanded uncertainty of U(μ_nf)=±4% from Ghanbarpour et al.[61]

In the Prasher model the terms α and k_m are calculated as

$$\alpha = \frac{2R_f k_m}{d_p} \tag{2.64}$$

$$k_m = k_f \left[1 + \frac{1}{4} Re \cdot Pr\right] \tag{2.65}$$

where the fluid radius R_f can be calculated from the fluid diameter d_f as previously discussed for particular characteristic Reynolds and Prandtl numbers for the particular problem. Due to the fact that whilst the Prasher model for thermal conductivity gives good results but is relatively complicated Ghanbarpour *et al.*developed a non-linear approximation as

$$\frac{k_{nf}}{k_f} = 1 + A_1\phi + A_2\phi^2 \tag{2.66}$$

where A_1 and A_2 are fitting parameters to be determined from the underlying experimental data. For the particular problem studied by Ghanbarpour *et al.*they calculated values for mass fractions from 3% to 50% and temperatures from 293 K to 333 K of $A = 30000$, $m = 2.5$, $A_1 = 3.5$ and $A_2 = 2.5$ respectively. With regards to nanofluid viscosity correlations, they considered the Einstein, Batchelor, Krieger & Dougherty and Corcione models of the form

$$\frac{\mu_{nf}}{\mu_f} = 1 + 2.5\phi \qquad \text{: Einstein} \tag{2.67}$$

$$\frac{\mu_{nf}}{\mu_f} = 1 + 2.5\phi + 6.5\phi^2 \qquad \text{: Batchelor} \tag{2.68}$$

$$\frac{\mu_{nf}}{\mu_f} = \left(1 - \frac{\phi}{\phi_{\max}}\right)^{-[\mu]\phi_{\max}} \qquad \text{: Krieger \& Dougherty} \tag{2.69}$$

$$\frac{\mu_{nf}}{\mu_f} = \left(1 - 34.87\left(\frac{d_p}{d_f}\right)^{-0.3}\phi^{1.03}\right)^{-1} \qquad \text{: Corcione} \tag{2.70}$$

where $[\mu]$ is the intrinsic viscosity which is just $[\mu] = 2.5$ for spherical nanoparticles. Referring to these results which as shown in Figure 2.5, Figure 2.6 and Figure 2.7 respectively it is seen that the Krieger & Dougherty viscosity formula gives relatively good results for a wide range of mass fractions at low temperatures, whilst at high temperatures the optimal viscosity model appears to be a combination of the Krieger & Dougherty and Corcione models.

When Ghanbarpour *et al.*further analysed their results they concluded that the Krieger & Dougherty viscosity model gives an accuracy of 10% on average for a combination of weight fraction ranges, but they were unable to determine an optimal viscosity correlation of the wide range of weight fraction measurements of their experimental data.

We comment that the conventional Krieger & Dougherty viscosity model is numerically ill-conditioned as $\phi \to \phi_{\max}$ since

$$\lim_{\phi \to \phi_{\max}}\left[1 - \frac{\phi}{\phi_{\max}}\right]^{-[\mu]\phi_{\max}} = \infty \tag{2.71}$$

Although it is possible to avoid this singularity in an *ad-hoc* manner by ignoring the value of μ_{nf}/μ_f at the volume fraction where $\phi = \phi_{max}$ by only considering the domain (ϕ_{min}, ϕ_{max}) i.e. by ignoring the nanofluid viscosity is the limit of low concentrations, which has been observed to be experimentally problematic when fitting thermal conductivity and viscosity models, and by disregarding the discontinuity at $\phi = \phi_{max}$ this approach will technically introduce an additional artificial statistical uncertainty component in the viscosity ratio calculation $u^2(\mu_{nf}/\mu_f)$ of the form

$$\frac{\partial}{\partial\phi_{max}}\left(\frac{\mu_{nf}}{\mu_f}\right) = \frac{\frac{-[\mu]\phi}{\left(1-\frac{\phi}{\phi_{max}}\right)\phi_{max}} - [\mu]\ln\left(1-\frac{\phi}{\phi_{max}}\right)}{\left(1-\frac{\phi}{\phi_{max}}\right)^{[\mu]\phi_{max}}} \tag{2.72}$$

$$u^2(\phi_{max}) = \left[\frac{\partial}{\partial\phi_{max}}\left(\frac{\mu_{nf}}{\mu_f}\right)\right]^2 u^2(\phi_{max}) \tag{2.73}$$

where in general

$$u^2(\phi) \approx \left(\frac{\partial\phi}{\partial w}\right)^2 u^2(w) + \left(\frac{\partial\phi}{\partial\rho_p}\right)^2 u^2(\rho_p) + \left(\frac{\partial\phi}{\partial\rho_f}\right)^2 u^2(\rho_f) \tag{2.74}$$

using the conventional experimental measurement uncertainty of the Guide to the Uncertainty of Measurement usually abbreviated as the GUM [53] for the correct statistical uncertainty analysis of measurement uncertainties by treating the various components in the viscosity model as random variables.
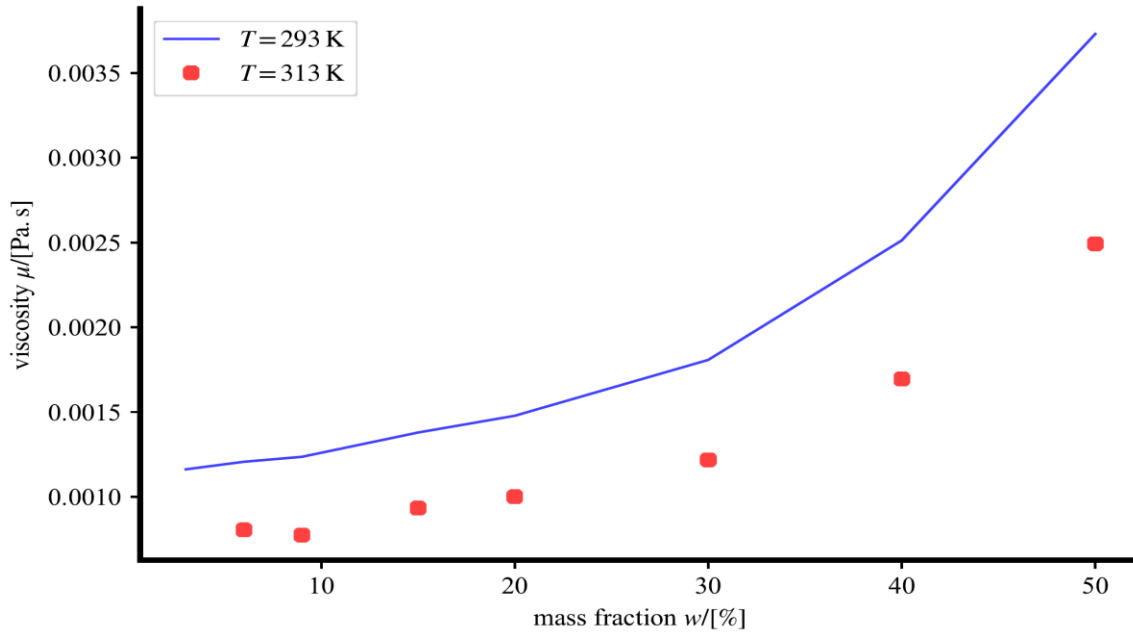
Figure 2-5 Analysis of Ghanbarpour et al.[61] data to validate the Krieger & Dougherty viscosity models by comparing the nanofluid viscosities at different temperatures
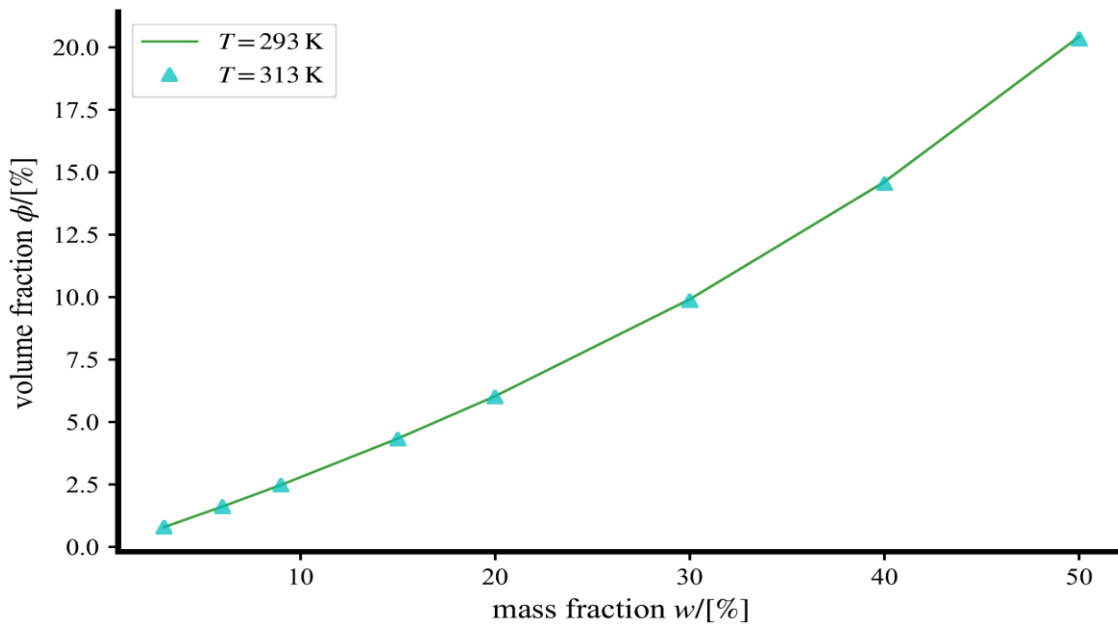
Figure 2-6 Analysis of Ghanbarpour et al.[61] data to validate the Krieger & Dougherty viscosity models by comparing the nanofluid mass fractions and volume fractions at different temperatures
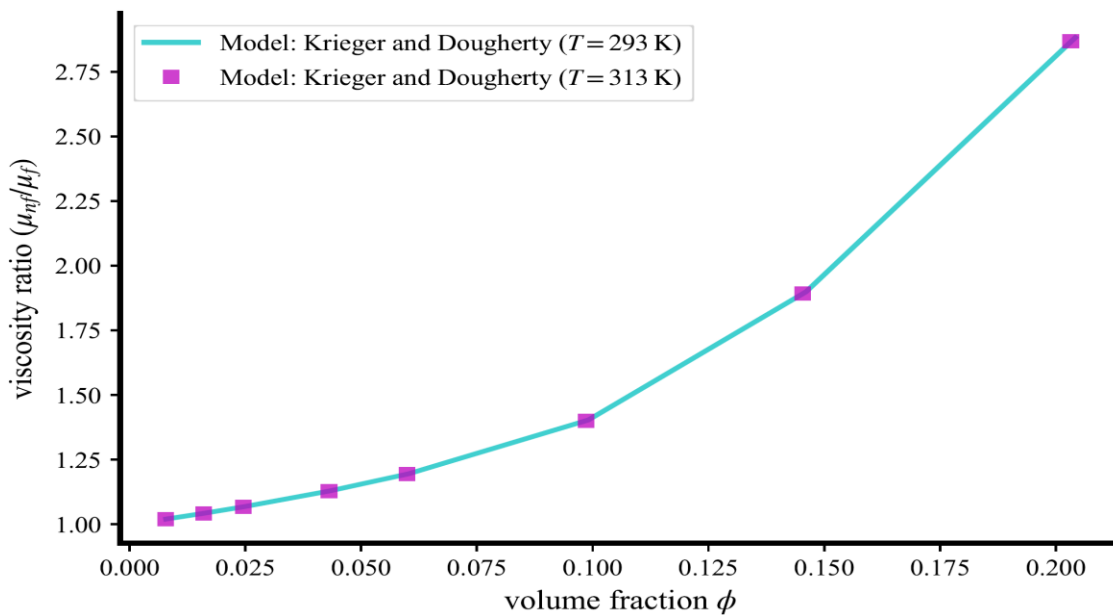
Figure 2-7 Analysis of Ghanbarpour et al.[61] data to validate the Krieger & Dougherty viscosity models by comparing the ratio of the nanofluid viscosity to the base fluid viscosity at different temperatures

The GUM first introduced to the international scientific community in the mid 1990's with later published editions and revisions in the early 2000's by uncertainty quantification researchers based at various national laboratories is an improvement on the earlier approach of Kline & McClintock

from the 1950's since the GUM incorporates statistical correlations and higher order statistical moments using a more modern approach in terms of Bayesian statistics and frequentist statistics and offers to ability to estimate probability density function distributions of experiment measurements at a more advanced and rigorous mathematical level. In the above calculation we comment that there would technically have an additional calculation to estimate the statistical uncertainty of the volume fraction ϕ_{max} by first calculating the corresponding uncertainty of the mass fraction w so that this incorporates the further uncertainties in the mass measurements that were used to produce the nanofluid. The above calculations would formally use an Ishikawa diagram, informally referred to as a "fish-bone diagram" by researchers in the field of uncertainty quantification (UQ), to track all the relevant terms when performing a rigorous experimental measurement uncertainty analysis and as result we comment that even with relatively simple algebraic models for the effective thermal conductivity and viscosity that the corresponding uncertainty analysis can quickly become very complicated.

Earlier viscosity models usually relied on data by Nguyen *et al.* [39] and one viscosity model equation fit was that by Abu-Nada [62] of the form where $T/[°C]$ and $\varphi/[\%]$

$$
\begin{aligned}
\mu_{Al_2O_3} = -0.155 &- \frac{19.582}{T} + 0.794\varphi + \frac{2094.47}{T^2} - 0.192\varphi^2 \\
&- 8.11\frac{\varphi}{T} - \frac{27463.863}{T^3} + 0.0127\varphi^3 + 1.6044\frac{\varphi^2}{T} + 2.1754\frac{\varphi}{T^2}
\end{aligned}
\tag{2.75}
$$

where the viscosity is in units of centi-poise.

A more systematic study of nanofluid viscosities was undertaken by Nwosu *et al.*[63] which established that whilst there are a wealth of various empirical studies and models for either nanofluid viscosities or relative viscosities that there is in fact very little formal rigorous theoretical justifications for the various models. Nwosu *et al.*in their investigation from then general literature determined that the main parameters in many nanofluid viscosity models are (i) volume fraction, (ii) temperature, (iii) packing fraction, (iv) nano-layer thickness, (v) particle shape and aspect ratio, (vi) aggregate radius, (vii) inter-particle spacing, and (viii) capping layer respectively. It is important to note that whilst these eight parameters are present to various extents in different viscosity model formulations that full experimental information on these various parameters are not necessarily available in all cases since for example Nwosu *et al.*utilized earlier reported data by Nguyen [39] to compare two possible viscosity models for a CuO based nano-fluid. This observation that not all nanofluid thermo-physical experimental studies consistently report on the same or even all of the relevant parameter information is a prevalent feature in both thermal conductivity as well as viscosity studies and in the particular case of nanofluid viscosity studies Nwosu *et al.*also remark that additional potentially relevant and useful experimental data such as (a) electromagnetic, (b) electro-viscous, (c) various dispersive energy-related phenomena, and (d) polarities amongst other parameters are also not available. We comment that this omission may be due to a combination of practical reasons such as the lack of specific or specialist laboratory instrumentation, disagreement between experimental and theoretical researchers of the need or relevance of particular information, or simple judgement calls.

Regardless of the particular reasons involved, the result is that nanofluid thermo-physical studies whether for thermal conductivities or viscosities has to incorporate an intrinsic lack of full and consistent experimental data and information. This type of problem but in the very different

context of nuclear fusion energy was studied by Baltz $et\ al.$[64] where there are over $N > 1000$ possible model parameters, no guarantee of convexity of the model $\mathbb{R}^N$ space, and the modelling challenge of a complex system with a high dimensionality is present. To address this problem where the intrinsic difficulty is that there is no single objective metric that fully captures both the underlying system quality and constraints Baltz $et\ al.$developed what they call the 'Optometrist Algorithm'. The basic idea of this algorithm is reliant of what is referred to as meta-parameters (MP's) where the MP's approximate the full dimensional $\mathbb{R}^N$ design space with a lower dimensional $\mathbb{R}^n$ design space where $n < N$ which captures the main intrinsic features of the model. To implement the algorithm which is a stochastic based algorithm the search for chosen representative MP's is first initialized, then a new state is chosen by moving in a random direction within the MP-space by simply adjusting the initial MP parameters by a relative amount where the original MP parameters are chosen in such a way that their values and dimensions are heterogeneous i.e. the $\mathbb{R}^n$ reduced space is mathematically consistent. After the initial perturbation the original higher dimensional $\mathbb{R}^N$ system parameters are recovered by undoing the the functional mapping that was used to generate the MP's. Measurements of the experimental outcome are then shown to a human operator who applies human judgement as to whether the perturbed state is 'about the same' or 'better' and the process repeated. In the algorithm implementation a judgement of 'about the same' is considered adequate to make the perturbed state as a new state so this search strategy avoids getting stuck in a higher dimensional local maxima, and as result algorithm is analogous to the Metropolis-Hastings acceptance algorithm for Monte Carlo optimization which allows for the acceptance of a search step that degrades the optimization function with some finite probability.

In the study by Nwosu $et\ al.$ they report that Hosseini et al.obtained useful results for the relative viscosity of nano-fluids in terms of (i) the base fluid viscosity, (ii) the hydrodynamic volume fraction, (iii) the nanoparticle diameter, (iv) the thickness of the capping layer, and (v) the temperature. In the absence of a complete and consistent theoretical model due to the lack of sufficient higher performance computing (HPC) power for either a full Boltzmann or full molecular dynamics (MD) simulation as discussed earlier we may reasonably assume that the above parameters are a reasonable approximation of the meta-parameters lower dimensional $\mathbb{R}^n$ design space for the viscosity model. The functional form of the Hosseini viscosity model as reported by Nwosu $et\ al.$takes the form

$$\frac{\eta_{nf}}{\eta_{bf}} = \exp\left[m + \alpha\left(\frac{T}{T_0}\right) + \beta(\phi_h) + \gamma\left(\frac{d}{1+r}\right)\right] \tag{2.76}$$

where ϕ_h is the hydrodynamic volume fraction, d is the nanoparticle diameter, r is the thickness of the capping layer, T_0 is a reference temperature, T the actual temperature of the mixture, and α, β, γ and m are empirical constants which must be determined from the experimental data. Of the various other viscosity models reported by Nwosu $et\ al.$the Kulkarni et al.model of the form

$$\ln\mu_{eff} = \exp(-(2.8751 + 53.54\phi - 107.12\phi^2)$$
$$+(1078.3 + 15.857\phi + 20.587)\frac{1}{T}) \tag{2.77}$$

is found to give relatively good results for predicting the temperature and volume fraction dependent viscosity for a wider temperature range. Although Nwosu $et\ al.$investigated various

choices of viscosity models using a genetic algorithm (GA) approach the fundamental challenge is regarding the identification of relevant functional forms for the viscosity which is necessary for both classical gradient-based as well as GA based optimizations. A similar type of issue also occurs if an artificial neural network (ANN) approach as discussed by Zhao *et al.*[65] is utilized since the neural network must be "trained" to optimize some choice of system response. In the work of Zhao et al. who used a radial basis function (RBF) based neural network for a mapping $\text{T}: X^n \rightarrow Y^q$ between two Euclidean spaces $X^n \subset \mathbb{R}^n$ and $Y^q \subset \mathbb{R}^q$ the system response was defined as a simple linear combination such that $y_k = \sum_{i=1}^{m} \omega_{ik} R_i(X)$ for $k = 1,2,\dots,q$. For this ANN viscosity study a four-input model of the nanoparticle volume concentration ϕ, nanoparticle diameter d, nanoparticle density ρ_{nf}, and base fluid viscosity μ_{bf} respectively, and a five-input model in terms of the same parameters plus the temperature were used. The response function $R_i(X)$ in this approach is not necessarily a linear function of the system input $X = [\phi, d, \rho_{nf}, \mu_{bf}]^{\text{T}}$ for the four-input model or $X = [\phi, d, \rho_{nf}, \mu_{bf}, T]^{\text{T}}$ for the five-input model and that the specific response function must be explicitly specified for a conventional forward training of the neural network. As a result, an ANN approach which also features in some thermal conductivity studies such as that by Ariana [66] which determines the optimal neural network node weights ω_{ik} has a qualitatively similar challenge as a GA approach since the functional forms must still be specified in order to perform the optimization. A slightly different approach to a GA and ANN optimization is the use of a Least Squares Support Vector Machine (LSSVM) approach as discussed by Meybodi [67] drawing from the field of artificial intelligence (AI) and using statistical learning concepts. The basic idea behind a LSSVM approach is that it is a special case of the more general Support Vector Machine (SVM) optimization problem that converts the original quadratic programming problem into an equivalent linear programming problem. In the special case where the dependent and independent variables of the LSSVM are linearly separable a linear regression problem results whilst in the general case a non-linear regression problem results of the form

$$y = \sum_{k=1}^{N} \beta_k (x_k)^{\text{T}} x + b \qquad \text{: Linear Regression} \tag{2.78}$$
$$y = \sum_{k=1}^{N} \beta_k K(x_k, x) + b \qquad \text{: Non-Linear Regression} \tag{2.79}$$

where $K(x_k, x)$ is the kernal-function. In order to perform the non-linear regression analysis the kernal function has to be explicitly specified before the optimization and similar to an ANN approach a radial basis function (RBF) approach is commonly applied since there are a lower number of 'tuning' i.e. fitting parameters where the RBF kernal function is of the form

$$K(x_k, x) = \exp\left(\frac{-\|x_k - x\|^2}{\sigma^2}\right), k = 1,2,\dots,N \tag{2.80}$$

where σ^2 is a squared bandwidth that must be first optimized beforehand with an external optimization technique before the LSSVM training can be undertaken. As a result it may be observed that the above-mentioned techniques whether they are designated as genetic algorithms (GA's), artificial neural networks (ANN's) or Least Squares Support Vector Machines (LSSVM's) are all in practical terms simply different optimization strategies and techniques for determining optimal model parameters for a particular choice of measurement model for either a nanofluid thermal conductivity or viscosity functional form.

The effect of the nanofluid pH values were considered in an earlier study by Timofeeva *et al.*[68] where it was originally concluded that the pH values in the nanofluid seems to depend on the structures and properties of the nanoparticles and not particularly on the solid/liquid interaction effects between the alumina nanoparticles and the water molecules. As a result based on this earlier observation by Timofeeva *et al.*a segment of many earlier researchers concluded that the pH of a nanofluid is really an effect from other factors and not a cause and hence various nanofluid models tended to disregard the pH value as a process parameter when constructing models for the effective thermal conductivity and effective viscosity. Later studies such as those by Meyer *et al.*[69] also undertook reviews of process parameters in both thermal conductivity as well as viscosity models and the issue as to whether the pH value was a cause & effect or a simple correlation of thermo-physical properties was still open to potentially differing interpretations based on the combination of available experimental data and the absence of a comprehensive fundamental physics-based *ab initio* study and theoretical model. Part of the motivation for the study of the influence of the various potential process parameters that may affect the effective viscosity μ_{eff} of a nanofluid as discussed by Meyer *et al.*is that a fluid's viscosity effects flow properties such as the Reynolds number, convective heat transfer coefficients and pressure drops for various flow configurations in pipes and channels. As a result if the viscosity is too high then this will have a detrimental effect of the pumping power required for various industrial systems that use the nanofluid as a working fluid as discussed in more detail by Mills [5]. The effect of the viscosity in for example a heat exchanger would typically be present by influencing pressure drops in such systems through the effect on the Reynolds number Re and consequently the fraction factor f. A practical example of how this may be studied is in terms of heat exchanger pressure drop equation as discussed by Mills of the form

$$\frac{\Delta P}{P_1} = \frac{G^2}{2\rho_1 P_1}\left[(1 - \sigma^2 + K_c) + \frac{f}{4}\frac{\rho_1}{\rho_m}\frac{A}{A_c} + 2\left(\frac{\rho_1}{\rho_2} - 1\right) - \frac{\rho_1}{\rho_2}(1 - \sigma^2 - K_e)\right] \qquad (2.81)$$

In the review article of Meyer *et al.* only two theoretical models for nanofluid viscosities were found in the reported literature as reported by Masoumi *et al.*[70] and Masoud Hosseini [71] respectively.

The earlier paper by Masoumi *et al.*[70] considered the effect of the Brownian motion of the nanoparticles within the base fluid and utilized a so-called 'apparent viscosity' μ_{app} so that the effective viscosity μ_{eff} was calculated as $\mu_{eff} = \mu_{bf} + \mu_{app}$ where μ_{bf} is the viscosity of the base fluid. In this approach a Brownian velocity $V_B = \frac{1}{d_p}\sqrt{\frac{18K_bT}{\pi\rho_p d_p}}$ was first calculated where K_b is the Boltzmann constant, d_p and ρ_p are the diameter and density respectively of the nanoparticle. Then a corresponding Reynolds was calculated using V_B such that $\text{Re}_B = \frac{1}{v_{bf}}\sqrt{\frac{18K_bT}{\pi\rho_p d_p}}$ and the authors made the assumption that there was a homogeneous distribution of nanoparticles within the base fluid such that in a cubical volume of the nanofluid mixture that the distance δ between the centres of the nanoparticles was $\delta = \left(\frac{\pi}{6\phi}\right)^{1/3}d_p$ where ϕ is the volume fraction. Once these assumptions were made the analysis then proceeded on the further assumption that the base fluid with the prevailing Brownian velocity flowed over the stationary nanoparticle which was assumed for simplicity as a spherical nanoparticle. The flow for the situation was then assumed as a creep flow i.e. a flow with a very small Reynolds number such that $Re \ll 1$ and an

expression for the viscosity derived by making the assumption that the nanoparticle kinetic energy was equal to the work done by the friction forces i.e. the surface total shear stresses acting on the assumed spherical nanoparticle surface. The final result by Masoumi *et al.* was

$$\frac{\mu_{app}}{\mu_{bf}} = \frac{\rho_p V_B d_p^2}{72 C \delta \mu_{bf}} \tag{2.82}$$

$$C = \frac{1}{\mu_{bf}} \left[(c_1 d_p + c_2) \phi + (c_3 d_p + c_4) \right] \tag{2.83}$$

In the above expression C is a correction factor and the constants were determined from earlier experimental results for Al_2O_3 nanoparticles of 13 nm and 28 nm sizes such that $c_1 = -0.000001133$, $c_2 = -0.000002771$, $c_3 = 0.00000009$ and $c_4 = -0.000000393$ respectively.

On the other hand, the later paper by Masoud Hosseini [71] proceeded on the assumption of dimensionless groups defined as $\pi_1 = \frac{\eta_{nf}}{\eta_{bf}}$, $\pi_2 = \phi_h$, $\pi_3 = \frac{d}{1+r}$ and $\pi_4 = \frac{T}{T_0}$ where η_{bf} is the nanofluid viscosity, η_{nb} is the base fluid viscosity, ϕ_h is the hydrodynamic volume fraction of the solid nanoparticles, d is the nanoparticle diameter, r is the thickness of the capping layer, T_0 is a reference temperature which was taken as $T_0 = 20$ °C for convenience, and T was the nanofluid mixture temperature. After this there was an assumption that $\frac{\eta_{nf}}{\eta_{bf}} = f_1 \left(\phi_h, \frac{d}{1+r}, \frac{T}{T_0} \right)$ where the function f_1 was then as an additional step assumed to take the form

$$\frac{\eta_{nf}}{\eta_{bf}} = \exp \left[m + \alpha \left(\frac{T}{T_0} \right) + \beta(\phi_h) + \gamma \left(\frac{d}{1+r} \right) \right] \tag{2.84}$$

where m was considered as a factor which was assumed to be representative of the nanofluid system and which encompassed information of the type of solid nanoparticles, the base fluid and their interactions, whilst α, β, γ were then simply considered as empirical constants which had to be determined from available experimental data. As a result both of the attempts by Masoumi *et al.*[70] and Masoud Hosseini [71] respectively to theoretically model the nanofluid viscosity are both based on a set of *ad-hoc* assumptions and simplifications and as a result cannot be strictly considered as meeting the requirements for a full and rigorous fundamental physics based *ab initio* mathematical representation of a real nanofluid physical system which at the present time can only be fully analysed from either an *ab initio* molecular dynamics or full Boltzmann simulation, and which are both considered to be numerically infeasible on existing high performance computing (HPC) and associated super-computing systems within South Africa.

Due to the absence of a comprehensive and reasonably complete theoretical framework to adequately model nanofluid properties Meyer *et al.*determined that the only remaining feasible option was to investigate empirical studies based on reported experimental data. One of the key observations by Meyer *et al.*in their review of the various empirical models reported in then literature was that there was a type of interaction effect between on the one hand how the nanoparticle size distribution affects the viscosity and on the other hand how agglomeration of the nanoparticles counter-acts this. From the available data, it was speculated that agglomeration effects alone was not sufficient to describe how the nanofluid viscosity would evolve for the

mixture and that the particle size distribution was sufficient for a nanofluid system composed of a mono-dispersed system of nanoparticles such that the relative viscosity η_r of the mixture could be approximated as

$$\eta_r = \left(\frac{\mu_1 \phi_1}{\mu_o}\right) \times \cdots \times \left(\frac{\mu_z \phi_z}{\mu_o}\right) = \prod_{i=1}^{z} \eta_r(\phi_i) \qquad (2.85)$$

where $\phi_i, i = 1,2,\ldots,z$ is the particle fraction for a particular class of nanoparticles in the overall nanofluid mixture. Of the various 'classical' or historical models for fluid/solid mixtures Meyer *et al.* observed that many of these earlier models were developed before the formal invention of nano-fluids which may be loosely considered as the period from around 1993 where Stephen Choi first proposed the modern concept of nano-fluids. As a result, additional factors over and above the classical parameters such as the nano-layer around the nanoparticles, the electrical double layer (EDL), zeta potentials, capping layers, inter-particle spacing and even nanoparticle magnetic properties in addition to the pH must also be considered. Amongst the most critical parameters affecting a nanofluid viscosity Meyer *et al.* reported temperature, volume fraction, shear rate $\dot{\gamma}/[\text{s}^{-1}]$ for the particular type of prevailing nanofluid flow, nanoparticle size, nanoparticle shape, and finally the pH and electrical conductivity of the suspension as potential contributing factors. From their review of the available literature, it was concluded that although the pH may have an insignificant affect for a specified volume concentration that the pH nevertheless has a major effect on the zeta potential which may be calculated from $Q = 4\pi\varepsilon_r\varepsilon_0 a\zeta$ where Q is the nanoparticle surface charge in coulombs, ε_r is the relative permittivity of the surrounding fluid, ε_0 is the free space vacuum permittivity and a is an estimate of the approximate radius of the nanoparticle particle, and that the pH modification of the nanofluid may reduce the nanofluid viscosity without detrimentally affecting the nanofluid stability. Nevertheless Meyer *et al.* caution that at the present time that there needs to be more research to determine the interaction between the zeta potential, the pH and the electrical conductivity and how these three inter-related parameters affect the nanofluid viscosity. Experimental results for the acidity/alkalinity levels of a nanofluid for different volume fractions ϕ and nanoparticle diameters d_p by Timofeeva *et al.*[68] are shown in Figure 2.8 from which it is seen that there appears to be a weak correlation of decreased pH values as the volume fraction decreases which is to be expected as water with no nanoparticles should have a neutral pH, however this behaviour exhibits a slight change for larger size nanoparticles.
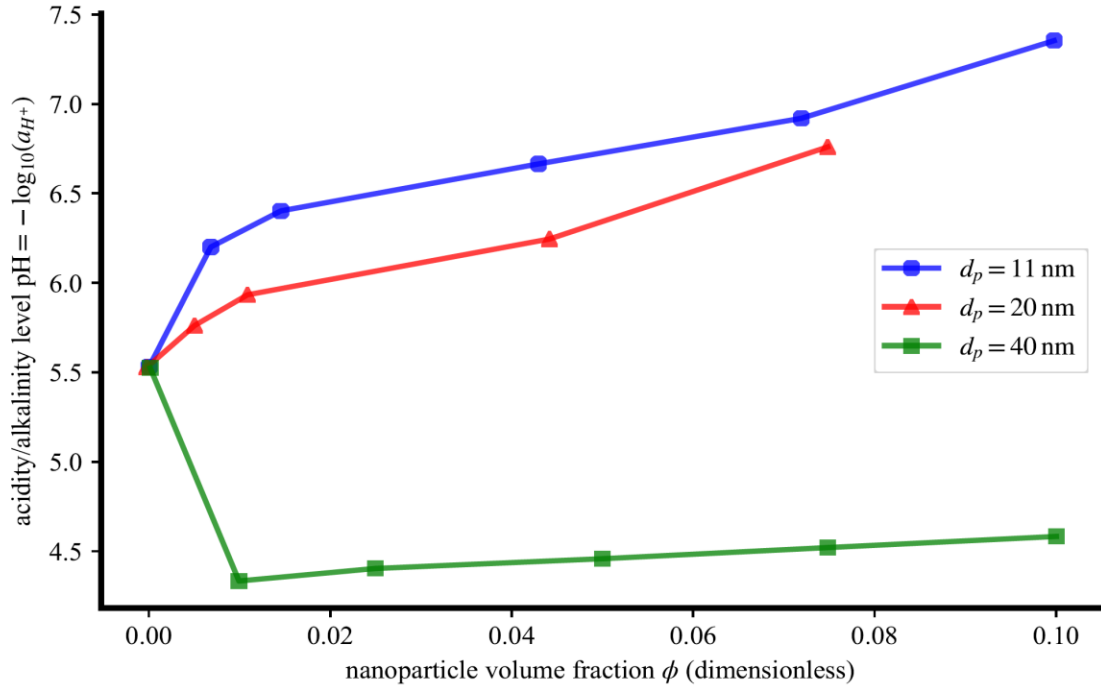
Figure 2-8 Illustration of nanofluid equilibrium pH concentration values for a water/alumina nanofluid based on experimental measurements by Timofeeva et al.[68]

Results for the zeta-potential ζ and shear rate $\dot{\gamma}$ based on experimental measurements by Zawrah *et al.*[72] are analysed from which it is observed that there is a definite trend of decreased ζ-potentials as the pH is increased and that the viscosity tends to increase with increasing volume fractions across a range of shear rates.

Earlier studies such as that by Konakanchi *et al.* [73] developed correlations for the pH of different types of nano-fluids including Al_2O_3/water mixtures based on experimental data of the form

$$\left(\frac{(pH)_{nf}}{(pH)_{bf}}\right) = \left[a_1\left(\frac{T}{T_0}\right)^2 + a_2\left(\frac{T}{T_0}\right) + a_3\right] \cdot [b_1\phi^2 + b_2\phi + b_3] \cdot \left[c_1\left(\frac{d}{d_0}\right)^2 + c_2\right] \tag{2.86}$$

$$(pH)_{bf} = 0.00015074T^2 - 0.11270782T + 26.73630875, 273 \leq T/[K] \leq 363 \tag{2.87}$$

where for a Al_2O_3/water nanofluid the regression coefficients are $a_1 = -0.1714584$, $a_2 = 0.376192$, $a_3 = -0.13514079$, $b_1 = -7.088066$, $b_2 = 1.463864$, $b_3 = 0.5181933$, $c_1 = 33.8946855$ and $c_2 = 12.0607088$ respectively for temperatures $273 \leq T/[K] \leq 363$, volume fractions $1 \leq \phi/[\%] \leq 5$ and nanoparticle diameters $10 \leq d/[nm] \leq 70$ with a maximum corresponding diameter of $d_0 = 100$ nm.

Due to the fact that the above correlation can give reasonably accurate results for the pH as a function of the temperature T, volume fraction ϕ and nanoparticle diameter d i.e. there exists some function such that $pH = f(T, \phi, d)$ it follows that the parameters T, ϕ, d are more fundamental than the pH i.e. the level of the nanofluid acidity/alkalinity is a physical consequence of the nanoparticle doping material and the bulk base fluid's properties. This observation is under-pinned by the fact that in various experimental pH studies of nano-fluids that the pH is usually modified either by the use of dispersants such as sodium dodecyle benzene sulfonate (SDBS) and/or the introduction of acid solutions such as hydrogen chloride (HCl) and sodium hydroxide (NaOH) in varying concentrations in order to produce differing pH levels. In practical terms this means that T, ϕ, d may suffice as meta-parameters when modelling the respective thermo-physical properties.

More recent experimental data on this specific aspect of Al_2O_3/water mixtures for an approximate nanoparticle diameter of $d = 50$ nm has subsequently been reported by Zawrah *et al.*[72] as summarized in Figure 2.9 and Figure 2.10 from which we comment that there is definitely a relation between the pH and the zeta potential ζ on the one hand, and between the viscosity μ and the shear rate $\dot{\gamma}$ on the other hand, however, the interaction between all three variables is nevertheless still an ongoing matter which requires further experimental data and investigation before it is possible to infer any physically meaningful correlations.

Due to this practical limitation on both an absence of an adequate and complete theoretical framework, and in addition due to the limited experimental data for the newer additional potential parameters it is advantageous from a mathematical modelling perspective to opt to construct nanofluid thermo-physical models for the thermal conductivity and viscosity in terms of the traditional reported parameters but with newer mathematical and statistical techniques. This approach is consistent with newer reported results in the literature such as that of Gupta [74] which models the thermal conductivity and viscosity in terms of parameters, and that by Murshed *et al.*[75] for viscosities from corresponding data from the literature as summarized in Figure 2.11.
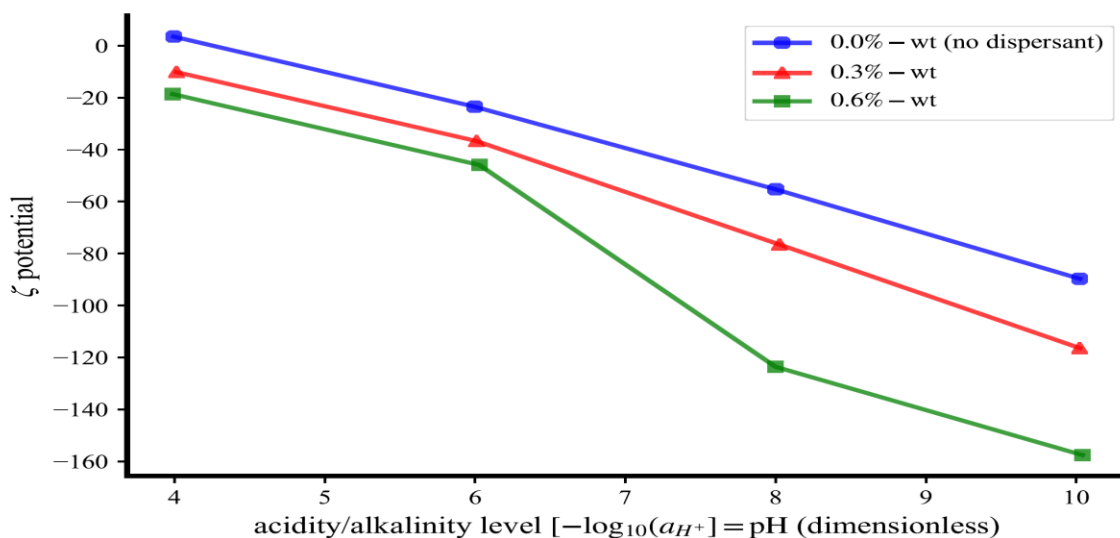
Figure 2-9 Illustration of nanofluid ζ potential and pH effects on viscosity based on experimental measurements by Zawrah et al.[72]

41
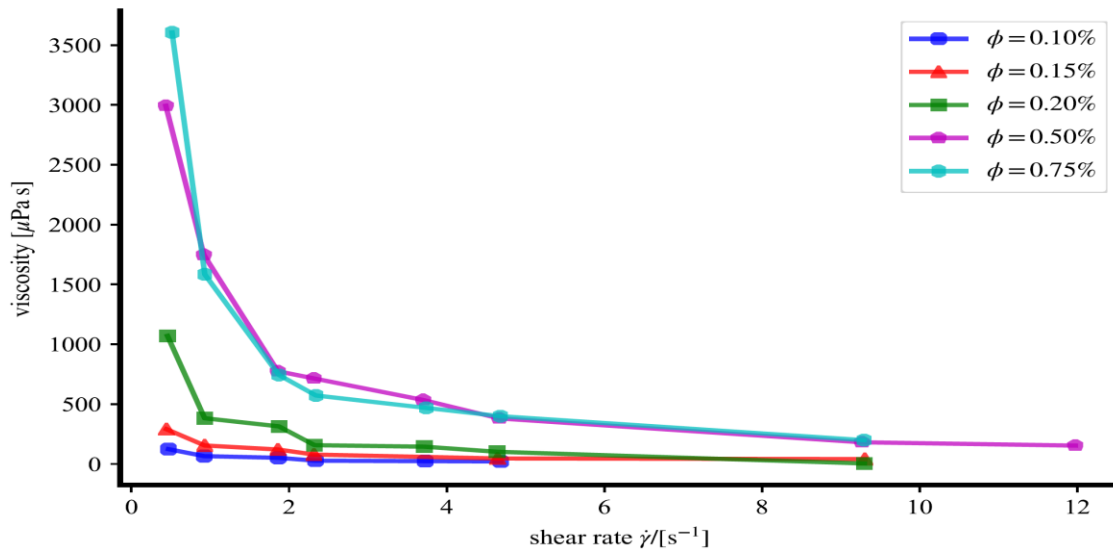
Figure 2-10 Illustration of nanofluid viscosity and shear rate effects on viscosity based on experimental measurements by Zawrah et al.[72]
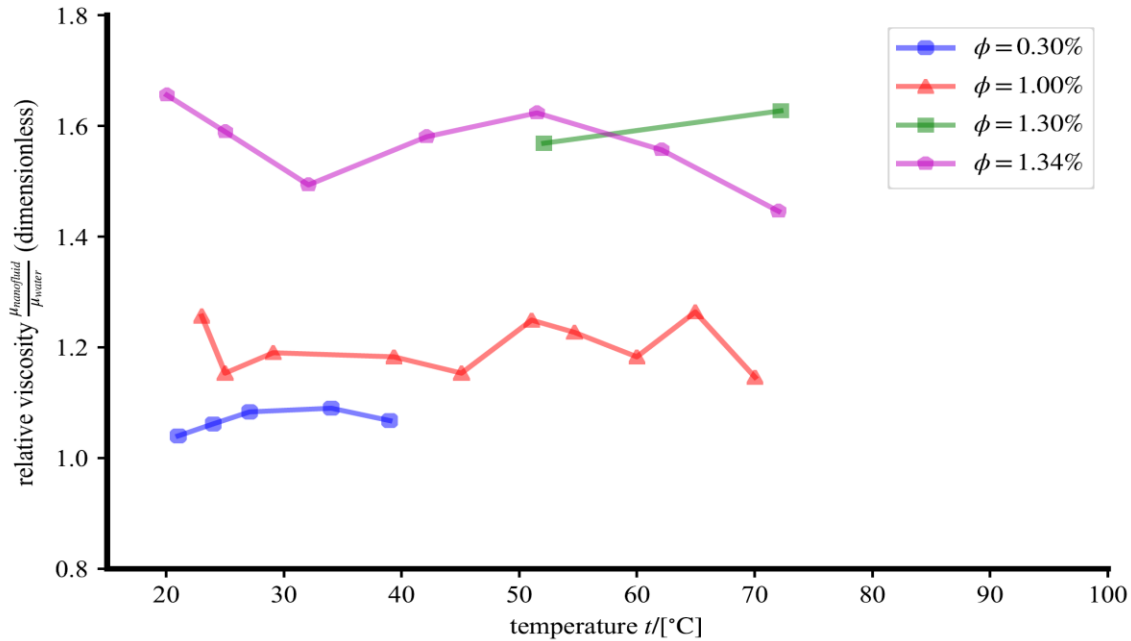
Figure 2-11 Illustration of nanofluid relative viscosity for a selection of temperatures and volume fractions based on experimental data by Murshed et al.[75]

2.3 Nanofluid Statistical Uncertainty Analysis Techniques

Earlier work conducted at the University of Pretoria by Mehrabi *et al.*[76] utilized thermal conductivity data reported by Masuda[1] *et al.*[77], Lee *et al.*[78], Das *et al.*[38], Putra *et al.*[79], Chon *et al.*[81], Li & Peterson [29], Li & Peterson [82], Kim *et al.*[83], Timofeeva *et al.*[68], Zhang *et al.*[84], Ju *et al.*[85], Murshed *et al.*[86], and Patel *et al.*[87] respectively. In this dissertation all of these data sources are utilized along with additional and newer reported data as documented in the literature review of this chapter as summarized in Table 2.5.

Considering information sources for nanofluid viscosity data utilization is made of earlier work by Meyer *et al.*[88] along with additional and newer data as documented in the literature review of this chapter as summarized in Table 2.6 noting that few studies report experimental data for both thermal conductivity and viscosity.

When extracting the statistical experimental data from above literature sources where tabulated values of experimental measurement points and their corresponding statistical uncertainties are not explicitly available we utilize the Java based graphical software package WebPlotDigitizer developed by Rohatgi [89] in order to obtain the nominal values of $[k_{eff}, t, d, \phi]^{\mathrm{T}}$, however this data must also include the statistical experimental uncertainties for each meta-parameter. The associated uncertainties for the meta-parameters are specified through the technical specifications provided by the Guide to the Expression of Measurement i.e. the GUM [53] where the expected

---

[1] The original paper is written in the Japanese language however the experimental data has been reported in the English language

value $\overline{q}$ for a quantity with n independent observations $q_k, k = 1,2, \dots, n$ is

$$\overline{q} = \frac{1}{n}\sum_{k=1}^{n} q_k \tag{2.88}$$

Since the individual observations q_k, be it for the base fluid temperature t, nanofluid volume fraction ϕ or nanoparticle diameter d_p, will have differing values due to random variations from both the physical mechanisms of experimental measurement as well as the intrinsic statistical uncertainties, the experimental variance of the individual observations is

$$s^2(q_k) = \frac{1}{n-1}\sum_{j=1}^{n} \left(q_j - \overline{q}\right)^2 \tag{2.89}$$

which is also known as the Experimental Standard Deviation of the Mean or ESDM. Following standard experimental measurement statistical practise the corresponding estimate of the variance is then

$$s^2(\overline{q}) = \frac{s^2(q_k)}{n} \tag{2.90}$$

The above formula are applicable in the event that there are indeed repeat measurements however in practice this will not always be the case and according to the GUM the corresponding variance may be estimated from a pool of information consisting of *inter alia*

• Previous measurement data from earlier experiments
• Prior laboratory experience or general knowledge of the behaviour and properties of the particular materials/instruments specific to the measurand
• Manufacturer specifications of either the instrument/equipment or specified reference materials
• Data from calibration certificates/reports
• Uncertainties assigned from reference data taken from handbooks

The above set of considerations are conventionally specified as so-called 'Type B' uncertainties to distinguish then from 'Type A' which are uncertainties obtained from statistical analyses. In order to perform a full uncertainty analysis of a measurement system it is necessary to 'convert' the Type B uncertainties into equivalent Type A uncertainties so that standard statistical analyses may be performed using for example Monte Carlo simulations which require estimates of standard uncertainties.

In the special case where no information of the standard uncertainty is available for a measurand X and only an estimate of the expected value x of X is available with an upper bound a_+ and lower bound a_- then the expected value and associated variance for X may be estimated as

$$\mu = \frac{a_- + a_+}{2} \tag{2.91}$$

$$u^2(x) = \frac{(a_+ - a_-)^2}{12} \tag{2.92}$$

under the assumption of a rectangular probability distribution which has been validated by Cox & Harris [90]. If a measurement x has a symmetric half-range such that $x_{\min} = \mu - R$ and $x_{\max} =$

$\mu + R$ then the equivalent standard uncertainty corresponding to a Gaussian probability density function distribution is just

$$u(x) = \frac{2R}{\sqrt{12}} \tag{2.93}$$

These results when the actual experimental repeat data points are available are applicable when $n \geq 4$ physical measurements are available however based on slightly subtle differences of approach using frequentist statistics and Bayesian statistics the above GUM based approximation becomes inaccurate if $n < 4$. A recent research paper by Cox & Shirono [91] addresses this issue through an analysis that incorporates the resolution between frequentist statistics i.e. statistics underpinned by Type A based observations and Type B based Bayesian statistics i.e. statistics underpinned by *a prior* probabilities of the physical system through the introduction of a correction factor ϕ.

The final summarized results for calculating the correct standard uncertainty $u(x)$ for a quantity X is then

$$x = \frac{1}{n}\sum_{i=1}^{n} x_i \tag{2.94}$$
$$S = \sum_{i=1}^{n} (x_i - x)^2 \tag{2.95}$$
$$s = \sqrt{\frac{S}{n-1}} \tag{2.96}$$

so that

$$u(x) = \phi \times \frac{s}{\sqrt{n}} \tag{2.97}$$

The correction factor is calculated as

$$\phi \equiv \phi_n(\alpha, \beta) \tag{2.98}$$
$$\phi = \left[\frac{n-1}{2}\frac{I\left(\frac{n-3}{2},\frac{1}{\alpha}\right)-I\left(\frac{n-3}{2},\frac{1}{\beta}\right)}{I\left(\frac{n-1}{2},\frac{1}{\alpha}\right)-I\left(\frac{n-1}{2},\frac{1}{\beta}\right)}\right]^{1/2} \tag{2.99}$$

The parameters in the above equation are

$$\alpha = \frac{2\sigma_{max}^2}{S} \tag{2.100}$$
$$\beta = \frac{2\sigma_{min}^2}{S} \tag{2.101}$$

and the integral which is the upper incomplete gamma function is defined as

$$I(v,z) = \int_z^{\infty} t^{(v-1)}e^{-t} \quad dt \tag{2.102}$$

Noting that the upper incomplete gamma function $\Gamma(s,x)$ and the lower incomplete gamma

function $\gamma(s, x)$ are defined as

$$\Gamma(s, x) = \int_x^\infty t^{(s-1)} e^{-t} \quad dt \tag{2.103}$$

$$\gamma(s, x) = \int_0^x t^{(s-1)} e^{-t} \quad dt \tag{2.104}$$

it follows that the integral $I(v, z)$ may then be calculated using a scaled upper incomplete gamma function. As per the observation by Cox & Shirono a simplification to the above formulae is to set $\sigma_{\min} = 0$ so that

$$\phi \approx \left[\frac{n-1}{2} \times \frac{I\left(\frac{n-3}{2}, \alpha\right)}{I\left(\frac{n-1}{2}, \alpha\right)} \right]^{1/2} \tag{2.105}$$

When implementing the above formulae in a practical experimental system with $n < 4$ physical measurements of say the effective thermal conductivity k_{eff} the analysis utilizes $\sigma_{\min}$ which is an estimate of the minimum square root of the variance based on good experimental judgement and $\sigma_{\max}$ is an estimate of the maximum square root of the variance. In the event that the actual experimental data points are not available from the summarized results in the open literature we will then utilize the simpler rectangular probability distribution assumption to calculate the equivalent standard uncertainty corresponding to a Gaussian probability distribution for the subsequent Monte Carlo analysis which is consistent with existing experimental statistics best practice guidelines as per the recommendations of the GUM. This can be simplified for a measurement x with an estimate for the maximum value $x_{\max}$ and the minimum value $x_{\min}$ as $\mu = \frac{x_{\min} + x_{\max}}{2}$, $a = \frac{x_{\max} - x_{\min}}{2}$ and $u(x) = \frac{a}{\sqrt{3}}$.

Frequently the term 'accuracy' is used in the literature for example ... *the accuracy of the water thermal conductivity was* $\pm 1\%$ *with repeatability of* 0.2%, however this unfortunately tends to introduce an element of subjectivity as to what the statistical standard uncertainty is. Technically an accuracy is a qualitative term indicating how close an estimate of a measurement is to the true value which is unknown by definition.

In scientific metrology, practise at many national laboratories the conventional practise is to specify the standard uncertainty of the measurement and the associated probability density function of the measurement as this gives a complete quantitative summary of the experimental measurement without any level of ambiguity such that as per the GUM [53] the combined standard uncertainty $u_c(y)$ of a measurand $y = f(x_1, x_2, \ldots, x_N)$ where x_i are variables is of the form

$$u_c^2(y) = \sum_{i=1}^{N} c_i^2 u^2(x_i) + 2 \sum_{i=1}^{N-1} \sum_{j=i+1}^{N} c_i c_j u(x_i) x(x_j) r(x_i, x_j)$$

$$+ \sum_{i=1}^{N} \sum_{j=1}^{N} \left\{ \left[\frac{1}{2} \left(\frac{\partial^2 f}{\partial x_i \partial x_j} \right)^2 + \frac{\partial f}{\partial x_i} \frac{\partial^3 f}{\partial x_i \partial x_j^2} \right] u^2(x_i) u^2(x_j) \right\} \tag{2.106}$$

where

$$r(x_i, x_j) = \frac{u(x_i, x_j)}{u(x_i)u(x_j)} \tag{2.107}$$

is a scaled covariance term and

$$c_i = \frac{\partial f}{\partial x_i} \tag{2.108}$$

are sensitivity coefficients of the underlying measurand model $y = f(x_1, ..., x_N)$. As per the discussion by Ramnath [92] the expanded uncertainty is calculated in terms of the standard uncertainty as

$$U = k_p u_c \tag{2.109}$$

where the coverage factor k_p for a specified probability level p, say $p = 0.95$ for a 95% confidence level, is calculated from the integral equation

$$\int_{-t_p}^{t_p} f(u; \nu_{eff}) \quad du = p \tag{2.110}$$

and the underlying probability density function under the assumption of the Central Limit Theorem (CLT) from the field of experimental statistics is assumed to follow a Student's t-distribution

$$f(t; \nu) = \frac{\Gamma\left(\frac{\nu+1}{2}\right)}{\sqrt{\pi\nu}\Gamma\left(\frac{\nu}{2}\right)} \left(1 + \frac{t^2}{\nu}\right)^{-\left(\frac{\nu+1}{2}\right)} \tag{2.111}$$

with a specified degrees-of-freedom ν where $\Gamma(t)$ is the Gamma function. The CLT assumption is known to be accurate in most practical experimental systems as the actual probability density function formally determined in terms of the Markov convolution integral tends to converge to a univariate/multivariate Gaussian probability density function which can be in for example a univariate case generalized using a Student's t-distribution if the corresponding degrees of freedom ν is known usually with the aid of the well known Welch-Satterthwaite formula

$$\nu_{eff} = \frac{u_c^4(y)}{\sum_{i=1}^{N} \frac{u)i^4(y)}{\nu_i}} \tag{2.112}$$

where ν_i are the associated degrees of freedom for x_i typically estimated as $\nu = n - 1$ for single quantities with n measurements or $\nu = n - m$ for least-squares fits with n measurements and m parameters, or as $\nu \approx \frac{1}{2}\left(\frac{\Delta u}{u}\right)^{-2}$ using the relative uncertainty $\frac{\Delta u}{u}$ in other cases where detailed statistical information is unknown. Generalizations to the effective degrees of freedom are possible as discussed by Willink [93] in the case of correlations between the variables x_i and x_j for $i \neq j$ to refine the calculation of the coverage factor k_p and to mathematically specify the shape of the measurand probability density function however this level of mathematical statistical detail necessary for a full rigorous measurement uncertainty analysis is usually either not performed or alternately not reported in many of the open literature sources that are in the public

domain.

Based on these limitations in order to estimate the standard uncertainty we will usually assume based on prior experimental laboratory experience unless otherwise specified that the quoted accuracy is simply an estimate of the expanded uncertainty, and that where both estimates of an accuracy and a repeatability are specified that these are respective components of the actual measurement uncertainty. In practical terms this means that if an accuracy A is specified either from a calculation or an estimate e.g. $A = 0.01$ corresponding to a $\pm 1\%$ accuracy we will assume a confidence level of 95.45% corresponding to a coverage factor of $k_p \approx 2$ so that the standard uncertainty is

$$u(x) = \frac{A \times x}{2} \tag{2.113}$$

In cases where both an accuracy estimate, say A, and an estimate of the repeatability, say R, are both specified we will then in accordance with standard uncertainty analysis techniques simply use the root-sum-squared technique to work out the corresponding standard uncertainty as

$$u_c^2 = \left(\frac{A \times x}{2}\right)^2 + R^2 \tag{2.114}$$

since the above terms implicitly already utilize a sensitivity coefficient in their quantification i.e. we assume that $u^2(x) = \sum c_i^2 \left(\frac{\partial f}{\partial x_i}\right)^2$ already includes the sensitivity coefficient weighted contributions of the various experimental uncertainties and since the repeatability contribution by conventional is usually simple added in a quadrature. In many practical cases where the functional equation for a measurand is unknown, such as in nanofluid studies due to the absence of a comprehensive physical theory and where only discrete data known, that under these circumstances from an experimental data analysis perspective it is occasionally possible for many experimentalist from prior experience to add in quadrature worst case estimates of the sensitivity weighted uncertainty contributions when developing an "uncertainty budget". The uncertainty calculated through summations of contributing terms in quadrature i.e. a root-sum-square type of calculation must be implemented in physical SI units for consistency i.e. if estimates of uncertainty contributions are in percentages then they must first be converted to equivalent quantities such as W m^{-1} K^{-1} for thermal conductivities and then added in quadrature as it is not mathematically justified to add percentages since this would result in statistical inconsistencies for the physical properties.

To illustrate how the worst-case estimates are occasionally used in a root-sum-squares calculation of an uncertainty budget in some laboratories consider the experimental measurement of the density of a quantity of water of volume $V = 99.8$ mL with a mass of $m = 103$ g. Using the actual physical definition of density we have

$$\rho = \frac{m}{V} = \frac{103 \times 10^{-3} \text{ kg}}{99.8 \times 10^{-6} \text{ m}^3} = 1032.1 \text{ kg m}^{-3}$$

Formal application of the GUM then yields the exact mathematical result, assuming an absence of correlation between the measured mass and volume, the formula

$$u^2(\rho) = \left(\frac{\partial \rho}{\partial m}\right)^2 u^2(m) + \left(\frac{\partial \rho}{\partial V}\right)^2 u^2(V) = \left(\frac{1}{V}\right)^2 u^2(m) + \left(\frac{-m}{V^2}\right)^2 u^2(V)$$

Supposing for illustrative purposes only that the laboratory has a mass balance with an accuracy of an equivalent standard uncertainty of $u(m) = \pm 0.5 \times 10^{-3}$ kg and that the volume measurement has an accuracy with an equivalent standard uncertainty of $u(V) = \pm 0.2 \times 10^{-6}$ m^3 it then follows that the formal uncertainty of the density is

$$u^2(\rho) = \left(\frac{1}{99.8 \times 10^{-6}}\right)^2 (0.5 \times 10^{-3})^2 + \left(\frac{-(103 \times 10^{-3})}{(99.8 \times 10^{-6})^2}\right)^2 (0.2 \times 10^{-6})^2$$
$$= \underset{=m\ \text{sens.}}{(1.002 \times 10^4)^2} \underset{=m\ \text{unc.}}{(0.5 \times 10^{-3})^2} + \underset{=V\ \text{sens.}}{(-1.0341 \times 10^7)^2} \underset{=V\ \text{unc.}}{(0.2 \times 10^{-6})^2}$$
$$= \underset{=\text{TOTAL}\ m\ \text{unc.}}{(5.01)^2} + \underset{=\text{TOTAL}\ V\ \text{unc.}}{(-2.0683)^2}$$
$$= 29.378$$

so that

$$u(\rho) = \sqrt{29.378} = 5.4201 \text{ kg m}^{-3}$$

In certain situations, it may be too complicated to work out the exact sensitivity coefficient or there may be insufficient information and the experimentalist may therefore based on prior experience make a judgement call that for example *"...the uncertainty contribution on the density due to the effect of volume uncertainty is less than* $[u(\rho)]|_{u(V)} = 3$ *kg m^{-3}"* and use this as a worst case estimate to calculate an upper bound for the uncertainty by adding in a root-sum-square sense so that

$$u^2(\rho) \leq \frac{1}{V^2} u^2(m) + \left([u(\rho)]|_{u(V)}\right)^2$$

This type of approximation where estimates of the product $\frac{\partial f}{\partial x_i} \times u(x_i)$ of the sensitivity coefficient $\frac{\partial f}{\partial x_i}$ and the uncertainty $u(x_i)$ is estimated based on an experimental judgement as Type B uncertainties rather than mathematically calculated using formal statistical theories as Type A uncertainties is permissible according to the GUM if underpinned by experimental good judgement based on physical reasoning. Under these circumstances the equivalent Type A uncertainty is then estimated using rectangular probability density function distributions in accordance with the maximal statistical entropy principle in order to infer conservative estimates of the equivalent Gaussian or Student t-distribution standard uncertainties in accordance with the GUM uncertainty analysis technique for physical measurement uncertainties.

For cases where the effects of both the accuracy as well as the repeatability are already included into a percentage estimate, say $q = 0.013$ for a final accuracy of 1.3% of an effective thermal conductivity k_{eff}, we will first calculate the corresponding range as

$$\Delta = q \times k_{eff} \tag{2.115}$$

Then using the above information we will simply assume a rectangular probability distribution as a conservative estimate so that the equivalent standard uncertainty is

$$u(k_{eff}) = \frac{\Delta}{\sqrt{3}} \tag{2.116}$$

under the assumption of maximum statistical entropy as discussed by Cox & Siebert [34]. In the context of statistical uncertainty analysis calculations for experimental measurements the maximal statistical entropy principle reduces to the simplification that in the absence of detailed knowledge of the underlying probability density function (PDF) for a measurement that the knowledge of the PDF is that of a rectangular PDF which maximizes the statistical entropy for the measurement system as per international best measurement uncertainty practice of the GUM for Type B uncertainty estimates where detailed mathematical statistical information is either not reported or available. As a result in order to infer the intrinsic aleatoric thermophysical data uncertainties requires a careful reading and examination of the combination of the reported information in the open literature.

2.4 Nanofluid Mathematical Modelling Techniques

In various fields of engineering many experiments are done using an improvement on the trial and error approach when there is no specific underlying mathematical model using what is nowadays referred to as the one-factor-at-a-time (OFAT) approach as discussed by Lye [95] in order to determine the behaviour and characteristics of a particular physical system. The OFAT approach which is sometimes considered as a more systematic standard and accepted scientific experimentation approach be it in terms of physical laboratory testing, mathematical theoretical predictions, or computational based numerical or symbolic based experimentation, investigates a particular engineering system by varying one factor at a time over an appropriate process parameter range such as for example a temperature range whilst holding the other process parameters such as for example an operating pressure at constant values in order to systematically gather experimental physical, theoretical or computational data for the particular system.

As an example of how the OFAT experimental approach would work in practice consider for example an experiment that varies the pressure p and temperature T of a gas in order to construct a model for the gas density ρ. The true fluid equation of state for a gas is constructed using the partition function from the fundamental definitions of statistical mechanics where it may be shown as discussed by Reif [10] that the average hydrostatic pressure $\bar{p}$ for a real gas takes the form $\frac{\bar{p}}{kT} = n + B_2(T)n^2 + B_3(T)n^3 + \cdots$ where $n = N/V$ is the number of molecules per unit volume and $B_2, B_3, \dots$ are the virial coefficients. For this experiment an approximate model for gas density is the ideal gas equation $p = \rho R_g T$ where $R_g = \mathcal{R}/M$ is the gas species constant defined as the ratio of the universal gas constant to that of the molecular mass M of the particular gas species. When the OFAT experimental approach is applied it will result in two sets of experimental data points as shown in Figure 2.12 and Figure 2.13 where in one set of experimental measurements one parameter such as the temperature is held constant while another such as the pressure is varied, whilst in the other set of experimental measurements the pressure is held constant whilst the temperature is varied.
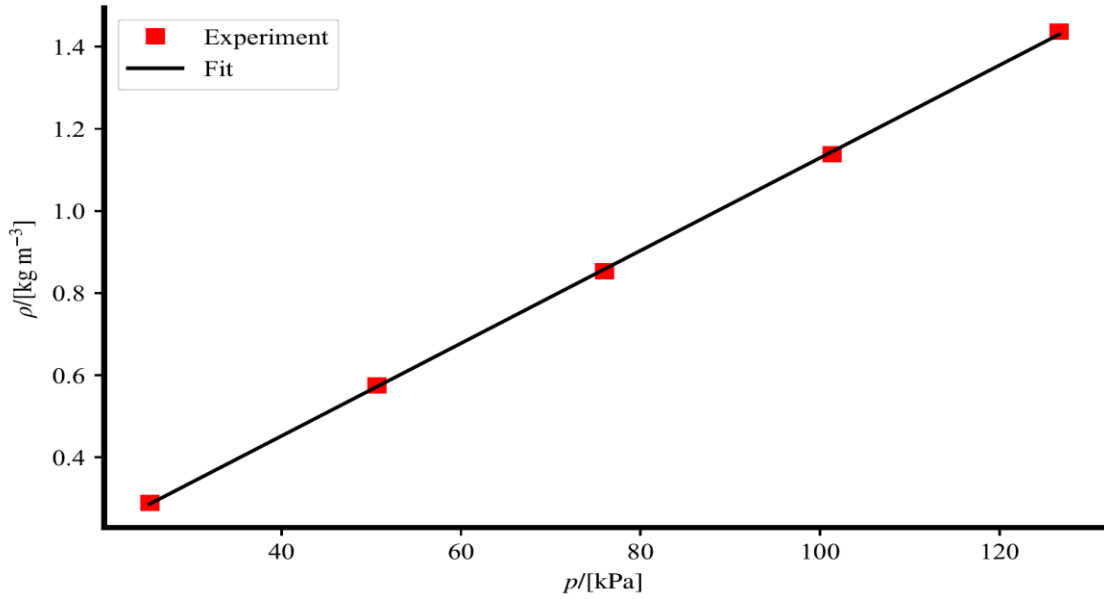
Figure 2-12 Illustration of one-factor-at-a-time (OFAT) experimental methodology to model gas density ρ=f(p,T) where experiment 1 is with a constant temperature T=298.15 K whilst the pressure is allowed to naturally vary
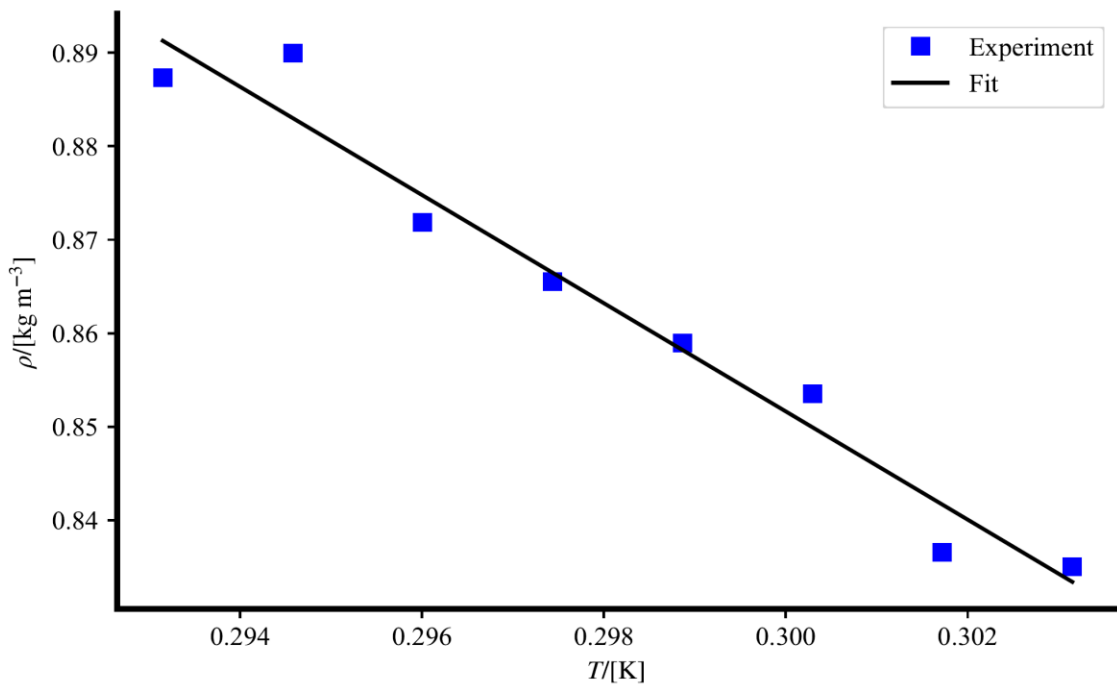
Figure 2-13 Illustration of one-factor-at-a-time (OFAT) experimental methodology to model gas density ρ=f(p,T) where experiment 2 is with a constant pressure at p=75.994 kPa whilst the temperature is allowed to naturally vary

As a result in the OFAT approach there will in general be N sets of experimental data for each of the process parameters if the measurand i.e. the quantity y to be measured in standard measurement science terminology is modelled in terms of the N parameters as a function $y = f(x_1, \dots, x_N)$ where $x_i, i = 1, \dots, N$ represent the various process parameters for the particular system. The challenge in this approach is to then use each of the underlying data sets to construct an approximation of the system's mathematical model using standard statistical analysis techniques. According to Lye the major disadvantage of the OFAT strategy is that it fails to consider the interaction effects between the various process parameters.

A consequence of this shortcoming is that different combinations of process parameters particularly when there are more than two process parameters such that $N \geq 2$ could in fact produce the same results but that these interaction effects would not be able to be discerned and incorporated when constructing the approximation to the mathematical model. These shortcomings in OFAT experiments were initially overcome using two-factor 2^k based statistical factorial experiments by users such as the US army [96] working in the field that is now commonly referred to as the design of experiments (DOE) as discussed by Telford [97]. Although in general there can be k factors and p levels as discussed by Spliid [175] in factorial designs in most practical applications statistical analysis is usually only considered for 2^k and 3^k factorial designs as discussed by Montgomery [99]. One particular approach when implementing k^p factorial designs is known as the Randomized Complete Block Design (RCBD) approach where if there are k process parameters say $x_1, \dots, x_k$ and each particular process parameter $x_i, i = 1, \dots, k$ has $L_1, \dots, L_k$ levels then if n is the number of repeat experiments for each factor/level if may be shown using combinatorial arguments that the total number N of experiments to complete the RCBD is $N = (L_1 \times L_2 \times \cdots \times L_k) \times n$. In the previous gas density illustrative example let $x_1 = p$ be the pressure and let $x_2 = T$ be the temperature and suppose x_1 has $L_1 = 3$ associated temperature measurements whilst x_2 has $L_2 = 4$ has associated pressure measurements. For convenience let the pressures be p_A, p_B, p_C and the temperatures be $T_\alpha, T_\beta, T_\gamma, T_\delta$ then the full set of factorial experiments may be summarized in Figure 2.14 which illustrates the RCBD for this design of experiment with a factorial design with $k = 3$ factors for pressures x_k and $p = 4$ levels for temperatures with $n = 1$ repeat experiments.
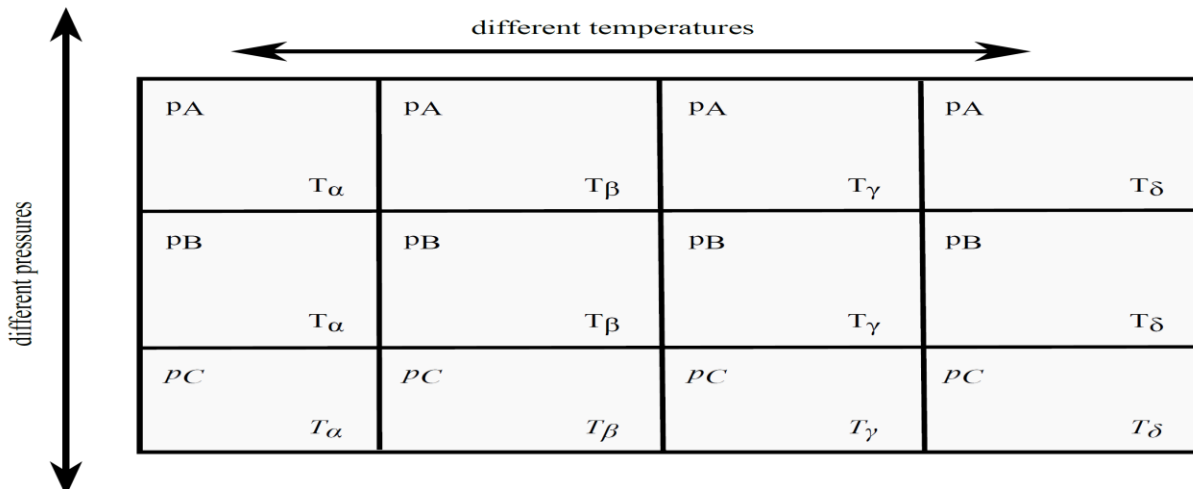
Figure 2-14 Illustration of a k^p factorial design experiment for a gas density example showing associated randomized complete block design configuration

Referring to this figure it may be observed that when implementing factorial designs that the information associated with each factor and level must both be known in order to perform the analysis. This requirement is not however generally able to be satisfied in nanofluid thermo-physical experiments since if for example the nanofluid thermal conductivity k_{eff} is modelled in terms of the process parameters of nanoparticle diameter d, volume fraction ϕ and base fluid temperature T such that $k_{eff} = f(d, \phi, T)$ then in many experimental studies not all of the parameters are independently reported.

A practical example is that some experimental studies only consider the effect of particle diameter d and volume concentration ϕ but disregard or do not accurately report data for the influence of the base fluid temperature T. This is limitation of reported data is present in varying extents in many experimental studies as not all experimentalist report on or agree on the same process parameters that are considered necessary of relevant in nanofluid thermal conductivity and viscosity model correlations. As a result due to the absence or lack of consistency in known process parameter information it is generally inadvisable to utilize a factorial based design of experiments approach unless a particular experiment has specifically included full complete reported measurement data for all the factors and levels.

Fortunately, an alternative to the factorial approach in the design of experiments where there is incomplete or inconsistent information is available in the form of the Response Surface Methodology (RSM) as discussed by Bezerra *et al.*[100]. As per the discussion by Bezerra *et al.* one of the disadvantages of factorial designs particularly for 3^k designs is that a very large number of experimental measurements is necessary if k is large. As an example if $k = 4$ corresponding to for example process parameters of $x_1 = d$ nanoparticle diameter, $x_2 = \phi$ volume fraction, $x_3 = T$ temperature and $x_4 = $ pH which is the level of hydrogen ion concentration in the nanofluid then the number of independent experimental data points is $N = 3^4 = 81$. This issue of the necessity of a relatively large number of experimental data points is not an issue in many RSM studies as the corresponding hyper-dimensional surface in $\mathbb{R}^k$ is usually of quadratic order i.e. it incorporates linear combinations of second order powers of the process parameters $x_1, \dots, x_k$ for the measurand model $y = f(x_1, \dots, x_k)$.

In the case of three process parameters x_1, x_2, x_3 the quadratic RSM surface takes then form

$$
\begin{aligned}
\hat{y}_{quadratic} = \beta_0 &+ \beta_1 x_1 + \beta_2 x_2 + \beta_3 x_3 \\
&+ \beta_{12} x_1 x_2 + \beta_{13} x_1 x_3 + \beta_{23} x_2 x_3 \\
&+ \beta_{11} x_1^2 + \beta_{22} x_2^2 + \beta_{33} x_3^2
\end{aligned}
\tag{2.117}
$$

as discussed by the NIST [101] whilst the corresponding cubic RSM model takes the form

$$
\begin{aligned}
\hat{y}_{cubic} = \hat{y}_{quadratic} \\
&+ \beta_{123} x_1 x_2 x_3 + \beta_{112} x_1^2 x_2 + \beta_{113} x_1^2 x_3 \\
&+ \beta_{122} x_1 x_2^2 + \beta_{133} x_1 x_3^2 + \beta_{223} x_2^2 x_3 \\
&+ \beta_{233} x_2 x_3^2 + \beta_{111} x_1^3 + \beta_{222} x_2^3 + \beta_{333} x_3^2
\end{aligned}
\tag{2.118}
$$

where β_0 is a nominal value, $\beta_i, i \in [1,2,3]$ are linear coefficients, $\beta_{ij}, i, j \in [1,2,3]$ are mixed

interaction effects, and $\beta_{ijk}, i, j, k \in [1,2,3]$ are the corresponding quadratic coefficients.

An advanced review of RSM is discussed further by Khuri & Mukhopadhyay [75] who extend and relate the original RSM to 2^k factorial designs and elaborate on an alternative to a 2^k factorial design known as the Plackett-Burman design which uses $n = (k + 1)$ experiments and offers considerable cost savings for large values of k when compared to classical 2^k and 3^k factorial designs. In this work Khuri & Mukhopadhyay also introduce methods to incorporate random effects in the RSM using generalized linear models (GLM's). Software implementations for RSM fits of data are discussed in Lenth [103] however it should be noted that that the conventional statistical RSM models are usually limited to second order models due to the high dimensional spaces that are considered. As an example a quadratic response surface in for example a 15 dimensional space is fitted for a model $y = f(\mathbf{x})$ where $\mathbf{x} = [x_1, \dots, x_{15}]^{\mathrm{T}} \in \mathbb{R}^{15}$, and as a result the conventional statistical regression linear and quadratic models are not suitable for our purposes as we have a relatively low number of process parameters, say for example the nanoparticle diameter, volume fraction, temperature, pH, and shape amongst other factors, and desire a higher order correlation for a low number of parameters.

Due to these issues the use of artificial neural network (ANN) and artificial intelligence techniques as discussed by Safikhani $et\ al.$[104] has become increasingly popular in the modelling of nanofluid properties. One particularly popular ANN approach is known as the Grouped Method of Data Handling (GMDH) where for M data points consisting of n inputs and a single output, which corresponds to our particular nanofluid modelling problem, involves the optimal determination of parameters for a Ivakhnenko polynomial of the form

$$y = a_0 + \sum_{i=1}^{n} a_i x_i + \sum_{i=1}^{n} \sum_{j=1}^{n} a_{ij} x_i x_j + \sum_{i=1}^{n} \sum_{j=1}^{n} \sum_{k=1}^{n} a_{ijk} x_i x_j x_k + \cdots \qquad (2.119)$$

in an analogous manner as earlier discussed where the general idea is to determine the optimal values of the parameters for an appropriate cost function. For GMDH type neural networks a common choice of Ivakhnenko polynomial is a low second order polynomial such that the GMDH-ANN reduces to solving

$$\hat{y} = a_0 + a_1 x_i + a_2 x_j + a_3 x_i x_j + a_4 x_i^2 + a_5 x_j^2 \qquad (2.120)$$
$$a_0, a_1, a_2, a_3, a_4, a_5 \leftarrow \min \sum_{i=1}^{M} [\hat{y} - y_i]^2 \qquad (2.121)$$

where the input parameters would in our particular problem correspond to $x_1 = T_{nf}$, $x_2 = d_p$ and $x_3 = \phi$ respectively, whilst the single output would correspond to either $y = k_{nf}$ or alternately $y = \mu_{nf}$. A more general extension of the GMDH-ANN scheme is known as a Multi-Layer-Perceptron (MLP) neural network as outlined by Ariana $et\ al.$[66] where the neuron output n_j is

$$n_j = f\left(\sum_{r=1}^{N} w_{jr} x_r + b_j\right) \qquad (2.122)$$

where now there may be multiple possible model outputs $n_1, n_2, \dots$ such as for example $n_1 = k_{nf}, n_2 = \mu_{nf}, n_3 = h_{nf}, \dots$ and f is referred to as an activation or transfer function, x_r is the input value of the neuron, w_{jr} are relevant weighting factors, b_j are respective bias coefficients, and where in general different types of activation/transfer functions and hidden neuron layers are possible. Following the earlier research work by Ariana $et\ al.$[66] a Levenberg-Marquardt

optimization technique is recommended for the training algorithm, and it has been further confirmed that a single hidden layer in the MLP network is generally sufficient to approximate any multivariable function as precisely as desired. For a single hidden layer different possible numbers of neurons are possible and this is generally determined through the minimization of appropriate statistical measures. Two common statistical indicators are the Absolute Average Relative Deviation (AARD%) and the Mean Square Error (MSE) defined as

$$AARD\% = \frac{100}{N} \sum_{i=1}^{N} \left(\left| \frac{k_i^{exp} - k_i^{cal}}{k_i^{exp}} \right| \right) \tag{2.123}$$

$$MSE = \frac{1}{N} \sum_{i=1}^{N} \left(k_i^{exp} - k_i^{cal} \right)^2 \tag{2.124}$$

with analogous expressions for the nanofluid effective viscosity μ_{nf} and which may be used to estimate the neural network with the highest accuracy corresponding to the smallest MSE or AARD% values. A regression coefficient (R^2) value for the associated data may also be estimated and different possible approaches to estimating the correlation coefficient R^2 are technically possible. One particular choice reported by Ariana *et al.*[66] is

$$R^2 = \frac{\sum_{i=1}^{N} \left(k_i^{exp} - \overline{\Delta k} \right)^2 - \sum_{i=1}^{N} \left(k_i^{exp} - \Delta k_i^{cal} \right)^2}{\sum_{i=1}^{N} \left(k_i^{exp} - \overline{\Delta k} \right)^2} \tag{2.125}$$

where N is the number of experimental data points, k_i^{exp} is the actual experimental data point value, k_i^{cal} the corresponding model predicted value, and $\overline{\Delta k}$ the average value of the particular experimental data points. Additional refinements to a MLP-ANN scheme are possible using a Radial Basis Function (RBF) approach as discussed by Zhao *et al.*[65] in an analogous manner to the MLP-ANN approach, where statistical indicators include Root Mean Squared Error (RMSE), Mean Absolute Percentage Error (MAPE), Sum of Squared Error (SSE) and again a linear correlation R^2 value defined as

$$RMSE = \left(\frac{1}{t} \sum_{j=1}^{t} |P_j - Q_j| \right)^{1/2} \tag{2.126}$$

$$MAPE = \frac{100\%}{t} \sum_{j=1}^{t} \left| \frac{P_j - Q_j}{P_j} \right| \tag{2.127}$$

$$SSE = \sum_{j=1}^{t} \left(P_j - Q_j \right)^2 \tag{2.128}$$

$$R^2 = 1 - \frac{\sum_{j=1}^{t} (P_j - Q_j)^2}{\sum_{j=1}^{t} (P_j)^2} \tag{2.129}$$

where now P_i is the actual data value, Q_i the corresponding model predicted value and t the total number of data-points where we note that the equation for the correlation coefficient R^2 now takes a slightly different algebraic form.

One issue that affects neural network modelling is that of over-fitting as discussed by Ahmadloo & Azizi [105] where the limitation is that the model can only produce good predictions for the specified data points and is unable to make adequate predictions for other input data values. The conventional approach to avoid neural network over-fitting is the early stopping technique where

the underlying data points in a set S_{data} are divided into three random sub-sets of $S_{training}$, $S_{validation}$ and $S_{testing}$ respectively. First $S_{training}$ is used to obtain the respective weighting and bias values for the neural network, and then $S_{validate}$ is used to ensure accuracy and generality of the model predictions. Training of the neural network is stopped when the error of the validation set increases, and then S_{test} is used to make an assessment of the final performance and quality of the fitted neural network model. Although the use of neural network models offers relatively good quality of predictions for nanofluid thermal conductivities the utility of this approach is still challenging for the prediction of nanofluid viscosities as recently reported by Hemmati-Sarapardeh *et al.*[106] who utilizing particle swarm optimization (PSO) and genetic algorithm (GA) approaches report that average absolute relative errors are typically $\pm 10\%$ at low volume fractions however may be as large as $\pm 40\%$ for volume fractions larger than 5%. As a result, careful attention should considered in the choice of activation or transfer function which is inclusive of linear $f(x) = x$, sigmoid $f(x) = 1/[1 + e^{-x}]$, sinusid $f(x) = \sin(x)$, tansig $f(x) = [2/(1 + e^{-2x})] - 1$, arctan $f(x) = \arctan(x)$ and binary step $f(x) = x$ for $x < 0, -x$ for $x > 0$ activation functions for both hidden as well as output layers as illustrated in Figure 2.15.

The neuron values are generally normalized to unity i.e. the neuron value x is scaled such that $0 \le x \le 1$ for convenience to avoid numerical ill-conditioning issues when constructing the particular neural network. From the literature review conducted the conventional practise by many researchers is to utilize a single hidden layer and opt for sigmoid transfer functions for the input/hidden layer and linear functions for the hidden/output layer when constructing the neural network by utilizing approximately 80% of the data for training, 10% for validation and 10% for testing, although occasionally two hidden layers have been reported in some studies.
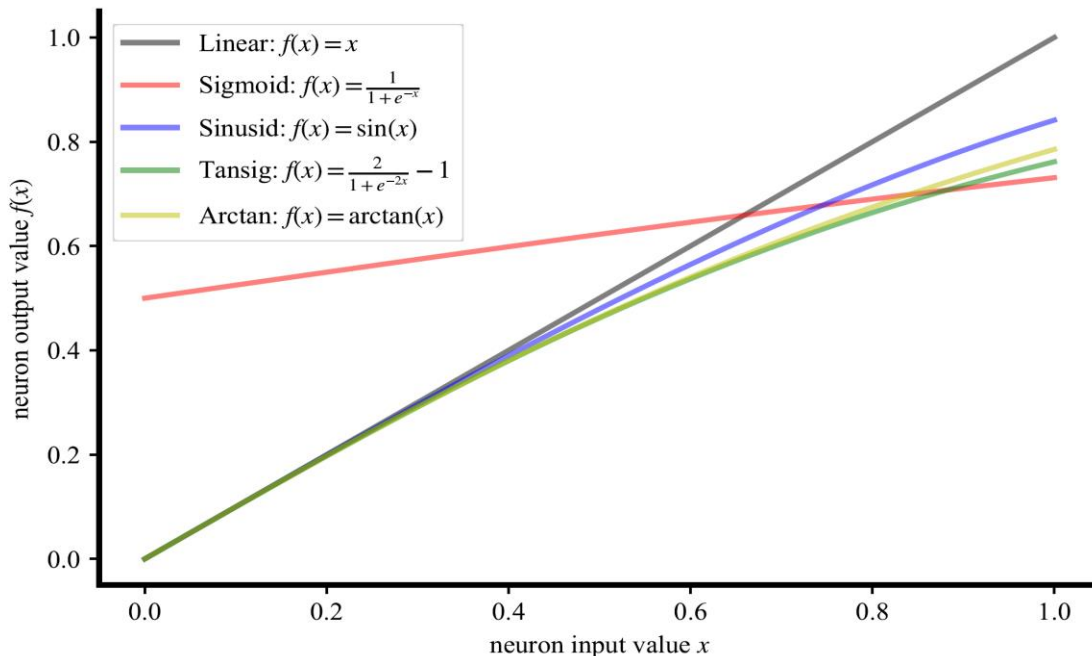
Figure 2-15 Illustration of typical neural network transfer/activation function behaviours

56

2.5 Nanofluid CFD Simulation Techniques

Once the statistical modelling process has been completed to model the effective thermal conductivity and effective viscosity in terms of the available representative meta-parameters by building and constructing the database as previously explained it is then necessary to utilize the thermodynamic data properties in for example computational fluid dynamics (CFD) simulations where the two main aspects of this application are defining appropriate governing equations for the mass, momentum and energy conservation equations of a nanofluid and in defining the auxiliary thermodynamic relations of the nanofluid in terms of the joint PDF.

Let $\mathbf{a} = (a_1, a_2, a_3)$ be a vector in $\mathbb{R}^3$ and $\mathbf{T}$ be a tensor representation in $\mathbb{R}^3$ then using standard vector/tensor analysis the gradient of a vector is defined as $\nabla \mathbf{a} = \frac{\partial \mathbf{a}}{\partial x_j} \otimes \mathbf{e}_j = \frac{\partial a_i}{\partial x_j} \mathbf{e}_i \otimes \mathbf{e}_j$. By applying these definitions it may then be shown that the outer product is $\mathbf{u} \otimes \mathbf{v} = \mathbf{u}\mathbf{v}^{\mathrm{T}}$, the gradient of a vector is $\nabla \mathbf{a}$ and the divergence of a tensor is $\nabla \cdot \mathbf{T} = \frac{\partial T_{ij}}{\partial x_j} \mathbf{e}_i$ where $e_i, i \in [1,2,3]$ are basis vectors. The following simplified working definitions then follow such that

$$\mathbf{u} \otimes \mathbf{v} = \begin{bmatrix} u_1 v_1 & u_1 v_2 & u_1 v_3 \\ u_2 v_1 & u_2 v_2 & u_2 v_3 \\ u_3 v_1 & u_3 v_2 & u_3 v_3 \end{bmatrix} \tag{2.130}$$

$$\nabla \mathbf{a} = \begin{bmatrix} \frac{\partial a_1}{\partial x_1} & \frac{\partial a_1}{\partial x_2} & \frac{\partial a_1}{\partial x_3} \\ \frac{\partial a_2}{\partial x_1} & \frac{\partial a_2}{\partial x_2} & \frac{\partial a_2}{\partial x_3} \\ \frac{\partial a_3}{\partial x_1} & \frac{\partial a_3}{\partial x_2} & \frac{\partial a_3}{\partial x_3} \end{bmatrix} \tag{2.131}$$

$$\nabla \cdot \mathbf{T} = \begin{bmatrix} \frac{\partial}{\partial x_1}(T_{11}) + \frac{\partial}{\partial x_2}(T_{12}) + \frac{\partial}{\partial x_3}(T_{13}) \\ \frac{\partial}{\partial x_1}(T_{21}) + \frac{\partial}{\partial x_2}(T_{22}) + \frac{\partial}{\partial x_3}(T_{23}) \\ \frac{\partial}{\partial x_1}(T_{31}) + \frac{\partial}{\partial x_2}(T_{32}) + \frac{\partial}{\partial x_3}(T_{33}) \end{bmatrix} \tag{2.132}$$

Substituting these formulae into the single-phase model for nano-fluids by Moraveji [49] then yields the following system of four simultaneous partial differential equations for two dimensional problems such that in steady state they take the form

$$\frac{\partial}{\partial x}[\rho u] + \frac{\partial}{\partial y}[\rho v] = 0 \tag{2.133}$$

$$\rho u \frac{\partial u}{\partial x} + \rho v \frac{\partial u}{\partial y} = -\frac{\partial p}{\partial x} + \frac{\partial}{\partial x}\left[\frac{4}{3}\mu\frac{\partial u}{\partial x} - \frac{2}{3}\mu\frac{\partial v}{\partial y}\right] + \frac{\partial}{\partial y}\left[\mu\frac{\partial u}{\partial y} + \mu\frac{\partial v}{\partial x}\right] \tag{2.134}$$

$$\rho u \frac{\partial v}{\partial x} + \rho v \frac{\partial v}{\partial y} = -\frac{\partial p}{\partial y} + \frac{\partial}{\partial x}\left[\mu\frac{\partial v}{\partial x} + \mu\frac{\partial u}{\partial y}\right] + \frac{\partial}{\partial y}\left[\frac{4}{3}\mu\frac{\partial v}{\partial y} - \frac{2}{3}\mu\frac{\partial u}{\partial x}\right] \tag{2.135}$$

$$\frac{\partial}{\partial x}[\rho c u T] + \frac{\partial}{\partial y}[\rho c v T] = \frac{\partial}{\partial x}\left(k\frac{\partial T}{\partial x}\right) + \frac{\partial}{\partial y}\left(k\frac{\partial T}{\partial y}\right) \tag{2.136}$$

In the above system of PDE's which are simply the well known Navier-Stokes equations for fluid mechanics problems and which may be conveniently solved with any convenient CFD solver such as Ansys Fluent if k_{eff} and μ_{eff} are specified an equation of state is necessary to calculate the nanofluid density ρ_{nf} and nanofluid enthalpy h_{nf} for mathematical completeness. Whilst the Pak & Cho formula may be conveninetly used to estimate the nanofluid enthalpy with the aid of a corresponding nanofluid specific heat capacity $c_{p,eff}$ as previously discussed a mixed model for the nanofluid density developed by Teng & Hung [33] of the form $\rho_{nf} = (1 - \phi)\rho_{bf} + \phi\rho_p$ usually yields good results with accuracies from -1.50% to $+0.06\%$ for temperatures from $10°C$ to $40°C$ for alumina/water mixtures. As a result in order to complete the equation of state for the nanofluid density we must provide equations for the water density and alumina nanoparticles density. For water the standard practise in many research laboratories is to use the Committee for Weights and Measures (CIPM) formula for Vienna Standard Mean Ocean Water (VSMOW) which is considered as a representative average chemical/isotopic composition for water throughout the world in which pure water is needed for very high accuracy chemical and physical experiments.

A more comprehensive but far more complex formula by the International Association for the Properties of Water and Steam (IAPWS) based on a Helmholtz free energy function $F = F(T,V)$ which is a thermodynamic function in terms of the absolute temperature T and volume V is available. Different approaches to deduce the density ρ from $F(T,V)$ such as taking the partial derivative with respect to volume at a constant temperature such that $\left(\frac{\partial F}{\partial V}\right)_T = -p$, or alternately by constructing the Gibbs free energy in terms of the Helmholtz energy so that $G = F + pV$ and taking the partial derivative of the Gibbs free energy in terms of the pressure at a constant temperature so that $\left(\frac{\partial G}{\partial p}\right)_T = V$ are theoretically possible in order to relate the density as a function of pressure p and temperature T. Whilst these approaches have their own respective merits mainly in the field of chemical physics in our particular case a simple algebraic application of the CIPM formula for water density as summarized by MetGen [107] is sufficient.

The CIPM water density formula for the density $\rho/[\text{kg m}^{-3}]$ in terms of the pressure $p/[\text{Pa}]$ and temperature $t/[°C]$ takes the form

$$\rho(t) = a_5\left[1 - \frac{(t+a_1)^2(t+a_2)}{a_3(t+a_4)}\right]; \quad p = 101325 \ \text{Pa} \tag{2.137}$$

where the values of the constants are

$$a_1 = -3.983035 \ °C \tag{2.138}$$
$$a_2 = 301.797 \ °C \tag{2.139}$$
$$a_3 = 522528.9°C^2 \tag{2.140}$$
$$a_4 = 69.34881 \ °C \tag{2.141}$$
$$a_5 = 999.974950 \ \text{kg m}^{-3} \tag{2.142}$$

The corresponding expanded uncertainty of the above formula for a coverage factor of $k = 2$ which is roughly equivalent to a confidence interval of 95.45% is

$$U_\rho = b_1 + b_2 t + b_3 t^2 + b_4 t^3 + b_5 t^4 \tag{2.143}$$

where the values of the constants are

$$b_1 = 8.394 \times 10^{-4} \ \text{kg m}^{-3} \tag{2.144}$$
$$b_2 = -1.28 \times 10^{-6} \ \text{kg m}^{-3} \tag{2.145}$$
$$b_3 = 1.10 \times 10^{-7} \ \text{kg m}^{-3} \tag{2.146}$$
$$b_4 = -6.09 \times 10^{-9} \ \text{kg m}^{-3} \tag{2.147}$$
$$b_5 = 1.16 \times 10^{-10} \ \text{kg m}^{-3} \tag{2.148}$$

Pressure effects on the water density are accounted for through the use of a simple multiplicative factor K_p such that the corrected density at a pressure different from a standard atmospheric pressure is

$$\rho_{corrected} = \rho(t) \times K_p \tag{2.149}$$

where the multiplicative correction factor is calculated as

$$K_p = 1 + (c_1 + c_2 t + c_3 t^2)(p - 101325) \tag{2.150}$$

The values of the constants in the above formula are
$$c_1 = 5.074 \times 10^{-10} \ \text{Pa}^{-1} \tag{2.151}$$
$$c_2 = -3.26 \times 10^{-12} \ \text{Pa}^{-1}{}^\circ\text{C}^{-1} \tag{2.152}$$
$$c_3 = 4.16 \times 10^{-15} \ \text{Pa}^{-1}{}^\circ\text{C}^{-2} \tag{2.153}$$

Values for the thermal conductivity $\lambda/[\text{W m}^{-1} \ \text{K}^{-1}]$ of water are calculated with the formulae reported by Ramires $et\ al.$[140] based on experimental data from transient hot wire measurements with an accuracy of $\pm 0.5\%$ of the form

$$\lambda^* = -1.48445 + 4.12292 T^* - 1.63866(T^*)^2,$$
$$\text{for} \ \ 274 \le T/[\text{K}] \le 370 \tag{2.154}$$
$$T^* = \frac{T}{298.15} \tag{2.155}$$
$$\lambda^* = \frac{\lambda(T)}{\lambda(298.15)} \tag{2.156}$$
$$\lambda(298.15 \ \text{K}, 0.1 \ \text{MPa}) = (0.6065 \pm 0.0036) \ \text{W m}^{-1} \ \text{K}^{-1} \tag{2.157}$$

According to Teng & Hung [33] the expected density of the nanoparticles which in their experiments was procured from suppliers is approximately

$$\rho_p \approx 3880 \ \text{kg m}^{-3} \tag{2.158}$$

which we will assume is a representative density value for Al_2O_3 nanoparticles since many laboratories in their experimental investigations tend to purchase their nanoparticles from the same suppliers for consistency of results.

Expressions for the viscosity of water are also necessary and traditionally the viscosity of water has been calculated in terms of the Vogel equation as discussed by Seeton [109] of the form

$$\eta_t = (\eta_\infty)^{\left[\frac{t-t_1}{t-t_\infty}\right]} \qquad : \text{Classical Vogel} \tag{2.159}$$

$$\ln(\mu) = A + \frac{B}{T-T_0} \qquad : \text{Vogel-Fulcher-Tammann (modified Vogel)} \tag{2.160}$$

In the classical Vogel equation $\eta_t \equiv \eta(t)$ is the viscosity at a temperature $t/[°C]$ in degrees Celsius, $\eta_\infty = \lim_{t\to\infty}\eta(t)$ is the limit of the viscosity as $t \to \infty$, t_1 is the corresponding temperature for when $\eta = 1$, and t_∞ is the corresponding temperature at which $\eta \to \infty$ from which it is seen that the original Vogel equation is both non-linear as well as mathematically complex. Later more comprehensive collaborations to investigate the viscosity of water by Huber *et al.*[110] improved on the earlier reported formulae by the International Association for the Properties of Water and Steam (IAPWS) thermodynamic properties of water and steam by constructing a new set of water viscosity μ formulae such that

$$\overline{\mu} = \overline{\mu}_0(\overline{T}) \times \overline{\mu}_1(\overline{T},\overline{\rho}) \times \overline{\mu}_2(\overline{T},\overline{\rho}) \tag{2.161}$$

$$\overline{\mu} = \frac{\mu}{\mu^*} \tag{2.162}$$

where $\overline{T} = \frac{T}{T^*}$, $\overline{\rho} = \frac{\rho}{\rho^*}$ and $\overline{p} = \frac{p}{p^*}$ are non-dimensionalized variables for specified reference constants $T^* = 647.096$ K, $\rho^* = 322.0$ kg m^{-3}, $p^* = 22.064$ MPa and $\mu^* = 1 \times 10^{-6}$ Pa s respectively.

Of various formulations that were investigated by Huber *et al.* the final optimal set of equations takes the form

$$\overline{\mu}_0(\overline{T}) = \frac{100\sqrt{\overline{T}}}{\sum_{i=0}^{3}\frac{H_i}{(\overline{T})^i}} \tag{2.163}$$

$$\overline{\mu}_1(\overline{T},\overline{\rho}) = \exp\left[\overline{\rho}\sum_{i=0}^{5}\left(\frac{1}{\overline{T}}-1\right)^i \sum_{j=0}^{6} H_{ij}(\overline{\rho}-1)^j\right] \tag{2.164}$$

$$\overline{\mu}_2 = \exp(x_\mu Y) \tag{2.165}$$

where H_i is specified in Table 2.2 and H_{ij} is specified in Table 2.3 respectively, and more complex formulae for the calculation of $\overline{\mu}_2$ in terms of μ_x and Y are available in terms of parameters summarized in Table 2.1 for water and where Y is calculated by the formula

$$Y(\xi) = \frac{1}{5}q_C\xi(q_D\xi)^5\left(1 - q_C\xi + (q_C\xi)^2 - \frac{765}{504}(q_D\xi)^2\right) \tag{2.166}$$
$$\text{if } 0 \le \xi \le 0.3817016416 \text{ nm}$$

or alternately by the formula

$$Y(\xi) = \frac{1}{12}\sin(3\psi_D) - \frac{1}{4q_C\xi}\sin(2\psi_D) + \frac{1}{(q_C\xi)^2}[1 - \frac{5}{4}(q_C\xi)^2]\sin(\psi_D)$$
$$- \frac{1}{(q_C\xi)^3}\{[1 - \frac{3}{2}(q_C\xi)^2]\psi_D - \| (q_C\xi)^2 - 1 \|^{3/2} L(w)\}$$
$$\text{if } \xi > 0.3817016416 \text{ nm}$$

(2.167)

where

$$\psi_D = \arccos(1 + q_D^2\xi^2)^{-1/2}$$

(2.168)

$$L(w) = \begin{cases} \ln\left(\dfrac{1+w}{1-w}\right) & \text{for } q_C\xi > 1 \\ 2\arctan \| w \| & \text{for } q_C\xi < 1 \end{cases}$$

(2.169)

and the variable w is defined by the equation

$$w = \left|\frac{q_C\xi-1}{q_C+1}\right|^{1/2} \tan\left(\frac{\psi_D}{2}\right)$$

(2.170)

As a result the function $Y(\xi)$ contains the wave numbers q_C and q_D which are constants that must be calculated for the particular choice of fluid which is specified in as indicated in Table 2.1 for water.

Constant	Value
x_μ	0.068
q_C^{-1}	1.9 nm
q_D^{-1}	1.1 nm
ν	0.630
γ	1.239
ξ_0	0.13 nm
Γ_0	0.06
$\overline{T}_R$	1.5

Table 2. 1 Coefficients for calculation of Y

i	H_i
0	1.67752
1	2.20462
2	0.6366564
3	−0.241605

Table 2. 2 Coefficients H_i for use in formula for $\overline{\mu}_0(\overline{T})$

i	j	H_{ij}
0	0	5.20094×10^{-1}
1	0	8.50895×10^{-2}
2	0	-1.08374
3	0	-2.89555×10^{-1}
0	1	2.22531×10^{-1}
1	1	9.99115×10^{-1}
2	1	1.88797
3	1	1.26613
5	1	1.20573×10^{-1}
0	2	-2.81378×10^{-1}
1	2	-9.06851×10^{-1}
2	2	-7.72479×10^{-1}
3	2	-4.89837×10^{-1}
4	2	-2.57040×10^{-1}
0	3	1.61913×10^{-1}
1	3	2.57399×10^{-1}
0	4	-3.25372×10^{-2}
3	4	6.98452×10^{-2}
4	5	8.72102×10^{-3}
3	6	-4.35673×10^{-3}
5	6	-5.93264×10^{-4}
other i	other j	set to zero

Table 2. 3 Coefficients H_{ij} for use in formula for $\overline{\mu}_1(\overline{T})$

The above formulae for the viscosity of water are currently the most advanced correlations used in very high accuracy scientific research work in thermodynamics national laboratories and the motivation for the need of these formulae is due to changes which occurred with the adoption of the International Temperature Scale of 1990 (ITS-90) which resulted in some minor discrepancies with the more conventional formulae that was issued by the International Association for the Properties of Water and Steam (IAPWS). With more recent fundamental physics research to redefine the International System of Units (Le Systéme Internationa d'Unités, SI) in terms of the fundamental constants of nature such as the Planck constant $\hbar$ in 2018/2019 the existing ITS-90 temperature scale will no longer be fundamentally defined in terms of the triple point of water and as a result the properties of water such as some formulae for the density and viscosity at accuracy levels of parts-per-million (ppm) and parts-per-billion (ppb) will potentially change slightly due to the choice of the definition of the temperature scale and the most recent values that will be issued by the CODATA Task Group on Fundamental Physical Constants under the guidance of the Consultative Committee of Units (CCU) operating under the international legal jurisdiction of the BIPM (Bureau International des Poids et Mesures). Based on potential adjustments to the Boltzmann constant k_B as per the discussion by Ramnath [111] these adjustments in the new international temperature scale will mainly occur below 20 K and above 1300 K and as a result modifications to the fundamental physical properties of water is not expected to drastically change particularly for engineering measurements which would not be affected at accuracy levels not close to ppm uncertainty levels.

As a result, in the case of industrial applications, the viscosity may be simply approximated as

$$\overline{\mu} \approx \overline{\mu}_0(\overline{T}) \times \overline{\mu}_1(\overline{T}, \overline{\rho}) \qquad (2.171)$$

Further simplifications for a restricted temperature at a standard pressure of 0.1 MPa then yield a simple polynomial expression for the dimensionless of the form

$$\overline{\mu} = \sum_{i=1}^{4} a_i(\tilde{T})^{(b_i)}, 253.15 \leq T/[\text{K}] \leq 383.15 \qquad (2.172)$$

$$\tilde{T} = \frac{T}{300 \ \text{K}} \qquad (2.173)$$

where the values of the constants a_i and b_i are listed in Table 2.4.

i	a_i	b_i
1	280.68	−1.9
2	511.45	−7.7
3	61.131	−19.6
4	0.45903	−40.0

Table 2. 4 Coefficients a_i and b_i for use in simplified water viscosity formula

In the above system of equations which are used for calculating the density, thermal conductivity and viscosity of water which is used as the base fluid in a water/alumina nanofluid mixture and which are algebraically complex we comment that these systems of equations can nevertheless be simply packaged as sub-routines in for example Matlab or GNU Octave as documented in the Appendix. Consequently this system of equations for the base fluid may then subsequently be utilized as inputs in the copula mathematical models to then in turn calculate the effective thermal conductivity k_{eff} and effective viscosity μ_{eff} for specifying the auxiliary thermodynamic relations if a single-phase nanofluid modelling approach is used.

The previously specified system of four coupled PDE's for steady state problems fully captures the conservation equations for mass, x momentum, y momentum and energy respectively using the single-phase nanofluid modelling scheme which we have opted to utilize in this dissertation for conceptual simplicity, although we comment that some researchers utilize multi-phase mathematical modelling schemes in certain application studies.

When single-phase nanofluid equations are supplied with auxiliary relations for the nanofluid effective thermal conductivity k_{eff}, effective viscosity μ_{eff}, effective density ρ_{nf} and effective specific heat capacity c_{eff} the fluid system is considered mathematically closed and may then in principle be solved with any convenient numerical technique such as finite difference, finite volume or finite element codes. The physical equations in this section provide the mechanism to work out the absolute values of the nanofluid effective thermal conductivity k_{eff} and effective viscosity μ_{eff} from the enhancement ratios k_{nf}/k_{bf} and μ_{nf}/mu_{bf} that are frequently reported in the open literature since we desire the actual physical absolute values in order to construct a database of nanofluid thermophysical properties in order to construct our respective mathematical models.

2.6 Construction of a Nanofluid Thermophysical Database

A comprehensive review of the experimental data for nanofluid effective thermal conductivity and effective viscosity for water/alumina mixtures based on this literature review has been performed that can be utilized to extract the relevant information in order to generate a database for the effective thermal conductivity of the form

$$\mathbf{K}_{eff} = \left[\frac{k_{eff}}{[\mathrm{W} \quad \mathrm{m}^{-1} \quad \mathrm{K}^{-1}]} \quad \frac{u(k_{eff})}{[\mathrm{W} \quad \mathrm{m}^{-1} \quad \mathrm{K}^{-1}]} \quad \frac{T}{[\mathrm{K}]} \quad \frac{u(T)}{[\mathrm{K}]} \quad \frac{d_p}{[\mathrm{m}]} \quad \frac{u(d_p)}{[\mathrm{m}]} \quad \phi \quad u(\phi) \right] \tag{2.174}$$

with similar information for the viscosity $\mathbf{V}_{eff}$ where the volume fraction ϕ is dimensionless in order to avoid unnecessary inconsistencies in the physical units used since for example when specifying the uncertainty of ϕ when specified as a percentage as another 'percentage of a percentage'.

Nominal values for the effective thermal conductivity are used as expected values for k_{eff} and the corresponding uncertainties are calculated using the supplied information where available whilst in the absence of supplied uncertainties the standard uncertainty is assumed, and when no information is supplied for a particular experimental dataset in the literature we assume as $u(k_{eff}) = \pm 1\%(k = 1)$ in unless otherwise specified in order to calculate the corresponding physical uncertainty $u(k_{eff})/[\mathrm{W} \quad \mathrm{m}^{-1} \quad \mathrm{K}^{-1}]$ in natural units. This assumption of a standard uncertainty for the effective viscosity as $u(\mu_{eff})(k = 1) = \pm 1\%$ is also assumed in the absence of any existing reported experimental uncertainties for the measured effective viscosities using representative experimental uncertainties obtained from the literature review of this chapter.

Temperature information for T and $u(T)$ are also extracted from the available information if available whilst the uncertainty in temperature is assumed as $u(T) = \pm 0.5$ K unless otherwise specified. We comment that whilst this temperature uncertainty may appear large it is in fact a reasonable physical experimental uncertainty estimate since although a point temperature measurement with a thermocouple of PRT/Pt100 temperature sensor in a fluid bath that contains the nanofluid may be measured to say 0.1 K that the actual effective uncertainty should in fact take into account the homogeneity and temperature stability of the fluid bath which would for the majority of practical cases using commercially supplied equipment generally not exceed accuracy levels with a standard uncertainty of ± 0.5 K since the homogeneities would usually be around 0.2 K to 0.3 K whilst the temporal stability of the bath would vary based on the quality of the temperature PID controllers such that the effective accuracy i.e. expanded uncertainty of the fluid temperature would usually be a fraction of a degree.

Estimates for the nanoparticle size d_p and its corresponding uncertainty $u(d_p)$ are obtained either from information reported by the authors in the literature sources or alternately from dynamic light scattering DLS information supplied within the literature sources consulted where the expected value of the DLS graphs are used to approximate the nanoparticle information as $d_p \approx \mu$ and $u(d_p) \approx \sigma$ respectively as previously discussed. When no information on the uncertainty of the nanoparticle diameter is reported in for example datasets in the literature where the authors used the manufacturer supplied information we assume that the standard uncertainty is

$u(d_p)(k = 1) = \pm 5$ nm from observations of typical dynamic light scattering measurements obtained from the literature review of this chapter.

In order to estimate the corresponding uncertainty $u(\phi)$ for the volume fraction ϕ in the absence of further information we approximate this quantity as

$$\phi = \omega \frac{\rho_{nf}}{\rho_p} \tag{2.175}$$

$$u^2(\phi) = \left(\frac{\rho_{nf}}{\rho_p}\right)^2 u^2(\omega) + \left(\frac{\omega}{\rho_p}\right)^2 u^2(\rho_{nf}) + \left(\frac{-\omega\rho_{nf}}{\rho_p^2}\right)^2 u^2(\rho_p) \tag{2.176}$$

where

$$\omega = \frac{W_p}{W_{nf}} \tag{2.177}$$

$$u^2(\omega) = \left(\frac{1}{W_{nf}}\right)^2 u^2(W_p) + \left(\frac{-W_p}{W_{nf}^2}\right)^2 u^2(W_{nf}) \tag{2.178}$$

The above formulae are used by first specifying a volume fraction, say $\phi = 0.05$ corresponding to a volume fraction of 5%, and then working out the nanofluid density as

$$\rho_{nf} = (1 - \phi)\rho_f + \phi\rho_p \tag{2.179}$$

by assuming that the nanoparticle density for alumina oxide is roughly $\rho_p = 3880$ kg m^{-3} with a corresponding standard uncertainty of $u(\rho_p)(k = 1) = \pm 50$ kg m^{-3} unless otherwise specified. Once the nanofluid density is estimated it is then used to calculate the corresponding mass fraction ω as

$$\omega = \frac{\rho_p}{\rho_{nf}} \phi \tag{2.180}$$

Then once ω is known we set a nominal value of the nanofluid weight as $W_{nf} = 1$ kg so that the corresponding nanoparticle mass may be calculated as

$$W_p = \omega W_{nf} \tag{2.181}$$

In order to proceed with the uncertainty estimates we then assume a typical expanded uncertainty of mass measurements for a commercial industrial laboratory as $U(m)(k = 2) = \pm(0.0002\% + 3$ µg) for masses from 0 g to 6 g, $U(m)(k = 2) = \pm(0.0002\% + 0.1$ mg) for masses from 6 g to 300 g, and $U(m)(k = 2) = \pm(0.0002\% + 1$ mg) for masses from 300 g to 1 kg respectively so that

$$u(m)/[kg] = \frac{1}{2}\begin{cases} 0.0002 \times 10^{-2}m + 3 \times 10^{-9}, & 0 \le m/[kg] \le 6 \times 10^{-3} \\ 0.0002 \times 10^{-2}m + 0.1 \times 10^{-6}, & 6 \times 10^{-3} \le m/[kg] \le 0.3 \\ 0.0002 \times 10^{-2}m + 1 \times 10^{-6}, & 0.3 \le m/[kg] \le 1 \end{cases} \tag{2.182}$$

As a result the uncertainty $u(W_p)$ may be calculated so that the corresponding uncertainty for ω can also be calculated, and subsequently be used to calculate the the uncertainty in the volume fraction ϕ. For this approximate uncertainty analysis we also need an estimate for the uncertainty of the nanofluid density $u(\rho_{nf})$ however since this is defined in terms of the volume fraction ϕ we approximate the nanofluid density uncertainty with that of the water density uncertainty since these uncertainties are considered to be reasonably close to each other for the typical volume fractions below 10% that are encountered in water/alumina nanofluids.

We comment that technically there is also an uncertainty contributing factor to the water density and nanofluid density expressions due to the effect of the uncertainty in temperature of the respective fluids however we disregard this uncertainty contribution for simplicity due to the relatively narrow operating temperature ranges for existing nanofluids which is usually in-between ambient temperature and about 75 °C from the majority of information sources consulted in the literature review. Under these circumstances the standard uncertainty for a volume fraction of 5% with $\phi = 0.05$ works out to $u(\phi) = \pm0.0022843$ i.e. $100 \times \frac{u(\phi)}{\phi} \approx 4.56\%$. As a result typical optimistic nominal standard statistical uncertainties at a $k = 1$ i.e. 1σ standard deviation confidence level is in most practical cases $u(k_{eff}) = \pm1\%$, $u(T) = \pm0.5$ K, $u(d_p) = \pm5$ nm and $u(\phi) = \pm4.56\%$ for most practical nanofluid experimental data reported in the open literature.

In order to construct a thermophysical database that may be used for meaningful physical predictions the underlying data should be statistically consistent to the extent that is physically possible. Whilst advanced mathematical statistical techniques from the field of metrology are available at key comparison level using concepts such as the degrees of equivalence and the Largest Consistent Subset (LCS) approach as discussed by Cox [112] in order to utilize data that is statistically meaningful these advanced techniques are reliant on the assumption that there is an accurate estimate of the associated statistical uncertainty for an underlying data-point regardless of whether the uncertainty is small or large. Restated it is considered more important to have an higher confidence in the stated claimed accuracy of a data-point than for the data-point to have an artificially small accuracy since if the uncertainty of the data-point is small/large it may then be appropriately utilized or disregarded using variations of statistical outlier techniques in a statistically rigorous manner. In the event that the assumption of estimates of the statistical uncertainties with high levels of confidence are available, which is distinct from an assumption of small accuracies since it is technically possible to high confidence in accuracies that are small or large, then the application of statistical outlier techniques becomes more challenging in the absence of verified and validated uncertainties i.e. error bars on the underlying data-points. This challenge has both physical as well as statistical causes in the field of nanofluid studies since there are physical difficulties such as adequately accounting for a single representative nanoparticle diameter in an agglomeration of nanoparticles each with varying sizes as well as statistical difficulties such as the estimation of covariance terms when calculating uncertainties of meta-parameters. Physical challenges such as *in situ* measurements of agglomerations of nanoparticles within the base fluid as opposed to SEM, TEM and DLS measurements of dry nanoparticles supplied by manufacturers prior to mixing in a wet base fluid are not considered experimentally feasible at the present time of writing, whilst statistical challenges such as estimating covariances between nanoparticle diameters and the base fluid temperature where random fluctuations at the

nanoscale level are known to exist are also similarly considered infeasible in the absence of a comprehensive physical nanofluid theory. The absence of an established physical nanofluid theory also manifests ambiguities even when quantitative nanoparticle diameter information with associated diameter uncertainties is available since different investigators may either use a number weighted average for d_p i.e. the averaged value $\langle d_p \rangle$ is calculated as a simple arithmetic average from observed SEM or TEM images or occasionally $\langle d_p \rangle$ is calculated as an area averaged value i.e. the observed nanoparticle diameters with larger surface areas are considered more relevant to nanofluid heat transfer studies since larger nanoparticle surface areas are able to transfer larger amounts of heat within the nanofluid. One example of this ambiguity was in earlier results reported by Lee *et al.*[78] where the number averaged estimate for d_p was $\langle d_p \rangle_N = (24.4 \pm 1.0)$ nm whilst the area averaged estimate for d_p was $\langle d_p \rangle_A = (38.4 \pm 2)$ nm. Different investigators would calculate the averaged nanoparticle diameter with different experimental equipment and potentially also different mathematical techniques where there is the additional possibility that even if similar experimental data was obtained that different computer software routines using either spreadsheets like MS Excel or scripting codes like Matlab to perform the calculations could then still introduce additional discrepancies. Unfortunately in the absence of the raw experimental data which is frequently unavailable in the reported open literature where usually only the final results and correlations are documented the only practical recourse to address these potential subjectivities and ambiguities is through larger aleatory based experimental uncertainties.

An example of one of the challenges posed for estimating statistical covariance terms is in for example the calculation of the volume fraction ϕ which we demonstrated earlier requires knowledge and quantification of the nanofluid density and its associated uncertainty value. Our approach involved a physical approximation based on the assumption of the conventional correlation expression $\rho_{nf} = (1 - \phi)\rho_f + \phi\rho_p$ that relates ρ_{nf} and ϕ and whilst this expression may be used in an implicit form of the GUM to simultaneously solve for ϕ and ρ_{nf} this mathematical form requires numerical data of both the volume fraction ϕ, nanofluid density ρ_{nf}, temperature T and nanoparticle density ρ_p and we comment that ideally both the nanofluid thermophysical properties k_{eff} and μ_{eff} as well as the remaining auxiliary thermodynamic quantities of the nanofluid density ρ_{nf} and enthalpy h_{nf} should all be determined, however in practice due to experimental constraints and limitations recourse is frequently made to the utilization of existing correlations and as a result accurate estimates of for example the volume fraction uncertainty are implicitly reliant on various assumptions and approximations which then results in a lower level of confidence in uncertainty estimates. The inclusion of additional experimental data-points whilst mitigating these limitations will not necessarily completely eliminate these issues if the underlying data is in principle still reliant on the same set of assumptions and approximations. Due to these theoretical limitations the remaining mathematical modelling option is to consider all the known experimental data-points to be equally valid albeit with a larger estimate of the associated uncertainties to account for the lower level of statistical confidence such that the higher statistical uncertainty estimates translates into a higher level of confidence in accordance with the maximum statistical entropy concept as discussed earlier.

Taking into account the fact that most of the existing correlations for nanofluid thermophysical data as reported in the literature have reported accuracy levels that range from 5% to 10% and that at least at the present time of writing that physical *in situ* experimental measurements of the

nanoparticle agglomerations within the base fluid itself are not possible we therefore opt based on the existing combination of inconsistent and/or contradictory experimental data to conservatively specify the statistical uncertainties of the meta-parameters and thermophysical data accounting for the absence of detailed and rigorous mathematical/statistical uncertainty analysis in the available literature resources that were consulted as

$$\left.\begin{array}{l} u(k_{eff})(k=1) = \pm 2.5\% \\ u(\mu_{eff})(k=1) = \pm 2.5\% \end{array}\right\} \text{thermophysical properties} \qquad (2.183)$$

Due to the lack of consistency as reported in the open literature by various investigators who did not adequately report probability density function distributions and associated confidence levels it was assumed for simplicity that the corresponding representative uncertainties in the absence of specific error bar information were

$$\left.\begin{array}{l} u(T)(k=1) = \pm 1 \ \text{K} \\ u(d_p)(k=1) = \pm 7.5 \ \text{nm} \\ u(\phi)(k=1) = \pm 5\% \end{array}\right\} \text{thermophysical meta} - \text{parameters} \qquad (2.184)$$

2.7 Conclusions

In this chapter information sources obtained from the open literature were used to construct the thermal conductivity database as summarized in Table 2.5 whilst that used to construct the viscosity database is summarized in Table 2.6 and of which both databases incorporate estimates of the respective aleatory physical experimental uncertainties from a critical analysis of the documented information sources that were consulted. The effective thermal conductivity $k_{eff}(T, d_p, \phi)$ and effective viscosity $\mu_{eff}(T, d_p, \phi)$ are formally four dimensional functions mathematically constructed in a $\mathbb{R}^n$ space with $n = 4$ and cannot be directly visualized in a normal three dimensional space.

Due to the size of this experimental information the final numerical nanofluid data contained in the database for the effective thermal conductivity k_{eff} and effective viscosity μ_{eff} are reported in graphical form as iso-surfaces and histograms for convenience. The database that was constructed in this chapter only considers unique experimental data-sets i.e. in many of the sources referred to from the open literature such as various review articles there is a duplication of data so we only considered independent data-sets where available in order to avoid introducing systemic/biased errors.

By analysing the iso-surfaces for representative low, medium and high range values as calculated with the interquartile statistical ranges of reported experimental data for k_{nf} and μ_{nf} it was determined that multiple regions for the meta-parameter inputs can exhibit the same value of k_{nf} or μ_{nf} so that convexity is not guaranteed on a global domain. As a result it is concluded that no unique nanofluid mathematical model is completely possible in a global domain due to the lack of convexity of the model inputs. From a qualitative analysis of the graphical data it is concluded that unique nanofluid mathematical models may be constructed if the analysis is restricted to smaller

domains of meta-parameter values to avoid non-monotonic predictions. The final thermal conductivity database accounting for and eliminating duplicate data results yielded $N_k = 566$ multidimensional experimental data-points, whilst the final viscosity database with a similar criteria results yielded $N_\mu = 558$ multidimensional experimental data-points and which are utilized in the next chapter for constructing the copula based mathematical models.

A review of existing mathematical techniques involving multiple layer perceptron neural network (MLP-NN) schemes was also investigated in order to specify an appropriate existing nanofluid mathematical model and this is considered later in the dissertation to benchmark against when comparing the developed copula model predictions.

Key	Year	Author	Comments
K1	1993	Masuda *et al.*[104]	Transient hot wire $t/[°C] \in [32,47,67]$
K2	1999	Lee *et al.*[83]	$d/[nm] = 38.4$, $t/[°C] = 21$, $\phi/[\%] \in [1,2,3,4]$
K3	1999	Wang *et al.*[191]	Steady-state parallel plate, γ-Al_2O_3, $d_p = 28$ nm,$t = 24$ °C, various ϕ
K4	2003	Putra *et al.*[139]	$d_p = 131.2$ nm, $t/[°C] \in [21,51]$, $\phi/[\%] \in [1,4]$
K5	2004	Das *et al.*[38]	Thermal oscillation method, t, k_{nf}, ϕ, diameter $d = 38.4$ nm
K6	2005	Chon *et al.*[32]	$t, \frac{k_{nf}}{k_f}, \phi, d$
K7	2006	Li & Peterson [88]	Data #1: $t, \frac{k_{nf}-k_f}{k_f}, \phi$, diameter $d = 36$ nm (low temp)
K8			Data #2: $t, \frac{k_{nf}-k_f}{k_f}, \phi$, diameter $d = 36$ nm (high temp)
K9	2006	Kim *et al.*[76]	transient hot wire, $d_p = 38$ nm,
			$\phi/[\%] \in [0.3,0.5,0.8,1.5,2.0,3.0]$, $t = 25$ °C
K10	2007	Wang & Mujumdar [192]	$\phi, \frac{k_{eff}}{k_b}, d, t$, selected pH values
K11	2007	Timofeeva *et al.*[184]	ϕ, k_{nf}, d ambient 23°C
K12	2007	Zhang *et al.*[204]	t, k_{nf}, ϕ average diameter $d = 20$ nm
K13	2007	Li & Peterson [26]	Data #1: t, k_{nf}, ϕ, d, diameter $d = 36$ nm
K14			Data #2: t, k_{nf}, ϕ, d, diameter $d = 47$ nm
K15	2008	Li & Kleinstreuer [89]	Data #1: $\phi/[\%], \frac{k_{eff}}{k_b}, t$;
K16			Data #2: $t, \frac{k_{eff}}{k_f}, \phi/[\%]$
K17	2008	Murshed *et al.*[121]	Data #1: $t, \frac{k_{nf}}{k_f}, d, \phi$, diameter $d = 80$ nm
K18			Data #2: $t, \frac{k_{nf}}{k_f}, d, \phi$, diameter $d = 150$ nm
K19	2008	Ju *et al.*[72]	$d_p/[nm] \in [20,30,45]$, $\phi/[\%] \leq 10$
K20	2009	Beck *et al.*[15]	t, k_{nf}, d, ϕ, contains standard deviations of k_{nf}. Observed a very large variation in nanoparticle d_p sizes quoted by manufacturers and own measurements at Georgia Institute of Technology (USA). Concluded that type of crystalline phase i.e. $\alpha/\gamma/\delta$-Al_2O_3 actually has very little practical effect on k_{nf} and that d_p is more significant. Measured std. dev. for α-Al_2O_3 with TEM as $38 \leq \sigma/[nm] \leq 95$, $\sigma/[nm]$ from 2 to 5 for γ-phase, and $\sigma/[nm]$ for δ-phase about 110. Hence in practical terms quite challenging to quantify agglomerations.
K21	2009	Mintsa *et al.*[117]	Data #1: t, k_{nf}, d, ϕ, $d = 47$ nm,$\phi = 4\%$
K22			Data #2: t, k_{nf}, d, ϕ, $d = 36$ nm,$\phi = 3.1,6,9\%$
			Concluded that nanofluid correlations are considered good if within $\pm 5\%$ of predictions. Hence we can assume $u(k_{eff}) = \pm 2.5\%$.
K23	2010	Teng *et al.*[182]	Data #1: $\omega, \frac{k_{nf}}{k_f}, d, t$ meas. 10 °C
K24			Data #2: $\omega, \frac{k_{nf}}{k_f}, d, t$ meas. 30 °C
K25			Data #3: $\omega, \frac{k_{nf}}{k_f}, d, t$ meas. 50 °C
K26	2010	Beck *et al.*[16]	t, k_{nf}, ϕ, d, diameter $d = 12$ nm contains std. dev
K27	2010	Chandrasekar *et al.*[29]	Data #1: $\phi, \frac{k_{eff}}{k_f}$ room temperature

Key	Year	Author	Comments
K28	2010	Patel *et al.*[136]	$d_p/$[nm] $\in$ [11,45,150], $t/$[°C] $\in$ [20,30,40,50]
			and $\phi/$[%] $\in$ [0.5,1.0,2.0,3.0]
K29	2011	Longo & Zilio [93]	Data #1: $t, \frac{k_{nf}}{k_f}, d, \phi$ stirred fluid
K30			Data #2: $t, \frac{k_{nf}}{k_f}, d, \phi$ sonicated fluid
K31	2012	Yiamsawasd *et al.*[201]	t, k_{nf}, d, ϕ, diameter $d = 120$ nm
K32	2012	Buschmann [25]	t, k_{nf}, ϕ, diameter between 30 nm to 80 nm
K33	2014	Ghanbarpour *et al.*[52]	Data #1: t, w, ϕ, k
			particle diameter from DLS measurements
K34	2014	Aybar *et al.*[12]	Various reported values for thermal conductivity of nanoparticle as $k_{Al_2O_3}/$[W m^{-1} K^{-1}] $\in$ [36,40,46]. Unique experimental data by Ho *et al.*[64].
K35	2015	Ariana [9]	Established that t, ϕ, d_p sufficient to model k_{eff}. No unique additional independent reported experimental data-sets.

Table 2. 5 Summary of open literature sources for thermal conductivity database

Key	Year	Author	Comments
V1	1993	Masuda *et al.*[104]	Transient hot wire $t/$[°C] $\in$ [32,47,67]
V2	1999	Wang *et al.*[190]	Overview of experimental apparatus for k_{eff}
V3	2007	Nguyen *et al.*[126]	Discusses hysteresis effects & equipment
V4	2007	Pak & Cho [132]	Observed that h_c for $\phi = 3\%$ was 12% smaller than pure water
V5	2007	Timofeeva *et al.*[184]	Determined that elongated/dendritic nanostructures are more efficient in enhancing thermal conductivity than spherical structure at the same ϕ concentration
V6	2007	He *et al.*[62]	h_c insensitive to d_p for certain conditions; TiO$_2$ data only.
V7	2008	Lee *et al.*[84]	Definite nonlinear μ_{eff} observed for $0.01 \leq \phi/$[%] $\leq$ 0.3 but linear trend for k_{eff} observed for same ϕ. Accuracy is assumed as $U(d_p) = \pm 5$ nm so $\sigma(d_p)/$[nm] $\in$ [2.5,10] in most likely circumstances so assume $u(d_p) \approx \pm 7.5$ nm. In authors estimate viscosity accuracy as $\pm 1.8\%$ so assume $u(\mu_{eff}) \approx \pm 2.5\%$.
V8	2008	Murshed *et al.*[121]	Data #3: $t, \frac{\mu_{nf}}{\mu_f}, d, \phi$, diameter $d = 80$ nm
V9	2008	Nguyen *et al.*[127]	Data #1: $\phi/$[%], $\frac{\mu_{nf}}{\mu_f}, d$ room temperature. Critical damage
V10			temperature $t_{cr} = 70$ °C; Data #2: t, μ, d, ϕ for 47 nm
V11			Data #3: t, μ, d, ϕ for 36 nm. Shown that
			$\mu_r = (\mu_{nf}/\mu_w) \approx$ const. for $\phi < 4\%$ with T, ϕ non-linear for $7 < \phi/\% < 9$.
V12	2008	Tavman *et al.*[180]	Hamilton-Crosser model for k_{eff} yields consistent results, Einstein model for μ_{eff} is inconsistent
V13	2009	Duangthongsuk & Wongwises [42]	$\phi/$[%] $\in$ [0.2,0.6,1.0,1.5,2.0] and $15 \leq t/$[°C] $\leq$ 35 for TiO$_2$, $(k_{nf}/k_w) = a + b\phi$ & $(\mu_{nf}/\mu_w) = a + b\phi + c\phi^2$.
V14	2009	Pastoriza-Gallego *et al.*[134]	Experimented up to 25 MPa determined that d_p has subtle effect on density and significant effect on μ_{eff}.

			This is suggestive that there appears to be correlations between a nanofluid's thermodynamic auxiliary relations of k_{nf}, μ_{nf}, ρ_{nf} and h_{nf}. Potentially an area of rewarding future research results using molecular dynamics.
V15	2009	Turvat [185]	Validated 3ω method with transient hot wire experiments
V16	2009	Anoop *et al.*[8]	Newtonian behaviour exhibited for $0.5 \leq \phi/[\%] \leq 6.0$, manufacturer $d_p = 50$ nm but agglomeration DLS is $\mathcal{A}_I = 94.7$ nm by number and $\mathcal{A}_N = 138.8$ nm by intensity: no clear relationship between d_p & $\mathcal{A}$
V17	2010	Chandrasekar *et al.*[29]	Data #2: $\phi, \frac{\mu_{eff}}{\mu_f}$ room temperature
V18	2010	Duangthongsuk & Wongwises [43]	h_c almost 26% greater for $\phi/[\%] \leq 1$ but lower by 14% for higher concentrations $\phi/[\%] \leq 2$
V19	2010	Kwek *et al.*[82]	d_p has limited effect on μ_{eff} which is more affected by T
V20	2010	Lee *et al.*[85]	$\phi, \frac{\mu_{nf}}{\mu_f}$, constant heat flux experiment, thermal convection/Δp drop
V21	2011	Khanafer & Vafai [74]	Data #1: $\phi, \frac{\mu_{nf}}{\mu_f}, d$ ambient temperatures
V22			Data #2: ϕ, μ_{nf}, d, t variable temperatures
V23	2011	Longo & Zilio [93]	Data #3: $t, \frac{\mu_{nf}}{\mu_f}, d, \phi$ stirred fluid
V24			Data #4: $t, \frac{\mu_{nf}}{\mu_f}, d, \phi$ sonicated fluid
V25	2011	Pastoriza-Gallego *et al.*[135]	d_p has minimal effect on ρ but more significant on μ_{eff}
V26	2012	Mahbubul *et al.*[97]	Observed contradictory effects on μ_{eff} and T, and definite effects on μ_{eff} based on d_p
V27	2012	Fedele *et al.*[46]	Newtonian behaviour for μ_{eff} for small ϕ but nonlinear behaviour at higher ϕ
V28	2014	Ghanbarpour *et al.*[52]	Data #2: ϕ, t, μ, w , particle diameters from DLS measurements
V29			Data #3: w, μ temperature 293 K
V30			Data #4: w, μ temperature 313 K
V31	2015	Meyer [113]	Confirmed nonlinear behaviour of μ_{eff} with increased ϕ and identified application of nanofluids in nuclear reactor cooling and solar ponds
V32	2015	Adio *et al.*[4]	Confirmed problematic under predictions of classical models, and identified potential to use certain nanofluids above 55 ˚C without unnecessary increases in pumping power based on μ_{eff}
V33	2015	Meybodi [112]	Outlier detection discussion
V34	2017	Murshed & Estellé [122]	$T, \phi, \frac{\mu_{nf}}{\mu_f}$

Table 2. 6 Summary of open literature sources for viscosity database

$$k_{nf} = 0.66984 \, \text{W/m.K}$$
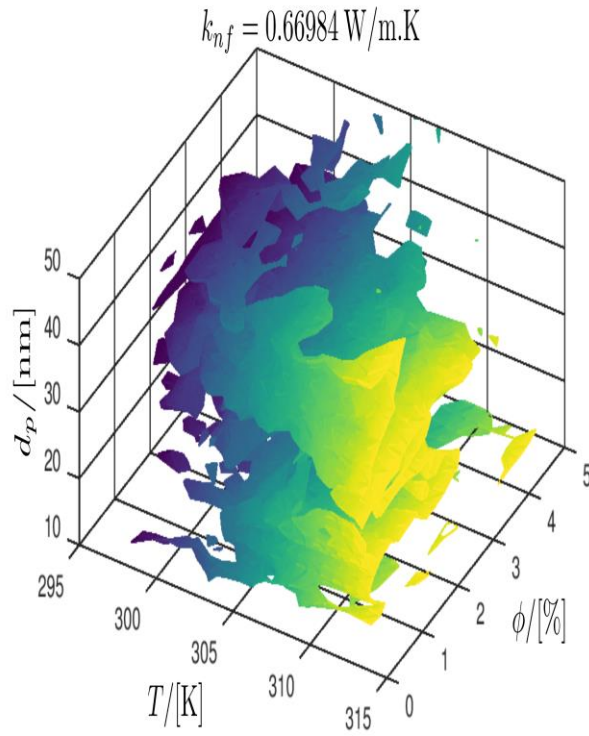
Figure 2-16 Visualization of nanofluid effective conductivity isosurface low-range with $k_{nf} = \overline{k_{nf}} - \frac{1}{2}IQR(k_{nf})$

$$k_{nf} = 0.7042 \, \text{W/m.K}$$
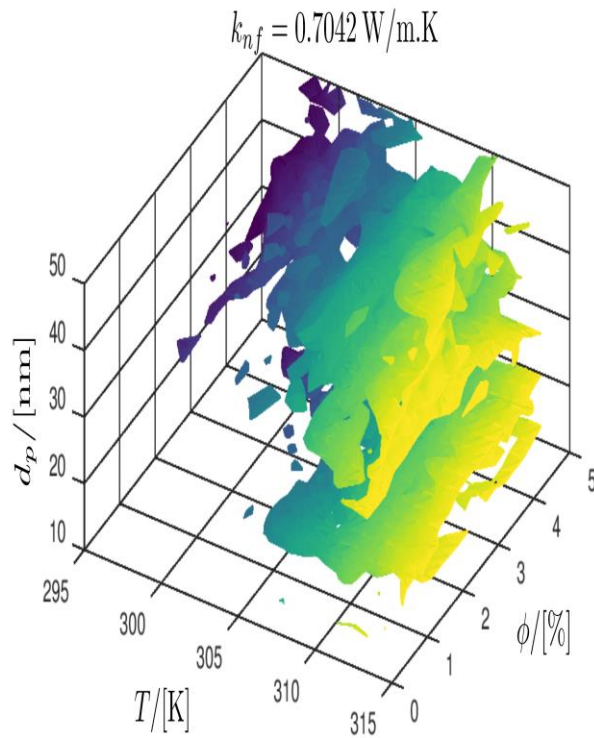
Figure 2-17 Visualization of nanofluid effective conductivity isosurface mid-range with $k_{nf} = \overline{k_{nf}}$

73

$$k_{nf} = 0.73855 \, \text{W/m.K}$$
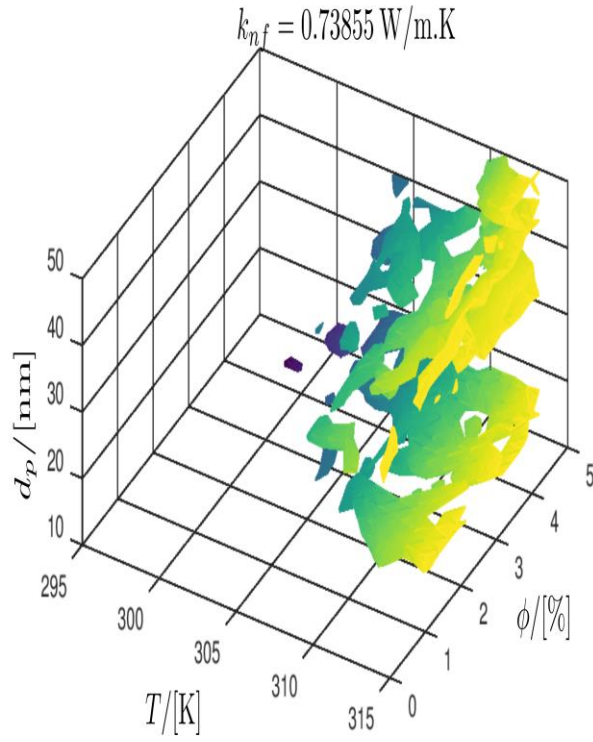
Figure 2-18 Visualization of nanofluid effective conductivity isosurface high-range with $k_{nf} = \overline{k_{nf}} + \frac{1}{2}IQR(k_{nf})$
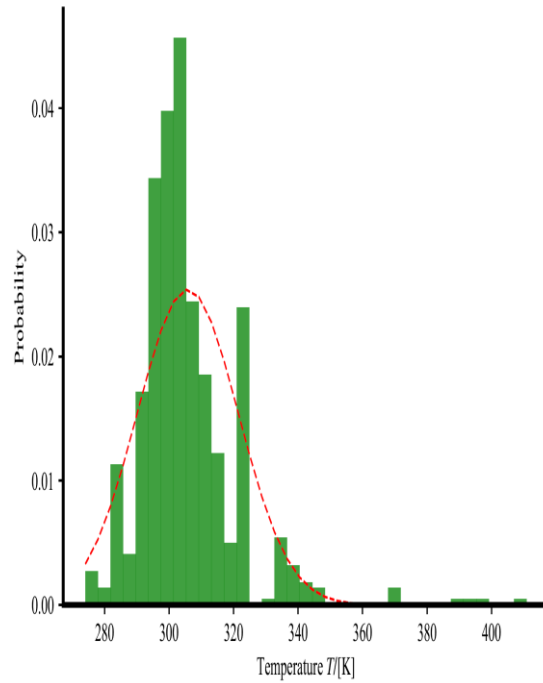
Figure 2-19 Statistical summary of T in $k_{nf}(T, \phi, d_p)$ *database*
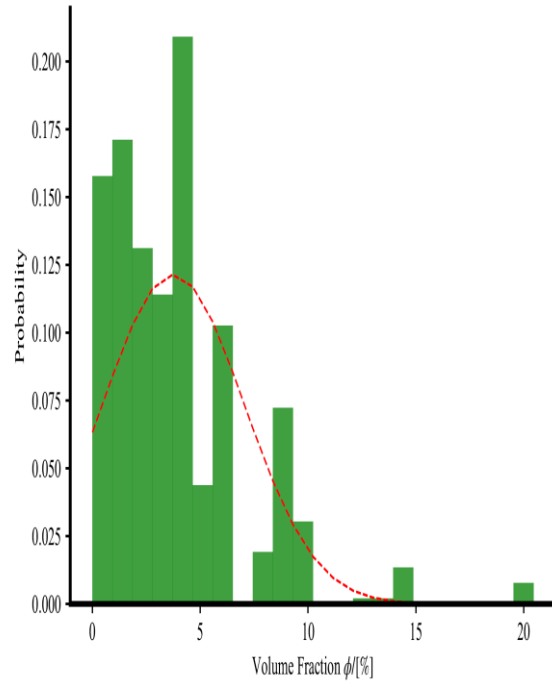
Figure 2-20 Statistical summary of ϕ measurements in $k_{nf}(T, \phi, d_p)$ database
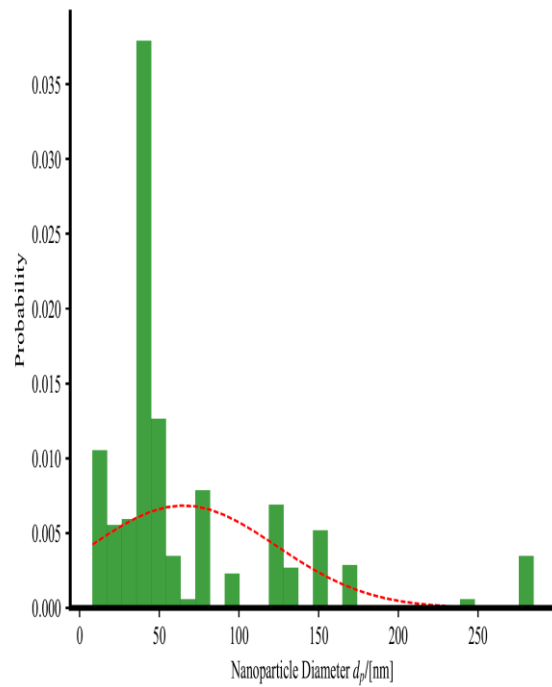
Figure 2-21 Statistical summary of d_p measurements in $k_{nf}(T, \phi, d_p)$ database
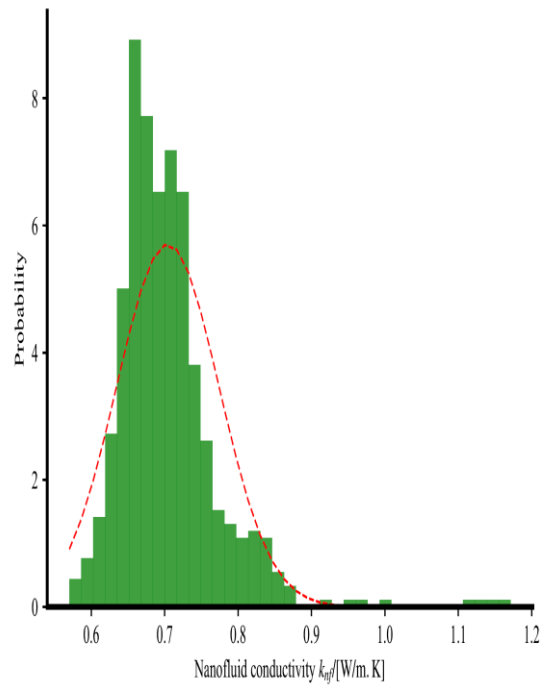
Figure 2-22 Statistical summary of k_nf measurements in $k_{nf}(T, \phi, d_p)$ database
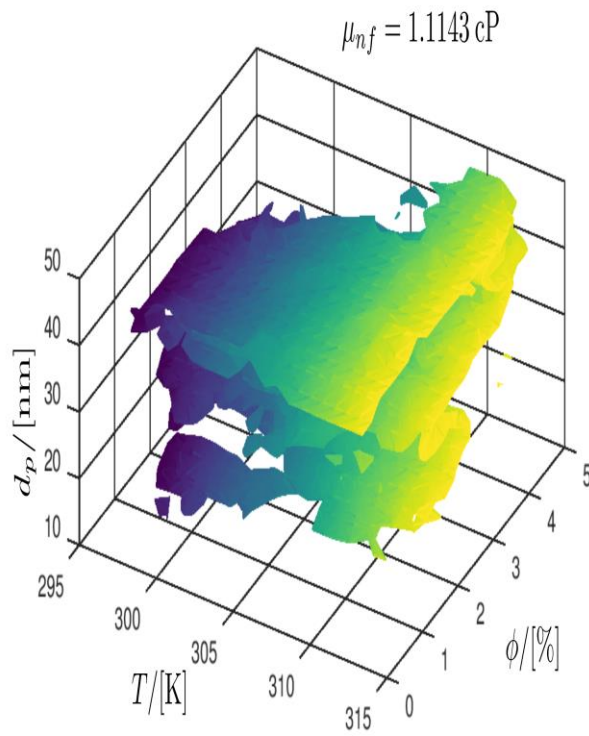
Figure 2-23 Visualization of nanofluid effective viscosity isosurface low-range with $\mu_{nf} = \overline{\mu_{nf}} - \frac{1}{2}IQR(\mu_{nf})$
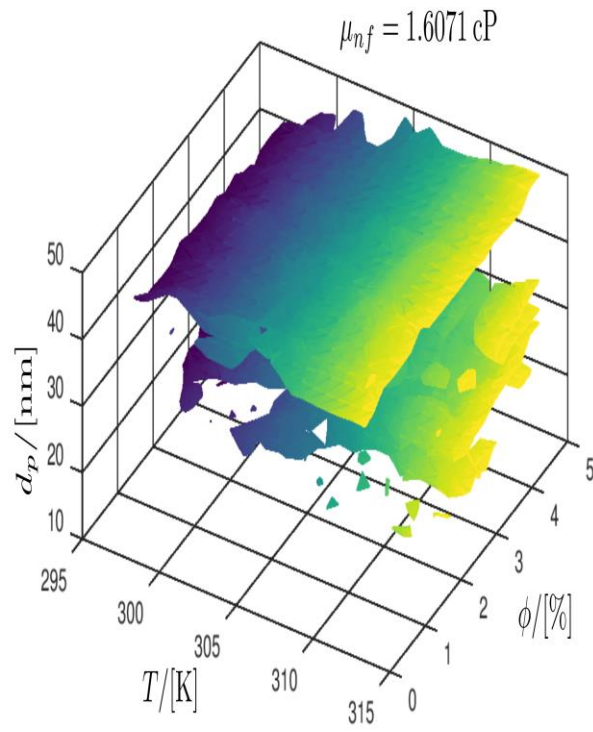
Figure 2-24 Visualization of nanofluid effective viscosity isosurface mid-range with $\mu_{nf} = \overline{\mu_{nf}}$
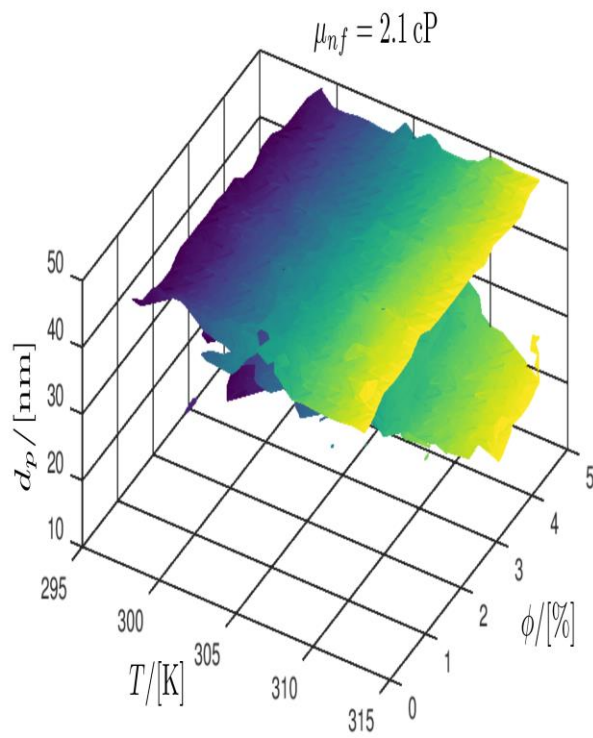
Figure 2-25 Visualization of nanofluid effective viscosity isosurface high-range with $\mu_{nf} = \overline{\mu_{nf}} + \frac{1}{2}IQR(\mu_{nf})$
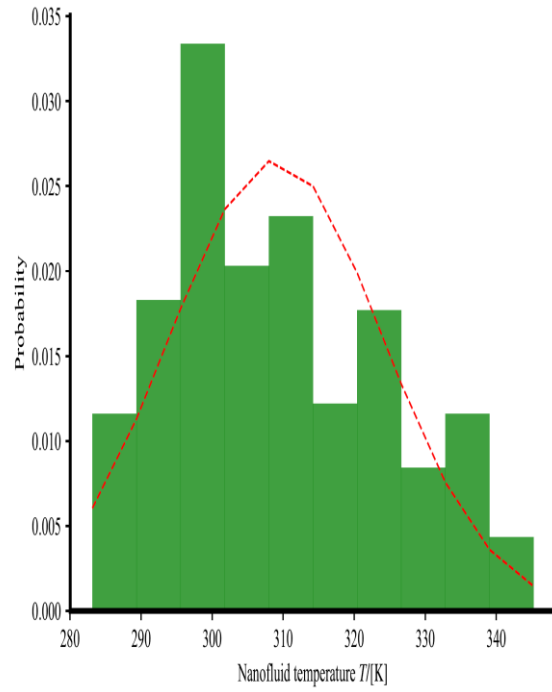
Figure 2-26 Statistical summary of T measurements in $\mu_{nf}(T, \phi, d_p)$ *database*
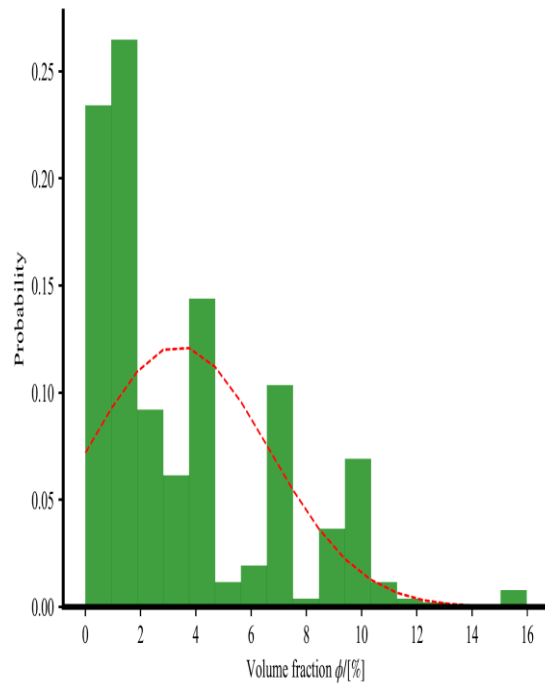
Figure 2-27 Statistical summary of ϕ measurements in $\mu_{nf}(T, \phi, d_p)$ *database*

78
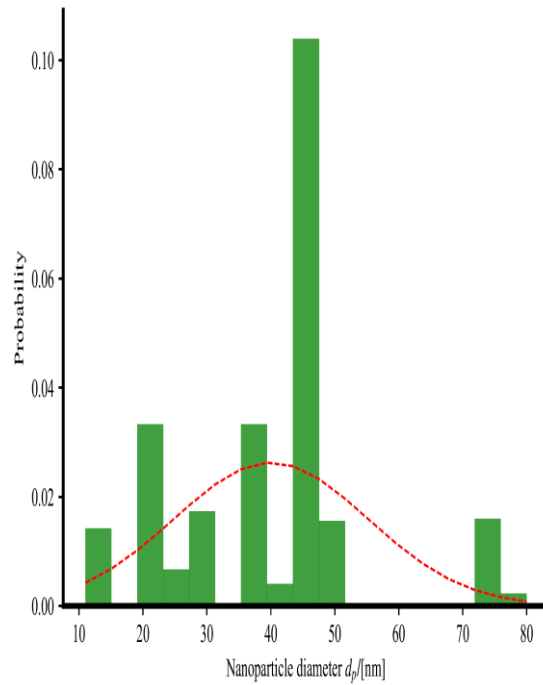
Figure 2-28 Statistical summary of d_p measurements in $\mu_{nf}(T, \phi, d_p)$ database
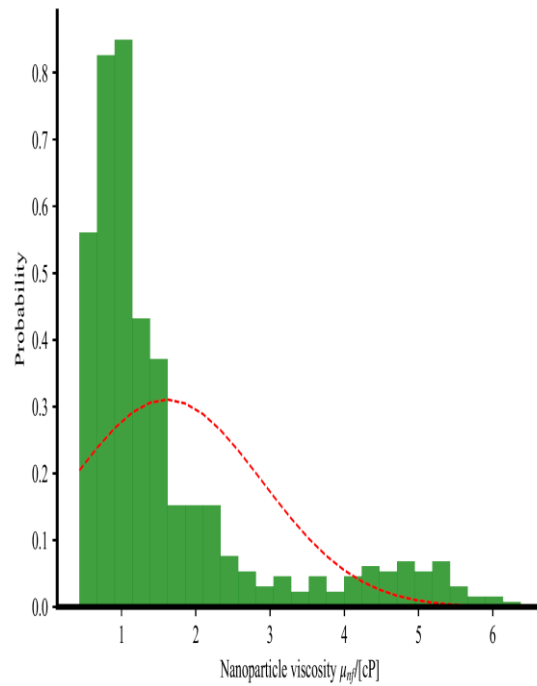
Figure 2-29 Statistical summary of μ_nf measurements in $\mu_{nf}(T, \phi, d_p)$ database

3 Mathematical Modelling Techniques

3.1 Analysis of Nanofluid Physical and Algebraic Characteristics

In this dissertation, the mathematical modelling approach for the statistical analysis taking into account the existing mathematical techniques discussed in the previous chapter is based on the approach for non-linear univariate models $y = f(x_1, \dots, x_M)$ as discussed by Press $et\ al.$[132]. In the case of a multi-dimensional input $\mathbf{x} = [x_1, \dots, x_M]^{\mathrm{T}} \in \mathbb{R}^N$ where $N \in \mathbb{N}$ is an integer corresponding to the number of components of $\mathbf{x}$ the measurand is assumed to to built up in terms of a linear combination of possibly non-linear basis functions $X_k(\mathbf{x})$ such that

$$y = \sum_{k=1}^{M} a_k X_k(\mathbf{x}) \tag{3.1}$$

where M is the number of parameters. Under these conditions a χ^2 merit function may be formed such that

$$\chi^2 = \sum_{i=1}^{N} \left[\frac{y_i - \sum_{k=1}^{M} a_k X_k(\mathbf{x}_i)}{\sigma_i} \right]^2 \tag{3.2}$$

where N is the number of experimental data points. The optimal values of the parameters $a_k, k = 1, \dots, M$ occurs when χ^2 is a minimum and this can be formally determined when

$$\frac{\partial \chi^2}{\partial a_k} = 0; \quad k = 1, \dots, M \tag{3.3}$$

The above system of equations is formally a non-linear equation of the form $\mathbf{F}(\mathbf{x}) = \mathbf{0}$ and conventional techniques such the multi-variable Newton's method, quasi-Newton's method, steepest descent, and homotopy/continuation methods as discussed by Burden & Faires [133] are available however due to the complexities involved in solving systems of non-linear equations it is generally easier to minimize the χ^2 merit function using classical optimization techniques. In most practical cases an unconstrained optimization is usually sufficient to minimize the χ^2 merit function since the terms $a_k, k = 1, \dots, M$ are simply parameters to obtain an optimal best fit however in general one may also impose additional constraint specifications using for example penalty functions and Lagrange multipliers in order to ensure physical meaningful results. One approach to determining the optimal parameters using an unconstrained optimization as discussed by Bertsekas [134] involves a simple line search such that the steps to determine the optimal parameters then take the form:

1. Set $f(\mathbf{x}) = \chi^2(\mathbf{a})$ where $\mathbf{x} = \mathbf{a}$
2. Guess an initial value $\mathbf{x}_0$ and choose a maximum number of iterations $N_{\max}$
3. For $i = 1, 2, \dots, N_{\max}$ perform the following steps
   (a) set $\mathbf{u}_i = \dfrac{-\nabla f(\mathbf{x}_{i-1})}{\|\nabla f(\mathbf{x}_{i-1})\|}$
   (b) set $\mathbf{x}_i = \mathbf{x}_{i-1} + \lambda_i \mathbf{u}_i$ where λ_i is the value that minimizes $F(\lambda_i) = f(\mathbf{x}_{i-1} + \lambda_i \mathbf{u}_i)$

The above unconstrained optimization can be directly and conveniently implemented using the scientific Python scipy package if the algebraic model for the data is known, however in the area of nanofluids the specific type of algebraic model is considered unknown. As a result in practical terms various different possible algebraic models must be individually investigated and each of the associated model parameters determined as per the above explanation. Due to the wide variety of different possible models, each of which may differ from other possible models both in terms of the specific algebraic form as well as in terms of the number of parameters to be fitted, this parameter fitting optimization approach to construct algebraic models is considered both excessively onerous as well as computationally demanding.

Once the above algorithm has been implemented for a particular choice of algebraic model the optimization then yields the values $a_1, \ldots, a_M$ for that particular model and we can then use a Monte Carlo boot strapping approach to generate synthetic data from sampling from the original data in order to construct estimates of the parameter uncertainties. This approach to characterize the uncertainties of the parameters $a_1, \ldots, a_M$ themselves for a particular model by using boot strapped synthetic data can be implemented using extended lambda distributions (ELD's) as developed earlier by Harris & Cox [135] and recently implemented by Ramnath [92]. The ELD's of the fitted parameters are constructed in terms of four scalar ELD parameters a, b, c, d such that the univariate quantile function $Q(\rho)$ takes the form

$$Q(\rho) = \begin{cases} d + c\left[\frac{a\rho^b - (1-\rho)^b + 1 - a}{b}\right] & \text{if } b \neq 0 \\ d + c\{a\ln(\rho) - \ln(1 - \rho)\} & \text{if } b = 0 \end{cases} \tag{3.4}$$

The relationship between the quantile function $Q(\rho)$ in terms of a parameter $\rho \sim R[0,1]$ which is a random number to generate the associated random variable η for the PDF $g(\eta)$ for the respective χ^2 parameters $a_k, k = 1, \ldots, M$ is

$$\frac{1}{Q'(\rho)} = g(\eta) \tag{3.5}$$
$$\eta = Q(\rho) \tag{3.6}$$
$$\rho = G(\eta) \tag{3.7}$$
$$g(\eta) = \frac{1}{c\{a\rho^{(b-1)} + (1-\rho)^{(b-1)}\}} \tag{3.8}$$

where the limits of the respective parameter random variables are

$$d - \frac{ac}{b} \leq \eta \leq d + \frac{c}{b} : b > 0 \tag{3.9}$$
$$-\infty < \eta < \infty : b \leq 0 \ \& \ a \neq 0 \tag{3.10}$$
$$0 \leq \eta < \infty : b \leq 0 \ \& \ a = 0 \tag{3.11}$$

The corresponding mean μ and variance σ^2 of the fitted parameters in terms of the ELD parameters a, b, c, d are then calculated according to Willink [136] as

$$\mu = d + \frac{c(1-a)}{b+1} \tag{3.12}$$

$$\sigma^2 = \begin{cases} \left(\frac{c}{b}\right)^2 \left[\frac{a^2+1}{2b+1} - \frac{2a\Gamma(b+1)^2}{\Gamma(2b+2)} - \left(\frac{a-1}{b+1}\right)^2\right] & \text{if } b \neq 0 \\ c^2 \left[a^2 + \frac{\pi^2 a}{3} - 2a + 1\right] & \text{if } b = 0 \end{cases} \tag{3.13}$$

where Γ is the Gamma function. For the optimally fitted parameter values the corresponding covariance matrix may be estimated as

$$\mathbf{C} = \boldsymbol{\alpha}^{-1} \tag{3.14}$$

$$\alpha_{k\ell} = \frac{1}{2}\frac{\partial \chi^2}{\partial a_k \partial a_\ell} \tag{3.15}$$

where the evaluation of the matrix $\boldsymbol{\alpha}$ components $\alpha_{k\ell}$ are calculated at the optimal parameter value $\mathbf{a}_{optimal}$ from the previously mentioned optimization.

If the process parameter $\mathbf{x}$ and the fitted parameter $\mathbf{a}$ are now combined into a new variable $\mathbf{z} = [\mathbf{x}, \mathbf{a}]$ for convenience where $y = f(z_1, \dots, z_n)$ then the final uncertainty of the optimally fitted y for the thermal conductivity or the viscosity, for a particular choice of algebraic model, is then with the aid of the application of the GUM of the form

$$u^2(y) = \sum_{i=1}^{n} c_i^2 u^2(z_i) + 2\sum_{i=1}^{n-1}\sum_{j=i+1}^{n} c_i c_j u(z_i)u(z_j)r(z_i, z_j)$$

$$+ \sum_{i=1}^{n}\sum_{j=1}^{n}\left\{\left[\frac{1}{2}\left(\frac{\partial^2 f}{\partial z_i \partial z_j}\right)^2 + \frac{\partial f}{\partial z_i}\frac{\partial^3 f}{\partial z_i \partial z_j^2}\right]u^2(z_i)u^2(z_j)\right\} \tag{3.16}$$

$$c_i = \frac{\partial f}{\partial z_i} \tag{3.17}$$

$$r(z_i, z_j) = \frac{u(z_i, z_j)}{u(z_i)u(z_j)} \tag{3.18}$$

The above estimate may then be used for the uncertainty from a particular mathematical algebraic model to estimate the E_n normalized errors between the experimental data points with their associated uncertainties and a particular model's predictions to check for accuracies and consistencies. Based on the literature review conducted as discussed in the previous chapter effective thermal conductivity data is utilized from the open scientific literature as summarized in Table 2.5 and effective viscosity data is utilized from the open scientific litertaure as summarized in Table 2.6 for the mathematical model construction process in this chapter.

The set of thermal conductivity and viscosity data is first used to build up a database of thermo-physical data in terms of a selection of meta-parameters (MP's) following the existing methodology by Gupta [74]. Referring to the work by Gupta for consistency with existing nanofluid modelling approaches the relevant physical MP's for thermal conductivity would model or be representative in some mathematical or statistical sense of *iter alia* of particle shape, particle material and base fluid, temperature, particle size, additives, acidity i.e. pH value, and clustering physical effects. On the other hand MP's for viscosity would model or be representative again in some mathematical or statistical sense of *inter alia* of morphology, shear rate, temperature and volume concentration physical effects respectively. From the earlier discussion in the previous

chapter of the available literature it was concluded that not all relevant physical effects are necessarily statistically independent quantities since for example the pH value of the nanofluid can reasonably be approximated with correlations of other physical effects. In addition there is the practical experimental constraint that not all physically relevant or pertinent information of physical effects is readily available either from reported data or in a format that is mathematically or statistically meaningful as inputs for a mathematical modelling of the thermo-physical properties. The absence of certain experimental information such as for example the nanofluid pressure $p/[\text{Pa}]$ or shear rate $\dot{\gamma}/[\text{s}^{-1}]$ is understandable as in certain contexts it is obvious that the experimental measurements were for example performed at atmospheric pressures such that $p = p_{atm}$, or that a certain quantity such as the shear rate $\dot{\gamma}$ is not necessarily physical meaningful in for example stationary fluids where the conventional definitions such as $\dot{\gamma} = \frac{v}{h}$ for parallel plate Couette flows with a nominal flow velocity v and wall spacing h, $\dot{\gamma}_{ij} := \frac{\partial v_i}{\partial x_j} + \frac{\partial v_j}{\partial x_i}$ for general flow conditions, $\dot{\gamma} = \frac{4Q}{\pi r^3}$ for Newtonian pipe flows with a volumetric flow rate $Q/[\text{m}^3 \quad \text{s}^{-1}]$ and pipe radius $r/[\text{m}]$, or possibly in terms of wall stresses such that $\tau_w = \dot{\gamma}\mu$ where τ_w is the wall shear stress and μ is the viscosity respectively apply for a particular experimental set-up, are not necessarily relevant or applicable. For such situations the absence of certain physical information such as the fluid working pressure may be assumed with little detrimental effect since for example many laboratories would have an ambient pressure reasonably close to a standard atmospheric pressure, however the absence of other possibly pertinent physical effects may not be possible to mitigate against without potentially altering the underlying validity of the experimental data. One particular example would be in how to combine experimental data for stationary fluids where $\dot{\gamma} = 0$ and flowing fluids where $\dot{\gamma} \neq 0$. In this particular case the obvious answer is to simply treat $\dot{\gamma}$ as an additional parameter however this is not an ideal approach since the underlying process parameters should be consistent for the physical fluid experiment. In certain nanofluid experimental studies it has been speculated that under certain nanoparticle concentrations that the nanofluid may exhibit non-Newtonian flow characteristics and this observation was reported by Meyer *et al.*[69] in their review paper where they considered rheological effects and remarked that in the case of zinc oxide ZnO and zirconium dioxide ZrO_2 nanoparticles suspended in a poly-alpha olefin (PAO6) base fluid that for low shear rates in the range $0 \leq \gamma/[\text{s}^{-1}] \leq 700$ that the nanofluid exhibited Newtonian flow characteristics whilst at high shear rates in the range $10^6 \leq \dot{\gamma}/[\text{s}^{-1}] \leq 10^7$ that the nanofluid started to exhibit a non-Newtonian flow rheology behaviour. Meyer *et al.*report that in this case correlations for the relative viscosity of the form $\eta_r/[10^{-2}\text{P}] = 52.80 - 9.76 \times 10^{-7}\dot{\gamma} + 0.172\varphi - 0.912T + 1.02 \times 10^{-8}\dot{\gamma}T + 4.24 \times 10^{-3}T^2$ for the low shear rate and $\eta_r/[10^{-2}\text{P}] = 53.78 - 9.25 \times 10^{-7}\dot{\gamma} + 0.202\varphi - 0.937T + 9.65 \times 10^{-9}\dot{\gamma}T + 4.39 \times 10^{-3}T^2$ for the high shear rate flow were obtained from the available experimental data. This modelling approach is equivalent to a functional expression for the relative viscosity of the form $\eta_r^{(v_I)} = a + b\dot{\gamma} + c\varphi dT + e\dot{\gamma}T + fT^2$ for flows with low shear rates, and of the form $\eta_r^{(v_{II})} = A + B\dot{\gamma} + C\varphi + DT + E\dot{\gamma}T + FT^2$ for flows with high shear rates where relevant constants are used for the two different flow conditions. This approach is mathematically consistent with the Response Surface Methodology (RSM) since the underlying functional form is composed of linear combinations of products of relevant dimensional groups i.e.

$$y_i = \sum_{j=1}^{N} \left[\alpha_j \left(\prod_{k=1}^{M} (\pi_k)^{(\beta_j)} \right) \right] \tag{3.19}$$

where y_i is a quantity that is being modelled, say for example $y_1 = k_{eff}$ for $i = 1$ and $y_2 = \mu_{eff}$ for $i = 2$, and π_k are relevant dimensional groups that are appropriately defined for the particular experimental data. In this particular modelling approach there could be in fact additional functional groups π_k such as the shear rate for example however in the absence of available data for all the dimensional groups the functional relation is simply a low order approximation which disregards higher order powers of other functional groups. As a result this modelling approach is consistent with conventional engineering dimensional analysis techniques such as the well known Buckingham-Pi theory however the key difference in the area of nanofluid studies is that the functional groups are unknown since there does not at the present time exists a consistent and wholly encompassing theoretical framework to consistently and completely model nanofluid thermo-physical properties. In the particular case of the absence of rheological property data this modelling approach is consistent with the assumption that coefficients such as a and e that are multiplicative factors of the shear rate $\dot{\gamma}$ are negligible so that $\eta_r^{(v_I)} \approx a + c\varphi dT + fT^2$ under the assumption that $a \approx 0$ and $e \approx 0$ in the absence of known and verified information of the shear rate $\dot{\gamma}$ with a corresponding assumption for similar terms of other dimensional groups.

As a result in the absence of certain physical experimental information and data such as for example pH values and shear rates our modelling approach is to avoid unsubstantiated assumptions and to simply utilize the available reported experimental data and information. Whilst this approach has physical validity for the available experimental data a remaining and potentially challenging issue presents itself in terms of how to incorporate physically relevant qualitative information that may not be easily amenable to appropriate quantitative simplifications and summaries. Examples of such potential modelling issues presents itself in terms of clustering effects for the effective thermal conductivity k_{eff} and morphology effects for the effective viscosity μ_{eff} respectively. In order to understand why this may be a potentially difficult modelling challenge consider how the nanoparticle diameter size d may be initially approximated from the experimental data such as for example reported dynamic light scattering information as shown in Figure 3.1 where the expected values are $z_1^{avg}/[\text{nm}] = 90.9$, $z_2^{avg}/[\text{nm}] = 98.7$ and $z_3^{avg}/[\text{nm}] = 121.9$ for the weight percentages of $w_1 = 0.5\%$, $w_2 = 1.0\%$ and $w_3 = 1.5\%$.
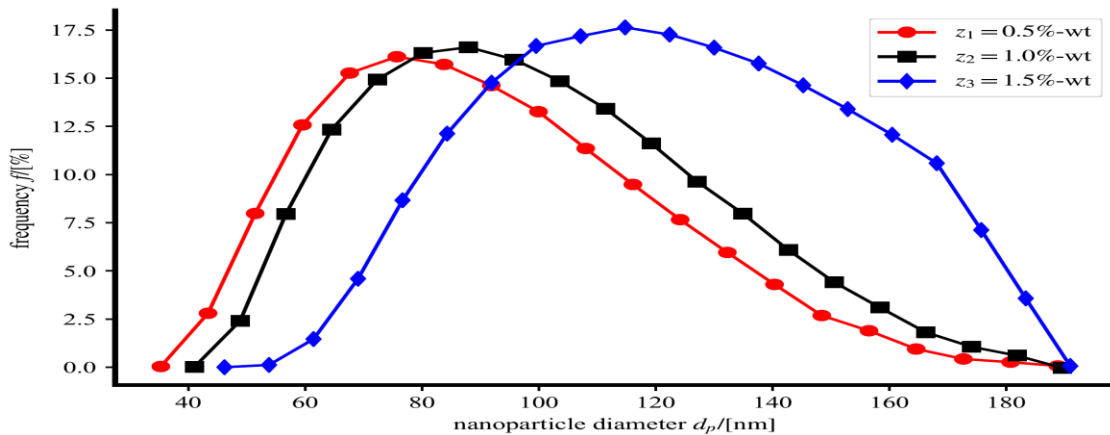
Figure 3-1 Illustration of typical experimental nanoparticle size data distributions based on data reported by Teng & Hung [33] which exhibits Gaussian or extended lambda distribution probability density function characteristics

In general based on physical intuition it is reasonable to expect that the underlying probability density function (PDF) for the nanoparticle diameter size would approximately follow a Gaussian PDF with an expected value μ and a standard deviation σ as qualitatively shown in the figure. One particular generalization of the classical Gaussian distribution that is more powerful is known as the extended lambda distribution (ELD) as previously discussed which models an underlying statistical distribution in terms of parameters a, b, c, d which are formally defined in terms of statistical moments as shown in Figure 3.2.
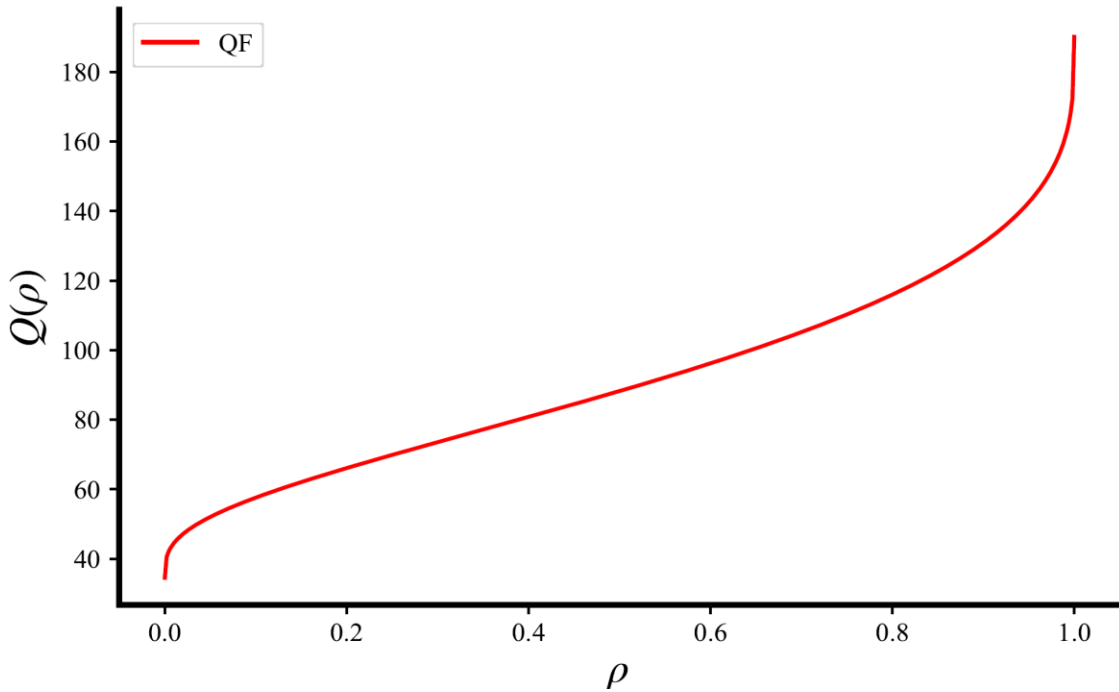
Figure 3-2 Illustration of corresponding quantile function for DLS frequency data

In order to use an extended lambda distribution we would first extract the underlying numerical data for the reported graphical data from Figure 3.1 and normalize it so that $\int_{-\infty}^{\infty} g(\eta) \, d\eta = 1$. Then since there are a finite number of discrete points and not an arbitrarily large number of points as in a full Monte Carlo simulation we would apply a standard curve fit regression using the standard least squares approach. The approach by Ramnath [92] for extracting the ELD parameters may be summarized as first setting

$$p_1 = 0.025, p_2 = 0.25, p_3 = 0.75, p_4 = 0.975 \tag{3.20}$$

and then calculate the terms ξ' and ξ'' defined as

$$\xi' = \frac{\theta_{p_4} - \theta_{p_1}}{\theta_{p_3} - \theta_{p_2}}, \xi'' = \frac{\theta_{p_4} - \theta_{p_2}}{\theta_{p_3} - \theta_{p_1}} \tag{3.21}$$

where the quantiles are calculated as $\theta_{p_i} = Q(p_i)$ respectively using the relations $\eta = Q(\rho)$ and $G(\eta) = \rho$ where $G(\eta) = \int_{-\infty}^{\eta} g(\xi) \, d\xi$ is corresponding distribution for the PDF $g(\eta)$ for the random variable η. Once ξ' and ξ' are calculated then the parameters a, b, c, d may be sequentially calculated as

$$\frac{p_1^b - (1-p_1)^b}{p_2^b - (1-p_2)^b} = \xi', b < 1.4 \tag{3.22}$$

$$a = \frac{\xi''\{(1-p_1)^b - (1-p_3)^b\} + (1-p_4)^b - (1-p_2)^b}{\xi''(p_1^b - p_3^b) + p_4^b - p_2^b} \tag{3.23}$$

$$c = \frac{b(\theta_{p_2} - \theta_{p_1})}{\{ap_2^b - (1-p_2)^b\} - \{ap_1^b - (1-p_1)^b\}} \tag{3.24}$$

$$d = \theta_{p_1} - \frac{c}{b}[ap_1^b - (1-p_1)^b + 1 - a] \tag{3.25}$$

An example of a reconstructed probability density function (PDF) that is generated from just the quantile parameters using the above formulae is shown in Figure 3.3 below whilst the orginal data compared to the extended lambda distribution (ELD) fit is shown in Figure 3.4.
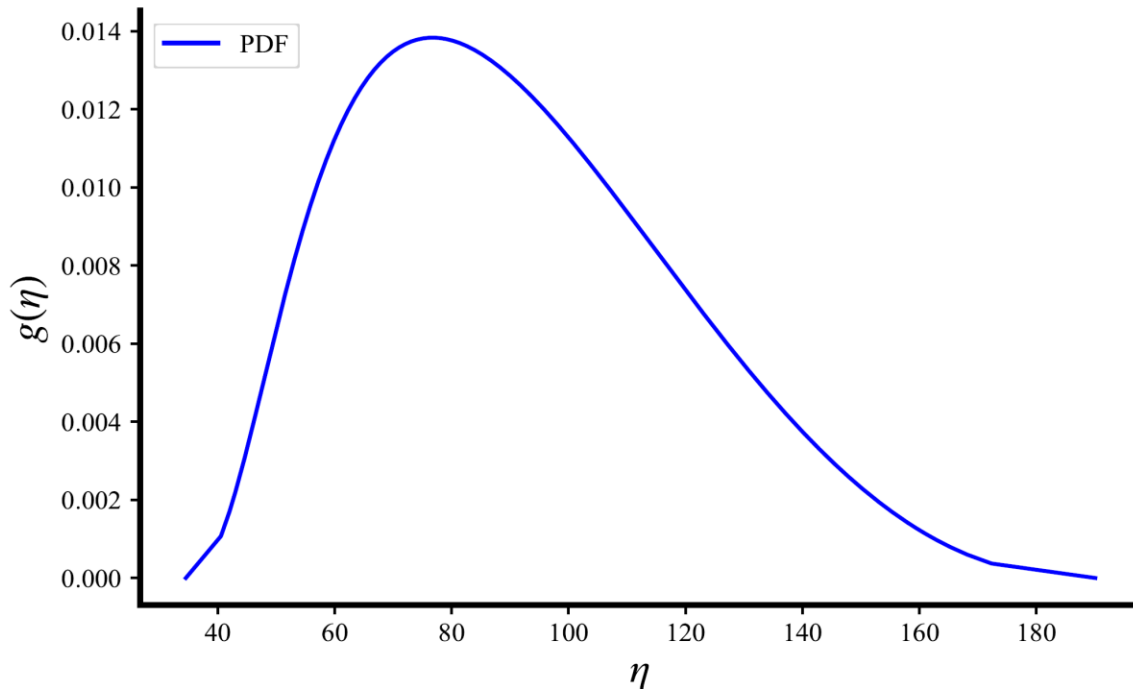
Figure 3-3 Illustration of corresponding PDF approximation constructed from quantile function of DLS frequency data
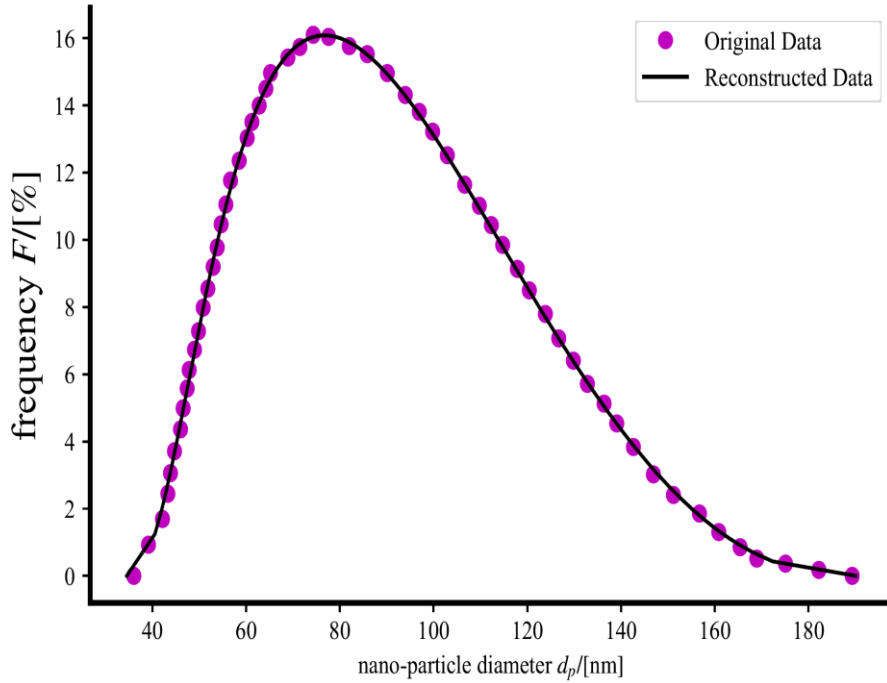
Figure 3-4 Illustration of comparison of original DLS frequency data and corresponding predictions from quantile function modelling approach for univariate probability density function scheme

When the above statistical scheme is applied to the extracted dynamic light scattering numerical data of the nanoparticle diameters d_p/[nm] from the reported graphical results in Figure 3.1 it results in the reconstructed data as shown in Figure 3.4 respectively from which it may be concluded that an extended lambda distribution can reasonably be used to approximate and reconstruct a variety of univariate PDF's.

The approach of using quantile function concepts such as extended lambda distributions to model univariate probability density functions which are of similar shape and characteristics to Gaussian distributions but which possibly exhibit slight asymmetries and/or skewness effects is now considered in many experimental statistics studies such as for example wind energy studies as reported by Anastasiades & McSharry [137]. The application of quantile functions consequently offers a relatively quick and simple approach to model the statistical behaviour of univariate parameters $a_1, \ldots, a_M$ in algebraic models $y = f(\mathbf{x}; \mathbf{a})$ where y is a quantity that is being modelled in terms of a univariate or multivariate input $\mathbf{x}$, $\mathbf{a}$ is a vector of parameters, and where the specific algebraic form of the model is known. Whilst the model parameter fitting process is relatively simple as outlined above we comment that the main challenge is in determining the specific type of algebraic model to investigate of which there may be numerous possibilities. In most practical cases the nanofluid thermal conductivity model k_{nf}^{M} will only depend on a parameter $\mathbf{a}$ and the viscosity model μ_{nf}^{M} will only depend on a parameter $\mathbf{b}$ however we consider the possibility that there may be interaction effects between the thermal conductivity and viscosity in which case both models will then formally depend on both $\mathbf{a}$ and $\mathbf{b}$. Considering the review of thermal conductivity and viscosity models by Yang *et al.*[138] that incorporate the

influence of both temperature and volume fraction as summarized in Table 3.1 we opt to first consider the model of the nanofluid thermal conductivity and viscosity utilizing potential functional characteristics as shown in Table 3.2 where k_p is the thermal conductivity of the nanoparticle and analytical models $k_{bf}^A(\mathbf{x})$ and $\mu_{bf}^A(\mathbf{x})$ are used to determine the base fluid thermophysical properties in order to illustrate how to mathematically model probability density function distributions of the uncertainties of the parameters in nanofluid models which will use the previous extended lambda distributions.

Author	Model
Kole & Dey [139]	$\log(\mu_{nf}) = Ae^{-BT}, A = -225.245\phi^2 + 18.404\phi + 1.749, B = 575.835\phi^3 - 32.101\phi^2 + 0.148\phi + 0.01$ for Al_2O_3-care engine coolant for $0.1 \le \phi/[\%] \le 3.5$
Namburu et al.[140]	$\log(\mu_{nf}) = Ae^{-BT}, A = 1.8375\phi^2 - 29.634\phi + 165.56, B = (4 \times 10^{-9})\phi^2 - 0.001\phi + 0.0186$ for CuO-EG/W for $2 \le \phi/[\%] \le 10$
Sharma et al.[141]	$\frac{\mu_{nf}}{\mu_{bf}} = 1.4\left(1 + \frac{\phi}{100}\right)^{11.3}\left(1 + \frac{T_{nf}}{70}\right)^{-0.038} + \left(1 + \frac{d_p}{170}\right)^{-0.061}$ for Si-water mixture
Nambura et al.[142]	$\log(\mu_{nf}) = Ae^{-BT}, A = 0.1193\phi^3 - 1.9289\phi^2 - 2.245\phi + 167.17, B = (-7 \times 10^{-6})\phi^2 - 0.0004\phi + 0.0192$ for SiO_2-EG/W for $2 \le \phi/[\%] \le 10$
Xuan et al.[143]	$k_{nf} = k_f\frac{k_p + 2k_f + 2\phi(k_p - k_f)}{k_p + 2k_f - \phi(k_p - k_f)} + \frac{1}{2}\rho_p C_p\phi\sqrt{\frac{k_B T}{3\pi\mu_f R_{cl}}}$ where R_{cl} is an apparent radius of the cluster
Koo & Kleinstreuer [144]	$k_{eff} = k_f\frac{k_p + 2k_f + 2\phi(k_p - k_f)}{k_p + 2k_f - \phi(k_p - k_f)} + (5 \times 10^4)\theta\rho_f C_{pf}\phi f(T,\phi)\sqrt{\frac{k_B T}{\rho_f d_p}}$ for CuO with $f(t,\phi) = (-6.04\phi + 0.4705)T + 1722.3\phi - 134.63$ where θ is the fraction of the liquid volume that travels with the nanoparticle

Table 3. 1 Selection of nanofluid thermophysical models that incorporate volume fraction and temperature effects

Model	Expression
$k_{nf}^M = k_{bf}^A\left[\frac{k_p + 2k_{bf}^A + 2\phi(k_p - k_{bf}^A)}{k_p + 2k_{bf}^A - \phi(k_p - k_{bf}^A)}\right] + a_1\phi\{(a_2\phi + a_3)T + a_4\phi + a_5\}\sqrt{\frac{T}{d_p}}$	
$\mu_{nf}^M = \exp\left[(d_p)^{b_1}(b_2\phi^2 + b_3\phi + b_4)\exp\{(b_5\phi^2 + b_6\phi + b_7)T\}\right]$	
$k_{nf}^M = \{a_1 + a_2(\phi_p)^{a_3}(d_p)^{a_4}\left(\frac{\mu_{nf}^M}{\mu_{bf}}\right)^{a_5} + a_6\frac{\phi_p}{T} + a_7\frac{(\phi_p)^2}{T^3} + a_8\frac{\phi_p}{T^2}\}k_{bf}^A$	
$\mu_{nf}^M = \left(1 + b_1(d_p)^{b_2}\phi^{b_3}\right)^{-1}\mu_{bf}^A$	

Table 3. 2 Selection of different possible proposed nanofluid models of effective thermal conductivity and viscosity

In order to formulate the approach to determine the parameters assume that the experimental data consist of N_k points for the thermal conductivity and N_μ points for the viscosity such that

$$D_k = \left\{k_{nf}^{(i)}, \mathbf{x}_i^k\right\}, i \in [1, \dots, N_k] \tag{3.26}$$

$$D_\mu = \left\{\mu_{nf}^{(j)}, \mathbf{x}_j^\mu\right\}, j \in [1, \dots, N_\mu] \tag{3.27}$$

where $\mathbf{x}^k$ or $\mathbf{x}^\mu$ for either the known thermal conductivity or viscosity data is as previously specified. Although $\mathbf{x}$ contains more information than is necessary to calculate the properties of the base fluid which are completely specified in terms of the temperature T and pressure p if there is a large variation in operating pressure, and whilst ϕ and d_p do not effect the properties of the base fluid we retain for simplicity the dependence on a vector of inputs for the analytical expressions $k_{bf}^A(\mathbf{x})$ and $\mu_{nf}^A(\mathbf{x})$. In general N_k may not necessarily be equal to N_μ depending on the particular available information either from a particular set of experiments or from data sources reported in the literature.

In the above generalized system for $k_{nf}^M(\mathbf{x}; \mathbf{a}, \mathbf{b})$ and $\mu_{nf}^M(\mathbf{x}; \mathbf{a}, \mathbf{b})$ the parameters $\mathbf{a}$ and $\mathbf{b}$ are constant and $\mathbf{x}$ is a variable input to account for different nanoparticle diameters d_p, volume concentrations ϕ and operating temperatures T at which the nanofluid will be used in practice. These assumptions are consistent with more recent results for example predictions for the nanofluid density ρ_{nf} as recently reported by Sharifpur *et al.*[35] which tend to restrict the choice of meta-parameters for nanofluid models to T, d_p and ϕ due to the limited range of operating pressures for many existing applications of in nanofluids. Whilst this assumption may not necessarily be appropriate for all physical applications such in some heat exchangers where the nanofluid is used as a coolant and is subjected to high operating pressures which may impact in some unknown sense on the nanofluid thermophysical properties that cannot be adequately adressed through the interaction of k_{nf} and μ_{nf} it is relatively simple to address at an abstract mathematical modelling level since we may in principle choose any appropriate choice of inputs $\mathbf{x} = [x_1, \dots, x_q]^T$ for an appropiate choice of $q \in \mathbb{N}$. An example of this approach is setting $q = 5$ and letting $\mathbf{x} = [T, d_p, \phi, p, \dot{\gamma}]^T$ to model pressure effects with p and shear strain effects with $\dot{\gamma}$ for particular nanofluid systems and configurations if there is an adequate knowledge of available experimental data for all of the model inputs $x_1, \dots, x_q$.

If a single-phase modelling approach for nanofluids is utilized to mitigate against the high computational costs of multi-phase models as discussed earlier by Moraveji & Ardehali [49] and more recently by Safaei *et al.*[58] then formally the interaction effects between the nanofluid thermal conductivity k_{nf}, viscosity μ_{nf}, density ρ_{nf} and enthalpy h_{nf} or equivalently the nanofluid specific heat c_{nf} should in principle be studied, although in practice only k_{nf} and μ_{nf} are usually considered to be correlated, whilst ρ_{nf} and h_{nf} are in various reported nanofluid models generally considered to be uncorrelated due to an absence of a available information. The corresponding mathematical problem under this particular set of assumptions and approximations as outlined is to then determine the optimal values of $\mathbf{a}$ and $\mathbf{b}$ that minizes the resultant errors in nanofluid thermophysical predictions with the use of the constructed equations for some domain Ω of input values $\mathbf{x} \in \Omega \subset \mathbb{R}^q, q = 3$. For simplicity the domain Ω may be considered as the hypercube constructed as a cartesian product such that $\Omega = [\min(x_1), \max(x_1)] \times [\min(x_2), \max(x_2)] \times [\min(x_3), \max(x_3)]$.

Conventional least squares regression analysis techniques as discussed by Press *et al.*[132] are usually applicable for the linear least squares form where the output y is constructed as a linear combination of possible non-linear functions such that $y = \sum_{k=1}^{N} a_k X_k(\mathbf{x}_k)$ however the particular problem in this research investigation is mathematically a fully non-linear multivariate

regression analysis problem. As a result traditional linear least squares univariate regression techniques for models of the form $z = f(x; \mathbf{a})$ where x is a univariate input, $\mathbf{a}$ is a vector parameter and z is a univariate output as investigated by Saunders [145] are not applicable since our problem is of the form $\mathbf{z} = \mathbf{f}(\mathbf{x}; \mathbf{c})$ if we consider instead a vector of model inputs $\mathbf{x}$, a vector of model parameters $\mathbf{c}$ and a vector of model outputs $\mathbf{z}$ where in our particular case we could simply set $z_1 = k_{nf}$ and $z_2 = \mu_{nf}$. Fortunately this more generalized mathematical problem for experimental measurement studies has a statistical solution in terms of the GUM Supplement 2 i.e. GS2 [146] if the non-linear multivariate functions can be expressed as a vector equation $\mathbf{h}(\mathbf{y}, \mathbf{x}) = \mathbf{0}$ where $\mathbf{x}$ is a vector input, $\mathbf{y}$ is a vector output and $\mathbf{0}$ is the zero-vector of dimension $\text{card}(\mathbf{y}) \times 1$. In the event that this model can be constructed then the GS2 multivariate Monte Carlo methodology reduces to solving the system

$$\mathbf{h}(\boldsymbol{\eta}_r, \boldsymbol{\xi}_r) = \mathbf{0}, r = 1, 2, \dots, M \tag{3.28}$$

where M is the number of Monte Carlo simulation events, $\boldsymbol{\xi}_r$ is a sampled random variable from the multivariate probability density function (PDF) distribution for $\mathbf{x}$, and $\boldsymbol{\eta}_r$ is the resultant solution which corresponds to an equivalent sampled value from the PDF of $\mathbf{y}$. Under these circumstances the expected value $\boldsymbol{\mu}$ of $\mathbf{y}$ and the covariance matrix $\mathbf{V}$ of $\mathbf{y}$ may then be approximated as

$$\boldsymbol{\mu} = \frac{1}{M}[\mathbf{y}_1 + \cdots + \mathbf{y}_M] \tag{3.29}$$
$$\mathbf{V} = \frac{1}{M-1}[(\mathbf{y}_1 - \boldsymbol{\mu}) \cdot (\mathbf{y}_1 - \boldsymbol{\mu})^{\mathrm{T}} + \cdots + (\mathbf{y}_M - \boldsymbol{\mu}) \cdot (\mathbf{y}_M - \boldsymbol{\mu})^{\mathrm{T}}] \tag{3.30}$$

In order to exploit the above results a mathematically equivalent function $\mathbf{h}(\mathbf{y}, \mathbf{x}) = \mathbf{0}$ is constructed in terms of an equivalent χ^2 system built up in terms of known experimental data where the solution is the resulting parameters from the χ^2 optimization as opposed to the nanofluid thermophysical properties. Following this approach first construct two χ^2 functions, χ_k^2 corresponding to the thermal conductivity data and χ_μ^2 corresponding to the viscosity data, such that

$$\chi_k^2 \stackrel{\text{def}}{=} \sum_{i=1}^{N_k} w_i^2 \left[k_{nf}^{\mathrm{D}}(\mathbf{x}_i^k) - k_{nf}^{\mathrm{M}}(\mathbf{x}_i^k; \mathbf{a}, \mathbf{b}) \right]^2 \tag{3.31}$$
$$\chi_\mu^2 \stackrel{\text{def}}{=} \sum_{j=1}^{N_\mu} w_j^2 \left[\mu_{nf}^{\mathrm{D}}(\mathbf{x}_j^\mu) - \mu_{nf}^{\mathrm{M}}(\mathbf{x}_j^\mu; \mathbf{a}, \mathbf{b}) \right]^2 \tag{3.32}$$

where w_i is an estimate of the uncertainties of the observed thermal conductivity values $k_{nf}^{\mathrm{D}}(\mathbf{x}_i), i \in [1, \dots, N_k]$ and w_j is similarly an estimate for the uncertainties of the observed viscosity values $\mu_{nf}^{\mathrm{D}}(\mathbf{x}_j), j = 1, \dots, N_\mu$. It may be now be observed that χ_k^2 and χ_μ^2 are now both technically functions of $\mathbf{a}$ and $\mathbf{b}$ for the specified data-sets D_k and D_μ since in general the nanofluid thermal conductivity and viscosity models are considered to be coupled. This problem is technically a multi-objective optimization since the χ_k^2 optimization determines the values of the parameters $\mathbf{a}$ and $\mathbf{b}$ for the optimal fit of the nanofluid thermal conductivity whilst the χ_μ^2 optimization determines the corresponding values of $\mathbf{a}$ and $\mathbf{b}$ for the optimal fit of the nanofluid viscosity, however for our particular problem since the nanofluid thermal conductivity and viscosity are both intrinsic physical properties they each carry equal weighting. Due to the fact that

in nanofluid mathematical studies both the thermal conductivity and viscosity are in general considered to be equally important thermophysical properties that must be modelled, unless otherwise specified for specific types of equipment/instruments that utilize the nanofluid as a working fluid, a simultaneous non-linear system of both of these merit functions in terms of an equivalent system equations may be constructed of the form

$$
\left.
\begin{aligned}
h_1(a_1, \ldots, a_m, b_1, \ldots, b_n) &= \frac{\partial \chi_k^2}{\partial a_1} \\
&\vdots \\
h_m(a_1, \ldots, a_m, b_1, \ldots, b_n) &= \frac{\partial \chi_k^2}{\partial a_m} \\
h_{(m+1)}(a_1, \ldots, a_m, b_1, \ldots, b_n) &= \frac{\partial \chi_k^2}{\partial b_1} \\
&\vdots \\
h_{(m+n)}(a_1, \ldots, a_m, b_1, \ldots, b_n) &= \frac{\partial \chi_k^2}{\partial b_n} \\
h_{(m+n+1)}(a_1, \ldots, a_m, b_1, \ldots, b_n) &= \frac{\partial \chi_\mu^2}{\partial a_1} \\
&\vdots \\
h_{(2m+n)}(a_1, \ldots, a_m, b_1, \ldots, b_n) &= \frac{\partial \chi_\mu^2}{\partial a_m} \\
h_{(2m+n+1)}(a_1, \ldots, a_m, b_1, \ldots, b_n) &= \frac{\partial \chi_\mu^2}{\partial b_1} \\
&\vdots \\
h_{(2m+2n)}(a_1, \ldots, a_m, b_1, \ldots, b_n) &= \frac{\partial \chi_\mu^2}{\partial b_n}
\end{aligned}
\right\} \text{coupled} - \text{system} \tag{3.33}
$$

The above system of equations form a coupled simultaneous system of non-linear equations in general, however the particular coupling effects will formally depend on the particular functional mathematical expressions that are used for $k_{nf}^{\mathrm{M}}(\mathbf{x}; \mathbf{a}, \mathbf{b})$ and $\mu_{nf}^{\mathrm{M}}(\mathbf{x}; \mathbf{a}, \mathbf{b})$.

In the special case that the mathematical expression for the nanofluid thermal conductivity k_{nf} does not depend on the nanofluid viscosity μ_{nf} and logically vice versa then the above system of equations may be uncoupled which then simplifies the subsequent calculations. As an example if the thermal conductivity only depends on the parameter **a** then then $\partial \chi_k^2 / \partial b_i = 0$ automatically whilst of the viscosity only depends on the parameter **b** then $\partial \chi_\mu^2 / \partial a_i = 0$ automatically so that the coupled system may be simplified as

$$\left.\begin{array}{rcl} \dfrac{\partial \chi_k^2}{\partial a_1} &=& 0 \\[2mm] &\vdots& \\[2mm] \dfrac{\partial \chi_k^2}{\partial a_m} &=& 0 \\[2mm] \dfrac{\partial \chi_\mu^2}{\partial b_1} &=& 0 \\[2mm] &\vdots& \\[2mm] \dfrac{\partial \chi_\mu^2}{\partial b_m} &=& 0 \end{array}\right\} \quad \text{uncoupled} - \text{system} \tag{3.34}$$

Making the observation that in any real nanofluid system there would almost inevitably be some sort of interaction effects however weak between the transport properties of the nanofluid's thermal conductivity, viscosity, density and enthalpy. For fluid systems where it necessary to consider the interaction effects between the nanofluid thermal conductivity and viscosity and an equal importance cannot be assigned then more advanced multi-objective optimization techniques can be used to determine the Pareto optimal solution for the parameters **a** and **b** in the event that there is a coupling between the nanofluid thermal conductivity and viscosity models in for example systems where the convective heat transfer coefficient must be accurately determined from the nanofluid thermal conductivity but viscosity effects that influence power requirements for the pumping of the nanofluid must also be accounted for.

When this system of equations are solved the results for $a_1, \dots, a_m$ and $b_1, \dots, b_n$ for each of the Monte Carlo simulation events may then be conveniently stored in matrices such that

$$\mathbf{A} = \begin{bmatrix} A_{1,1} & \cdots & A_{1,m} \\ \vdots & \vdots & \vdots \\ A_{r,1} & \cdots & A_{r,m} \\ \vdots & \vdots & \vdots \\ A_{M,1} & \cdots & A_{M,m} \end{bmatrix} \tag{3.35}$$

and

$$\mathbf{B} = \begin{bmatrix} B_{1,1} & \cdots & B_{1,m} \\ \vdots & \vdots & \vdots \\ B_{r,1} & \cdots & B_{r,m} \\ \vdots & \vdots & \vdots \\ B_{M,1} & \cdots & B_{M,m} \end{bmatrix} \tag{3.36}$$

In the above system of matrices each column will therefore store the corresponding Monte Carlo univariate data for a particular model parameter which can then be post-processed in order to determine its characteristic statistical properties, whilst the correlation effects between the model parameters may be recovered from the covariance matrix as previously discussed.

The above ELD technique may then be applied to the univariate data for $a_1, \dots, a_m$ and $b_1, \dots, b_n$

to work the corresponding expected values $\mu_{a_1}, \ldots, \mu_{a_m}$ and $\mu_{b_1}, \ldots, \mu_{b_n}$ and similarly the corresponding standard deviations may also be worked out as $\sigma_{a_1}, \ldots, \sigma_{a_m}$ and $\sigma_{b_1}, \ldots, \sigma_{b_n}$ respectively. Once the statistical information for the model parameters of k_{nf} and μ_{nf} have been determined then the corresponding uncertainties in the predicted nanofluid properties may be calculated with the aid of the Guide to Uncertainty in Measurement i.e. the GUM [53] such that the uncertainty for the nanofluid effective thermal conductivity is

$$
\begin{aligned}
u^2(k_{nf}) = &\sum_{i=1}^{q} \left(\frac{\partial k_{nf}}{\partial x_i}\right)^2 u^2(x_i) + \sum_{j=1}^{m} \left(\frac{\partial k_{nf}}{\partial a_j}\right)^2 u^2(a_j) \\
&+ \sum_{j=1}^{n} \left(\frac{\partial k_{nf}}{\partial b_j}\right)^2 u^2(b_j) + (\text{higher order \& correlation effects})
\end{aligned}
\tag{3.37}
$$

and similarly the uncertainty for the nanofluid effective viscosity is calculated as

$$
\begin{aligned}
u^2(\mu_{nf}) = &\sum_{i=1}^{q} \left(\frac{\partial \mu_{nf}}{\partial x_i}\right)^2 u^2(x_i) + \sum_{j=1}^{n} \left(\frac{\partial \mu_{nf}}{\partial b_j}\right)^2 u^2(b_j) \\
&+ \sum_{j=1}^{m} \left(\frac{\partial \mu_{nf}}{\partial a_j}\right)^2 u^2(a_i) + (\text{higher order \& correlation effects})
\end{aligned}
\tag{3.38}
$$

where q is the number of nanofluid meta-parameters, and m and n are respectively the number of parameters for the nanofluid effective thermal conductity and viscosity models. The above system of equations will simplify in the special case of uncoupled systems since the partial derivatives will evaluate to zero if there is no interaction effects. As a result this modelling scheme has therefore developed a potential mathematical analysis approach with the aid of the Monte Carlo based GUM Supplement 1 technique to in the case of algebraic models compute the parameters $a_1, \ldots, a_M$ and their associated uncertainties $u(a_1), \ldots, u(a_M)$ for arbitrary nanofluid effective thermal conductivity algebraic models, the parameters $b_1, \ldots, b_N$ and their associated uncertainties $u(b_1), \ldots, u(b_N)$ for arbitrary nanofluid effective viscosity models, and similarly for coupled arbitrary nanofluid effective thermal conductivity and effective viscosity models where there are interaction effects. The developed mathematical approach in this research investigation therefore solves the original research challenge of how to incorporate the modelling and incorporation of intrinsic aleatoric thermophysical data uncertainties so that the derived thermophysical predictions, in terms of the algebraic model and the associated parameters, now exhibits behaviour, properties and characteristics which is statistically consistent. Unfortunately this powerful mathematical functionality is reliant on the need for the specification of an appropriate algebraic model. As previously discussed at the present time of writing there does not yet exist a relatively complete theory of nanofluids which would inform the specification of an appropriate algebraic model. In the absence a particular choice of algebraic model defined in terms of a suitable selection of meta-parameters and algebraic equation parameters the remaining option is to perform an Exploratory Data Analysis (EDA) of possible algebraic models. Nevertheless if an appropriate algebraic model is selected either from an informed physical reasoning perspective or in terms of a statistical hypothesis testing approach our developed mathematical approach may still offer a potentially useful approach for the modelling of nanofluid thermophysical properties.

Due to the fact that many researchers have reported findings in the open literature on the relative performance and functionality of various algebraic nanofluid thermophysical property models these validated results may be used in lieu of a statistical hypothesis testing approach to obtain an approximation of the general form of the algebraic model by qualitatively comparing and contrasting algebraic models in order to infer possible trial functions that may then be investigated more fully with our developed mathematical approach.

For nanofluid systems where the nanofluid properties are defined in terms of enhancements to the base fluid properties knowledge of the base fluid density ρ_{bf}, thermal conductivity k_{bf} and viscosity μ_{bf} are also necessary to complete the mathematical modelling process. Under these circumstances the CIPM water density formula as discussed by Harvey *et al.*[147] is used to calculate the base fluid density $\rho/[\text{kg m}^{-3}]$ in terms of the water temperature $t/[°\text{C}]$, the thermal conductivity for water $k_{bf}/[\text{W m}^{-1} \text{ K}^{-1}]$ is in specified in terms of a formula by Ramires *et al.*[108], and an analytical expression for the viscosity of water $\mu_{bf}/[\text{Pa s}]$ is approximated using an expression by Huber *et al.*[110]. As a result the actual nanofluid properties such as effective thermal conductivities and effective viscosities may be calculated or at least approximated from the reported data in the open literature using these formulae as a first step to convert from nanofluid enhancements relative to a base fluid such as water and back to the original actual nanofluid thermophysical properties in pursuing our developed mathematical approach even if not all of the data and results from the open literature is in a convenient and easy to use form.

In order to implement and demonstrate the developed mathematical approach of this research investigation utilization and analysis of the experimental data reported by Ghanbarpour *et al.*[61] for a water/alumina nanofluid mixture which documents the dynamic light scattering (DLS) measurements of the nanoparticle diameters, the nanofluid thermal conductivity $k_{nf}/[\text{W m}^{-1} \text{ K}^{-1}]$ for combinations of temperatures $T/[\text{K}]$ and mass fractions $w/[\%]$, and the nanofluid viscosity $\mu_{nf}/[\text{Pa s}]$ also for combinations of temperatures $T/[\text{K}]$ and mass fractions $w/[\%]$ is considered for illustrative purposes as summarized in Table 3.3. For this particular data-set there are constant uncertainties for the measured thermal conductivity and viscosity values of the nanofluid and as a result the weighting factors w_i and w_j are constant and may then be factored out since they will not effect the merit function optimization.

The first step is to use the DLS data obtained from transmission electron microscopy measurements and obtain estimates for the expected value of the nanoparticle diameter d_p and its associated uncertainty $u(d_p)$. This is achieved by fitting the DLS data with an extended lambda distribution such that the ELD parameters are calculated as $a = 0.35843$, $b = 0.22358$, $c = 63.78722$ and $d = 186.40116$.

The known ELD parameters can then be used to calculate the expected value and variance which for the particular data produce results as $\mu = 219.84710$ and $\sigma = 56.64047$ respectively from the analytical formulae so that

$$d_p = 219.847 \text{ nm} \tag{3.39}$$
$$u(d_p) = 56.640 \text{ nm} \tag{3.40}$$

T/[K]	k/[W/m.K]	phi	T/[K]	mu/Pa.s]	phi
2.93147E+02	5.92310E-01	0.00000E+00	2.93009E+02	1.00000E-03	0.00000E+00
3.03036E+02	6.10802E-01	0.00000E+00	3.03041E+02	7.94118E-04	0.00000E+00
3.12926E+02	6.33075E-01	0.00000E+00	3.12969E+02	6.47059E-04	0.00000E+00
3.22912E+02	6.50303E-01	0.00000E+00	3.22997E+02	5.58824E-04	0.00000E+00
2.93052E+02	6.09961E-01	5.84426E-03	2.93105E+02	1.18382E-03	5.84362E-03
3.03040E+02	6.34751E-01	5.72208E-03	3.02833E+02	9.77941E-04	5.72465E-03
3.12927E+02	6.43159E-01	5.59806E-03	3.12964E+02	8.30882E-04	5.59760E-03
3.22913E+02	6.57866E-01	5.46971E-03	3.22993E+02	6.98529E-04	5.46867E-03
2.93054E+02	6.20045E-01	1.19870E-02	2.93104E+02	1.22059E-03	1.19858E-02
3.03042E+02	6.43574E-01	1.17379E-02	3.03035E+02	1.00000E-03	1.17381E-02
3.13128E+02	6.74663E-01	1.14798E-02	3.13066E+02	8.08824E-04	1.14815E-02
3.23020E+02	7.13323E-01	1.12204E-02	3.22992E+02	7.27941E-04	1.12212E-02
2.93057E+02	6.41473E-01	1.84516E-02	2.93002E+02	1.24265E-03	1.84537E-02
3.03045E+02	6.63742E-01	1.80706E-02	3.03034E+02	1.02206E-03	1.80711E-02
3.12934E+02	6.84755E-01	1.76837E-02	3.13066E+02	7.94118E-04	1.76784E-02
3.23118E+02	7.13319E-01	1.72750E-02	3.22890E+02	7.64706E-04	1.72842E-02
2.93065E+02	6.86851E-01	3.24533E-02	2.93099E+02	1.38971E-03	3.24510E-02
3.03053E+02	7.12902E-01	3.17925E-02	3.02929E+02	1.13971E-03	3.18008E-02
3.13038E+02	7.22566E-01	3.11144E-02	3.12859E+02	9.41176E-04	3.11267E-02
3.23023E+02	7.29710E-01	3.04186E-02	3.22888E+02	8.30882E-04	3.04281E-02
2.93069E+02	7.14582E-01	4.53617E-02	2.93097E+02	1.48529E-03	4.53592E-02
3.03057E+02	7.40633E-01	4.44502E-02	3.03028E+02	1.22794E-03	4.44529E-02
3.13044E+02	7.59121E-01	4.35140E-02	3.12959E+02	1.00735E-03	4.35221E-02
3.22937E+02	8.00302E-01	4.25621E-02	3.22988E+02	8.75000E-04	4.25571E-02
2.93185E+02	8.20459E-01	7.53057E-02	2.92885E+02	1.81618E-03	7.53491E-02
3.02975E+02	8.38955E-01	7.38676E-02	3.02919E+02	1.50000E-03	7.38760E-02
3.12962E+02	8.57443E-01	7.23593E-02	3.12952E+02	1.24265E-03	7.23609E-02
3.22948E+02	8.73410E-01	7.08090E-02	3.22982E+02	1.06618E-03	7.08037E-02
2.93200E+02	9.16257E-01	1.12435E-01	2.92966E+02	2.50735E-03	1.12484E-01
3.03091E+02	9.46093E-01	1.10351E-01	3.02903E+02	2.06618E-03	1.10391E-01
3.13176E+02	9.65838E-01	1.08162E-01	3.13040E+02	1.69853E-03	1.08192E-01
3.22969E+02	9.99460E-01	1.05974E-01	3.23173E+02	1.47794E-03	1.05927E-01
2.93232E+02	1.11415E+00	1.59667E-01	2.92829E+02	3.72059E-03	1.59779E-01
3.03024E+02	1.13643E+00	1.56890E-01	3.02874E+02	3.05147E-03	1.56933E-01
3.13009E+02	1.14358E+00	1.53968E-01	3.12916E+02	2.48529E-03	1.53996E-01
3.22899E+02	1.16963E+00	1.50983E-01	3.22849E+02	2.17647E-03	1.50998E-01

Table 3. 3 Experimental nanofluid thermal conductivity and viscosity data by Ghanbarpour et al.[61]

Different possible choices of quantifying the nanoparticle size are technically possible since this quantification is usually undertaken either with scanning electron microscope (SEM) or transmission electron microscope (TEM) images which may be used to estimate the effective nanoparticle diameter d_p with different weighting schemes, whilst dynamic light scattering

95

(DLS) measurements quantify the hydrodynamic size R_{hyd} of the Al_2O_3 nanoparticles instead defined as

$$R_{hyd} \overset{\text{def}}{=} \frac{1}{N^2} \left\langle \sum_{i \neq j} \frac{1}{r_{ij}} \right\rangle \tag{3.41}$$

where N is the number of nanoparticles, r_{ij} is the distance between particle i and particle j, and $\langle \cdot \rangle$ is the corresponding ensemble average that is appropriately defined. Different ensemble average schemes are possible and include the microcanonical ensemble (isolated system with E, V, N constant), canonical ensemble (closed system, V and N constant, but energy exchange is possible so E is not constant) and grand canonical ensemble (open system with V constant, but energy exchange and particle exchange possible so E and N are not constant) average schemes. In general the above hydrodynamic length, either a hydrodynamic radius R_{hyd} or equivalent diameter D, obtained from dynamic light scattering measurements is considered an equivalent type of mean effective diameter based on how monochromatic light such as that from a laser is scattered by the population of nanoparticles, however we comment that this equivalent DLS based diameter is not necessarily correlated to the nanoparticle diameter d_p due to the particular choice of ensemble $\langle \cdot \rangle$ average used in the calculation from the physical experimental light scattering measurements and how the nanoparticles are clustered or agglomerated together. Different techniques are available to analyse the light scattering information in order to construct the auto-correlation function that is then used to work out the ensemble average and include first-order and second-order correlation schemes that can be used to model how the transmitted light through the collection of nanoparticle decays over time, however the experimental technique is generally considered more reliable when (i) the underlying particles do not interact with each other through collisions, and when (ii) there are no electrostatic forces between the ions of the particles. Both of these preferred conditions are not fully satisfied in the case of nanofluids since the nanoparticles in agglomerations by definition interact with each other and condition (i) can only be more fully satisfied in the special case of dilute mixtures i.e. for situations in the Einstein concentration limit, and that there is the experimentally observable and verified phenomenon of the nanolayer in many nanoparticles which produces a charge distribution around the outer surface of a nanoparticle and which consequently induces electrostatic forces between individual nanoparticles in the agglomeration which makes up the ensemble that is physically measured through the light scattering data. As a result through a combination of physical and statistical issues the use of dynamic light scattering data and results in certain situations may be less consistent than simpler number or area averaged SEM/TEM based estimates of the nanoparticle diameter d_p, or alternative experimental techniques such as X-ray diffraction based measurements.

In general the SEM/TEM based estimates use either arithmetic or equivalent area averages to estimate d_p which for this data set is roughly $d_p \approx 75$ nm whilst the DLS estimate is $D \approx 220$ nm. This observation illustrates that the variation of sizes between individual nanoparticles i.e. 'collections of molecules' such that $d_p/[\text{nm}] = \mathcal{O}(10^1)$ and that of agglomerations i.e. collections of "clumped together nanoparticles' such that $\mathcal{A}/[\text{nm}] = \mathcal{O}(10^2)$ may approach an order of magnitude. Relatively few data sources in the open literature consistently report on measurements of both SEM/TEM nanoparticle diameters and DLS based diameters and in certain sources such as that by Ho *et al.*[122] the SEM/TEM nanoparticle is 33 nm whilst light

scattering measurements of the hydrodynamic diameter range from 129 nm at a volume fraction of $\phi = 0.1\%$ to 167 nm at a volume fraction of $\phi = 4\%$ suggesting that the hydrodynamic diameter itself is a function of the temperature and volume concentration. As per the earlier discussion in the previous chapter in this dissertation we will generally utilize estimates of the nanoparticle diameter d_p where available as a convenient meta-parameter since anecdotal experimental evidence from the literature review is suggestive that the nanoparticle diameter d_p is a more statistically relevant choice of meta-parameter than that of the agglomeration size $\mathcal{A}$. At the present of writing there does not exist a definitive explanation as to why this is the case in the absence of a relatively complete theory of nanofluids however we postulate in this dissertation that this could potentially be the case through a combination of two underlying physical reasons namely that (i) the nanoparticle diameter d_p is a more physically relevant scale in nanofluids due to the fact there exists complex and potentially random flow characteristics that manifests at length scales from 0.1 nm to 1 nm i.e. for flows at length scales approximately the same size as individual nanoparticles, and that (ii) shear stresses within the fluid "break up" the original 'dry' agglomerations that are used to manufacture the nanofluid so that the new effective or 'wet' agglomeration may physically differ in size from the original 'dry' agglomeration. Many investigators have speculated that one of the potential underlying causes as to why nanofluids may be so effective in terms of heat transfer characteristics is due to their high specific-surface-area (SSA) which means that an indication of nanoparticle diameters may offer a better indication of the heat transfer properties of a nanofluid than that of an agglomeration size based on clusters of nanoparticles. As previously discussed at the present time of writing there does not exists a convenient and easy to use experimental technique to perform *in situ* physical measurements of nanoparticles that have already been doped in a base fluid since it is considered physically impossible to resolve the motion and geometry of individual collections of molecules within a fluid due both to the random Brownian motion of the molecules as well the challenging experimental constraints posed by the relevant length scales. Whilst SEM and TEM techniques can resolve two dimensional images at a sub-nanometre length scale and that atomic force microscope (AFM) measurement can to a certain extent measure three dimensional geometries that the accuracy of AFM measurements at the present time of writing is rough ± 0.3 nm at the 3σ standard level and is expected to reduce to about 0.2 nm in the next eight years by 2024 as discussed by Hussain *et al.*[148] however this is strictly for dry samples and no techniques exist that can directly as opposed to indirectly measure wet samples.

The combination of these two potential physical manifestations therefore leads us to suspect that it is potentially more useful to simply use an estimate of the nanoparticle diameter d_p as a conservative choice of meta-parameter, since a choice of d_p would potentially enable a CFD analyst to better refine predictions of the flow characteristics at the interface of nanoparticles and the surrounding fluid medium, whether with single-phase or multi-phase nanofluid models, and to more accurately simulate the potential break-up of agglomerations of nanoparticles as a potential future area of research investigation. Regardless of the extent to which these postulates may physically be exhibited and which in principle could only be adequately investigated at an *ab initio* level using molecular dynamics simulations the choice of nanoparticle diameters is the conventional modelling choice in the majority of investigations that have been reported in the open literature and we thus opt to utilize the prevailing existing convention for consistency and simplicity.
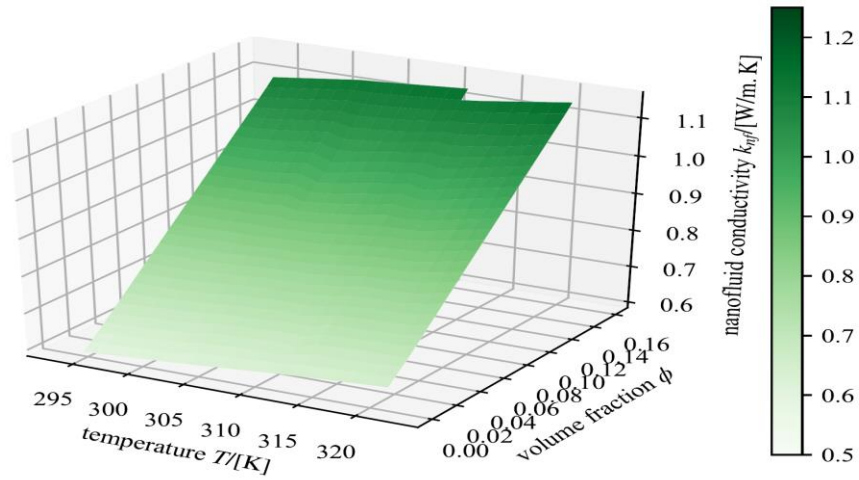
Figure 3-5 Visualization of water/alumina nanofluid thermal conductivity behaviour as a function of temperature and nanoparticle volume concentration
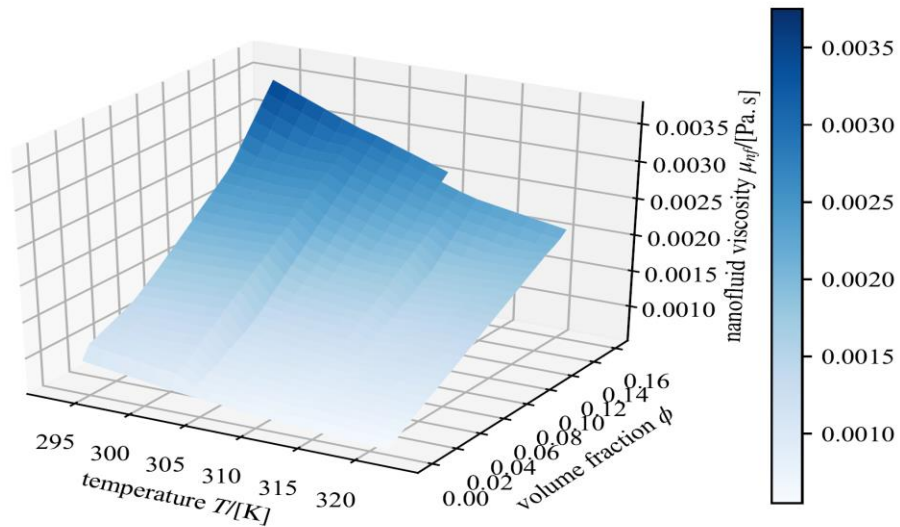
Figure 3-6 Visualization of water/alumina nanofluid viscosity behaviour as a function of temperature and nanoparticle volume concentration

Since the same nanofluid is used in the experimental results of Ghanbarpour *et al.*[61] the above nanoparticle diameter values are considered constant and as a result k_{nf} and μ_{nf} may be visualized as functions of the remaining inputs of the temperature T and volume fraction ϕ when the volume fractions are recovered from the weight fractions.

Due to the fact that nanofluids are prepared with mass fractions it is necessary to convert between the mass fraction w and volume fraction ϕ which are related by the following equations

$$\frac{1-w}{w}\frac{\rho_p}{\rho_f} = \frac{1-\phi}{\phi} \tag{3.42}$$

$$\phi = \frac{1}{1+\left(\frac{1-w}{w}\right)\frac{\rho_p}{\rho_f}} \tag{3.43}$$

In order to perform the conversion between mass fractions w and volume fractions ϕ assume a density and thermal conductivity for the nanoparticles as

$$\rho_p = 3880 \ \text{kg} \ \text{m}^{-3} \tag{3.44}$$
$$k_p = 18 \ \text{W} \ \text{m}^{-1} \ \text{K}^{-1} \tag{3.45}$$

The results for the volume fractions when processed using these formulae are illustrated in Figure 3.5 and Figure 3.6 respectively. For illustrative purposes only assume standard uncertainties at a 1σ confidence level for the temperature T as ± 0.5 K, for the volume fraction ϕ as $\pm 2.5\%$ and for the nanofluid thermal conductivity as $\pm 2.5\%$ so that the uncertainties in the Monte Carlo simulation are

$$\left. \begin{array}{lcl} u(d_p) & = & 56.640 \ \text{nm} \\ u(T) & = & 0.5 \ \text{K} \\ u(\phi) & = & 0.003775 \\ u(k_{nf}) & = & 0.029241 \end{array} \right\} \tag{3.46}$$

In order to illustrate the methodology consider the uncoupled nanofluid thermal conductivity model of the form

$$k_{nf}^{\text{M}} = k_{bf}\frac{k_p+2k_{bf}+2\phi(k_p-k_{bf})}{k_p+2k_{bf}-\phi(k_p-k_{bf})} + (a_1\phi^2 T + a_2\phi T + a_3\phi^2 + a_4)\sqrt{\frac{T}{d_p}} \tag{3.47}$$

The above equation k_{nf}^{M} is a new proposed nanofluid effective thermal conductivity algebraic model that we postulate may offer a potentially useful mathematical model for a water/alumina nanofluid based on an analysis of different possible algebraic models that were considered in the course of the literature review from the previous chapter. Rearranging this equation then yields

$$\sqrt{\frac{T}{d_p}}\phi^2 T a_1 + \sqrt{\frac{T}{d_p}}\phi T a_2 + \sqrt{\frac{T}{d_p}}\phi^2 a_3 + \sqrt{\frac{T}{d_p}}a_4 = k_{nf} - k_{bf}\frac{k_p+2k_{bf}+2\phi(k_p-k_{bf})}{k_p+2k_{bf}-\phi(k_p-k_{bf})} \tag{3.48}$$

As a result the nominal fitted values of the constants for the thermal conductivity model $k_{nf}^{\text{M}}(\mathbf{x}^k, \mathbf{a})$ using a least squares solution from the experimental data previously summarized in Table 3.3 produces the initial results as shown in Figure 3.7 where the nominal starting values are

$$\left. \begin{array}{lcl} a_1 & = & 2.041489 \times 10^{-6} \\ a_2 & = & 8.373330 \times 10^{-8} \\ a_3 & = & -5.816567 \times 10^{-4} \\ a_4 & = & -9.099597 \times 10^{-7} \end{array} \right\} \text{nominal starting values} \tag{3.49}$$
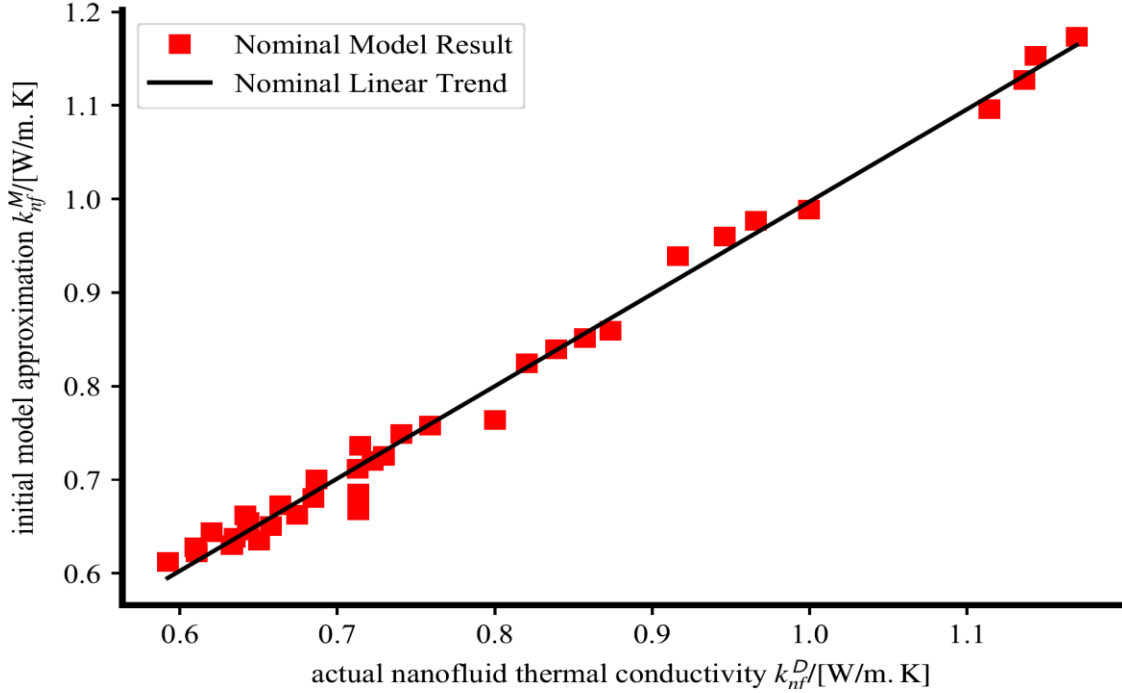
Figure 3-7 Illustration of nominal least squares fitted model results

These values may then be utilized as approximate starting solutions solutions for the χ_k^2 minimization by solving $\partial\chi_k^2/\partial a_i = 0, i = 1, \dots, m$ in the implementation of the corresponding Monte Carlo simulation using for example $M = 500$ simulation events for convenience in mathematical algebraic modelling approach. In order to perform the simulation analytical expressions for the partial derivative terms of the nanofluid models are necessary which can be readily computed with the aid of commercial computer algebra systems (CAS's) such as Mathematica or in mixed symbolic/numerical open source programs using toolboxes like OctSymPy which combines the symbolic capability of the Python CAS library sympy with the numerical functionality of Gnu Octave as discussed by McDonald [106]. The general form for an uncoupled thermal conductivity model using our notation takes the form

$$\frac{\partial\chi_k^2}{\partial a_i} = -2\sum_{j=1}^{N_k} \left\{ \left[k_{nf}^{\mathrm{D}}(\mathbf{x}_j^k) - k_{nf}^{\mathrm{M}}(\mathbf{x}_j^k, \mathbf{a}) \right] \cdot \frac{\partial k_{nf}^{\mathrm{M}}(\mathbf{x}_j^k, \mathbf{a})}{\partial a_i} \right\} \tag{3.50}$$

Monte Carlo simulations for the above optimization may be performed assuming Gaussian distributions for the PDF's of the uncertainties in temperature, nanoparticle diameter and volume concentration where sampled values ξ are in general generated as

$$\xi = \mu + \sigma r \tag{3.51}$$

where μ is the expected value which we assume is the measured value in the experimental data-set D_k, σ is the standard uncertainty of the measured values as previously specified, and r is a

random number sampled from the appropriate PDF distribution such as either a rectangular distribution $R[0,1]$ or alternately from a Gaussian PDF distribution. The results from the Monte Carlo simulation are summarized in Table 3.4 as indicated below.

k_{nf}^{M} parameter a_i	ELD a_i	ELD b_i	ELD c_i	ELD d_i	ELD μ_i	ELD σ_i
	2.52280E-01	2.54902E-01	2.02777E-06	1.08463E-06	2.29286E-06	1.60029E-06
	8.19417E-01	5.79271E-02	2.19306E-08	6.79756E-08	7.17190E-08	3.28875E-08
	8.17021E-02	4.17837E-01	-7.93275E-04	-1.28865E-04	-6.42650E-04	4.43652E-04
	1.12220E+00	2.89914E-02	-1.31776E-07	-8.36055E-07	-8.20406E-07	2.41523E-07

Table 3. 4 Summary of nanofluid thermal conductivity Monte Carlo simulation results using extended lambda distribution parameters

so that

$$
\left.\begin{aligned}
a_1 &= (2.29286 \times 10^{-6}) \pm (1.60029 \times 10^{-6}) \\
a_2 &= (7.17190 \times 10^{-8}) \pm (3.28875 \times 10^{-8}) \\
a_3 &= (-6.42650 \times 10^{-4}) \pm (4.43652 \times 10^{-4}) \\
a_4 &= (-8.20406 \times 10^{-7}) \pm (2.41523 \times 10^{-7})
\end{aligned}\right\} \tag{3.52}
$$

When these results are post-processed the corresponding model uncertainties can then be calculated as

$$
u^2(k_{nf}^{M}) = \left(\frac{\partial k_{nf}^{M}}{\partial T}\right)^2 u^2(T) + \left(\frac{\partial k_{nf}^{M}}{\partial \phi}\right)^2 u^2(\phi) + \left(\frac{\partial k_{nf}^{M}}{\partial d_p}\right)^2 u^2(d_p) + \sum_{j=1}^{4}\left(\frac{\partial k_{nf}^{M}}{\partial a_j}\right)^2 u^2(a_i) \quad (3.53)
$$

as summarized in Table 3.5.

Referring to this table it is observed that the normalized errors defined as

$$
E_n = \frac{y^{\text{model}} - y^{\text{actual}}}{\sqrt{U^2(y^{\text{actual}}) + U^2(y^{\text{model}})}} \tag{3.54}
$$

from standard measurement theory practice are all less than unity i.e. $\| E_n \| \leq 1$ for all the reported experimental measurement data points and as a result it is concluded that the method developed has been statistically validated and verified.

By inspecting the percentage errors it is also observed that all of the calculated results from the proposed model and associated uncertainty analysis deviate by less than 5% as shown in Figure 3.8 which is consistent with the original results by Ghanbarpour *et al.*[61] however our approach allows for the explicit mathematical calculation of the nanofluid thermal conductivity uncertainties directly in terms of the physical uncertainties $u(T)$, $u(\phi)$ and $u(d_p)$, and specifically quantifies the parameter uncertainties $u(a_j), j = 1,2,3,4$ for our particular choice of thermal conductivity model.

T	phi	knfData	U(knfData)	knfModel	U(knfModel)	En	Error
293.15	0.00000	0.59231	0.05848	0.61560	0.02700	0.36155	3.932
303.04	0.00000	0.61080	0.05848	0.62583	0.02757	0.23239	2.460
312.93	0.00000	0.63308	0.05848	0.63336	0.02810	0.00437	0.045
322.91	0.00000	0.65030	0.05848	0.63823	0.02861	-0.18545	-1.857
293.05	0.00584	0.60996	0.05848	0.63024	0.02723	0.31441	3.325
303.04	0.00572	0.63475	0.05848	0.64068	0.02785	0.09153	0.934
312.93	0.00560	0.64316	0.05848	0.64824	0.02844	0.07821	0.791
322.91	0.00547	0.65787	0.05848	0.65309	0.02899	-0.07313	-0.726
293.05	0.01199	0.62004	0.05848	0.64595	0.02889	0.39716	4.178
303.04	0.01174	0.64357	0.05848	0.65655	0.02956	0.19794	2.015
313.13	0.01148	0.67466	0.05848	0.66433	0.03021	-0.15705	-1.532
323.02	0.01122	0.71332	0.05848	0.66911	0.03080	-0.66892	-6.198
293.06	0.01845	0.64147	0.05848	0.66270	0.03380	0.31429	3.309
303.04	0.01807	0.66374	0.05848	0.67353	0.03446	0.14415	1.474
312.93	0.01768	0.68476	0.05848	0.68134	0.03507	-0.05010	-0.499
323.12	0.01727	0.71332	0.05848	0.68636	0.03565	-0.39355	-3.779
293.06	0.03245	0.68685	0.05848	0.69977	0.06093	0.15295	1.881
303.05	0.03179	0.71290	0.05848	0.71132	0.06131	-0.01863	-0.221
313.04	0.03111	0.72257	0.05848	0.71975	0.06159	-0.03317	-0.390
323.02	0.03042	0.72971	0.05848	0.72506	0.06174	-0.05471	-0.638
293.07	0.04536	0.71458	0.05848	0.73490	0.10574	0.16819	2.844
303.06	0.04445	0.74063	0.05848	0.74741	0.10578	0.05607	0.915
313.04	0.04351	0.75912	0.05848	0.75661	0.10560	-0.02079	-0.331
322.94	0.04256	0.80030	0.05848	0.76247	0.10520	-0.31428	-4.727
293.18	0.07531	0.82046	0.05848	0.82034	0.27427	-0.00043	-0.015
302.98	0.07387	0.83896	0.05848	0.83577	0.27359	-0.01137	-0.379
312.96	0.07236	0.85744	0.05848	0.84778	0.27226	-0.03470	-1.127
322.95	0.07081	0.87341	0.05848	0.85602	0.27027	-0.06290	-1.991
293.20	0.11243	0.91626	0.05848	0.93363	0.60247	0.02870	1.896
303.09	0.11035	0.94609	0.05848	0.95518	0.60119	0.01504	0.960
313.18	0.10816	0.96584	0.05848	0.97266	0.59843	0.01134	0.706
322.97	0.10597	0.99946	0.05848	0.98527	0.59431	-0.02376	-1.420
293.23	0.15967	1.11415	0.05848	1.09086	1.20857	-0.01925	-2.091
303.02	0.15689	1.13643	0.05848	1.12294	1.20788	-0.01115	-1.187
313.01	0.15397	1.14358	0.05848	1.15028	1.20432	0.00556	0.586
322.90	0.15098	1.16963	0.05848	1.17193	1.19788	0.00192	0.197

Table 3. 5 Summary of nanofluid thermal conductivity uncertainty analysis validation results using normalized errors and percentage errors
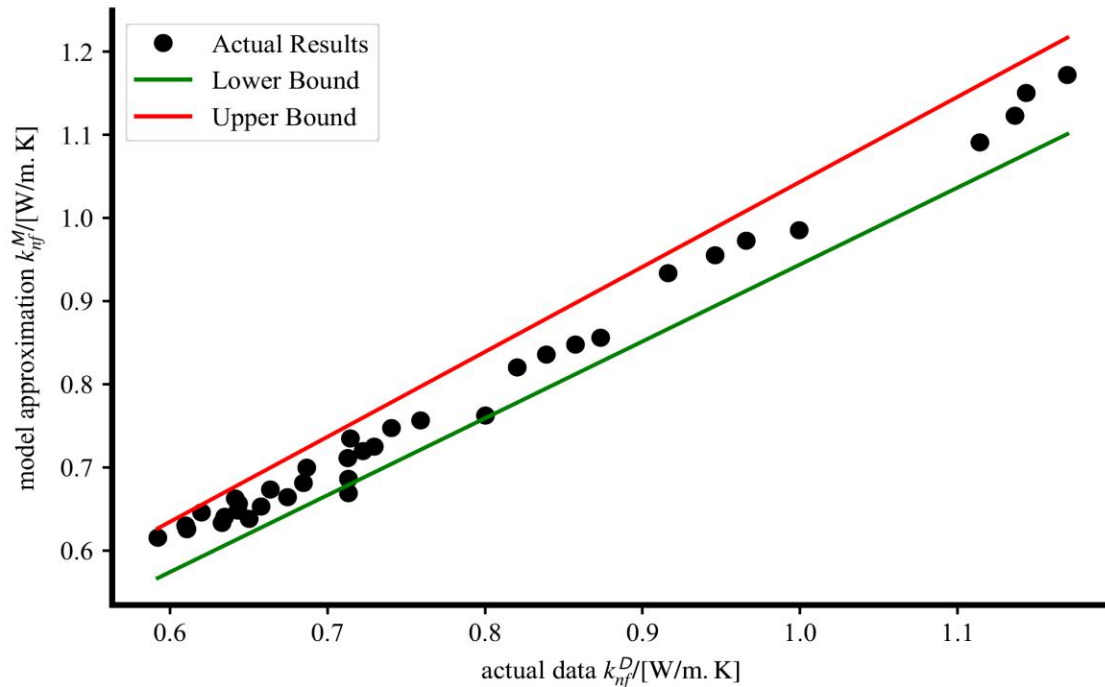
Figure 3-8 Illustration of lower and upper 5% bound limits for nanofluid thermal conductivity results

A key advantage of our developed methodology is that it allows for the analytical incorporation of the influence of all three meta-parameters T, ϕ and d_p on the nanofluid thermal conductivity which was previously mainly restricted to viscosity models. This completes the implementation of our developed mathematical modelling approach that addresses the original research objective of how to incorporate aleatory statistical uncertainties so that resultant model predictions are statistically consistent and accurate.

As a result it has therefore been demonstrated how experimental measurement uncertainties may be mathematically incorporated as parameter uncertainties into explicitly defined mathematical models using multivariate Monte Carlo based numerical simulations as an extension to nonlinear multivariate regression analysis and parameter estimation techniques. This methodology which has been outlined is completely general and can incorporate both coupled nanofluid thermal conductivity and viscosity models where there are interaction effects as well as in uncoupled models where interaction effects are not present. When the technique is numerically implemented estimates for nanofluid model parameter expected values, variances and correlations are all quantified in terms of probability density function statistical distributions which then allows for the explicit analytical calculation of the resultant nanofluid uncertainties that is inclusive of both the uncertainties in physical equipment/instrumentation that utilize a nanofluid as a working fluid as well as the intrinsic aleatory uncertainties of the nanofluid model itself in accordance with the Guide to Uncertainty in Measurement (GUM) based specifications for rigorous high accuracy experimental measurement research work, however this approach is mathematically and numerically challenging. The mathematical challenge is in identifying what algebraic model to

103

utilize and the numerical challenge is in terms of determining the starting estimates of the parameter values for the merit function optimization. An additional challenge that is also sometimes not fully appreciated by many researchers is that convergence is only formally mathematically possible in the case of convex functions in higher dimensional spaces as discussed in more detail by Johansson [150].

The first mathematical modelling approach in this research investigation therefore considered arbitrary algebraic models where univariate probability density functions were used to model and characterize the statistical information of the parameters so that the combination of the chosen algebraic model and parameters adequately and accurately incorporated the relevant underlying experimental measurement information used to build the nanofluid mathematical model. The next logical research question for mathematical completeness that must now be addressed is how to model two dimensional bivariate data and we comment that in general this may be achieved through the use of bivariate PDF's using for example copulas which may be in principle be extended to arbitary dimensions as outlined by Ramnath [151], however although multivariate PDF's may be adequately modelled if the underlying statistical data is available this is only possible if the underlying data is quantitative in nature. The modelling challenge in nanofluids studies is that the clustering of the nanoparticles and the associated morphology is intrinsically qualitative in nature and not easily amenable to a simple and straightforward quantitative summary.

To understand why this observation presents a modelling challenge we considered scanning electron microscope (SEM) and transmission electron microscope (TEM) images from earlier reported experimental work by Ghodsinezhad [152] in order to make an assessment as to how the morphology of nanofluids could be potentially be modelled. It is clear from an assessment of the typical SEM and TEM images that the nanoparticle clustering/morphology is inevitability always represented as two dimensional images although the nanoparticle matter within the base fluid is physically a three dimensional object. Whilst in principle these results may be summarized by considering the nanoparticle matter $\mathcal{N}$ as being composed of an aggregate of N_p individual nanoparticles each with their own univariate diameter statistical distribution $g_i(\xi)$ in terms of an ELD parameter $\mathbf{p}_i = [a_1, b_i, c_i, d_i]^\mathrm{T}$ coupled with a spatial location say $\mathbf{r}_i$ that the clustering/morphology modelling aspect of the form

$$\mathcal{N} = \cup_{i=1}^{N_p} \mathbf{z}_i, \mathbf{z}_i = [\mathbf{r}_i, \mathbf{p}_i] \tag{3.55}$$

would prove more mathematically challenging since in general the individual nanoparticles would also have to have a corresponding orientation $\boldsymbol{\xi}_i$ relative to other nanoparticles within the aggregate mixture. At the present time of writing most nanofluid models utilize the nanoparticle size d_p as the main parameter instead of DLS measurements of the agglomeration size since the relationship between an individual nanoparticle size where $\mathcal{O}(d_p)\sim 10$ nm and that of a collection of nanoparticles which make up the agglomeration within the base fluid such that the agglomeration size is $\mathcal{O}(\mathcal{A})\sim 100$ nm is unclear. Due to the irregular shape of nanoparticles the size is usually by convention defined in terms of the area of the solid/liquid interface where the specific surface area (SSA) of the nanoparticle is measured by the Brunauer-Emmett-Teller (BET) approach in order to determine the average particle size d_p whilst the average hydrodynamic

diameter for the particle nanoparticle type and base fluid is estimated using the dynamic light scattering (DLS) approach as discussed by Liu *et al.*[153] where the BET and DLS measurements then quantify the particle size and agglomeration sizes respectively and who have recently attempted to construct a new nanofluid thermal conductivity model with both particle and agglomeration sizes, and where we note that variation between the individual particle size d_p and that of the agglomeration size $\mathcal{A}$ may differ by a factor of almost four i.e. $d_p \sim \frac{1}{4}\mathcal{A}$ for certain nanofluid mixtures however no definite correlations are available due to the wide variety of nanofluid manufacturing techniques and *in situ* operating conditions. Since much of the existing literature only specifies the nanoparticle size d_p, volume fraction ϕ and base fluid temperature T, under the assumption of local thermodynamic equilibrium (LTE) within the nanofluid and usually omits the DLS based agglomeration size $\mathcal{A}$ we will for simplicity assume that k_{eff} and μ_{eff} may be adequately modelled using just d_p, ϕ and T as meta-parameters since anecdotal experimental evidence from the literature review suggests that this may reasonably be the case for water/alumina nanofluids.

This type of mathematical model has recently been studied in more mathematical detail by Mahdavi [154] who investigated the nanoparticle interaction effects using both Eulerian/Eulerian and Eulerian/Lagrangian approaches using a set of mathematical modelling assumptions for the slip velocities between the solid/fluid phases and the interactions between the solid and liquid phases based on a continuum hypothesis underpinned by an approximate mean free path λ of the water molecules of $\lambda = 0.3$ nm and an approximate nanoparticle diameter of $d_p = 100$ nm so that a continuum hypothesis is mathematically valid since the Knudsen number is $Kn = (\lambda/d_p) \ll 1$. The conventional Knudsen number ranges for varying flow regimes are usually specified as

$0 \leq Kn \leq 0.01$	: Continuum flow regime	(3.56)
$0.01 \leq Kn \leq 0.1$	: Slip flow regime	(3.57)
$0.1 \leq Kn \leq 10$	: Transitional flow regime	(3.58)
$10 \leq Kn < \infty$	: Molecular flow regime	(3.59)

where the above-mentioned delimited flow regimes the conventional Navier–Stokes equations whether solved with commercial, opensource or custom written CFD research codes are strictly only mathematically valid for a Knudsen number range of $0 \leq Kn \leq 0.01$ and deteriorate in physical performance as the Knudsen number approaches the transitional flow regime.

In general as discussed earlier there does not existing a full rigorous physical theory for liquids and as a result mean free paths are usually calculated using the kinetic theory of gases although this is not strictly justified for the high number densities n of the form

$$n = \frac{\bar{p}}{k_B T} \tag{3.60}$$

where $\bar{p}$ is the average pressure, $k_B = 1.3806488 \times 10^{-23}$ J K^{-1} the Boltzmann constant and T the absolute temperature. Using a simplified analysis of the molecular cross-sections as discussed by Reif [10] as shown in Figure 3.9 it may be shown that the scattering cross-section σ_0
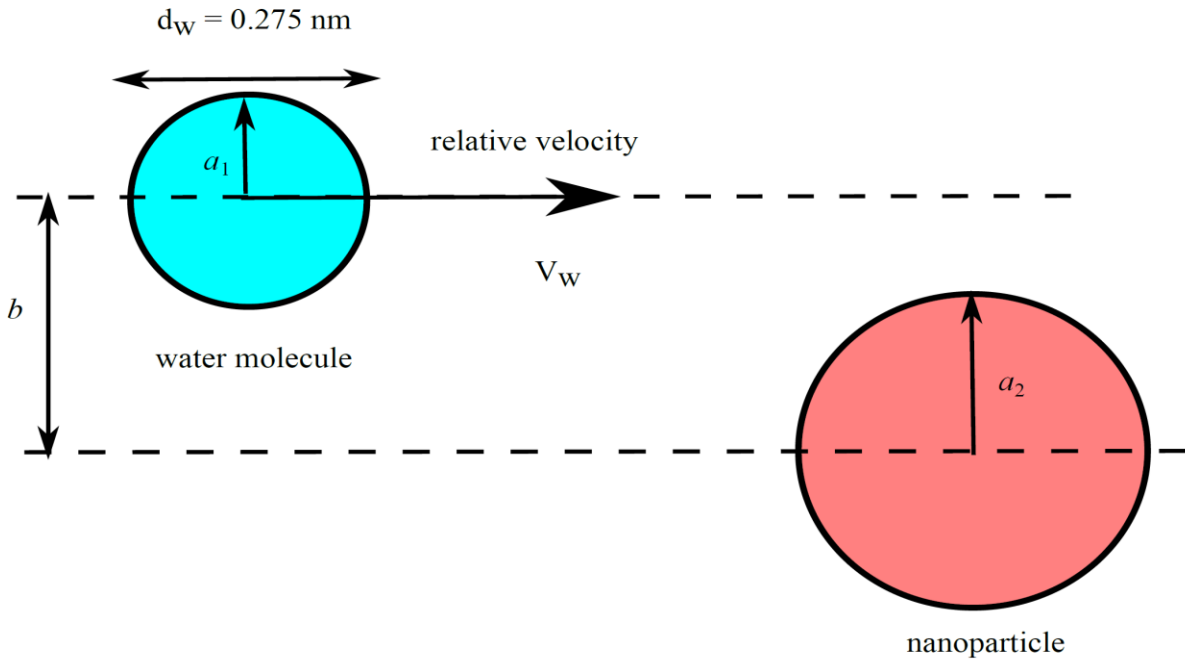
Figure 3-9 Conceptual illustration of the collision between two hard spheres for modelling the interaction of a water molecule of radius a_1 and a nanoparticle of radius a_2 with an impact parameter of b

for two dissimilar molecules is of the form

$$\sigma_0 = \pi(a_1 + a_2)^2 \tag{3.61}$$

so that the mean free path ℓ is approximately

$$\ell \approx \frac{1}{\sqrt{2}n\sigma_0} \tag{3.62}$$

Using an approximate estimate of $d_w = 0.275$ nm for the diameter of a water molecule, noting that a hard sphere model is only an approximation of the probability distribution of the spatial positions of the constituent atoms, and the above simplified mean free path estimates from statistical mechanics an approximate model validity range in terms of the nanoparticle diameters for a continuum based hypothesis may be established as shown in Figure 3.10.

Referring to the above model validity results it may be observed that a continuum hypothesis is mathematically valid only for a particular size of nanoparticle and that in general the model validity will also depend on the base fluid operating temperature and pressure. In the particular case of a water/alumina nanofluid the continuum modelling assumption is only valid for nanoparticles with a diameter d_p such that $d_p/[\text{nm}] \geq 15$ and the modelling assumption will fail if $d_p/[\text{nm}] < 15$ at standard atmospheric temperatures and pressures, however there are two provisos for this validity limit.
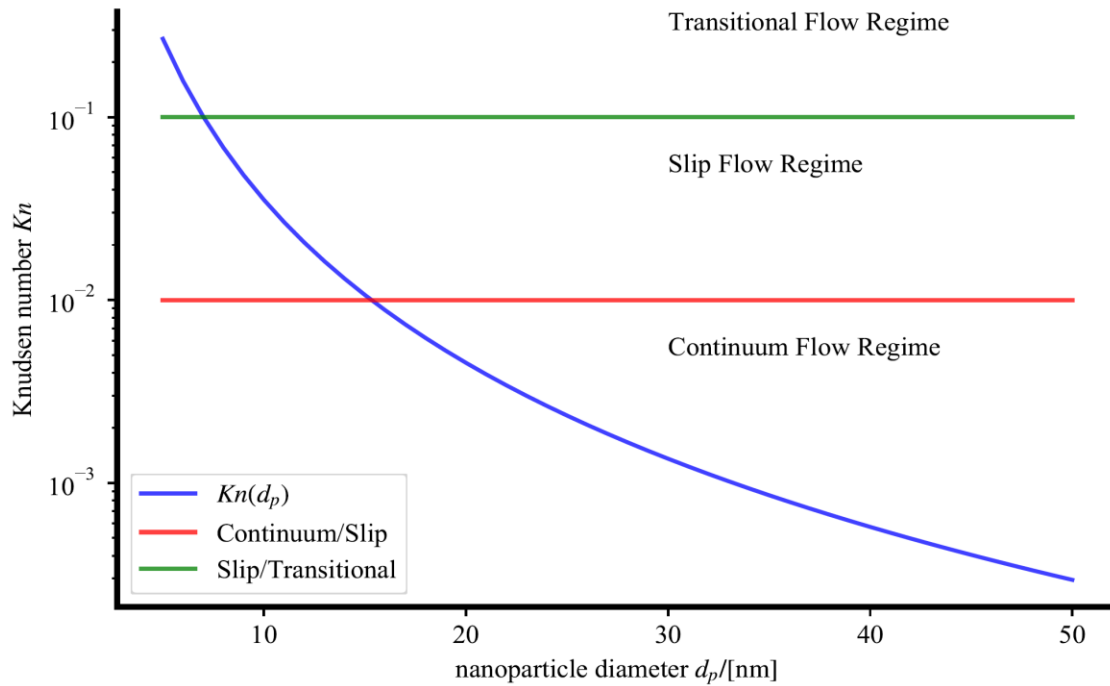
Figure 3-10 Illustration of continuum modelling hypothesis validity limits with variation in nanoparticle diameter for a water/nanoparticle nanofluid mixture at T=300 K and p=101.325 kPa

The first observation is that the Knudsen number calculation is a rough approximation using the kinetic theory of gases which is based on further approximations of the base fluid and nanoparticle physical properties, and the second observation that the modelling approach is implicitly based on the assumption that there is a representative molecular diameter or equivalent length scale for the nanoparticle contrary to the underlying wave nature of molecular systems which at a fundamental level are based on probabilistic molecular orbital dynamic effects.

Considering the first observation in a recent study by Uddin *et al.*[155] calculated a Knudsen number range of $0.0042 \leq Kn \leq 0.42$ for a typical range of nanofluids using water as the base fluid with the aid of the kinetic theory of gases as a rough approximation under the assumption that the water molecule mean free path was $\lambda = 0.42$ nm and that the collision cross-section area was equivalent to a water molecule radius of 0.15 nm and concluded that a continuum modelling assumption was reasonable. Although in the calculations performed by Uddin *et al.*the lower Knudsen number limit of $Kn(d_p)|_{low} = 0.0042$ is below the threshold of the generally accepted upper Knudsen number limit $Kn_{max} = 0.01$ of continuum flows it is seen that higher Knudsen number limit of $Kn(d_p)_{high} = 0.42$ is substantially larger than the upper limit of $Kn_{max} = 0.01$ and well into the transitional flow regime as shown in Figure 3.11.
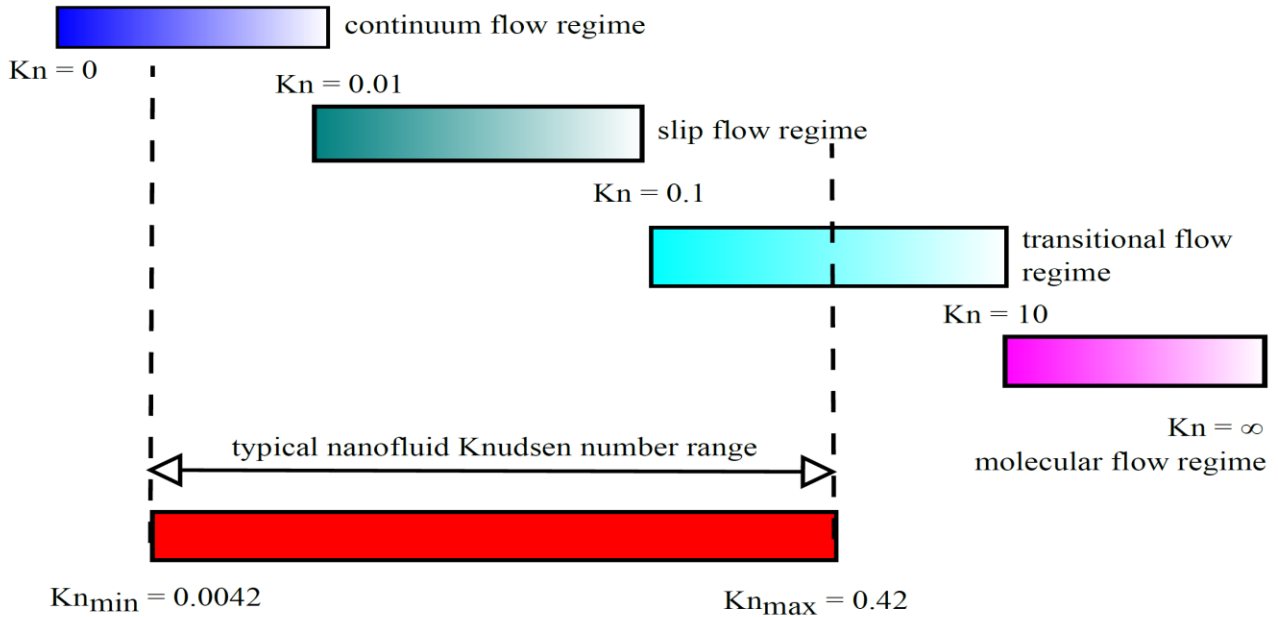
Figure 3-11 Illustration of overlapping physics flow regimes that occur when modelling a nanofluid using a continuum hypothesis due to the wide range of typical nanofluid Knudsen number ranges

As a result utilizing the conventional assumptions reported in the literature as discussed by Uddin *et al.*it is seen that the Knudsen number overlaps the continuum flow regime, slip flow regime and extends well into the transitional flow regime. The practical consequence of this observation is that a continuum modelling hypothesis can only mathematically model nanofluids for a range of nanoparticle diameters. Earlier *ab initio* computational physics simulations by Hadjiconstantinou [156] using a direct numerical solution of the Boltzmann equation determined that second-order slip boundary conditions could extend the Navier-Stokes equations up to a maximum Knudsen number of $Kn_{max} \leq 0.3$ however this reduced the accuracy of the predicted fluid velocity behaviour to $\| u(\mathbf{v}) \| \approx 5\%$ and it was observed that whilst qualitative fluid behaviour could be adequately captured that quantitative predictions became increasingly inaccurate as the Knudsen number increased beyond the Knudsen number limit of continuum flows, and that certain physical fluid phenomena at nanoscale level could no longer be accurately predicted.

In the event that smaller nanoparticle diameters are present in the nanofluid there will then be higher localized Knudsen numbers in the water medium surrounding these smaller nanoparticles and a continuum based CFD analysis in the fluid regions around these smaller nanoparticles will become mathematically invalid and hence potentially physically inaccurate. Although more advanced techniques such as modified boundary conditions, typically either with modified first order or second order boundary conditions for extended Navier-Stokes numerical simulations to incorporate Maxwell/velocity-slip and Smoluchowski/temperature-jump conditions as discussed by Ramnath [157] do exist, the use of these alternatives to retain a continuum modelling hypothesis is limited to modest increases of Knudsen number. These extensions to the $\mathcal{O}(Kn)$ based Navier-Stokes equations for higher Knudsen numbers are typically not extended by more than $Kn_{max} \approx 0.2$ either with $\mathcal{O}(Kn^2)$ Burnett hydrodynamics based equations as discussed by Singh *et al.*[158]

108

or alternative higher order models such as the Kogan-Galkin-Friedlander equations as discussed by Rogozin [159] which are both analyses based on the Boltzmann equation. Whilst the Boltzmann equation is able to fully model and resolve the underlying physical fluid behaviour at any length scale without any simplifications it is still nevertheless even with mathematical modelling approximations such as the Bhatnagar-Gross-Krook (BGK) or ellipsoidal statistical S-model for the collision integral term as discussed by Sharipov & Seleznev [160] still nevertheless extremely mathematically complex to solve. In practical terms a Boltzmann equation solution for a computational physics based *ab initio* flow is therefore usually implemented with an equivalent molecular dynamics based simulation for arbitrary Knudsen number flows where the molecular dynamics simulation results are used to "calibrate" the optimal second-order boundary conditions for an extended Navier-Stokes system of equations.

Due to the physical fact that any actual nanofluid will have a range of possible nanoparticle diameters for example $5 \leq d_p/[\text{nm}] \leq 50$ as experimentally measured using for example dynamic light scattering measurements there is always then the possibility of violations of the underlying modelling validity assumptions and hence potential errors of numerical simulations performed with a continuum modelling hypothesis if smaller particles are present in the base fluid. These potential model validity limits can be addressed by either more refined mathematical modelling, modifications such as higher order boundary conditions using slip velocities to extend the validity for moderately higher Knudsen numbers, or by more direct particle based simulations. By considering the full collection of all possible shapes and sizes of both nanoparticles as well as water molecules present within the volume of the nanofluid mixture the probabilities of collisions and interactions at the molecular level may instead be considered without any underlying continuum modelling hypothesis.

This type of idea is similar to the concept of electron density $\rho(\mathbf{r}) = \sum_{k=1}^{N} n_k \parallel \varphi_k(\mathbf{r}) \parallel^2$ encountered in the field of quantum chemistry where the electron density is a measure of the probability of an electron occupying an infinitesimal element of space around the immediate neighbourhood of the spatial point $\mathbf{r}$ and is suggestive that nano-fluids properties at an *ab initio* level may be studied as a many-bodies problems at a microscopic level i.e. a system where quantum mechanics effects are unavoidable and where classical mechanics breaks down and is unable to adequately capture the molecular interaction effects between the base fluid molecules and the nanoparticles.

At the present time of writing it is unclear if nanofluid properties can be adequately fully recovered from a conventional molecular dynamics (MD) simulations which is essentially in practical terms a conventional classical mechanics problem using Newton's second law $\mathbf{F} = m\ddot{\mathbf{x}}$ to model the behaviour of the particle displacement $\mathbf{x}$ for a specified force field $\mathbf{F}$ which is usually but not necessarily always constructed in terms of an assumed or approximate potential energy term that models the interaction effects between molecules using for example the classical Lennard-Jones potential, or if quantum mechanical effects at a more fundamental quantum chemical level are an unavoidable necessity to fully reconstruct the interaction potential energy term. The challenge with a molecular dynamics simulation apart from the heavy computational costs in which simulations are typically only possible for a few femto-seconds is that there is no simple and consistent scheme in order to deduce the underlying potential energy interaction term for a specified many-particle system. Quantum chemistry simulations nowadays typically adopt the well known density

functional theory (DFT) approach either with the more conventional historical Hartree-Fock approach or alternately the more modern Kohn-Sham approach for DFT simulations, although these earlier historical approaches have in some aspects been succeeded by newer approaches such as the post Hartree-Fock *ab initio* and Moller-Plesset perturbation theories. At the most fundamental level simulations at the quantum chemical level consists of solving the Schrodinger equation with an associated total molecular Hamiltonian however in this research investigation this *ab initio* research strategy is not considered due to the extreme complexity in deducing the underlying system potential energy term when building up the corresponding Hamiltonian $H = \sum_{n=1}^{N} \frac{1}{2m_n} (\mathbf{p}_n \cdot \mathbf{p}_n) + V(\mathbf{r}_1, \mathbf{r}_2, \dots, \mathbf{r}_n, t)$. Quantum chemical simulations using the Hartree-Fock approach have historically been used to simulate liquids such as water at the atomic and molecular level as originally pioneered by Stillinger [161] where the potential energy term for N molecules takes different forms where the potential energy disregards interaction effects if the molecules are far from each other such as in gaseous form, and where the potential energy term considers interaction effects when the N water molecules are closely spaced to each such as liquid form. As per the discussion by Stillinger one the inherent errors with the Hartree-Fock approximation when applied to water is that the predicted dipole moment for the single water molecule is too large and earlier theoretical chemical predictions for the dipole moment were 22% larger than contemporary experimental values because of charge distribution errors. Whilst Stillinger remarked that these errors could in principle be addressed with a full quantum mechanical simulation at the time due to the limited computational resources available the preferred approach was to utilize a modified form of the empirical Lennard-Jones 12-6 energy potential with semi-empirical modifications in order to account for the errors in the dipole moment calculations, and which would in turn also account for London dispersion attraction force effects on the potential energy function. Later studies that considered the use of quantum chemistry included that of Mrázek and Burda [162] who attempted to use quantum chemical simulations to predict the pH of a solute using the proprietary commercial computer code Gaussian that is not readily available to many researchers and who tentatively speculated that that may be theoretically possible if very large clusters of surrounding molecules were considered in the bulk medium. A simplified molecular dynamics simulation for Al_2O_3, C_2H_5OH and $C_2H_4OH_2$ nanoparticles with H_2O molecules was performed by Lu & Fan [163] who used a *NVT* canonical ensemble with N particles and a system volume V at a temperature T a Lennard-Jones potential energy term of the form

$$\phi(r_{ij}) = \begin{cases} 4\varepsilon_{ij} \left[\left(\frac{\sigma_{ij}}{r_{ij}} \right)^{12} - \left(\frac{\sigma_{ij}}{r_{ij}} \right)^{6} \right] & \text{if } r_{ij} < r_{cut} \\ 0 & \text{if } r_{ij} \geq r_{cut} \end{cases} \tag{3.63}$$

where the intermolecular force may be recovered from the potential energy term as

$$\mathbf{f}(r_{ij}) = -\nabla\phi(r_{ij}) = \frac{48\varepsilon_{ij}}{\sigma_{ij}} \left[\left(\frac{\sigma_{ij}}{r_{ij}} \right)^{13} - \frac{1}{2} \left(\frac{\sigma_{ij}}{r_{ij}} \right)^{7} \right] \frac{\mathbf{r}_{ij}}{r_{ij}} \tag{3.64}$$

A similar approach was later also adopted by Li *et al.*[164] for a simulation of copper oxide nanoparticles in order to study the effect of the nano-layer where Li *et al.*developed their own research code using a half time step Verlet algorithm, adapting their symbol notation slightly for

consistency, of the form

$$v\left(t + \frac{\delta t}{2}\right) = v\left(t - \frac{\delta t}{2}\right) + \frac{F_i(t)}{m_i} \cdot (\delta t) \tag{3.65}$$

$$F_{ij}(t + \delta t) = -\frac{\partial \phi_{ij}(t+\delta t)}{\partial r_{ij}} \tag{3.66}$$

$$v(t) = \frac{1}{2}\left[v\left(t + \frac{\delta t}{2}\right)\right] + v\left(t - \frac{\delta t}{2}\right) \tag{3.67}$$

The above scheme was also again used by Sankar *et al.*[165] for a water-platinum nanofluid however Sankar *et al.*took the modelling process a step further by attempting to simulate the interaction effects within the nanoparticle material itselt by using a finitely extendable nonlinear elastic (FENE) potential

$$U_{FENE} = -Ae\ln\left[1 - \left(\frac{r}{B\sigma}\right)^2\right] \tag{3.68}$$

where A and B are experimental constants to account for the interaction between the platinum atoms within the nanoparticle itself. A Morse potential of the form

$$\Phi(r) = D_e[\exp\{-2\beta(r - R_e) - 2\exp\{-\beta(r - R_e)\}\}] \tag{3.69}$$

where D_e is the dissociation energy, R_e the equilibrium bond length and β is a constant whose dimension is in units of the reciprocal of length was then used to complete the modelling process. Although most of the reported studies within the literature therefore use the conventional Lennard-Jones potential energy modelling approach there are in fact alternative potential energy formulations such as the Flexible-3-Center (T3C) model as discussed by Sachdeva [166]. The utility of molecular dynamics also extends to studying the effects of shear rates as discussed by Sun *et al.*[167] who used an equilibrium molecular dynamics (EMD) simulation with the Green-Kubo formula to investigate shear rate effects for copper nanoparticles in argon where they used the Berthlot mixing rule

$$\sigma_{sl} = \frac{\sigma_{ss} + \sigma_{ll}}{2} \tag{3.70}$$

$$\varepsilon_{sl} = \sqrt{\varepsilon_{ss}\varepsilon_{ll}} \tag{3.71}$$

in order to estimate the Lennard-Jones potential energy parameters where the subscripts s and l denote the solid and liquid components in the nanofluid mixture. More recent work by Lou & Yang [168] has now also been utilized to investigate viscosities of nano-fluids such as water/alumina mixture using both the more conventional equilibrium molecular dynamics (EMD) as well as the more advanced non-equilibrium (NEMD) approaches. In the work of Lou & Yang they opted to use the TIP4P/2005 potential function for the water-water molecular interactions and they modelled the water-particle interactions using the CLAYFF force field approach which was originally developed for clay systems and justified this modelling approach with the reasoning that Al_2O_3 is one of the constituent components for the clay system in the CLAYFF force field model and used the LAMMPS software package to simulate the system for 800 ps for the NVT ensemble. A final further potential application of molecular dynamics in nanofluid thermo-physical properties is potentially in terms of modelling the chaotic movements in the nanoparticles

of the base fluid as recently reported by Cui *et al.*[169] however as previously mentioned this requires very powerful HPC capabilities for a full *ab initio* quantitative simulation which is presently unavailable in South Africa and this therefore not a feasible option at the present time of writing of this dissertation, although qualitative molecular dynamics studies using semi-empirical Lennard-Jones type of potentials are possible. In the event of a full molecular dynamics simulation the transport coefficients are recovered through the Green-Kubo relations as discussed by Frenkel & Smit [170] such that the shear viscosity η and thermal conductivity λ are calculated as

$$\eta = \frac{1}{Vk_BT}\int_0^\infty \langle \sigma^{xy}(0)\sigma^{xy}(t)\rangle \ dt \tag{3.72}$$

$$\lambda = \frac{1}{Vk_BT^2}\int_0^\infty \langle j_z^e(0)j_z^e(t)\rangle \ dt \tag{3.73}$$

where

$$\sigma^{xy} = \sum_{i=1}^N \left(m_i v_i^x v_i^y + \frac{1}{2}\sum_{j\neq i} x_{ij}f_y(r_{ij})\right) \tag{3.74}$$

$$j_z^e = \frac{d}{dt}\left[\sum_{i=1}^N z_i \frac{1}{2}\left(m_i v_i^2 + \sum_{j\neq i} v(r_{ij})\right)\right] \tag{3.75}$$

and

$$\dot{f} = \dot{\mathbf{r}}\frac{\partial f}{\partial \mathbf{r}} + \dot{\mathbf{p}}\frac{\partial f}{\partial \mathbf{p}} \tag{3.76}$$

is an arbitrary function defined in terms of the particular system's position vectors $\mathbf{r}_i(t)$ and momenta $\mathbf{p}_i(t)$ for $i = 1,2,\dots,N$ in the case of N particles. In the case where f is defined in terms of the positions $\mathbf{r}$ and the momenta $\mathbf{p}$ then the molecular dynamics simulation is said to follow the Lioville formulation for time-reversible systems and this approach is sometimes used to develop more efficient solution algorithms, however the Lioville formulation is mathematically equivalent to the more common Newton's laws of motion approach $m_i\ddot{x}_i = F_i$ if the force can be accurately specified or equivalently derived from an appropriate potential energy function that adequately describes the ground energy state as well as the interaction effects between different particles. Although the classical Newton equations of motion approach is simpler to model for the time evolution for the system for N particles in a volume V and with a total energy E since only initial conditions of particle positions $r_i(0)$ and momenta $p_i(0)$ at time $t = 0$ for particles $i = 1,2,\dots,N$ this approach is much more complicated if the system is to be studied for a constant temperature T or a constant pressure p. Whilst it is easier to hold the temperature or the pressure constant in a full Monte Carlo simulation this constraint is in general more complicated to implement in a molecular dynamics simulation since it then becomes necessary to construct an extended Lagrangian $\mathcal{L}$ for the system. The disadvantage with this approach is that the extended Lagrangian cannot in general be easily transformed into an equivalent Hamiltonian form $\mathcal{H}$ where the Hamiltonian is defined as $\mathcal{H}(q,p) \equiv p\dot{q} - \mathcal{L}(q,\dot{q},t)$ where q is a generalized coordinate and p is the momentum. The consequence of this limitation is that in the absence of a well defined Hamiltonian which can be used to construct the equivalent system of differential equations to model the time evolution of the system, that the connection to the underlying statistical mechanics for the N particle system cannot be fully established and hence in practical terms the transport properties such as the thermal conductivity and viscosity cannot in general be fully mathematically

justified unless it can be proven that the Hamiltonian fully captures the underlying statistical mechanics of the fluid physics.

The above formulae in a molecular dynamics simulation assume the validity of the ergodic hypothesis which is loosely speaking the assumption that the time average for some quantity say A of a many-particle system, say N molecules for a volume V and energy E, can either be computed by time averaging of A or by the ensemble average which is an average over all the corresponding quantum states for that particular many-particle system. In practical terms the ergodic hypothesis may be summarized as that the ensemble average for quantity A is $\langle A \rangle$ which may be approximated as a time average such that $\lim_{\tau \to \infty} A_\tau = \langle A_\tau \rangle$ where $A_\tau = \frac{1}{\tau} \int_0^\tau A(t) \quad dt$ for some sufficiently long time period τ of the molecular dynamics simulation so that

$$\langle A \rangle = \frac{1}{\tau} \int_0^\tau A(t) \quad d\tau \tag{3.77}$$

The variance $\sigma^2(A)$ of the quantity A is then formally calculated as

$$\sigma^2(A) = \langle A_\tau^2 \rangle - \langle A_\tau \rangle^2 \tag{3.78}$$
$$\sigma^2(A) = \frac{1}{\tau^2} \int_0^\tau \int_0^\tau \langle [A(t) - \langle A \rangle][A(t' - \langle A \rangle)] \rangle \quad dt \quad dt' \tag{3.79}$$

The term $\langle [A(t) - \langle A \rangle][A(t' - \langle A \rangle)] \rangle = C_A(t - t')$ is usually called the correlation function and in the special case where the simulation time τ is much larger than the characteristic decay time t_A^c for the system being studied then the variance and relative variance may then be approximated as

$$\sigma^2(A) \approx \frac{1}{\tau} \int_{-\infty}^\infty C_A(t) \quad dt \tag{3.80}$$
$$\sigma^2(A) \approx \frac{2t_A^c}{\tau} C_A(0) \tag{3.81}$$
$$\frac{\sigma^2(A)}{\langle A \rangle^2} \approx \frac{2t_A^c}{\tau} \frac{\langle A^2 \rangle - \langle A \rangle^2}{\langle A \rangle^2} \tag{3.82}$$

A potential benefit of molecular dynamics based studies is in terms of a direct *ab initio* numerical simulation approach for investigating the main physical based mechanisms such as the Brownian motion of the nanoparticles within the base fluid, the physical characteristics of the nanolayer around the nanoparticles, clustering effects and the mechanism of the heat transfer within the actual nanoparticles themselves. One particular example of this was reported by Aybar *et al.*[121] from an earlier literature survey where they reported that the enhancement of thermal conductivity did not seem to be affected by hydrodynamic effects caused by Brownian motion within the nanofluid, however the practical implementation challenge of very demanding high performance computing resources still remains a major obstacle for the further widespread adoption of molecular dynamics simulations in nanofluids as least within South Africa at the present time.

As a result due the above combination of modelling issues and complexities we now opt to consider a statistical modelling approach in terms of a reduced number of meta-parameters in order to perform a quantitative investigation of the effective thermal conductivity and effective viscosity, and comment that open source software codes as discussed by Pirhadi [171] and Fortunato &

Colina [172] may be utilized in more advanced quantum chemical and molecular dynamics *ab initio* based studies as more powerful HPC systems become more readily accessible within South Africa. Utilization of a statistical modelling approach in order to investigate nanofluid properties is consistent with earlier observations by Meyer *et al.*[88] and Nwosu *et al.*[173] who also recommended performing studies in terms of parametric variables in order to construct plausible near-generalized models for rheological characteristics such as the nanofluid viscosity. Part of the difference with our current approach is that we will not make any prior assumptions of a particular algebraic equation formulation of the effective thermal conductivity and viscosity by fitting parameters to a particular equation but instead allow the statistical experimental data distribution to naturally determine the most appropriate model equation. The difference is therefore that in existing studies a particular model is first chosen for a property such as the viscosity, using for example a Hosseini *et al.*model of the form $(\eta_{nf}/\eta_{bf}) = \exp[m + \alpha(T/T_0) + \beta(\phi_h) + \gamma(d/(1 + r))]$ where α, β, γ and m are unknown parameters as discussed by Nwosu *et al.*[173], where statistical techniques are subsequently applied to determine the optimal values of the various equation parameters, whilst in our approach we first use statistics techniques to pre-process the data which then suggests a plausible mathematical model to fit the data. The benefit of this approach is that we do not have to sequentially investigate a voluminous variety of possible analytical mathematical expressions for the effective thermal conductivity k_{eff} and effective viscosity μ_{eff} models for which there are over 30 for k_{eff} and over 30 for μ_{eff} as discussed by Sharifpur & Meyer [36] and as a result $30 \times 30 = 900 = \mathcal{O}(10^3)$ possible combinations of thermal conductivity – viscosity models to investigate and study, however a potential issue is the mathematical complexity that may arise when constructing the resultant mathematical models of the effective thermal conductivity and viscosity directly in terms of the underlying data.

Different techniques that construct models based directly on the underlying data are possible of which Artificial Neural Networks (ANN's) and Artificial Intelligence (AI) based approaches in various forms are quite popular in nanofluid studies for both thermal conductivity as well as for viscosity model constructions. An earlier study by Mehrabi *et al.*[174] utilized an Adaptive Neuro-Fuzzy Inference System (ANFIS) to construct a model of a water/alumina nanofluid where a database of experimental data from the literature was used to train the network using particle size, volume concentration and temperature where 80% of the data was used to construct the model and the remaining 20% was used as test data points to validate the ANFIS network model. Later work by Mehrabi *et al.*[76] utilized a Fuzzy C-Means clustering (FCM) approach to first pre-process the nanofluid thermophysical data extracted from the literature into two or more clusters of data and then developed a genetic algorithm with a polynomial neural network scheme formulated as Group Method of Data Handling (GMDH) scheme to model and predict a water/alumina nanofluid thermal conductivity again with a 80% data split for model construction and 20% data split for subsequent testing of the modelling predictions where the output z in terms of inputs x_i, x_j, x_k using the GMDH scheme took the mathematical form of a Volterra function series of the form

$$z = a_0 + \sum_{i=1}^{M} a_i x_i + \sum_{i=1}^{M} \sum_{j=1}^{M} a_{ij} x_i x_j + \sum_{i=1}^{M} \sum_{j=1}^{M} \sum_{k=1}^{M} a_{ijk} x_i x_j x_k + \cdots \qquad (3.83)$$

where x_i, x_j, x_k were data points for the nanoparticle size d, volume concentration ϕ and temperature t from the nanofluid thermophysical data extracted from the literature, M was the number of points in the underlying database, and a_i, a_{ij}, a_{ijk} were unknown model parameters

that were to be determined. It may be observed that the above Volterra series is mathematically equivalent to a high order Response Surface Methodology (RSM) model and as a result the modelling approach of genetic algorithms and neural networks amongst other modelling approaches is conceptually equivalent at a mathematical modelling level to traditional model parameter regression analysis techniques where in practical terms the main technical difference is in terms of how the parameters are determined through a numerical optimization of a suitable cost or χ^2-merit function defined in various different mathematically appropriate ways for the various modelling approaches, and as a result it is seen that the determination of the effective thermal conductivity and viscosity is in essence a classical regression analysis problem. As a result the problem is technically classified as a '*supervised learning*' problem as opposed to an '*unsupervised learning*' problem using the research terminology and nomenclature of machine learning as discussed by Raschka [175]. Due to the supervised learning nature of the problem there is an implicit simplification with regards to the input/output mathematical model as there is no need for a dimensional reduction through for example a principal component analysis since the principal components have been *a priori* selected as the nanoparticle size $d = x_1$, volume concentration $\phi = x_2$ and temperature $t = x_3$ for simplicity and we remark that in most practical cases it is not mathematically feasible to obtain data of higher dimensions since information of for example the nanofluid acidity/alkalinity with $pH = x_4$ or a physically meaningful parametrization of the nanoparticle agglomeration $\mathcal{A} = x_5$ effects is either unavailable due to experimental constraints, or is simply unknown in the absence of a full physics based nanofluid theory. This modelling assumption is conceptually illustrated in graphical form in Figure 3.12 where a dimensional reduction with 5 inputs is reduced to 3 inputs for a 2 output model so that $\mathbf{z} \approx \mathbf{f}(\mathbf{x})$ with $\mathbf{z} = [k_{eff}, \mu_{eff}]^T$ and $\mathbf{x} = [d, \phi, t]^T$.
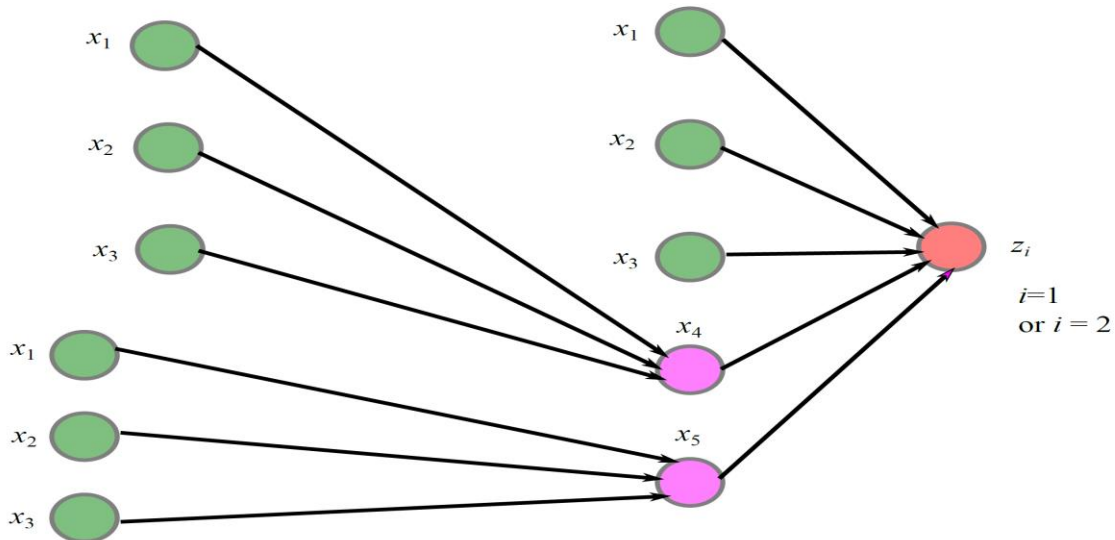

Figure 3-12 Conceptual illustration of dimensional reduction using an a priori principal component analysis modelling assumption with $d = x_1$, $\phi = x_2$, $t = x_3$, $pH = x_4$, $\mathcal{A} = x_5$ and outputs $z_1 = k_{eff}$ and $z_2 = \mu_{eff}$

A practical result is that dimensional reduction techniques essentially use higher dimensional

statistical correlation schemes in order to determine the most 'dominant' inputs and as a result in the absence of a holistic physical theory the mathematical model is usually an approximation that does not fully incorporate the interaction between all of the model inputs.

Whilst the use of Artificial Neural Networks (ANN's) to reconstruct the effective thermal conductivity and effective viscosity from supplied thermo-physical data has been reported in the literature one of the disadvantages of this approach as previously discussed is that it still requires the original dataset X even if the weights ω_{ik} are supplied since the function is approximated as $y_k = \sum_{i=1}^{m} \omega_{ik} R_i(X)$. In many ANN studies it is usually assumed that the supplied data set X is exact however there will always be a corresponding statistical uncertainty $u(X)$ associated with the dataset which has a physical basis due to experimental uncertainties from the particular laboratory equipment and instruments that were used to measure either the thermal conductivities or viscosities. The uncertainties of the inputs into a model building process are termed *aleatoric* uncertainties whilst the errors which result from inconsistencies in obtaining the 'best' model are termed *epistemic* uncertainties. In many experimental measurement fields of study particularly within physics and chemistry national laboratories the aleatoric uncertainties are statistically modelled in terms of appropriate probability density function distributions and these physical/chemical based statistical uncertainties are 'propagated' through the model either with full Monte Carlo, direct Markov convolution integral or occasionally Markov Chain Monte Carlo (MCMC) numerical simulations so that the output model parameters have corresponding statistically meaningful and appropriate PDF's. As a result the epistemic uncertainties are immediately quantified for consistency in subsequent numerical simulations that utilize the model and associated model parameters as conceptually illustrated in Figure 3.13 and Figure 3.14 using the case of the functional form of the water density $\rho(T)/[\text{kg}]$ as a function of the temperature $T/[\text{K}]$.
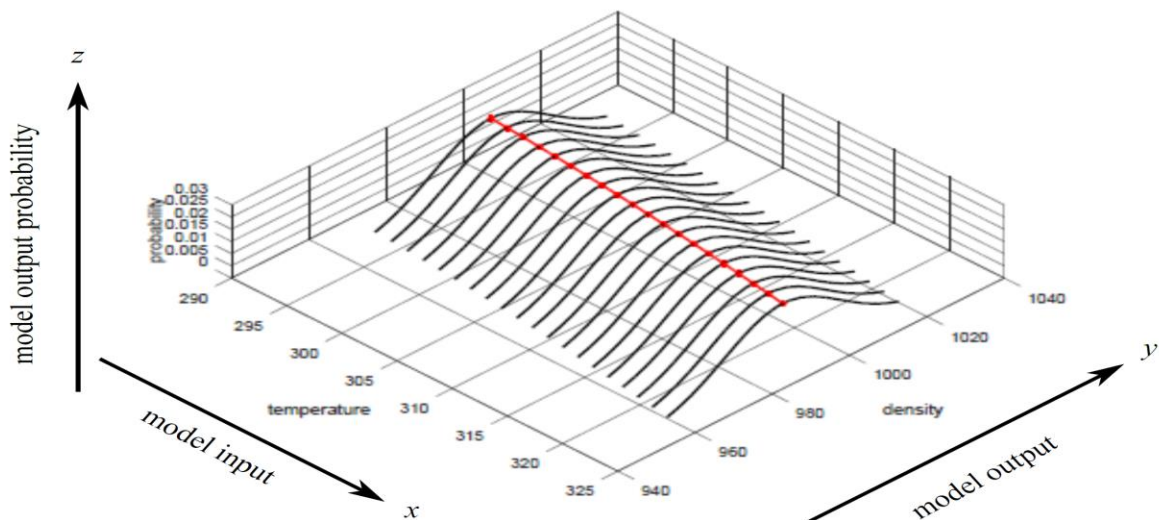

Figure 3-13 Illustration of how statistical aleatoric uncertainties for a n=2 dimensional model reside in a related $\mathbb{R}^{n+1}$ higher dimensional space where the model probability is explicit

116
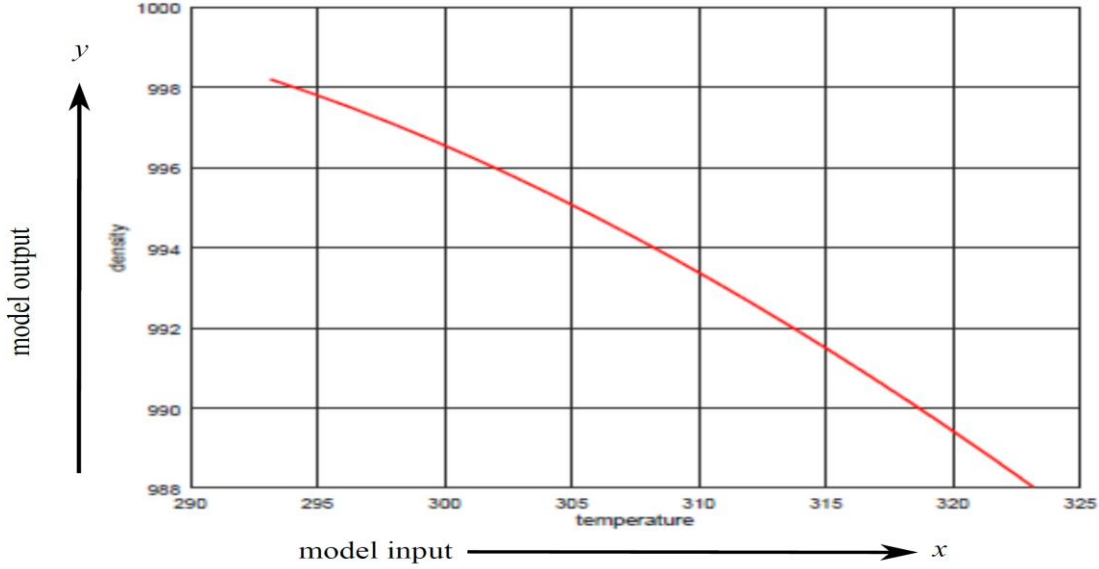
Figure 3-14 Illustration of how physical nominal measurements for a n=2 dimensional model reside in a $\mathbb{R}^n$ lower dimensional space where the model probability is implicit

An adaptation of an earlier interpretation by Tarantola [176] may be considered as an example who considered the more general situation where **d** is the model output data, **m** are the model parameters, and **g** is a model function. For this example corresponding uncertainties may be generated using an assumed density uncertainty of $u(\rho)(k=1) = \pm 15$ kg m^{-3} for an easier visualization to illustrate the general principle where the parameter uncertainties for a function will result in a corresponding uncertainty of a function and which then creates an additional dimension for the equivalent probability density function where in our simplified illustration the PDF $f(x)$ for $x = \rho(T)$ follows a Gaussian distribution such that $f(x) = \frac{1}{\sigma\sqrt{2\pi}} \exp\left[-\frac{1}{2}\left(\frac{x-\mu}{\sigma}\right)^2\right]$ where x is a random variable for the water density, μ is the expected value of the water density and $\sigma = 15$ kg m^{-3} for illustrative purposes only. In the case of the effective thermal conductivity $k_{eff}(T, d_p, \phi)$ and effective conductivity $\mu_{eff}(T, d_p, \phi)$ there would then be equivalent higher dimensional forms analogous to a simplified three dimensional illustrative example as shown in Figure 3.13.

A recent unpublished study by Levasseue *et al.*[177] has proposed a potential mechanism that may be used to determine the uncertainties of the constructed neural network that takes into account noise levels in the input data i.e. uncertainties $u(X)$ and training and architecture errors made by the network i.e. errors in the neural network node weightings $u(\omega_{ik})$. The approach of Levasseue *et al.*is claimed to offer superior performance to the conventional MCMC approach, as discussed by for example Forbes [178], through the tuning of a single hyper-parameter. The determination of the optimal weights ω is achieved by minimizing the integral $p(\mathbf{y}|\mathbf{x}, \mathbf{X}, \mathbf{Y}) = \int p(\mathbf{y}|\mathbf{x}, \omega)p(\omega|\mathbf{X}, \mathbf{Y})$ dω where $\mathbf{X} = \{\mathbf{x}_1, ..., \mathbf{x}_N\}$ are a set of input images and the output parameters are $\mathbf{Y} = \{\mathbf{y}_1, ..., \mathbf{y}_N\}$ where $p(\omega|\mathbf{X}, \mathbf{Y})$ are the plausible network parameters that must be determined in order to minimize the error. Levasseue *et al.*perform this optimization of the neutral network set of weights ω by minimizing the Kullback-Leibler (KL) divergence by selecting the value of ω to minimize $p(\mathbf{y}|\mathbf{x}) \approx \int p(\mathbf{y}|\mathbf{x})q(\omega)$ dω however the disadvantage

of their approach is that this high dimensional integral must be calculated with a high dimensional Monte Carlo integration as discussed by Press *et al.*[132] such that the multi-dimensional integral $I = \int_\Omega f(\mathbf{x}) \quad d\mathbf{x}$ for $\mathbf{x} \in \mathbb{R}^m$ is approximated as $I \approx V\frac{1}{N}\sum_{i=1}^N f(\mathbf{x}_i)$ for suitable sampled points $\mathbf{x}_i \in \mathbb{R}^m$ where for the neutral network problem m would correspond to the total number of paths between the set of input and output nodes. In general an artificial neural network will have a very large number of nodes and therefore there will be a corresponding large number of weights ω when training and constructing the ANN, as a result the determination of the ANN parameter uncertainties whilst theoretically possible is potentially unnecessarily complicated by the need for stratified sampling schemes in order to perform the high dimensional integration that is necessary. A similar type of problem occurs when modelling randomness in neural networks as discussed by Scardane & Wang [179] where in the case of feed-forward random weighted networks (RW-FFN) the output takes the form $f(\mathbf{x}) = \sum_{m=1}^B \beta_m h_m(\mathbf{x}; \mathbf{w}_m)$ which is a linear combination of B non-linear transformations. Typically in the field of neural networks the basis function $h_m(\mathbf{x})$ takes the additive form $h_m(\mathbf{x}) = g(\mathbf{a}_m^T\mathbf{x} + b_m)$ where $\mathbf{a}_m$ is an unknown vector, b_m is an unknown scalar, and researchers usually use a sigmoid function of the form $h_m(\mathbf{x}) = [1 + \exp\{\mathbf{a}_m^T\mathbf{x} + b_m\}]^{-1}$. Occasionally in some situations a radial basis function (RBF) approach is adopted usually with a Gaussian shape such that $h_m(\mathbf{x}) = \exp\{-\alpha_m \parallel \mathbf{x} - \mathbf{c}_m \parallel_2^2\}$. Regardless of whether the neutral network is modelled either in terms of additive functions or radial basis functions the issue of how to address randomness in neural networks in the case of RW-FFN's applies a stochastic assignment of a subset of the neural network weights i.e. a selection of some of the neural network weights are artificially randomized which is then carried forward to construct a simplified optimization problem that must be solved to recover the neural network weights. This optimization is often further simplified and cast into a standard linear least-squares problem, however whilst there exist many numerical numerical routines to solve least-squares problems the main challenge of how to 'randomize' a selection of the weights still remains.

A potentially simpler approach to the use of neural networks is to directly model the underlying experimental data with the corresponding uncertainties using a radial basis function (RBF) approach as discussed by Fasshauer [180] for the global domain of the associated meta-parameters. The use of radial basis functions has become increasingly popular for curve and surface fitting in higher-dimensional spaces using techniques such as the moving least squares (MLS) approach for which refinements such as the piece-wise moving least squares approximation method (PMLS) as discussed by Li *et al.*[181] exists for cases where there may be a large number of known discrete points and where the dimension of the space in which the discrete points reside in is high.

In this dissertation as previously discussed the focus is on low dimensional spaces since there is a relatively small number of known meta-parameters such as the nanoparticle size d, volume concentration ϕ and temperature t and as a result specialist techniques such as the PMLS approach are not necessary as the regular techniques such as the normal moving least squares approach can suffice for our underlying data-set obtained from the open literature. Special RBF approaches such as the Compactly Supported RBF approach (CSRBF) are available to reduce the computational cost for system with a large number of data points and high dimensional spaces as discussed by Skala [182], whilst special regularization techniques are also available to mitigate against ill-conditioned systems as discussed by Sarra & Cogar [183]. As a result whilst the use of radial basis function approach in its conventional forms may be considered to be sufficiently powerful for our mathematical modelling of the effective thermal conductivity k_{eff} and effective

viscosity μ_{eff} its use to also simultaneously model the resultant uncertainties in k_{eff} and μ_{eff} whilst not theoretically impossible is nevertheless problematic from a practical implementation point of view due to the potentially large number of radial basis function constants.

The research objective in this dissertation is to mathematically model a global function for k_{eff} and μ_{eff} for some restricted domain $T_{\min} \leq T \leq T_{\max}, \phi_{\min} \leq \phi \leq \phi_{\max}, d_{\min} \leq d_p \leq d_{\max}$ of the meta-parameters T, ϕ, d_p as previously discussed instead of utilizing specific algebraic functional forms from the literature for k_{eff} and μ_{eff} for restricted domains such as limited temperature ranges by optimizing the parameters for the various choices of the commonly used equations, where the developed mathematical model can be used to predict both values for the effective thermal conductivities and viscosities as well as their associated estimated uncertainties. Whilst predictions of thermophysical nanofluids properties has been investigated by many researchers in prior reported work for algebraic models as opposed to statistical models the incorporation of the associated statistical uncertainty analysis of the effective thermal conductivity and viscosity as opposed to a more conventional numerical error analysis has not featured predominantly.

3.2 Mathematical Analysis of Multivariate Copula Models

Based on the preceding analysis significant limitations have been identified as posed by the conventional functional form approach of choosing specific *a priori* algebraic functions and then performing optimizations particularly when the mathematical functional forms are unknown in the absence of a comprehensive nanofluid physical theory that is able to fully account for the interactions of all the relevant physical parameters. Due to these shortcomings in this dissertation the more rigorous mathematical modelling approach of using multivariate copulas to model and summarize the validated multivariate experimental data obtained from the literature review based on the recently reported success of the application of a copula based bivariate probability density function of an engineering fluid system by Ramnath [151] is investigated. A review of copulas by Kolev *et al.*[184] provides the equivalent informal mathematical definition for a n-dimensional copula C as the mapping $C: \mathbb{I}^n \rightarrow \mathbb{I}$ where $\mathbb{I} = [0,1]$ is the closed unit interval set where $X_1, X_2, \ldots, X_n$ are continuous random variables with a distribution function $H(x_1, \ldots, x_n)$, respective marginal distributions $F_{X_1}, \ldots, F_{X_n}$ and C maps every point $(x_1, \ldots, x_n) \in [-\infty, \infty]^n$ such that

$$H(x_1, \ldots, x_n) = C(F_{X_1}(x_1), \ldots, F_{X_n}(x_n)) \tag{3.84}$$

which is known as Sklar's theorem in the statistical literature. In order to illustrate the application of Sklar's theorem for the bivariate case let x and y be variables which have associated univariate marginal probability density function distributions $g_x(\xi_x)$ and $g_y(\xi_y)$ where ξ_x and ξ_y are corresponding random variables of x and y respectively. The model output $h = f(x, y)$ will then have a joint probability density function in terms of the underlying random variables ξ_x and ξ_y which can be used to predict the expected value of h along with the associated uncertainty for a specified confidence level. If the cumulative distributions for x is u and that for y is v defined as

$$u = \int_{-\infty}^{x} g_x(\xi_x) \ d\xi_x \tag{3.85}$$
$$v = \int_{-\infty}^{y} g_y(\xi_y) \ d\xi_y \tag{3.86}$$

then the application of Sklar's theorem defines the joint PDF as

$$f(x, y) = uv \frac{\partial^2 C}{\partial u \, \partial v} \tag{3.87}$$

This idea can be extended to higher dimensional models and in the case of the dimension $d = 3$ where there is a third random variable z with a univariate marginal PDF $g_z(\xi_z)$ where ξ_z is a random variable for z the cumulative distribution function w for z is defined as

$$w = \int_{-\infty}^{z} g_z(\xi_z) \ d\xi_z \tag{3.88}$$

In this case the trivariate PDF that couples the random variables x, y, z is then specified as

$$f(x, y, z) = uvw \frac{\partial^3 C}{\partial u \, \partial v \, \partial w} \tag{3.89}$$

where $C(u, v, w)$ is the trivariate copula function and $c(u, v, w) = \frac{\partial^3 C}{\partial u \, \partial v \, \partial w}$ is known as the copula density. A physical example of a trivariate joint PDF would be the previous mathematical example that we considered where the nanofluid effective thermal conductivity was some mathematical function expressed in terms of the temperature T and nanofluid volume concentration ϕ where we would apply the conceptual mathematical idea of a copula to this statistically model this relationship by setting the thermal conductivity as a random variable $k_{nf} = x$, the temperature as a random variable y and the volume concentration as a random variable $z = d_p$ and then construct the trivariate joint PDF $f(k_{nf}, T, \phi)$ in order to model the relationship between the random variables x, y, z. The marginal distributions u, v, w calculated in terms of the PDF's $g_x(\xi_x)$, $g_y(\xi_y)$ and $g_z(\xi_z)$ are relatively easy to calculate and can be modelled analytically either with extended lambda distributions as previously discussed or if necessary with higher-order B-splines as discussed by Harris *et al.*[185]. As a result in order to construct the mathematical model knowledge of the corresponding copula function $C(u, v, w)$ is necessary of which different types of copulas such as elliptical, generalized Archimedean, Liebscher, Fischer & Kock, Koehler-Symanowski and pair copula decompositions (PCD) approaches are possible as discussed by Fischer [186]. Considering the particular case of a pair copula decomposition we have following the approach of Fischer that in the case of a three dimensional model that in terms of conditional probabilities using the basic properties of statistical PDF's that

$$f(x_1, x_2, x_3) = f(x_3) \times f(x_2|x_3) \times f(x_1|x_2, x_3) \tag{3.90}$$

This is equivalent using Sklar's theorem in terms of the copula density $c(u_1, u_2, u_3)$ where $u_i = F(x_i)$, $i = 1,2,3$ is the cumulative distribution such that the joint PDF then takes the mathematical form

$$f(x_1, x_2, x_3) = c_{123}(F(x_1), F(x_2), F(x_3)) \times f(x_1) \times f(x_2) \times f(x_3) \tag{3.91}$$

120

Setting

$$u_i = F(x_i), i = 1,2,3 \tag{3.92}$$

and equating the above joint PDF's then gives

$$c_{123}(u_1, u_2, u_3) = \frac{f(x_2|x_3) \times f(x_1|x_2,x_3)}{f(x_1) \times f(x_2)} \tag{3.93}$$

Applying Sklar's theorem again with the definition of conditional density then gives

$$f(x_2|x_3) = c_{23}(F(x_2), F(x_3)) \times f(x_2) \tag{3.94}$$

Combining and substituting then gives

$$c_{123}(u_1, u_2, u_3) = \frac{c_{23}(u_2,u_3) \times f(x_1|x_2,x_3)}{f(x_1)} \tag{3.95}$$

Sequentially repeating the above steps again Fischer then derived a general expression for the corresponding copula density as

$$c_{123}(u_1, u_2, u_3) = c_{12}(u_1, u_2)c_{23}(u_2, u_3)c_{13|2}(h_{\theta 12}(u_1, u_2), h_{\theta 32}(u_3, u_2)) \tag{3.96}$$

if

$$h_\theta(u, v) \stackrel{\text{def}}{=} \frac{\partial C(i,v)}{\partial v} \tag{3.97}$$

The practical implication of this is that any higher dimensional copula can be constructed in terms of combinations of bivariate copulas as "building blocks" as illustrated in Figure 3.15.

In order to catalogue the different types of constructions that are mathematically possible a decomposition or D-vine distribution and a canonical or C-vine distribution are traditionally utilized.

The decomposition vine for a copula takes the form

$$f(x_1, \dots, x_d) = \left[\prod_{j=1}^{(d-1)} \prod_{i=1}^{(d-j)} c_{i,(i+j)|(i+1),\dots,(i+j-1)}\right] \times \left[\prod_{k=1}^{d} f_k(x_k)\right] \tag{3.98}$$

whilst the conical vine takes the form

$$f(x_1, \dots, x_d) = \left[\prod_{j=1}^{(d-1)} \prod_{i=1}^{(d-j)} c_{j,j+1|1,\dots,j-1}\right] \times \left[\prod_{k=1}^{d} f_k(x_k)\right] \tag{3.99}$$

joint PDF conductivity/viscosity
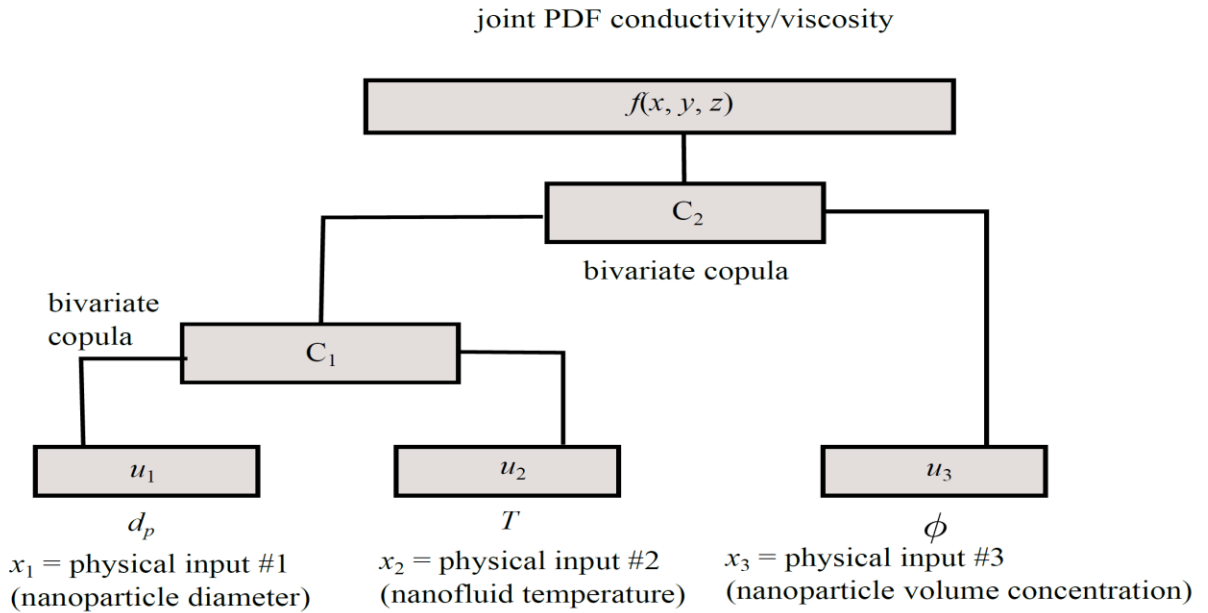
Figure 3-15 Illustration of how a pair-copula-decomposition can be used to sequentially build up higher dimensional joint probability density function distributions using the statistical information of the meta-parameters

Applying these results for $d = 3$ the joint PDF then takes the form

$$
\begin{aligned}
f(x_1, x_2, x_3) = {}& f(x_1)f(x_2)f(x_3) \\
& \times c_{12}(F(x_1), F(x_2)) \\
& \times c_{23}(F(x_2), F(x_3)) \\
& \times c_{13|2}(F(x_1|x_2), F(x_3|x_2))
\end{aligned}
\tag{3.100}
$$

Different strategies for calculating the conditional distributions are possible according to Aas [187] which take the forms for C-vines as

$$
F(x_j|x_1, x_2, \ldots, x_{j-1}) = \frac{\partial C_{j,j-1|1,\ldots,j-2}(F(x_j|x_1,\ldots,x_{j-2}), F(x_{j-1}|x_1,\ldots,x_{j-2}))}{\partial F(x_{j-1}|x_1,\ldots,x_{j-2})}
\tag{3.101}
$$

and for D-vines as

$$
F(x_j|x_1, x_2, \ldots, x_{j-1}) = \frac{\partial C_{j,1|2,\ldots,j-1}(F(x_j|x_2,\ldots,x_{j-1}), F(x_1|x_2,\ldots,x_{j-1}))}{\partial F(x_1|x_2,\ldots,x_{j-1})}
\tag{3.102}
$$

In general the total number of possible families of copula to consider for C-vines and D-vines following the technical results of Aas is $\frac{d(d-1)}{2}$ so for $d = 3$ corresponding to our particular modelling approach this then requires $\frac{3\times(3-1)}{2} = 3$ different choices of bivariate copula families to model the copula $c(u_1, u_2, u_3)$ whilst if $d = 4$ then $\frac{4\times(4-1)}{2} = 6$ different copula families are required in order to model the copula $c(u_1, u_2, u_3, u_4)$. Whilst the number of possible bivariate

122

copula family choices are extremely large for high dimensional models special statistical software exists as discussed by Brechmann & Schepsmeier [188] for fitting C-vines and D-vines where specialist goodness-of-fit tests exist for the determination and fitting of higher dimensional models as discussed by Schepsmeier [189] which we will utilize in testing possible copula models for our nanofluid thermophysical data from the previous chapter. In addition to C-vines and D-vines generated with the **R** statistical computing software [190] many researchers nowadays investigate multivariate empirical beta copulas as developed by Segers *et al.*[191] which is considered a special case of the Berstein copula in contemporary multivariate statistical research as determined from the earlier literature review. Although empirical copulas may offer high accuracy predictions as a future research topic the application of empirical copulas is disregarded in this dissertation due to its relatively heavy computational demands both for the construction of the copula itself and also for the calculation of the copula density. Parameter based copula models by contrast present a completely self-contained analytical specification of the nanofluid thermophysical properties that may be constructed for simplicity and ease of use. The non-parametric form of the empirical beta copula is

$$\mathbb{C}_n(\mathbf{u}) \stackrel{\text{def}}{=} \frac{1}{n} \sum_{i=1}^{n} \prod_{j=1}^{d} \mathbf{1} \left\{ \frac{R_{i,j}^{(n)}}{n} \leq u_j \right\}, \mathbf{u} = (u_1, \dots, u_d) \in [0,1]^d \tag{3.103}$$

where the test function is defined as

$$\mathbf{1} \left\{ \frac{R_{i,j}^{(n)}}{n} \leq u_j \right\} = \begin{cases} 1 & \text{iff condition is true} \\ 0 & \text{otherwise} \end{cases} \tag{3.104}$$

and where in this investigation as previously discussed just the marginal distributions u, v, w in $\mathbb{R}^3$ would be considered since there are $d = 3$ meta-parameters and logically extend this definition in the case of a four-dimensional statistical model. The non-parametric forms of copulas such as the above-mentioned empirical copulas may be used in mathematical modelling situations where a traditional two-parameter bivariate copula $C_\theta(u, v)$ is inadequate for the underlying (u, v) statistical data-set. Alternatives to empirical beta copulas are empirical Hazen and empirical Weibull copulas which may be constructed using the copBasic software package by Asquith [11]. Analytical trivariate copulas developed by De Capitani *et al.*[193] take the form for the distribution function as

$$F(x_1, x_2, x_3) = \prod_{i=1}^{3} \frac{1}{\left(1 + \lambda_i x_i^{-\theta_i}\right)^\varepsilon} \tag{3.105}$$

which when modified to include second order and third order interaction effects between the random variables x_1, x_2, x_3 then take the form

$$\begin{aligned} F(x_1, x_2, x_3) = [1 + \lambda_1 x_1^{-\theta_1} + \lambda_2 x_2^{-\theta_2} + \lambda_3 x_3^{-\theta_3} + \alpha_{12} \lambda_1 \lambda_2 x_1 x_2^{\theta_1 \theta_2} \\ + \ \alpha_{13} \lambda_1 x_1 x_3^{\theta_1 \theta_3} + \alpha_{23} \lambda_2 \lambda_3 x_2 x_3^{\theta_2 \theta_3} \\ + \ \alpha_{123} \lambda_1 \lambda_2 \lambda_3 x_1 x_2 x_3^{-\theta_1 \theta_2 \theta_3}]^{-\varepsilon} \end{aligned} \tag{3.106}$$

The above distribution function then results in the copula function

$$C(u_1, u_2, u_3) = [1 + \sum_{i=1}^{3} \left(u_i^{-\frac{1}{\varepsilon}} - 1\right) + \alpha_{12}\left(u_1^{-\frac{1}{\varepsilon}} - 1\right)\left(u_2^{-\frac{1}{\varepsilon}} - 1\right)$$

$$+ \ \alpha_{13}\left(u_1^{-\frac{1}{\varepsilon}} - 1\right)\left(u_3^{-\frac{1}{\varepsilon}} - 1\right) + \alpha_{23}\left(u_2^{-\frac{1}{\varepsilon}} - 1\right)\left(u_3^{-\frac{1}{\varepsilon}} - 1\right) \qquad (3.107)$$

$$+ \ \alpha_{123}\left(u_1^{-\frac{1}{\varepsilon}} - 1\right)\left(u_2^{-\frac{1}{\varepsilon}} - 1\right)\left(u_3^{-\frac{1}{\varepsilon}} - 1\right)]^{-\varepsilon}$$

where the following inequalities must be satisfied for the copula to be valid such that

$$\alpha_{12} \leq (\varepsilon + 1) \qquad\qquad (3.108)$$
$$\alpha_{13} \leq (\varepsilon + 1) \qquad\qquad (3.109)$$
$$\alpha_{23} \leq (\varepsilon + 1) \qquad\qquad (3.110)$$
$$\alpha_{123} \leq (\varepsilon + 1)\min(\alpha_{12}\alpha_{13}, \alpha_{12}\alpha_{23}, \alpha_{13}\alpha_{23}) \qquad\qquad (3.111)$$

The general form for two, three and four dimensional copulas as derived by Aas [187] for multivariate copulas is summarized such that

$$f(x_1, x_2) = f_1(x_1)f_2(x_2) \times c_{12}(F_1(x_1), F_2(x_2)) \qquad\qquad (3.112)$$

$$f(x_1, x_2, x_3) = f_1(x_1)f_2(x_2)f_3(x_3)$$
$$\times c_{12}(F_1(x_1), F_2(x_2)) \times c_{23}(F_2(x_2), F_3(x_3)) \qquad\qquad (3.113)$$
$$\times c_{13|2}(F(x_1|x_2), F(x_3|x_2))$$

$$f(x_1, x_2, x_3, x_4) = f_1(x_1)f_2(x_2)f_3(x_3)f_4(x_4)$$
$$\times \ c_{12}(F_1(x_1), F_2(x_2)) \times c_{13}(F_1(x_1), F_3(x_3)) \times c_{14}(F_1(x_1), F_4(x_4))$$
$$\times \ c_{23|1}(F(x_2|x_1), F(x_3|x_1)) \times c_{24|1}(F(x_2|x_1), F(x_4|x_1)) \qquad (3.114)$$
$$\times \ c_{34|12}(F(x_3|x_1, x_2), F(x_4|x_1, x_2))$$

In order to implement a copula model for the effective thermal conductivity k_{eff} or the effective viscosity μ_{eff} the copula function "*couples*" the respective random variables interactions with each other and "*uncouples*" their own independent marginal distributions. This mathematical modelling technique is considered both statistically appropriate and physically relevant for this research investigation due to the fact that the meta-parameters are formally considered as independent model inputs i.e. they are independent random variables so they each have their own independent marginal distribution and they then subsequently couple and interact with each other in a subsequent mathematical model for a nanofluid's respective property such as its effective thermal conductivity or effective viscosity. As an example if the effective thermal conductivity depends just on the base fluid temperature and the nanofluid volume concentration ϕ so that $k_{eff}(T, \phi)$ then we set $T = x_1$, $\phi = x_2$ and $k_{eff} = x_3$ and determine the joint PDF $f(x_1, x_2, x_3)$. Once the joint PDF is constructed then the remaining random variable $x_3 = k_{nf}$ for a specified value of $x_1 = T_{bath}$ and $x_2 = \phi_{bath}$ for example may then be calculated as a statistical expectation such that using the formal statistical definition $\langle k_{nf} \rangle = \mathbb{E}(x_3)$ it follows that

$$\mathbb{E}(x_3) = \int_{\mathbb{R}} x_3 f(T_{bath}, \phi_{bath}, x_3) \ dx_3 \qquad (3.115)$$

$$\langle k_{nf} \rangle = \int_{-\infty}^{\infty} x_3 f(T_{bath}, \phi_{bath}, x_3) \ dx_3 \qquad (3.116)$$

The above definition is equivalent to the one-dimensional definition of the expected value μ for a random variable x with a probability density function $f(x)$ such that the expected value is calculated as $\mu = \int_{-\infty}^{\infty} x f(x) \ dx$ with a variance $\sigma^2 = \int_{-\infty}^{\infty} (x - \mu)^2 f(x) \ dx$ since in the special case if the other random variables are fixed to a specific value, such as a specified temperature T or volume concentration ϕ, the joint PDF $f(T, \phi, d_p, k_{nf})$ will then simplify to a conditional probability. Following a similar line of reasoning the corresponding variance for the nanofluid thermal conductivity σ may then be equivalently calculated using the formal mathematical statistical definition as

$$\sigma^2 = \int_{-\infty}^{\infty} (x - \mu)^2 f(x) \ dx$$
$$= \int_{-\infty}^{\infty} x_3^2 f(T_{bath}, \phi_{bath}, x_3) \ dx_3 - \mu^2 \qquad (3.117)$$

The above working definitions for the expected value and corresponding variance may then in principle be extended for nanofluid models with more than three meta-parameters. As an example if the nanofluid thermal conductivity is mathematically modelled in terms of the temperature $x_1 = T$, the volume concentration $x_2 = \phi$, the nanoparticle diameter $x_3 = d_p$, the nanofluid pH value $x_4 = \text{pH}$ and the shear strain rate $x_5 = \dot{\gamma}$ so that the functional form is $k_{nf} = \text{fnc.}(x_1, x_2, x_3, x_4, x_5)$ we would construct the multivariate copula $f(x_1, x_2, x_3, x_4, x_5, x_6)$ by treating the nanofluid thermal conductivity as a random variable that is "coupled" through some sort of complicated mathematical equation with the other random variables so that the expected value of the effective thermal conductivity for a particular operating condition of the equipment, machine or instrument which is using the nanofluid as a working fluid, say for $T_{op} = x_1^*$, $\phi_{op} = x_2^*$, $d_{op} = x_3^*$, $\text{pH}_{op} = x_4^*$ and $\dot{\gamma}_{op} = x_5^*$ which are specified, may then be calculated as $\langle k_{nf} \rangle = \int_{-\infty}^{\infty} x_6 f(x_1^*, x_2^*, x_3^*, x_4^*, x_5^*, x_6) \ dx_6$ where x_6 is a dummy variable to evaluate the improper Riemann integral. For a general multidimensional data-set $\mathbf{X} = [x_1, x_2, \ldots, x_d]^{\mathrm{T}}$, be it for a nanofluid effective thermal conductivity k_{nf}, viscosity μ_{nf}, density ρ_{nf} or enthalpy h_{nf} where $x_j, j = 1, \ldots, d$ are appropriate meta-parameters the expected value μ and associated variance may be convenient calculated as $\mu = \int_{-\infty}^{\infty} x_d f(x_1, \ldots, x_d) \ dx_d$ and $\sigma^2 = \int_{-\infty}^{\infty} (x_d - \mu)^2 f(x_1, \ldots, x_d) \ dx_d$ where as previously discussed x_d is treated as a dummy variable to evaluate the respective integral formulae for the expected value and variance. Due to the fact that a copula may be used to construct the joint PDF for a random variable $\mathbf{X} = [x_1, \ldots, x_d]^{\mathrm{T}}$ for any dimension $2 \leq d \in \mathbb{N}$ this general approach may therefore in principle be extended to nanofluids with any appropriate choice of meta-parameters however the key requirement is that the underlying data is reliable and that it has an associated statistical uncertainty. This requirement is satisfied in our particular case since we have conducted a review of the available data k_{nf}, T, ϕ, d_p from the open literature and estimated the corresponding uncertainties $u(k_{nf}), u(T), u(\phi), u(d_p)$ either from accuracies documented in the respective literature sources or from good experimental judgement for all of the underlying data-points which are used in a Monte Carlo simulation to generate sampled values of the meta-parameters when constructing the copula statistical model.

As a result whilst a powerful mathematical approach to model and summarize the properties of nanofluid thermophysical properties in a manner that incorporates the underlying aleatoric statistical experimental measurement uncertainties has been identified this mathematical modelling technique is only as powerful as the quality of the underlying data that is incorporated into the mathematical model. Unfortunately the contemporary research status within the field of nanofluids is that much of the reported data is incomplete and where available there have been questions as to the overall reliability and consistency of the available experimental data.

Although the above expectation values are formally defined as iterated infinite integrals due to the mathematical requirement that the joint PDF normalizes to unity i.e. $\int_{\mathbb{R}^3} f(\mathbf{x}) \ \ \mathrm{d}x_1 \mathrm{d}x_2 \ \ \mathrm{d}x_3 = 1$ in the case of the PDF $f(x_1, x_2, x_3)$ with a similar normalization for $f(x_1, x_2, x_3, x_4)$ in practical terms the expectations are calculated as definite integrals due to the finite limits of the underlying data. As an example when manufacturing a water/alumina nanofluid the operating temperature would usually be from around room temperature of 20 °C to not higher than about 70 °C due to the fact that this is generally considered a critical temperature above which most nanofluid's performance will start to significantly degrade in terms of heat exchanger performance. In many practical cases it is not strictly necessary to analytically evaluate the above integrals since if the integrand is defined in terms of the marginal distributions and copula density then the integrand may be simply and conveniently numerically evaluated using a Monte Carlo integration as discussed by Press *et al.*[132]. The evaluation of a univariate integral will also feature later in this chapter when we demonstrate how to mathematically calculate the expected value and associated variance for the nanofluid thermal conductivity in terms of the conditional distributions constructed from the various bivariate copula families of the meta-parameters and which may also in principle be calculated with a Monte Carlo integration.

The mathematical modelling approach to calculate the effective thermal conductivity or viscosity from a joint PDF constructed in terms of a copula has been mathematically specified from the preceding analysis however a related and remaining challenge for completeness is how to sample from the underlying copula based joint PDF in order to for example perform further Monte Carlo simulations when estimating the uncertainty $u(h_c)$ of a convective heat transfer coefficient h_c that uses the nanofluid as working fluid in for example a heat exchanger. In order to address this issue consider for simplicity a nanofluid model with three meta-parameters such that $k_{nf} = $ fnc.(T, ϕ, d_p) where it is assumed that the meta-parameters are random variables that are statistically independent of each other i.e. the scientist/engineer that produces the nanofluid in the laboratory has the freedom to source a particular grade and type of nanoparticle from a supplier/manufacturer which then specifies the average nanoparticle diameter d_p, the scientist/engineer has the freedom to mix the base fluid and nanoparticles with appropriate mass or volume fractions which then specifies the nanoparticle volume concentration ϕ, and finally the scientist/engineer has the freedom the operate the particular machinery, equipment or instrumentation that uses the nanofluid at an appropriate temperature which then specifies the temperature T. Under these circumstances the meta-parameters are fixed as $x_1^* = T$, $x_2^* = \phi$ and $x_3^* = d_p$ so that the remaining parameter x_4 in the joint PDF $f(x_1, x_2, x_3, x_4)$ which represents the random variable for the effective thermal conductivity is now a free variable. For convenience let $x_4 = \xi$ so that the joint PDF simplifies to a one dimensional function $f(\xi)$ which after appropriate normalization for statistical consistency for a PDF such that $\int_{-\infty}^{\infty} f(\xi) \ \ \mathrm{d}\xi$ may now

represent an equivalent probability density function $g(\xi)$ for the nanofluid thermal conductivity where $g(\xi) = [f(\xi)]/[\max(f(\xi))]$. The problem of sampling random variables ξ from a PDF $g(\xi)$ may be solved by generating a random variable ρ from a standard rectangular normal distribution $R[0,1]$ i.e. $\rho \sim R[0,1]$ and then solving the integral equation

$$\xi \leftarrow \rho = \int_{-\infty}^{\xi} f(\eta) \ d\eta \tag{3.118}$$

The generation of the statistical sampling scheme as indicated above uses the cumulative distribution function $F(\xi) = \int_{-\infty}^{\xi} f(\eta) \ d\eta$ where η is a dummy variable and not the probability density function $f(\xi)$ due to the fact that the CDF is already naturally normalized. We recall that a univariate PDF will in general have a Gaussian or bell-shaped curve, with appropriate skewness and/or asymmetry deviations from a pure Gaussian distribution, so that even if $f(\xi)$ is further scaled such that $0 \leq f(\xi) \leq 1$ and we attempt to solve for $\rho = f(\xi)$ that this would potentially introduce systematic or biased errors since we would in general have to specify "which side of the Gaussian curve" to search for a solution of $\rho = f(\xi)$. The use of the cumulative distribution function $F(\xi)$ completely avoids this issue since it is unimodal so that there is always a unique solution to $\rho = F(\xi)$ and is considered the correct mathematical statistical technique to consistently and accurately sample from arbitrary statistical distributions. An illustration of the sampling scheme is shown in Figure 3.16 for an arbitrary probability density function (PDF) and its corresponding cumulative distribution function (CDF).
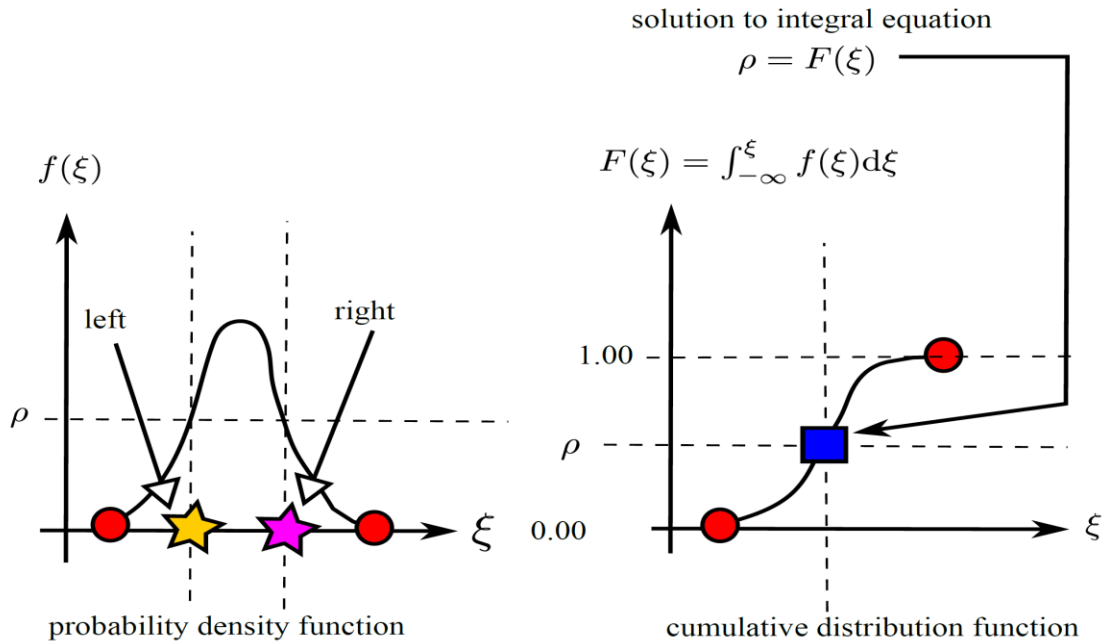

Figure 3-16 Illustration of proposed statistical sampling scheme for a nanofluid's thermophysical property from an equivalent univariate PDF obtained from a copula based joint PDF of the nanofluid's respective thermophysical property

In this example the domain of the PDF for the thermal conductivity is $\xi_{min} \leq \xi \leq \xi_{max}$ where ξ is a random variable for the thermal conductivity and for example we assume that $\xi_{min} = 0.679$ W m^{-1} K^{-1} and $\xi_{max} = 0.753$ W m^{-1} K^{-1} for example only. If we scale the PDF such that $0 \leq f(\xi) \leq 1$ and then attempt to solve the equation $\rho = f(\xi)$ for the corresponding value of the random variable ξ it is observed that the value of the solution of ξ will technically depend whether we searched "on the left" or "on the right" which is not statistically rigorous and mathematically inconsistent. On the other hand the CDF formally defined as $F(\xi) = \int_{-\infty}^{\xi} f(\xi) \ d\xi$ regardless of the magnitude of ξ, which may be a thermal conductivity in units of [W m^{-1} K^{-1}] or an absolute viscosity in units of [mPa s], is always by definition scaled such that $0 \leq F(\xi) \leq 1 \ \forall \ \xi \in [\xi_{min}, \xi_{max}]$ and will therefore always result in a statistically correctly and mathematically consistent value when sampling from an arbitrary probability density function. As a result if the various meta-parameters have specified values our mathematical model for a particular nanofluid property such as an effective thermal conductivity or an effective viscosity which is constructed in terms of copulas then reduces to a mathematical expression for the probability density function of the respective nanofluid property.

The nanofluid mathematical modelling approach in this research investigation is a low dimensional multivariate problem for conceptual simplicity so that the joint PDF may be readily constructed in terms of a copula mathematical model from known meta-parameter multivariate experimental data points, although the copula model may in principle be extended to arbitarily high dimensions if additional meta-parameters are known. In order to validate & verify the predictions for the mathematical model a simple normalized error E_n approach may be utilized where

$$E_n = \frac{y_a - y_p}{\sqrt{U^2(y_a) + U^2(y_p)}} \tag{3.119}$$

where y_a is the actual effective thermal conductivity or effective viscosity from the database, y_p is the predicted value using our mathematical model, and $U(y_a)$ and $U(y_p)$ are the associated expanded uncertainties for y_a and y_p respectively. The comparison between actual and predicted results can also be inspected for consistency using multivariate quantile-quantile plots as discussed by Dhar *et al.*[194].

In order to construct the copula model for the effective thermal conductivity $k_{eff}(T, d_p, \phi)$ the clustering of the multi-dimensional data-points using the results in Figure 3.17, Figure 3.18 and Figure 3.19 is first visualized in Figure 3.20 from which restrictions to the model's domain may be determined.

Based on the clustering of the data points as shown in Figure 3.20 a restricted domain for constructing the model is specified as

$$\left. \begin{array}{l} 0.5 \leq \phi/[\%] \leq 10 \\ 293.15 \leq T/[K] \leq 333.15 \\ 10 \leq d_p/[nm] \leq 75 \end{array} \right\} \tag{3.120}$$

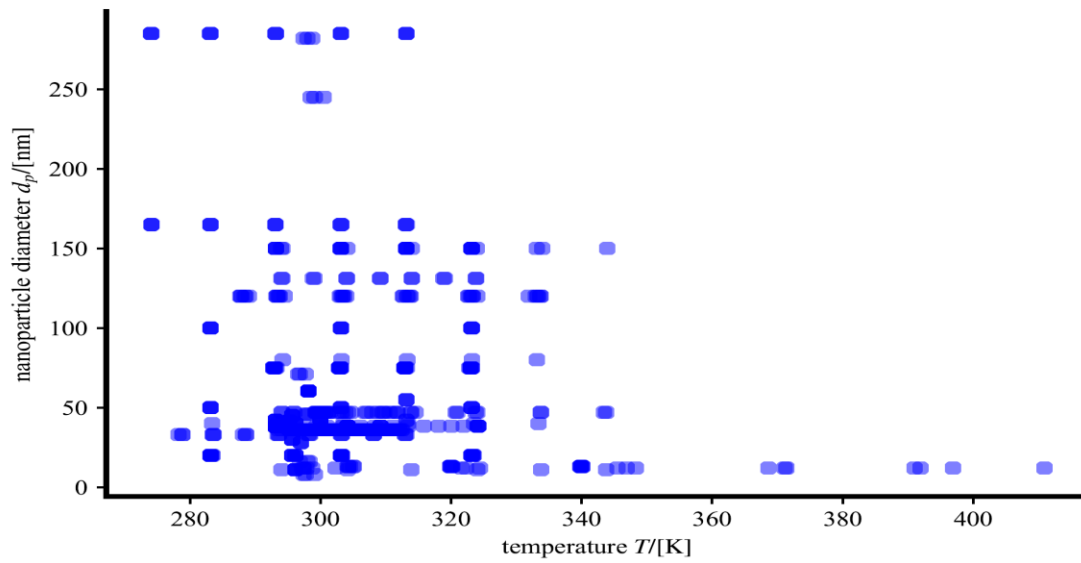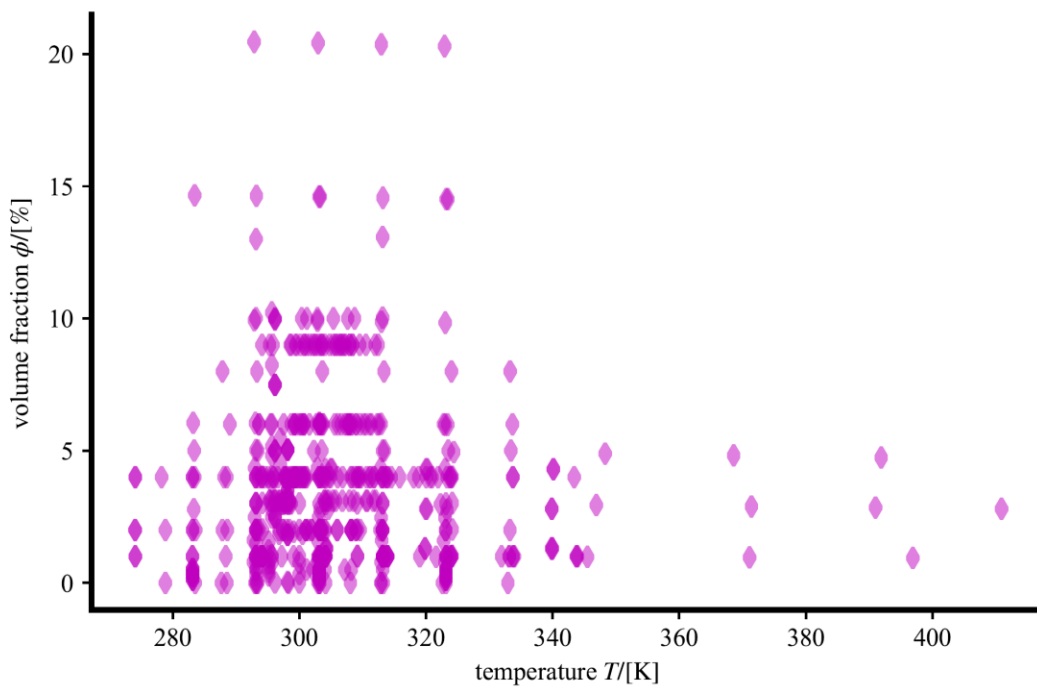*Figure 3-17 Illustration of typical T and d_p limits from thermal conductivity database*

Figure 3-18 Illustration of typical T and ϕ limits from thermal conductivity database
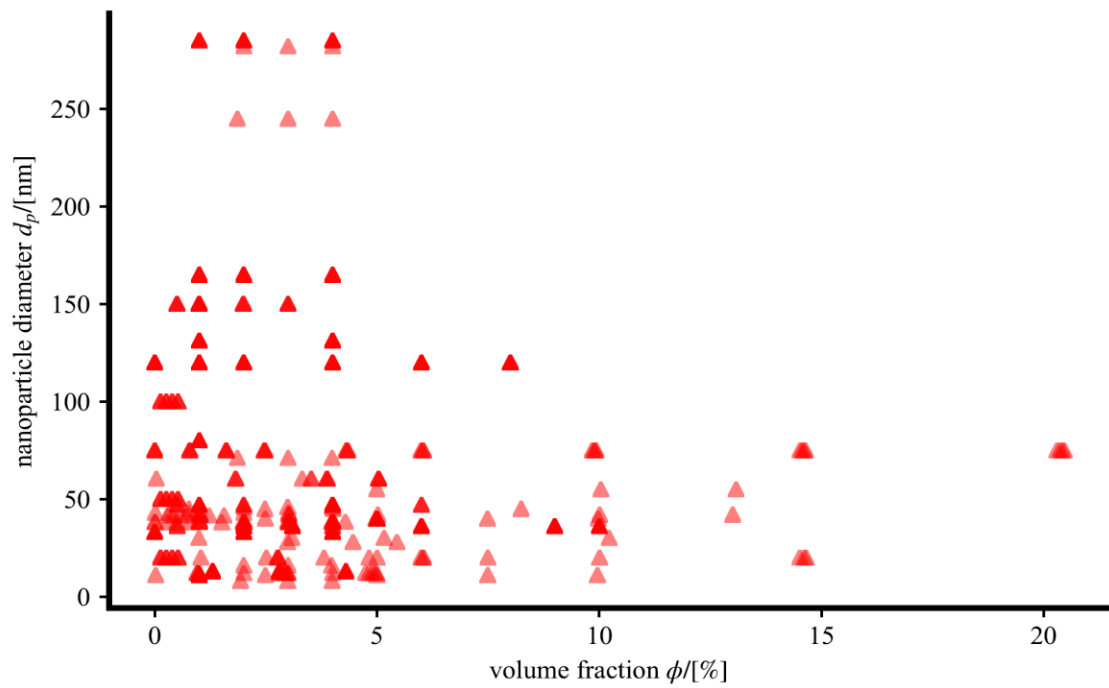
Figure 3-19 Illustration of typical ϕ and d_p limits from thermal conductivity database
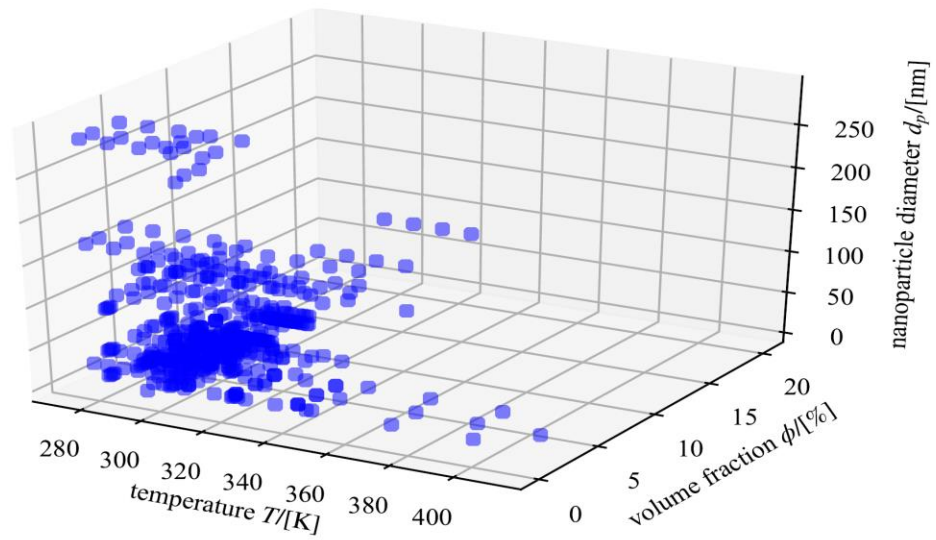

Figure 3-20 Illustration of visualization of clustering effects of T, ϕ and d_p experimental data points

The above choice of domain is to ensure that there are an adequate number of points in the $\mathbb{R}^3$ space of the underlying meta-parameters so that the meta-parameters are "clustered" near each other in order to avoid a higher dimensional "leverage" effect where inaccuracies occur if there are too few points to adequately perform predictions in certain regions of the $\mathbb{R}^3$ domain. An example of this "leverage" effect is if predictions for k_{eff} are performed at for example a point $\mathbf{x} = [348 \ \text{K}, 150 \ \text{nm}, 10\%]^T \in \mathbb{R}^3$ since the space in this neighbourhood is relatively "empty".

This numerical strategy of limiting the domain to regions of the meta-parameter hyper-space $\mathbb{R}^{(d-1)}$ which are sufficiently populated with known data-points therefore implicitly avoids inaccurate extrapolations to points that are not physically plausible such as for example nanofluid data points for $\phi/\% > 20$ or $T/[\text{K}] > 400$ which are not experimentally feasible. In the event that the model was defined in terms of $n \geq 4$ meta-parameters, for example if we constructed a model such that $k_{eff} = f(\mathbf{x})$ where $\mathbf{x} = [T, d_p, \phi, \text{pH}, \mathcal{A}]^T$ where the nanofluid pH and agglomeration size $\mathcal{A}$ were also considered, then a three-dimensional visualization of the clustering effect would not be possible and we would either have to plot a set of two dimensional visualizations x_1/x_2, x_1/x_3, x_1/x_4, x_2/x_3, x_2/x_4 and x_3/x_4 or utilize alternative algebraic techniques in order to determine an appropriate domain for the meta-parameter $\mathbf{x}$.

Although the copulas may be manually constructed in terms of building up the marginal distributions in terms of extended lambda distributions and using custom specified pair copula constructions (PCC's) with parametric schemes or non-parametric schemes as previously outlined it is generally more convenient and efficient to use the available professionally written statistical software.

Presently the most well known and widely utilized approach is the **R** package CDVine developed by Brechmann & Schepsmeier [188] which allows for constructing either C-vines or D-vines. In order to utilize the CDVine package after first selecting a convenient domain for T, ϕ and d_p we extract all the multi-dimensional data points from the thermal conductivity database that reside within this domain and then save 90% of these points in a multidimensional set D_e for building up a new experimental dataset and reserve the remaining 10% of the points in another multidimensional set D_t for testing the accuracy of our model predictions.

Using the representative standard uncertainties for each of the components in D_e we then use a Monte Carlo scheme to generate sampled statistical draws from D_e in order to build up a larger dataset that takes into account the statistical uncertainties to produce the Monte Carlo data for $\mathbf{x} = [k_{nf}, T, \phi, d_p]^T$ in natural physical units. The statistical data from the Monte Carlo simulation may then be used to construct the copula model where the mathematical modelling process is conceptually illustrated in Figure 3.21.

Motivated by an earlier dimensional group approach originally developed by Sharifpur *et al.*[46] who generated dimensional groups for the meta-parameters it is considered beneficial to modify the Monte Carlo data $\mathbf{x}$ by constructing the equivalent distribution functions for each component x_1, x_2, x_3, x_4 as per the recommendations of Brechmann *et al.*[188]. This implementation may be performed using the discrete form of the univariate distribution function as documented in the GUM Supplement 1 by the BIPM [195].
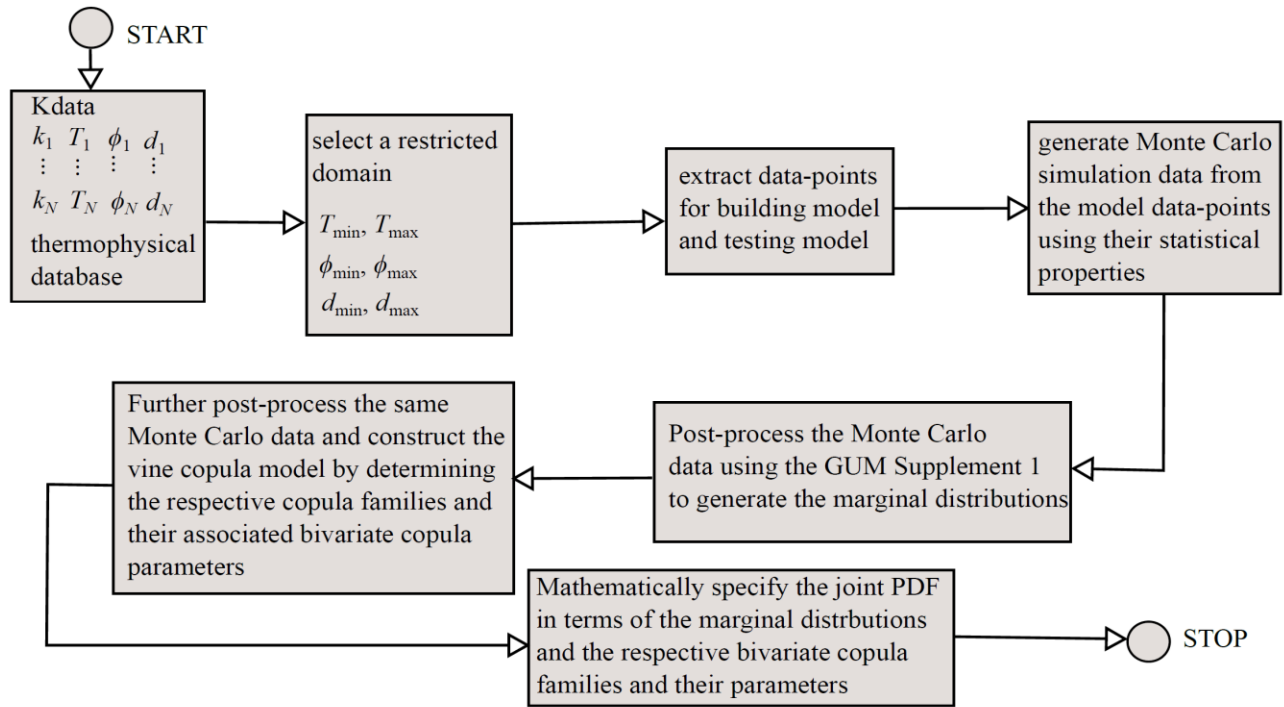
Figure 3-21 Conceptual illustration of mathematical modelling process to generate a copula model of nanofluid thermophysical properties for a four dimensional model using three meta-parameters

The results for the distribution functions for the random variables x_1, x_2, x_3, x_4 from the Monte Carlo simulation obtained from the database are analysed from where we comment that the distribution curves for the volume fraction ϕ and nanoparticle diameter d_p are not "smooth" since the curves are based on actual physical experimental data reported in the literature which tended to use discrete values of the mass fractions ω (which we converted into equivalent volume fractions ϕ) usually every 5% from 0% to 50% and where much of the nanoparticles used the existing manufacturer nanoparticle diameters such as 30 nm i.e. the meta-parameter values were discrete values of practical experimental quantities due to physical laboratory constraints. The results in this figure are scaled for easier visualization although natural units of $x_1/$ [W m^{-1} K^{-1}], $x_2/$[K], x_3 which is dimensionless and not expressed in percentage, and $x_4/$[m] and not units of nanometres are utilized, however it should be noted that the "copula data" values of u_1, u_2, u_3, u_4 are all dimensionless and all scaled by definition such that $0 \leq u_1, u_2, u_3, u_4 \leq 1$ so the physical units are not an issue in the copula fitting process since the corresponding physical units can always be recovered from the $u_i = F(x_i), i = 1,2,3,4$ marginal distribution relations which can either be approximated with an analytical expression such as for example an extended lambda distribution or with numerical interpolation schemes since the x_i and $F(x_i)$ data-points are univariate and unimodal curves.

For simplicity a kernal density estimate (KDE) approach may be utilized in order to work out the corresponding marginal probability density functions $f(x_1), f(x_2), f(x_3), f(x_4)$ for which from

the data obtained in the literature review results in constructed PDF's from which it may be observed that although the marginal PDF's for the thermal conductivity $f(k_{nf})$ and temperature $f(T)$ can obviously be modelled with analytical expressions such as for example the extended lambda distributions that for the present dataset that the concentration $f(\phi)$ and size distribution $f(d_p)$ PDF's are too complicated to be adequately analytically with simple mathematical formulae. As a result a simple approach to mathematically capture the marginal distributions is to export the kernel density estimate data to a file which may then be subsequently accessed for univariate interpolations where the KDE data ere obtained with the built-in **R** function for calculating a KDE of the various marginal PDF's as indicated below:

```
pdfdata <- read.table("D:/University of Pretoria/MODELLING/
CONDUCTIVITY/pdfMonteCarlo.txt", header = FALSE)
pdfxyresults <- density(pdfdata, bw = "nrd0", adjust = 1, kernel = c("gaussian"), weights =
NULL, window = kernel, give.Rkern = FALSE,n = 250)}
xvalues <- pdfxyresults$x
yvalues <- pdfxyresults$y
write.csv(xvalues, file = "D:/University of Pretoria/MODELLING/
CONDUCTIVITY/densityxvalues.csv")
write.csv(yvalues, file = "D:/University of Pretoria/MODELLING/
CONDUCTIVITY/densityyvalues.csv")
```

In the above fragment of **R** computer code a simple pdfMonteCarlo.txt file that contains a single column of the Monte Carlo data is loaded into the **R** workspace and after some computer coding implementation a total of $n = 250$ data-points is generated and which is then saved to file. As a result the marginal probability density functions $f(x_1), f(x_2), f(x_3), f(x_4)$ may then conveniently and simply evaluated with for example univariate spline routines. To avoid complicated scaling factors physical SI units should be utilized unless otherwise indicated since the four-dimensional joint PDF must formally satisfy the normalization condition

$$\int_{\mathbb{R}^4} f(x_1, x_2, x_3, x_4) = 1 \tag{3.121}$$

As a results the corresponding distribution functions $F(x_1), F(x_2), F(x_3), F(x_4)$ as illustrated in Figure 3.22, Figure 3.23, Figure 3.24 and Figure 3.25 respectively may then be used to calculate the equivalent copula coordinate values u_1, u_2, u_3, u_4 where the corresponding probability density functions are illustrated in Figure 3.26, Figure 3.27, Figure 3.28 and Figure 3.29 respectively.

Since the cumulative distributive function is unimodal by definition the equivalent copula value is simply specified as $u_j = F(x_j), j = 1,2,3,4$ so that the coordinates x_1, x_2, x_3, x_4 are naturally scaled to reside in the hyper-cube $[0,1] \times [0,1] \times [0,1] \times [0,1]$ as per the recommended technical guidelines specified by Brechmann *et al.*in order to conveniently utilize the CDvine software package.
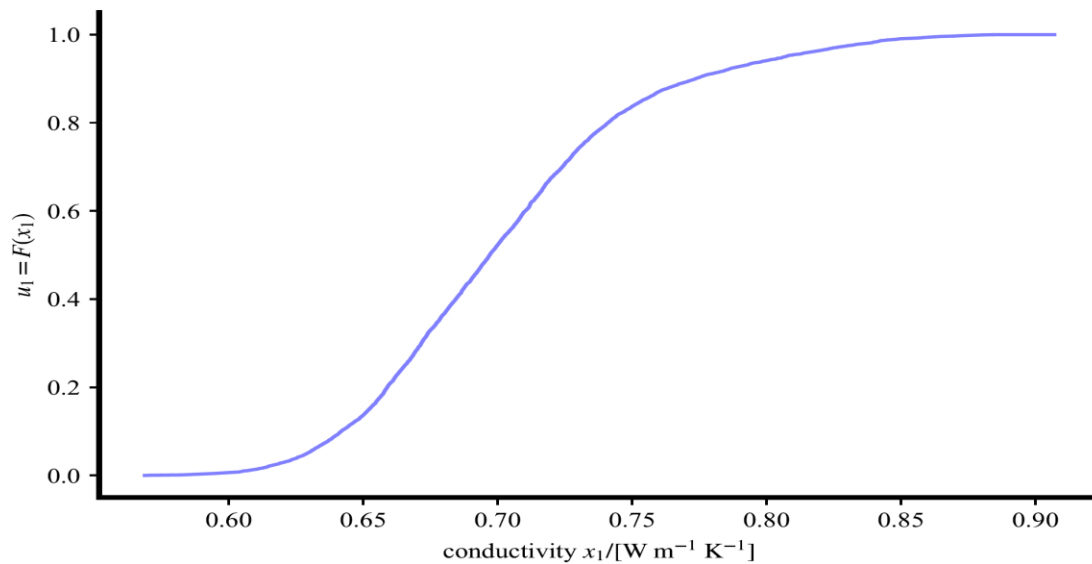
Figure 3-22 Illustration of marginal distribution function $F(x_1)$ of nanofluid conductivity for thermal conductivity database
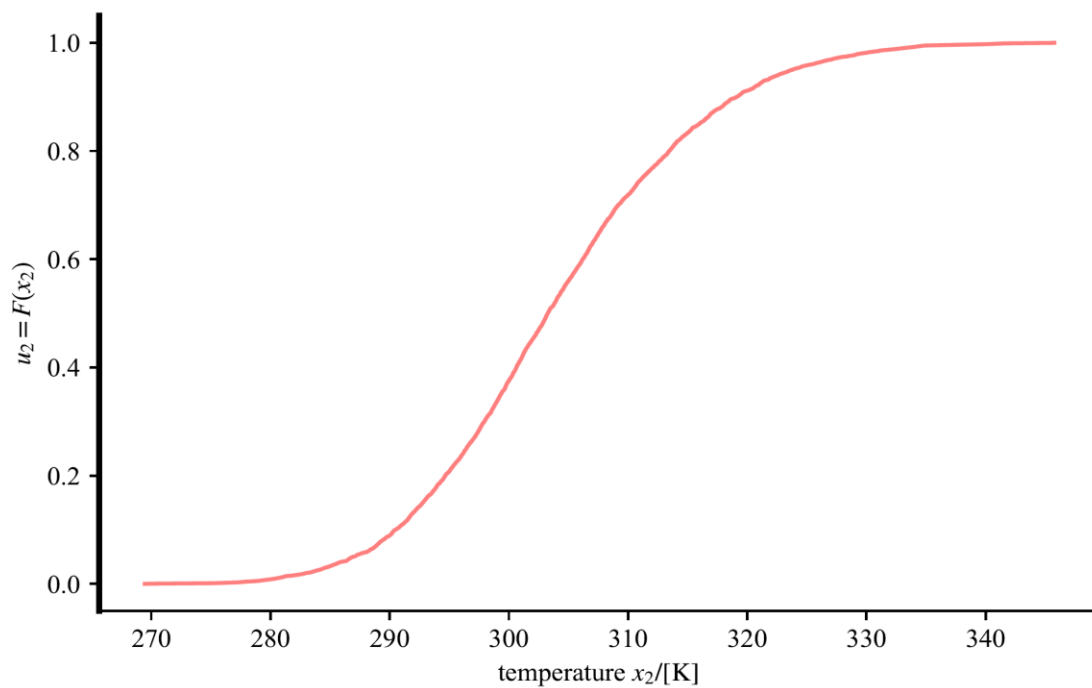
Figure 3-23 Illustration of marginal distribution function $F(x_2)$ of nanofluid temperature for thermal conductivity database
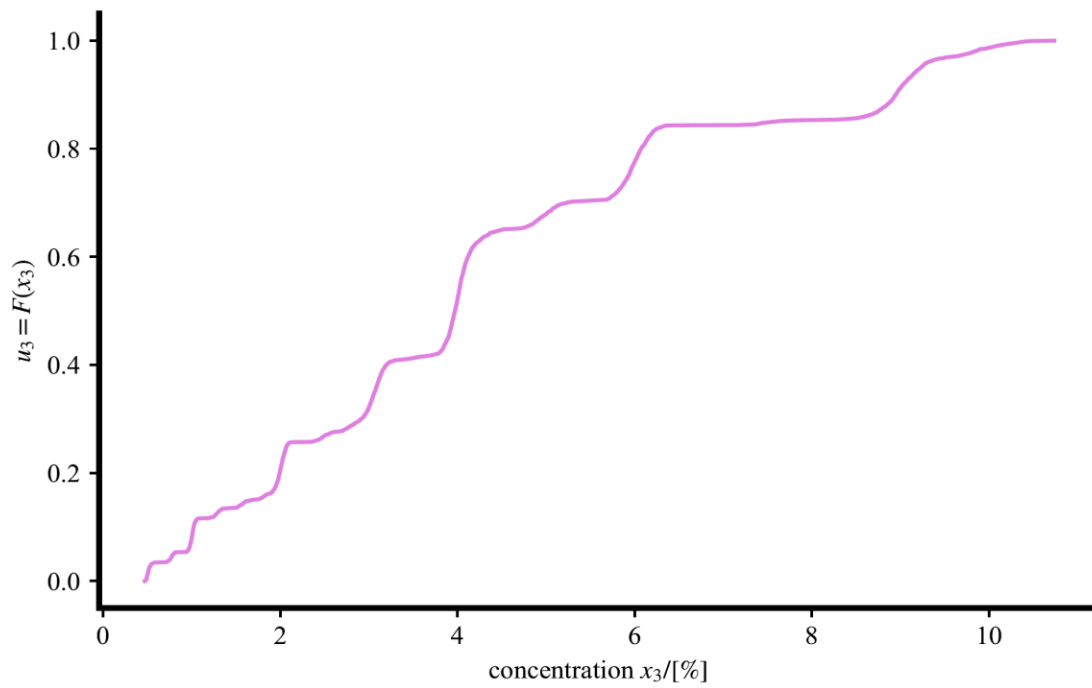
Figure 3-24 Illustration of marginal distribution function $F(x_3)$ of nanofluid concentration for thermal conductivity database
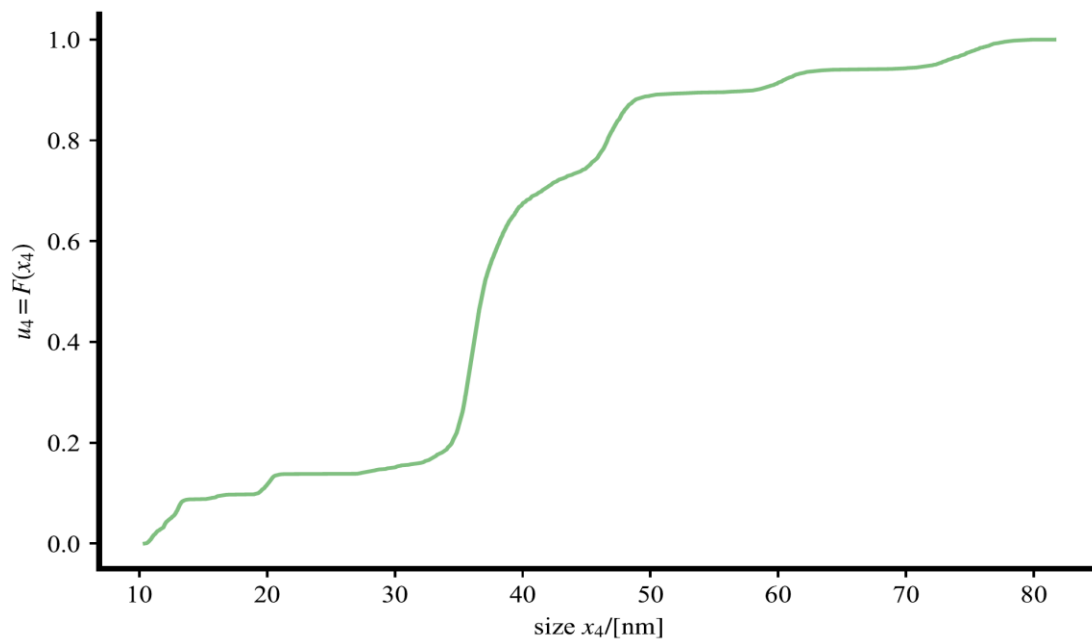
Figure 3-25 Illustration of marginal distribution function $F(x_4)$ of nanoparticle size for thermal conductivity database
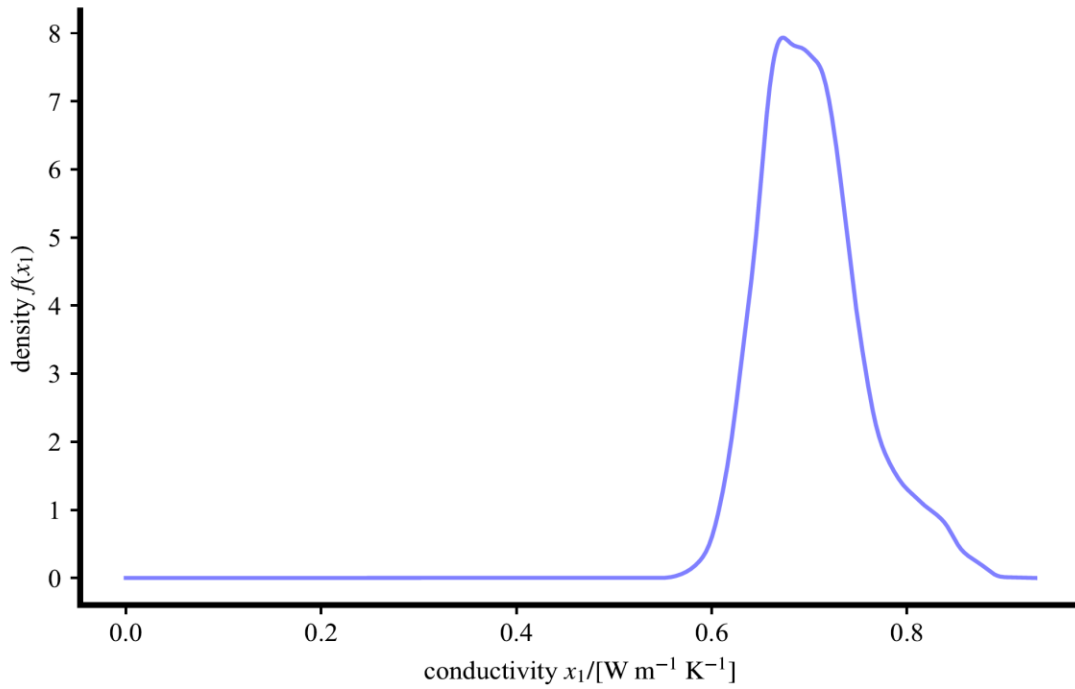
Figure 3-26 Illustration of marginal probability density function $f(x_1)$ using a kernel density estimate approach for the Monte Carlo simulations of random variable x_1 for thermal conductivity database
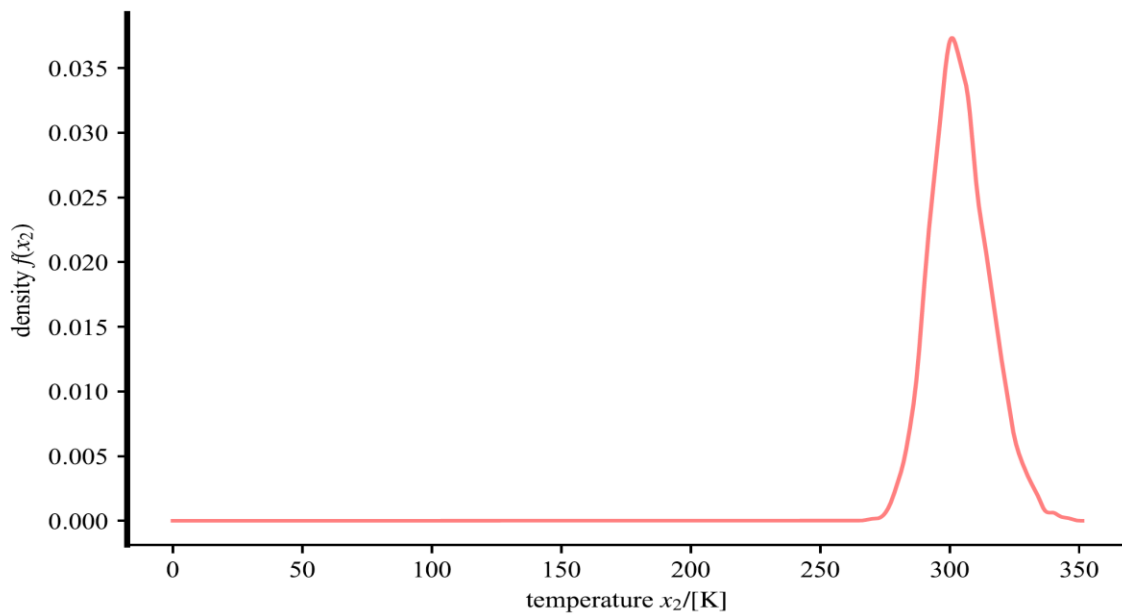
Figure 3-27 Illustration of marginal probability density function $f(x_2)$ using a kernel density estimate approach for the Monte Carlo simulations of random variable x_2 for thermal conductivity database

136
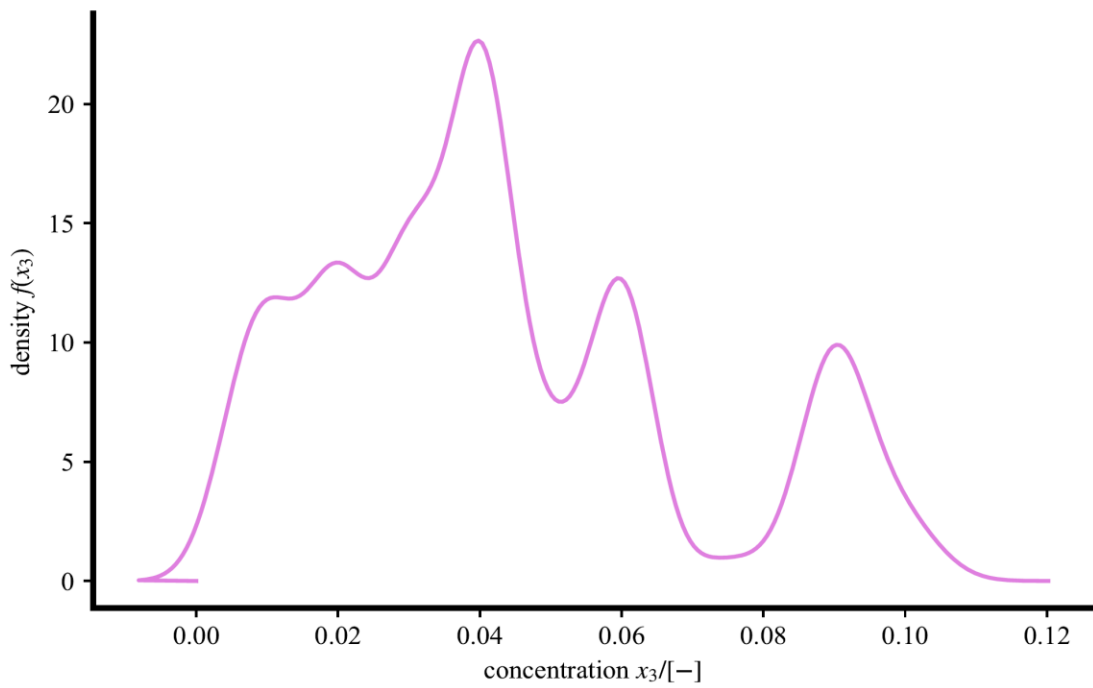
Figure 3-28 Illustration of marginal probability density function $f(x_3)$ using a kernel density estimate approach for the Monte Carlo simulations of random variable x_3 for thermal conductivity database
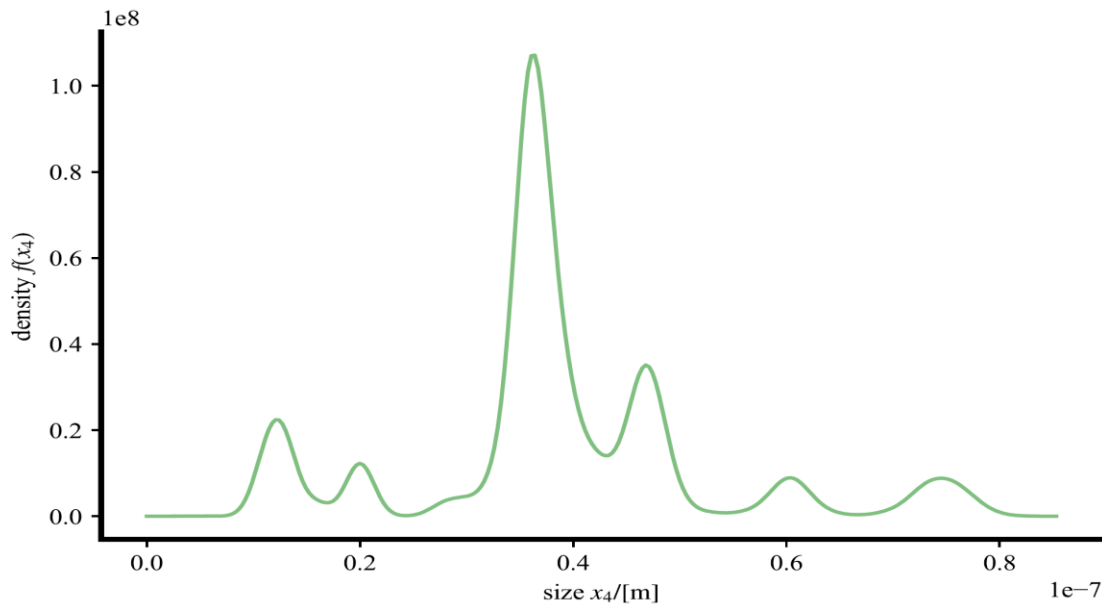
Figure 3-29 Illustration of marginal probability density function $f(x_4)$ using a kernel density estimate approach for the Monte Carlo simulations of random variable x_4 for thermal conductivity database

The next step is to select a tree structure for a C-vine scheme for our $d = 4$ dataset however this choice whilst unique in the special case that $d = 3$ is however not unique if $d \geq 4$. A combinatorial analysis may be used to demonstrate that since there are in general $\frac{d(d-1)}{2}$ different bivariate copula densities that must be selected as previously discussed.

The selection of the particular tree structure for a C-vine would in general depend on the either the intuition of the analyst, additional statistical hypothesis testing, or a combination of these two approaches. A selection of potential vine based copula models based on a combination of physical intuition and a mathematical modelling hypothesis is illustrated in Figure 3.30.

In general as per the the discussion by Nagler *et al.*[123] the tree structure of C-vines usually referred to as a R-vine is constructed in such a way as to satisfy the following general specifications for mathematical consistency such that:

1. For a d-dimensional random variable $\mathbf{x} = [x_1, \ldots, x_d]^\mathrm{T}$ the R-vine is constructed as a set of trees $T_m = (V_m, E_m)$ where $m = d - 1$ is the total number of trees where V_m is a set of vertices and E_m a corresponding set of edges
2. T_1 is an initial tree with nodes $V_1 = \{1, \ldots, d\}$ and edges E_1 where the random variables are chosen in any convenient order (in our model we set node 1 as the nanofluid thermal conductivity or viscosity for convenience)
3. For $m \geq 2$ the tree T_m has nodes $V_m = E_{m-1}$ and edges E_m
4. Whenever two nodes is a tree T_{m+1} are joined by some edge then the corresponding edges in the previous tree T_m must then share a common node for mathematical consistency

Due to the underlying statistical database in this investigation which contains the Monte Carlo data of four random variables i.e. $\mathbf{x} = [x_1, x_2, x_3, x_4]^\mathrm{T}$ the dimension of the data is $d = 4$ as as per the standard methodology of constructing C-vines there will then be $m = d - 1 = 3$ tree structures associated with the copula model.

Using the approach of Brechmann & Schepsmeier [188] the corresponding copula density for example in Model 1 as specified in Figure 3.30 in order to demonstrate the general principle is then calculated as

$$
\begin{aligned}
c(u_1, u_2, u_3, u_4) = {} & c_{1,2}(u_1, u_2) \times c_{1,3}(u_1, u_3) \times c_{1,4}(u_1, u_4) \\
& \times \ c_{2,3|1}(u_{2|1}, u_{3|1}) \times c_{3,4|1}(u_{3|1}, u_{4|1}) \\
& \times \ c_{2,4|1,3}(u_{2|1,3}, u_{4|1,3})
\end{aligned} \tag{3.122}
$$

where the notation of for example $C_{2,3|1}$ means that this is the bivariate copula function for the variables x_2 and x_3 that is independent of the variable x_1 i.e. this is a conditional distribution function. Slightly different expressions for the copula density $c(u_1, u_2, u_3, u_4)$ will occur depending on how the analyst opted to construct the tree structure for the copula model.
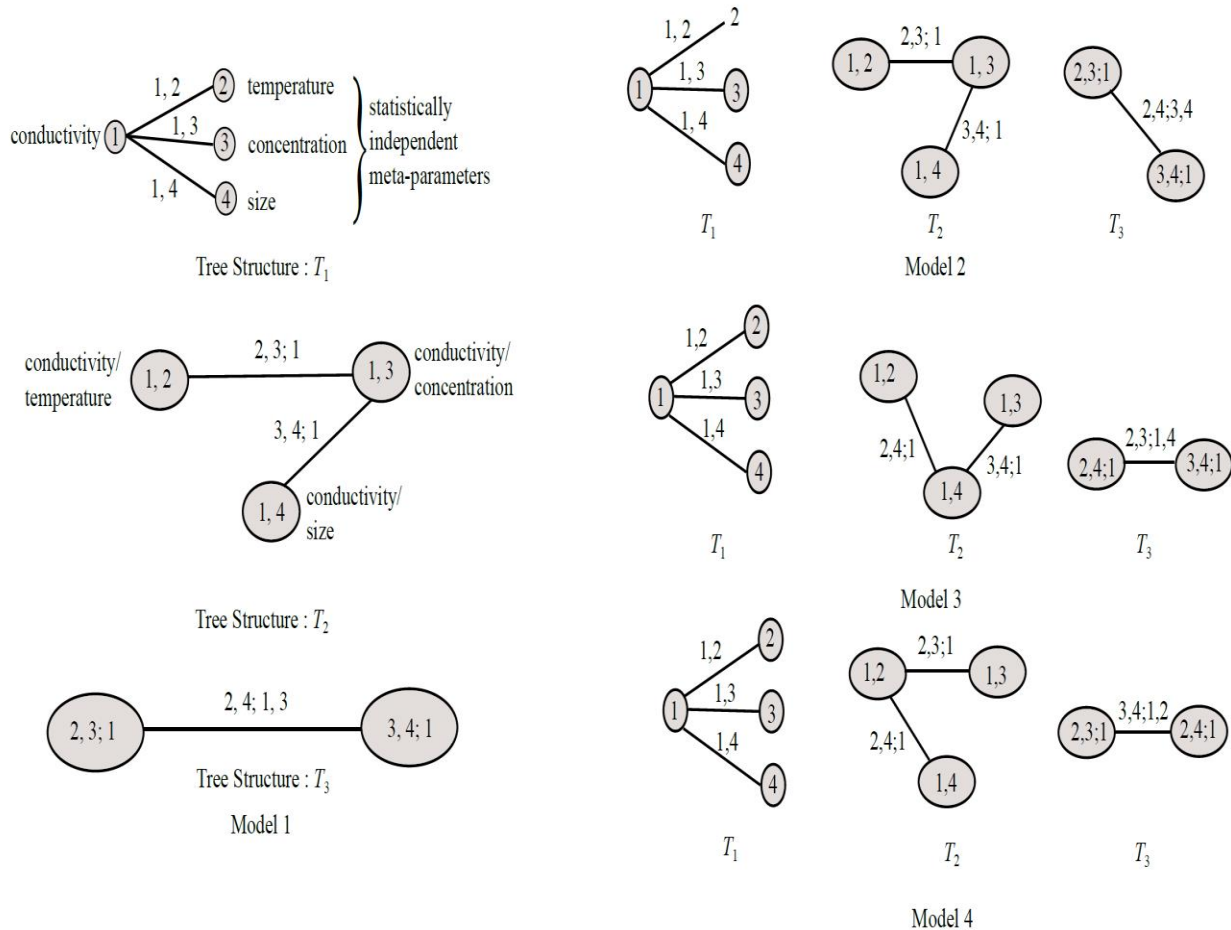
Figure 3-30 Illustration of different possible copula models constructed in terms of simplified R-vine tree structures for nanofluid thermophysical properties

For consistency in the analysis the lower case $f(x)$ will signify a probability density function, an upper case $F(x)$ will signify a cumulative distribution function for the PDF $f(x)$ i.e. $F(x) = \int_{-\infty}^{x} f(\xi) \, d\xi$, an upper case $C(x, y)$ will denote the bivariate copula function for random variables x and y, and a lower case $c(u, v)$ will signify a corresponding copula density function. The corresponding joint PDF may then be calculated in the general case for a four-dimensional model as

$$f(x_1, x_2, x_3, x_4) = f_1(x_1) \times f_2(x_2) \times f_3(x_3) \times f_4(x_4) \times c(u_1, u_2, u_3, u_4) \tag{3.123}$$

139

where for the specified scheme in Model 1 as previously illustrated $f_j(x_j), j = 1,2,3,4$ are the corresponding marginal distributions of the random variable x_j, $j = 1,2,3,4$ and $u_j, j = 1,2,3,4$ are the corresponding cumulative distribution functions $F(x_j)$ as previously discussed where $0 \leq u_j \leq 1$ by definition. From this equation it is seen that the construction of a pair copula construction (PCC) is critically dependent on a knowledge of the various conditional distributions terms such as $u_{2|1}$. In certain texts such as that by Nagler *et al.*[123] the definition of conditional distribution is occasionally written as $u_{j_e|D_e} := C_{j_e|D_e}(u_{j_e|\mathbf{u}_{D_e}})$ to simplify the notation however a mechanism of calculating the conditional distributions is still necessary for completeness. The mathematical trick used in copula modelling was originally discussed by Brechmann *et al.*[188] who explains the relevant technical implementation details where v_j is an arbitrary component of the vector $\mathbf{v}$ of the conditional random variables and $\mathbf{v}_{-j}$ is a corresponding vector defined as $\mathbf{v}\backslash\{v_j\}$ i.e. the vector that is made up of $\mathbf{v}$ but which excludes the element v_j. Using this scheme the mathematical trick in the field of copulas for calculating the conditional distribution is to then calculate the conditional distribution constructed through a sequential iteration scheme such that the univariate/multivariate conditional distribution is of the form

$$F(x|\mathbf{v}) = \frac{\partial}{\partial F(v_j|\mathbf{v}_{-j})} [C_{xv_j|\mathbf{v}_{-j}}(F(x|\mathbf{v}_{-j}), F(v_j|\mathbf{v}_{-j}))] \tag{3.124}$$

which is conveniently implemented in the CDVine software library.

The above univariate/multivariate conditional distribution $F(x|\mathbf{v})$ i.e. where it is desired to find the distribution function for some univariate random variable x, say for example to find a thermal conductivity, given a known multivariate random variable, say for example $\mathbf{v} = [x_2, x_3]^T$ for an experiment with a given bath temperature such as $x_2 = T_{bath} = 310$ K and a known nanoparticle diameter such as $x_3 = d_p = 37$ nm, as discussed is sequentially calculated through an iteration process of the various copula functions that were constructed in the previous trees for the particular R-, C- or D-vines that were used to build up the overall copula model. In the special case of a univariate/univariate conditional distribution $F(x|v)$ the formula reduces to

$$F(x|v) = \frac{\partial C_{xv}(F(x), F(v))}{\partial F(v)} \tag{3.125}$$

In order to illustrate how this formula works consider that we wish to calculate for example $F(x_1|x_2)$ where according to our previous model nanofluid thermal conductivity model we have $k_{nf} = \text{fnc.}(T, \phi, d_p)$ so that the joint PDF is $f(x_1, x_2, x_3, x_4)$ where $x_1 = k_{nf}$, $x_2 = T$, $x_3 = \phi$ and $x_4 = d_p$ respectively. To calculate the conditional distribution we first work out $F(x_1)$ from the statistical data and set it to say $u = F(x_1)$ noting that now $0 \leq u \leq 1$ by definition, and similarly we work out say $v = F(x_2)$ where again $0 \leq v \leq 1$. Now since two random variables are considered it is possible to simply construct the bivariate copula function $C(u, v)$ using any convenient and appropriate copula family such as a bivariate Gaussian or a bivariate Student's t-distribution, so that the conditional distribution is simply calculated as the partial derivative $F(x_1|x_2) = \frac{\partial C}{\partial v}$ which can either be calculated analytically if the bivariate copula has a simple formula or numerically using for example any convenient finite difference scheme.

In practical terms this means that conditional distributions in tree T_2 are defined in terms of the normal copula functions in tree T_1, then conditional distributions in tree T_3 are in turn defined in terms of functions from tree T_2 (which are in turn defined in terms of functions from tree T_1) and so on up to the final tree T_m where $m = d - 1$. Whilst an analyst may in principle write their own computer code to implement these mathematical techniques it is usually easier to use the existing statistical functions in software such as **R** which at its base level is written in ANSI compliant C for fast compilation and performance.

As a result the main challenge in copula modelling is to select an appropriate tree structure based on physical/mathematical intuition and/or statistical hypothesis testing, and then in the appropriate selection of bivariate copula models in each of the constituent "building blocks" used to construct the higher dimensional copula model. The selection of an appropriate bivariate copula for each of the underlying "building blocks" whilst conceptually simple is not a trivial undertaking if attempted manually through for example graphical comparisons of potential trial copulas since there are almost 40 different choices of bivariate copula families and since in the four dimensional case with $d = 4$ there are $\frac{d(d-1)}{2} = 6$ different bivariate copula building blocks there is then a need to select from a total of $40 \times 6 = 240$ possible bivariate copula families, which is why our recommended approach for constructing the "best" copula model is through the use of the Cdvine software library.

Due to the fact that the choice of tree structure is not unique for higher dimensional models there is then a variety of possible different combinations of models as previously illustrated in Figure 3.30 and of which each possible tree structure would have to be evaluated based on a combination of physical and mathematical criteria since not all potential combinations would necessarily be physically meaningful even if there are statistical correlations that are present. This issue is also a potential modelling challenge in for example some of the artificial intelligence (AI) and artificial neural network (ANN) approaches that were considered in the previous chapter due to the distinction between correlation and causality the resolution of which at least in the field of nanofluids remains an ongoing concern in the absence of a comprehensive physical theory and experimentally consistent high quality measurement data. The copula model construction may therefore be simplified using a conventional 'star-shaped' C-vine as illustrated in Figure 3.31.
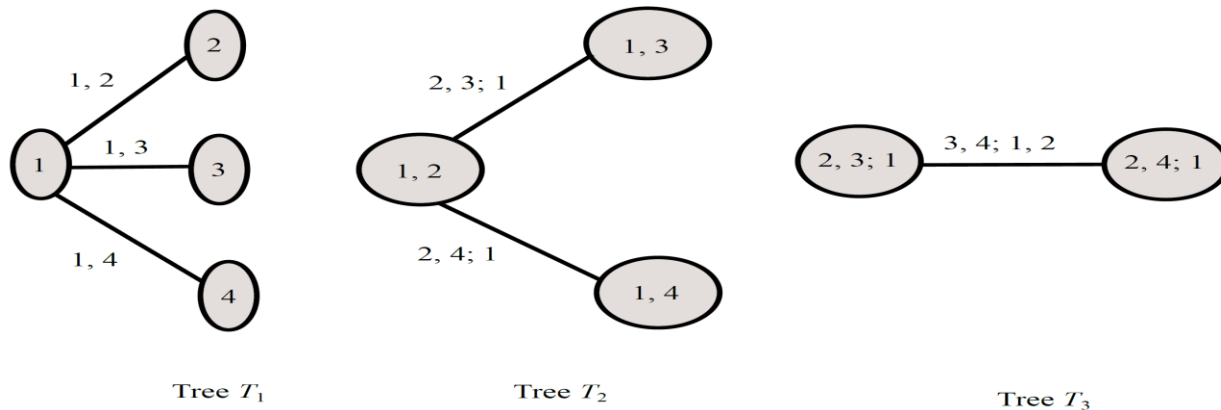

Figure 3-31 Illustration of four dimensional C-vine tree structures to model a four dimensional joint probability density function

As a result the joint PDF is then simply calculated as

$$f(x_1, x_2, x_3, x_4) = f_1(x_1) \times f_2(x_2) \times f_3(x_3) \times f_4(x_4) \times c(u_1, u_2, u_3, u_4)$$ (3.126)

where the corresponding copula density for a conventional C-vine is then

$$c(u_1, u_2, u_3, u_4) = c_{1,2} \times c_{1,3} \times c_{1,4} \times c_{2,3|1} \times c_{2,4|1} \times c_{3,4|1,2}$$ (3.127)

The above standard C-vine structure for a four dimensional copula is not necessarily as restrictive as it may seem as the four random variables x_1, x_2, x_3, x_4 can in turn be ordered in for example six different ways as summarized in Table 3.6 by simply changing the order of the columns in the Monte Carlo statistical data from a $N \times 6$ matrix where each column reports on each random variable.

Copula Model	Ordering Scheme of Tree Nodes
I	$x_1 = k_{nf}, \ x_2 = T, \ x_3 = \phi, \ x_4 = d_p$
II	$x_1 = k_{nf}, \ x_2 = \phi, \ x_3 = d_p, \ x_4 = T$
III	$x_1 = k_{nf}, \ x_2 = d_p, \ x_3 = T, \ x_4 = \phi$
IV	$x_1 = k_{nf}, \ x_2 = T, \ x_3 = d_p, \ x_4 = \phi$
V	$x_1 = k_{nf}, \ x_2 = \phi, \ x_3 = T, \ x_4 = d_p$
VI	$x_1 = k_{nf}, \ x_2 = d_p, \ x_3 = \phi, \ x_4 = T$

Table 3. 6 Selection of different possible four dimensional copula models based on a reordering of the tree nodes

In this dissertation as previously discussed in the literature review we restrict the analysis to three meta-parameters since this is considered physically meaningful for a nanofluid thermophysical property and there is an absence of verified and complete experimental information of other potential meta-parameters. As a result to avoid unnecessary complications with recursive definitions of the conditional distribution terms when constructing the copula since a low order copula has been utilized explicit formulae are feasible when building a four dimensional copula. The final results for a four dimensional copula density as reported by Barthel *et al.*[197] who investigated D-vines using h-functions defined as

$$h_{i|k}(u_i|u_k) = \frac{\partial}{\partial u_k} \mathbb{C}_{ik}(u_i, u_k)$$ (3.128)

$$h_{k|i}(u_k|u_i) = \frac{\partial}{\partial u_i} \mathbb{C}_{ik}(u_i, u_k)$$ (3.129)

$$h_{i|j;k}(u_i|u_j) = \frac{\partial}{\partial u_j} \mathbb{C}_{ij;k}(u_i, u_j)$$ (3.130)

$$h_{j|i;k}(u_j|u_i) = \frac{\partial}{\partial u_i} \mathbb{C}_{ij;k}(u_i, u_j)$$ (3.131)

When these explicit formulae are utilized it is then necessary to fit six bivariate copula for a conventional C-vine in standard form as summarized in Table 3.7 which provides explicit expressions for the first and second variables for each of the six copula building blocks.

Tree	Bivariate copula	First variable	Second variable
T_0	$\mathbb{C}_{12}(u_1,u_2)$	$v_1=u_1$	$v_2=u_2$
T_0	$\mathbb{C}_{13}(u_1,u_3)$	$v_1=u_1$	$v_2=u_3$
T_0	$\mathbb{C}_{14}(u_1,u_4)$	$v_1=u_1$	$v_2=u_4$
T_1	c_{12}	$v_1=u_1$	$v_2=u_2$
T_1	c_{13}	$v_1=u_1$	$v_2=u_3$
T_1	c_{14}	$v_1=u_1$	$v_2=u_4$
T_2	$c_{23\mid1}$	$v_1=\dfrac{\partial\mathbb{C}_{12}(u_1,u_2)}{\partial u_1}$	$v_2=\dfrac{\partial\mathbb{C}_{13}(u_1,u_3)}{\partial u_1}$
T_2	$c_{24\mid1}$	$v_1=\dfrac{\partial\mathbb{C}_{12}(u_1,u_2)}{\partial u_1}$	$v_2=\dfrac{\partial\mathbb{C}_{14}(u_1,u_4)}{\partial u_1}$
T_3	$c_{34\mid12}$	$v_1=\dfrac{\partial\mathbb{C}(a,b)}{\partial b}, a=\dfrac{\mathbb{C}_{13}(u_1,u_3)}{\partial u_1}, b=\dfrac{\mathbb{C}_{12}(u_1,u_2)}{\partial u_1}$	$v_2=\dfrac{\partial\mathbb{C}(a,b)}{\partial b}, a=\dfrac{\partial\mathbb{C}_{14}(u_1,u_4)}{\partial u_1}, b=\dfrac{\partial\mathbb{C}_{12}(u_1,u_2)}{\partial u_1}$

Table 3. 7 Illustration of the construction of a set of bivariate copula for building a four dimensional C-vine copula density
$c(u_1,u_2,u_3,u_4)=c_{12}\times c_{13}\times c_{14}\times c_{23\mid1}\times c_{24\mid1}\times c_{34\mid12}$

For convenience when the copula mathematical is constructed the built in conditional distribution function from the CDVine software library is utilized which takes the form for $u_{2\mid1}$ as

```
BiCopHfunc(u1val, u2val, family=C12family, par=C12theta1, par=C12theta2)$hfunc1
```

In the above computer code fragment C12family is a numerical term that specified the bivariate copula family for $C(u_1,u_2)$, par is a numerical value of the θ_1 parameter for copula $C(u_1,u_2)$, par2 is a numerical value of the θ_2 parameter for copula $C(u_1,u_2)$, and u1val and u2val are the specified values for which the conditional distribution must be evaluated where the $hfunc1 function-call extracts the corresponding partial derivative. Based on the preceding mathematical modelling analysis that we have performed the algorithm to build and construct a copula mathematical model for the nanofluid effective thermal conductivity may then be summarized as indicated in Table 3.8.

The mathematical modelling of the nanofluid thermal conductivity using a copula in this algorithm after suitable manipulation is now reduced to the standard statistical form and we may then conveniently and simply use the existing CDvine software library to calculate the six corresponding copula families and their associated parameters. The computer code to generate the mathematical model in **R** using the CDVine software library is then:

```
library(CDVine)
udata <- read.table("D:/University of Pretoria/MODELLING/ CONDUCTIVITY/Udata.txt",
header = FALSE)
CV <- CDVineCopSelect(data = udata, familyset = NA, type = "CVine", selectioncrit = "AIC")
optimized_families <- CV$family parameter_1 <- CV\$par parameter_2 <- CV$par2
```

When this computer code is implemented using the $N=4770$ Monte Carlo data-points for the thermal conductivity it then produces the results by typing the commands:

```
optimized_families print(parameter_1, digits = 10) print(parameter_2, digits = 10)
```

Step	Implementation
I	Load the physical statistical database information as a $N \times 4$ matrix into an appropriate computational workspace such that the columns of the data are ordered as k_{nf}, T, ϕ, d_p
II	Extract the physical data into univariate vectors such that $p_1 = [(k_{nf})_1, \ldots, (k_{nf})_N]^{\mathrm{T}}$, $p_2 = [T_1, \ldots, T_N]^{\mathrm{T}}$, $p_3 = [\phi_1, \ldots, \phi_N]^{\mathrm{T}}$, and $p_4 = [(d_p)_1, \ldots, (d_p)_N]^{\mathrm{T}}$
III	Convert the physical data into an equivalent copula data by constructing univariate distribution functions such that the random variables are $x_1 = F_1(p_1)$, $x_2 = F_2(p_2)$, $x_3 = F_3(p_3)$ and $x_4 = F_4(p_4)$ using the GUM Supplement 2
IV	Analytically specify the marginal distributions as $f_i(x_i) = \left\{ c_i \left[a_i \rho^{(b_i-1)} + (1-\rho)^{(b_i-1)} \right] \right\}^{-1}$ for $i = 1,2,3,4$ using the previously constructed extended lambda parameters where ρ is numerically solved from the equation $x_i = Q_i(\rho)$ where $Q_i(\rho) = d_i + (c_i/b_i)[a_i\rho^{b_i} - (1-\rho)^{b_i} + 1 - a_i]$ iff $b_i \neq 0$ whilst $Q_i(\rho) = d_i + c_i[a_i\ln(\rho) - \ln(1-\rho)]$ iff $b_i = 0$. Alternately if the data is too "messy" save the data as a $N \times 8$ matrix x1u1x2u2x3u3x4u4 so that univariate splines can simply and easily interpolate the relevant distributions $u_i = F(x_i)$.
V	Calculate the appropriate families and respective family parameter(s) for the bivariate copulas $c_{1,2}, c_{1,3}, c_{1,4}, c_{2,3|1}, c_{2,4|1}, c_{3,4|1,2}$ for a four-dimensional C-vine of x_1, x_2, x_3, x_4
VII	Specify the copula density as $c(u_1, u_2, u_3, u_4) = c_{1,2} \times c_{1,3} \times c_{1,4} \times c_{2,3|1} \times c_{3,4|1} \times c_{2,4|3}$
VIII	Calculate the joint PDF as $f(x_1, x_2, x_3, x_4) = f_1(x_1) \times f_2(x_2) \times f_3(x_3) \times f_4(x_4) \times c(u_1, u_2, u_3, u_4)$

Table 3. 8 Algorithm implementation for constructing a copula mathematical model of a nanofluid effective thermal conductivity transformed joint probability density function $f(x_1, x_2, x_3, x_4)$ with $x_1 = k_{nf}$, $x_2 = T$, $x_3 = \phi$ and $x_4 = d_p$

The above commands then produces the following computer output to screen as indicated below:

copula #	family	par	par2
1	10	1.92082298	0.884453438
2	1	0.336285905	0
3	20	1.17843781	0.986786
4	23	-0.214856871	0
5	2	0.016404251	9.776683
6	5	-0.774240094	0

Referring to the user manual of the CDVine software library then produces the following extracted information:

family #	family name
1	BB8 copula (Frank-Joe)
2	Gaussian copula
3	Rotated BB8 copula (180° survival BB8)
4	Rotated Clayton copula (90°)
5	Student t-copula
6	Frank copula

Copula	Family	Parameters
$c_{1,2}(u_1, u_2)$	BB8 (Frank-Joe) / family # 10	$\theta_1 = 1.92082298$ & $\theta_2 = 8.84453438E - 01$
$c_{1,3}(u_1, u_3)$	Gaussian / family # 1	$\theta_1 = 3.36285905 \times 10^{-1}$ & $\theta_2 = 0$
$c_{1,4}(u_1, u_4)$	Rotated BB8 (180° survival BB8) / family # 20	$\theta_1 = 1.17843781$ & $\theta_2 = 9.86785516 \times 10^{-1}$
$c_{2,3;1}(u_{2|1}, u_{3|1})$	Rotated Clayton (90°) / family # 23	$\theta_1 = -2.14856871 \times 10^{-1}$ & $\theta_2 = 0$
$c_{2,4;1}(u_{2|1}, u_{4|1})$	Student-t / family # 2	$\theta_1 = 1.64042514 \times 10^{-2}$ & $\theta_2 = 9.77668263$
$c_{3,4;1,2}(u_{3|1,2}, u_{4|1,2})$	Frank / family #5	$\theta_1 = -7.74240094 \times 10^{-1}$ & $\theta_2 = 0$

Table 3. 9 Summary of bivariate copulas for nanofluid effective thermal conductivity mathematical model constructed in terms of a conventional four-dimensional C-vine $c(u_1, u_2, u_3, u_4)$

Copula	Family	Parameters
$c_{1,2}(u_1, u_2)$	Rotated BB8 (90°) / family # 30	$\theta_1 = -1.96692$ & $\theta_2 = -0.93747$
$c_{1,3}(u_1, u_3)$	Frank / family # 5	$\theta_1 = 4.469618$ & $\theta_2 = 0$
$c_{1,4}(u_1, u_4)$	BB8 / family # 10	$\theta_1 = 1.438957$ & $\theta_2 = 0.953844$
$c_{2,3;1}(u_{2|1}, u_{3|1})$	BB8 / family # 10	$\theta_1 = 1.890264$ & $\theta_2 = 0.887141$
$c_{2,4;1}(u_{2|1}, u_{4|1})$	Frank / family # 5	$\theta_1 = 0.657003$ & $\theta_2 = 0$
$c_{3,4;1,2}(u_{3|1,2}, u_{4|1,2})$	Rotated BB8 (180°) / family # 20	$\theta_1 = 2.684825$ & $\theta_2 = 0.437763$

Table 3. 10 Summary of bivariate copulas for nanofluid effective viscosity mathematical model constructed in terms of a conventional four-dimensional C-vine $c(u_1, u_2, u_3, u_4)$

Using the above information the nanofluid effective thermal conductivity model is then conveniently analytically summarized in Table 3.9 where we have used the notation that the respective copula building blocks each have a parameter $\boldsymbol{\theta} = [\theta_1, \theta_2]^{\mathrm{T}}$ that captures the information of the outputs par and par2 from the CDVine program.

In the case where the particular copula only has one parameter the second parameter is then just set to $\theta_2 = 0$ for mathematical consistency and practical convenience when utilizing software implementations for reporting copula mathematical models.

A similar process may also be performed in order to construct a copula mathematical model for the nanofluid effective viscosity from the database reported in the previous chapter. Qualitative results for the viscosity copula model are shown in the following figures for the marginal distributions in Figure 3.32, Figure 3.33, Figure 3.34 and Figure 3.35 respectively, whilst the corresponding kernal density estimates (KDE's) of the corresponding marginal PDF's are shown in Figure 3.36, Figure 3.37, Figure 3.38 and Figure 3.39 respectively, whilst the copula families and associated parameters for the vine based copula modelling scheme for the effective viscosity is summarized in Table 3.10.
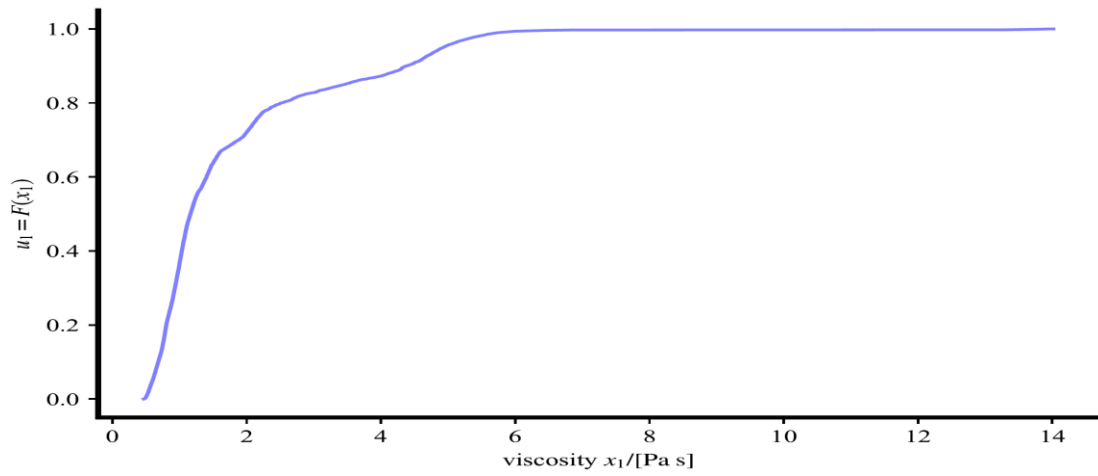
Figure 3-32 Illustration of marginal distribution function $F(x_1)$ of viscosity database Monte Carlo simulations of random variable x_1 of nanofluid effective viscosity results
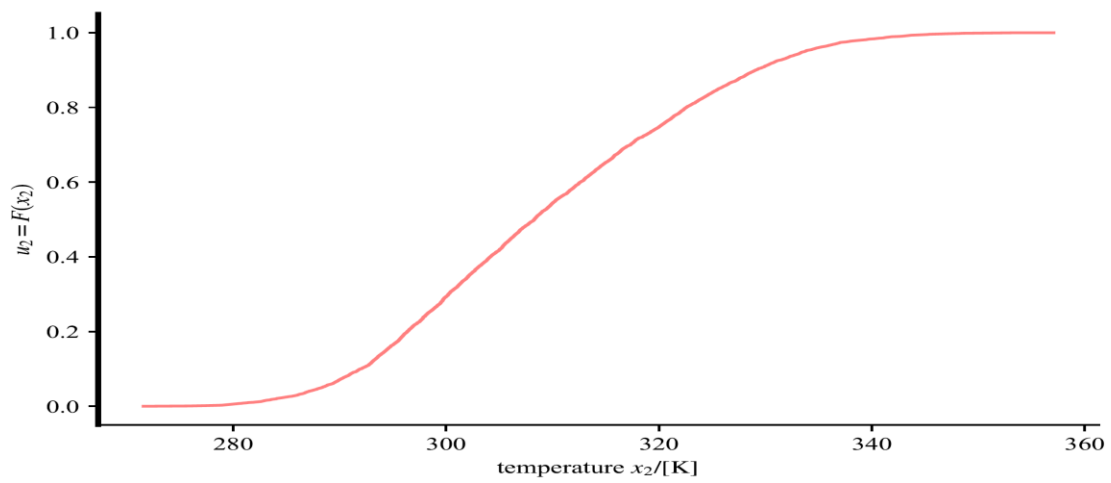
Figure 3-33 Illustration of marginal distribution function $F(x_2)$ of viscosity database Monte Carlo simulations of random variable x_2 of nanofluid effective viscosity results
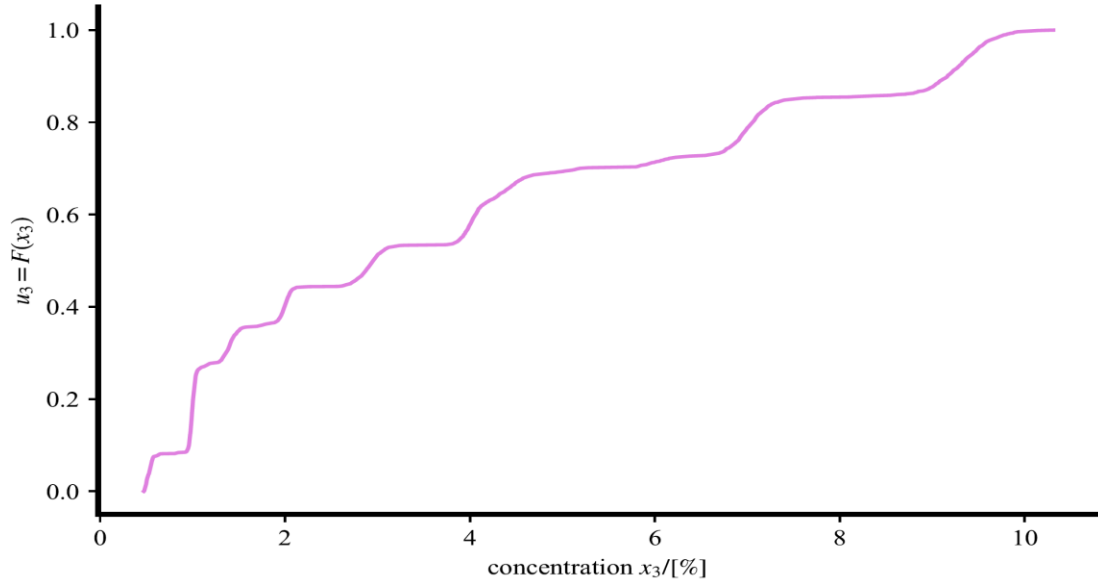
Figure 3-34 Illustration of marginal distribution function $F(x_3)$ of viscosity database Monte Carlo simulations of random variable x_3 of nanofluid effective viscosity results
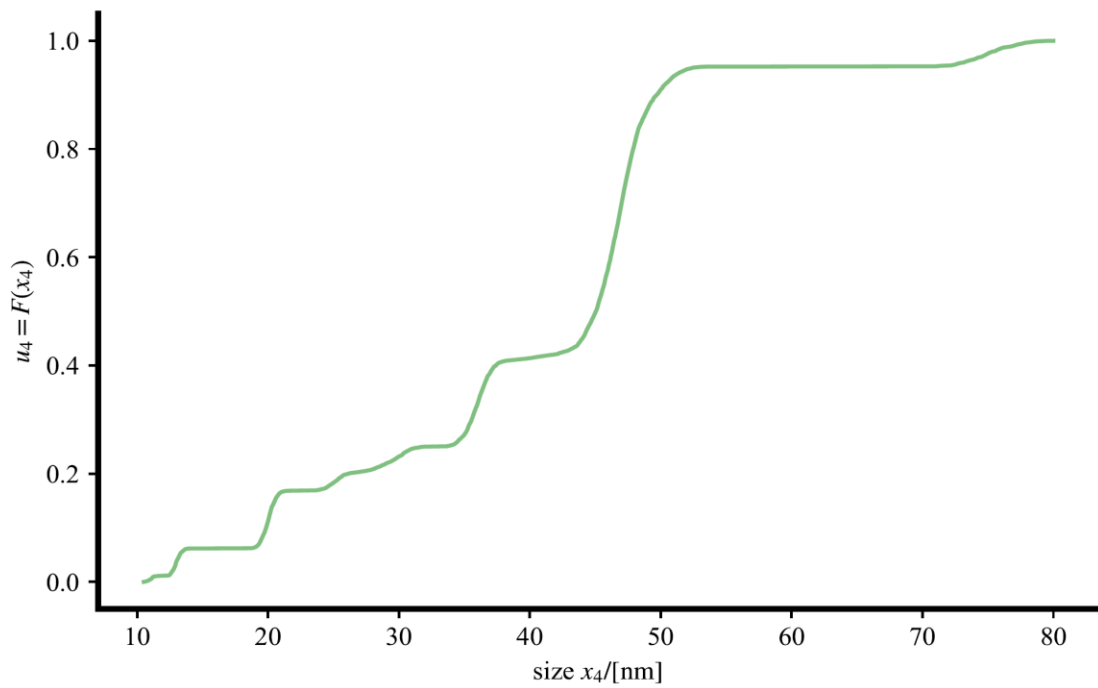
Figure 3-35 Illustration of marginal distribution function $F(x_4)$ of viscosity database Monte Carlo simulations of random variable x_4 of nanofluid effective viscosity results
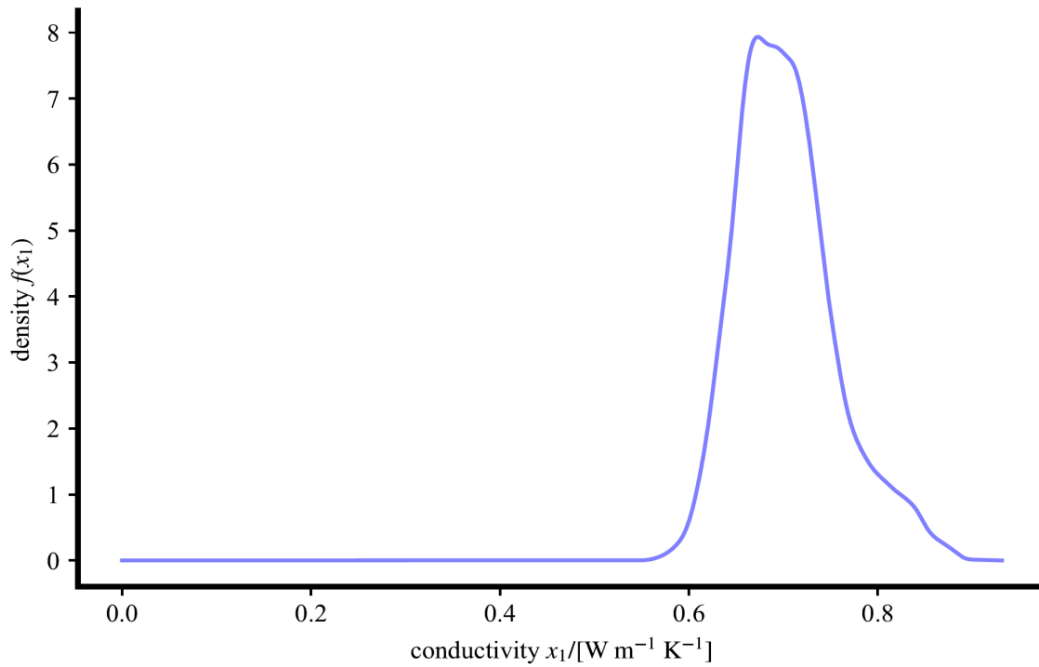
Figure 3-36 Illustration of marginal probability density functions $f(x_1)$ using a kernel density estimate approach for the Monte Carlo simulations of random variables x_1 for nanofluid effective viscosity
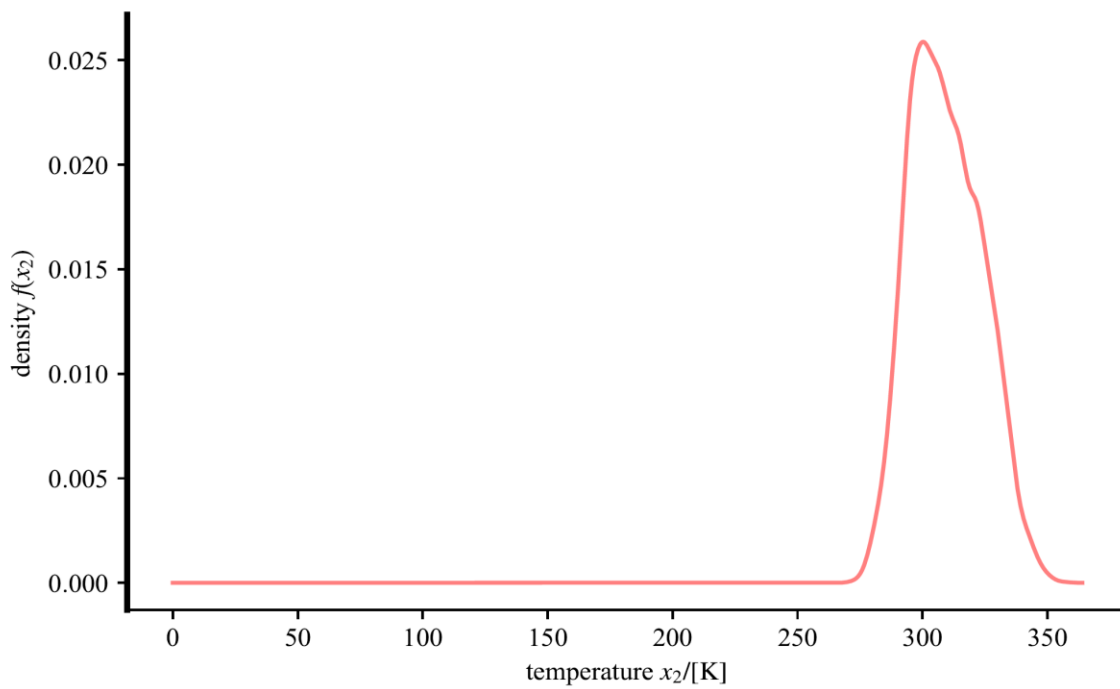
Figure 3-37 Illustration of marginal probability density functions $f(x_2)$ using a kernel density estimate approach for the Monte Carlo simulations of random variables x_2 for nanofluid effective viscosity

148
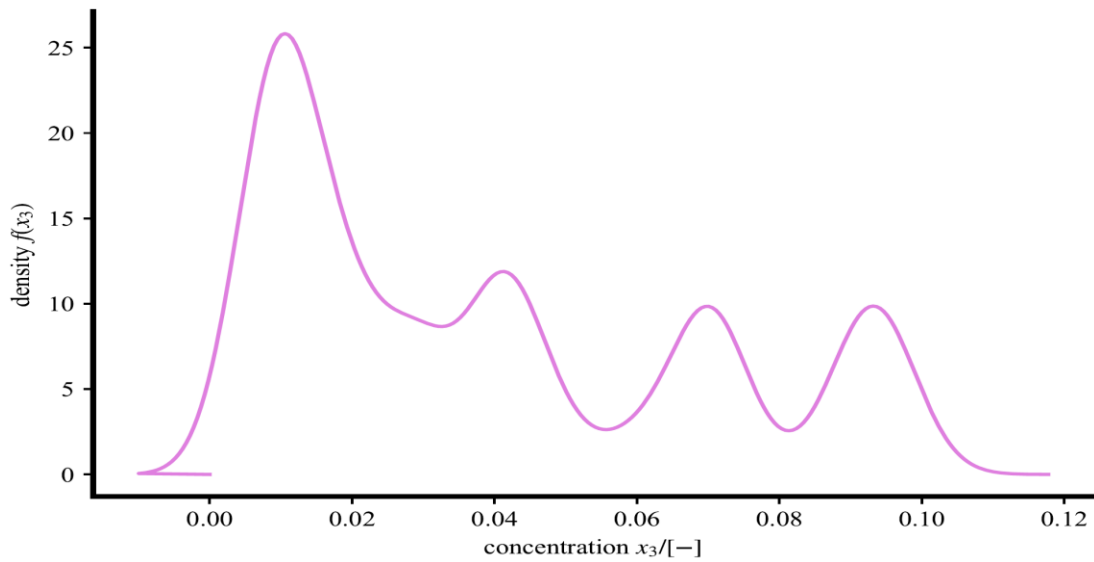
Figure 3-38 Illustration of marginal probability density functions $f(x_3)$ using a kernel density estimate approach for the Monte Carlo simulations of random variables x_3 for nanofluid effective viscosity

Figure 3-39 Illustration of marginal probability density functions $f(x_4)$ using a kernel density estimate approach for the Monte Carlo simulations of random variables x_4 for nanofluid effective viscosity

In general bivariate copulas are either elliptical of the form

$$C(u_1, u_2) = F(F_1^{-1}(u_1), F_2^{-1}(u_2)) \tag{3.132}$$

by the direct application of Sklar's theorem as previously discussed or they are Archimedian. A bivariate Archimedean copula takes the form
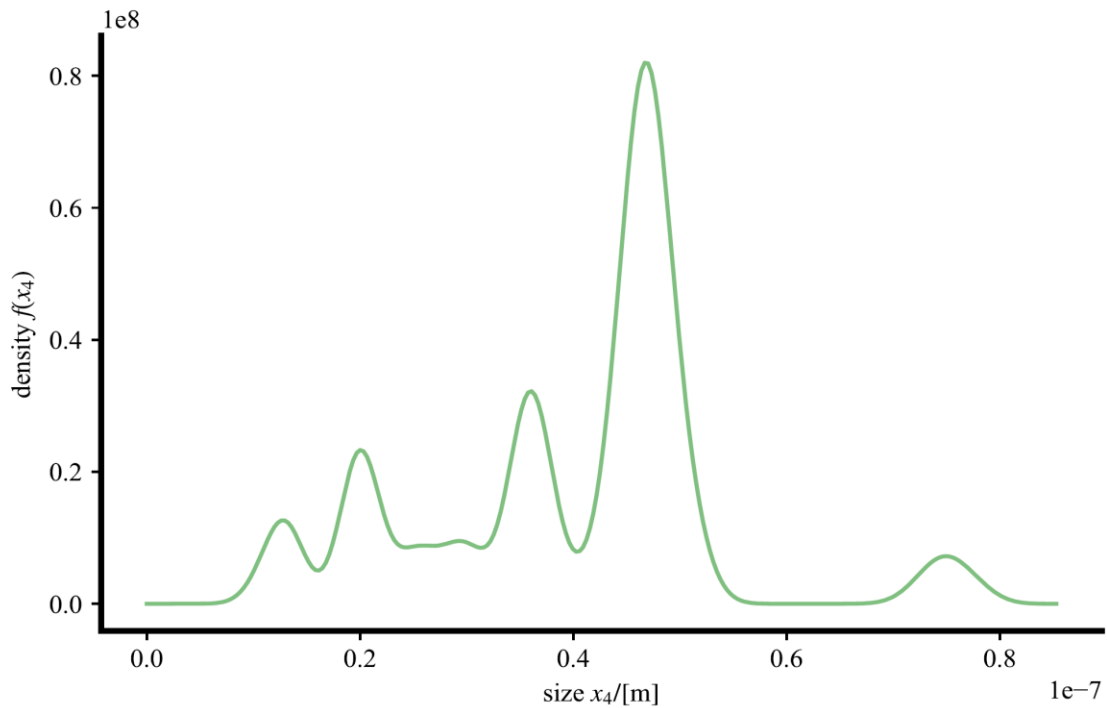
$$C(u_1, u_2) = \varphi^{[-1]}(\varphi(u_1) + \varphi(u_2)) \tag{3.133}$$

where φ is a generator that satisfies the following properties such that

$$\varphi : [0,1] \to [0, \infty] \tag{3.134}$$
$$\varphi(1) = 0 \tag{3.135}$$
$$\varphi^{[-1]}(t) = \begin{cases} \varphi^{-1}(t), 0 \le t \le \varphi(0) \\ 0, \varphi(0) \le t \le \infty \end{cases} \tag{3.136}$$

Although some explicit analytical formulae are available in the literature for certain types of copulas many copulas are in fact calculated in terms of special types of generating functions. The situation is analogous to how whilst power series expansions are in principle available for certain advanced types of mathematical functions, such as say Bessel functions or Abramowitz functions in the context of the linearized Boltzmann equation as discussed by Jiang & Luo [198], that they are nevertheless in practise rarely evaluated from first principles since software libraries are readily available in order to call and conveniently numerically evaluate these mathematical functions. A good example in the area of copulas is the well known bivariate Gaussian copula which whilst conceptually simple does not have a simple explicit mathematical function since it is defined as

$$C(u_1, u_2) = \Phi_2(\Phi^{-1}(u_1), \Phi^{-1}(u_2)) \tag{3.137}$$
$$\Phi_2(h, k) = \int_{-\infty}^{h} \int_{-\infty}^{k} \varphi_2(x_1, x_2) \ dx_1 \ dx_2 \tag{3.138}$$
$$\varphi_2(x_1, x_2) = \frac{1}{2\pi\sqrt{1-\rho^2}} \exp\left(-\frac{x_1^2 - 2\rho x_1 x_2 + x_2^2}{2(1-\rho^2)}\right) \tag{3.139}$$

where ρ is the correlation coefficient and the bivariate Gaussian copula value must be numerically solved when it has to be evaluated. Many copula families consequently do not possess simple analytical formulae and due to this fact in many practical situations it is sufficient to simple specify the families and their associated parameters as previously reported in Table 3.9 along with the associated marginal distributions since the function values can generally be evaluated with the aid of readily available statistical software library routines in languages such as **R** or equivalently in computer code written in for example Python. As a result in this dissertation the above specification of the bivariate copula families and their respective parameter(s) for each tree in the four-dimensional copula that we have investigated is considered to sufficient to fully describe and close the mathematical copula model for the water/alumina nanofluid.

From a practical implementation perspective in the joint PDF $f(x_1, x_2, x_3, x_4)$ since $x_1 = k_{nf}$ is the main quantity of interest and $x_2 = T$, $x_3 = \phi$ and x_4 are in our particular mathematical approach considered as meta-parameters we are therefore main interested in using the copula to

predict the characteristics of x_1 in terms of the other quantities. This mathematical effect is formally specified in terms of conditional distribution for x_1 and which is formally specified through repeated application of the formula

$$F(x_i|\mathbf{v}) = \frac{\partial C_{x_i v_j}(F(x_i|\mathbf{v}_{-j}), F(v_j|\mathbf{v}_{-j}))}{\partial F(v_j|v_{-j})}, x_i = x_1, \mathbf{v} = [x_2, x_3, x_4]^{\mathrm{T}} \tag{3.140}$$

where in our particular study we have $x_i = x_1$ and $\mathbf{v}$ due to our earlier choice of variable numbering for the C-vine copula scheme we opted to utilize. In the more general case where the are more meta-parameters such as $x_5 = \mathrm{pH}$ and $x_6 = \dot{\gamma}$ so that the conditional distribution would be specified as $F(x_i|\mathbf{v})$ where $\mathbf{v}$ is a vector of random variables to specify the conditional distribution. By repeated application of the iterated scheme for our four dimensional model there are then $3 \times 2 = 6$ different approaches in constructing the conditional distribution where each of the six possible approaches would require the construction of additional corresponding bivariate copula. One particular option is

$$F(x_1|x_2, x_3, x_4) = \frac{\partial C_{12|34}(u_{1|34}, u_{2|34})}{\partial u_{2|34}} \tag{3.141}$$

where the first copula is constructed of random variables such that

$$u_{1|34} = \frac{\partial C_{13|4}(u_{1|4}, u_{3|4})}{\partial u_{3|4}} \tag{3.142}$$

$$u_{2|34} = \frac{\partial C_{23|4}}{\partial u_{3|4}} \tag{3.143}$$

and this copula is in turn constructed of the random variables defined as

$$u_{1|4} = \frac{\partial C_{14}(u_1, u_4)}{\partial u_4} \tag{3.144}$$

$$u_{2|4} = \frac{\partial C_{24}(u_2, u_4)}{\partial u_4} \tag{3.145}$$

$$u_{3|4} = \frac{\partial C_{34}(u_3, u_4)}{\partial u_4} \tag{3.146}$$

The corresponding probability density may then be constructed as

$$f(x_1|x_2, x_3, x_4) = \frac{\mathrm{d}}{\mathrm{d}x_1} F(x_1|x_2, x_3, x_4) \tag{3.147}$$

so that the expected value of the thermal conductivity x_1 for specified values of x_2, x_3, x_4 is then

$$\mu = \int_{-\infty}^{\infty} x_1 f(x_1|x_2, x_3, x_4) \quad \mathrm{d}x_1 \tag{3.148}$$

with an equivalent variance

$$\sigma^2 = \int_{-\infty}^{\infty} (x_1 - \mu)^2 f(x_1|x_2, x_3, x_4) \ dx_1 \tag{3.149}$$

It is theoretically possible to also calculate the expected value directly from the distribution function however in this chapter the indirect approach is preferred for conceptual simplicity to illustrate the functionality of the copula mathematical modelling approach that we have utilized.

In the above approach the different possible approaches to calculating the conditional distribution are all considered mathematically consistent however in practical terms some possible choices may be considered preferable as not all possible bivariate copulas are amenable to closed form mathematical solutions or alternately if they are mathematically tractable then it is not necessarily the case that they are already implemented in available statistical software library routines. This issue is not necessarily a fundamental problem since nowadays the partial derivatives of two dimensional functions may be readily computed using computer algebra systems (CAS) such as the open source symbolic Python package sympy or the commercially available Mathematica software, or directly numerically evaluated using finite difference schemes in C/C++ or Matlab when determining the partial derivatives for the bivariate conditional distributions such as $u_{3|4} = \partial C_{34}(u_3, u_4)/ \partial u_4$.

Once the conditional distribution $F(x_1|x_2, x_3, x_4)$ has been constructed it may then be conveniently be used to sample random points from the corresponding probability density function for the thermal conductivity. In the next chapter we demonstrate how to utilize the developed copula models for performing predictions of nanofluid thermophysical properties.

In most practical CFD studies the use of auxiliary thermodynamic relations such as that for the density is mainly used to estimate the thermodynamic parameter value for known operating conditions. Under this scenario the problem is then how to use the joint PDF $f(x_1, x_2, x_3, x_4)$ to estimate the most likely value of x_1 if x_2, x_3, x_4 are specified. Assume for simplicity after appropriate conversion between physical data values p_1, p_2, p_3, p_4 and copula data values x_1, x_2, x_3, x_4 as previously discussed that the supplied values of the meta-parameters are x_2^*, x_3^* and x_4^* and simply substitute them in the joint PDF so that only free variable is now x_1. For this situation define a new function $g(\xi)$ such that

$$\xi = x_1 \tag{3.150}$$

$$g(\xi) = \frac{f(\xi, x_2^*, x_3^*, x_4^*)}{\int_{-\infty}^{\infty} f(\xi, x_2^*, x_3^*, x_4^*) \ d\xi} \tag{3.151}$$

The above function $g(\xi)$ is an equivalent probability density function for the random variable x_1 so that the expected value is then calculated as

$$x_1^* = \int_{-\infty}^{\infty} \xi f(\xi) \ d\xi \tag{3.152}$$

and then the physical data value, say p_1^* which corresponds to the copula data value x_1^*, is recovered from this copula data value by solving the equation

$$p_1^* \leftarrow x_1^* = F_1(p_1^*) \tag{3.153}$$

which completes the nanofluid mathematical modelling with copula process.

In many practical applications numerical simulations are usually performed with the finite volume based CFD solver Ansys Fluent with user defined functions for the auxiliary relations for convenience when implementing the numerical results in the computational simulations as discussed earlier by Maripia *et al.*[199] and later by Ghodsinezhad [152] who note the ongoing challenge of occasionally contradictory numerical results from experimental measurement data which sometimes exhibits discrepancies. These issues have subsequently been addressed by more advanced alternative mathematical modelling approaches such multiphase based schemes for nanofluid models as discussed by Mahdavi [154] as previously discussed in systems where a continuum modelling hypothesis is valid for nanoparticles with a diameter d_p such that $\mathcal{O}(d_p/[\text{nm}]) \sim 100$, and through improved slip models recently developed by Mahdavi *et al.*[200] for multiphase nanofluid modelling which incorporates Brownian and thermophoretic diffusion effects in addition to electrostatic effects in the calculation of the slip velocity and which gives good agreement with water/alumina experimental measurements. Newer improved mathematical models that combine aspects of the more conventional mixture and discrete phase model (DPM) approaches in a nanofluid numerical studies as recently developed have also been reported in the literature by Mahdavi *et al.*[201] and as a result continuum based nanofluid models for computational fluid dynamic simulations using multiphase modelling approaches are still an active and rewarding area of research that is complementary to particle based simulations using *ab initio* molecular dynamics simulations without any particular modelling approximations or simplifications as increased high performance computing (HPC) super-computing resources start to become available to researchers.

As a result the previous formulae as outlined above may be used to first calculate the base fluid thermodynamic properties of density ρ_w, thermal conductivity k_w, viscosity μ_w and enthalpy h_w for water. Then once the base fluid properties are known the water temperature is set as the nanofluid temperature T assuming local thermodynamic equilibrium and similarly the volume fraction ϕ and nanoparticle size d_p are also specified in the copula model. Once the copula model has these inputs the corresponding PDF for the nanofluid thermal conductivity or viscosity is complete and it can then be used to estimate the expected value $\mu = \int_{-\infty}^{\infty} x_d f(\mathbf{x}) \quad dx_d$ of either k_{nf} or μ_{nf} which is then used as the values for the auxiliary thermodynamic properties in for example a finite volume based CFD code that is used to perform any subsequent computational simulations.

In this dissertation the research focus and scope has been limited to the building, construction and development of a mathematical model for the nanofluid thermophysical properties using copulas so we have opted to use the **R** based CDVine software library for convenience. Whilst the numerical application of mathematical copula models can in principle be natively implemented in other software languages we comment that in many practical situations it may be easier and more convenient to simply interface a Python code to **R** using for example the rpy2 interface as discussed by Belopolsky *et al.*[202] or to interface a code written in the C/C++ language to a **R** based copula function using the Rcpp based application programming interface as discussed by Eddelbuettel *et al.*[203]. The practical consequence of this is that since many commercial and open source CFD codes now offer the ability to incorporate either scripts written in Python and user defined functions (UDF's) written in the C language it is not strictly necessary to rewrite the professionally

developed statistical **R** based copula libraries which have already been extensively validated and verified (V&V'ed) from a software engineering quality perspective, but to simply call this functionality for calculating the nanofluid thermophysical properties from the associated software routines implemented in **R** with any convenient software interfacing routine for computational applications that utilize the developed multivariate copula mathematical models to calculate the nanofluid thermophysical properties.

3.3 Conclusions

In this chapter investigations have been performed of the physical characteristics and limitations of the existing mathematical and statistical modelling approaches for nanofluids and compared and contrasted the available techniques in order to determine the optimal approach in applying and constructing copula mathematical models of thermophysical properties. From this research investigation two new mathematical techniques have been developed to incorporate the aleatory uncertainties into mathematical models of nanofluid thermophysical properties such that both models are able to predict both values for the nanofluid properties as well the associated uncertainties in the respective predictions.

The first mathematical modelling technique that was developed is applicable to algebraic based models where the model is defined in terms of a specified analytical algebraic function of input variables and model parameters with associated parameter uncertainties such that the predictions of results and uncertainties may be conveniently calculated with the application of the law of propagation of uncertainties (LPU) as encapsulated by the Guide to the Expression of Uncertainty in Measurement (GUM) either analytically through the use of multivariate calculus techniques or with a pure numerical Monte Carlo based propagation scheme using the specified parameter values and uncertainties in conjunction with the algebraic model. Novel research aspects of this mathematical approach are the functionality to model either independent nanofluid thermophysical properties such as just the effective thermal conductivity or just the effective viscosity as uncoupled systems, or in addition the functionality to also model coupled effective thermal conductivity and effective viscosity values simultaneously which is considered a more physically realistic approach since the application of these predictions are at a fundamental level always considered simultaneously when solving the mass, momentum and energy conservation equations using the single-phase formulation of the Navier-Stokes equations for nanofluids.

This first mathematical development which we investigated now offers the functionality for constructing either uncoupled or coupled model constructions of the nanofluid auxiliary thermodynamic properties of thermal conductivity and viscosity and may be usefully applied to obtaining optimal mathematical expressions for the nanofluid's properties in situations where a particular piece of equipment or instrument has an overall performance and quality that is simultaneously critically dependent on both a thermal conductivity and a viscosity such as certain types of heat exchangers where the overall heat exchanger performance/quality depends on the convective heat transfer coefficient h_c and the pumping power P which are functions that are simultaneously dependent on the nanofluid's effective thermal conductivity and effective viscosity. Due to the fact that many mechanical engineers working in industry have a preference for the use of simple to apply algebraic formulae in spreadsheet environments such as MS Excel for the calculation of fluid properties it is recommended that this first mathematical modelling

approach be further investigated and developed such that a selection of equations, their parameters and the associated parameter uncertainties as determined with this technique are available to potential users within the South African industry sector.

A second mathematical development which was investigated is applicable to statistical based models where the model is defined in terms of higher dimensional copulas where the joint probability density function of the respective nanofluid thermophysical properties and meta-parameters were built using Monte Carlo simulations of the previously determined database of statistical information through the use of canonical vines constructed through a tree based scheme of bivariate copulas. This model is also in principle completely specified by a set of constants for the marginal distributions and a set of copula families with their associated parameters. The mathematical model for the water/alumina nanofluid effective thermal conductivity using the second mathematical approach developed in this dissertation has marginal distribution functions for the meta-parameters $k_{nf}/[\text{W} \quad \text{m}^{-1} \quad \text{K}^{-1}] = x_1$, $T/[\text{K}] = x_2$, $\phi = x_3$ and $x_4/[\text{m}] = d_p$ and which are suitable for univariate spline interpolations of $u_i = F(x_i), i = 1,2,3,4$. The corresponding marginal probability density functions may then be calculated in terms of these specified distribution functions through the application of the fundamental mathematical statistical relation $f_i(x_i) = \frac{\text{d}}{\text{d}x_i}[F_i(x_i)]$, and the corresponding bivariate copula densities have analytical expressions that are completely specified for mathematical completeness. Analogous results following a similar mathematical modelling approach for the copula model of the water/alumina nanofluid effective viscosity were also performed however it is concluded that additional experimental data for the nanofluid viscosity is necessary as only preliminary qualitative results are feasible due to the limited number of points from the constructed database.

Since the mathematical technique in this second approach may readily applied to higher dimensional models with additional parameters such as the nanofluid pH value and shear strain rate it is recommended that the application of copulas be further investigated for both higher dimensional copula models of specific nanofluid properties as well as higher dimensional coupled nanofluid property systems where experimental data-sets of coupled simultaneous nanofluid properties are available in order to refine the interaction effects between the model inputs for higher accuracies and confidence in the predicted results with potential future application in the field of reliability engineering studies and operations that utilize nanofluids.
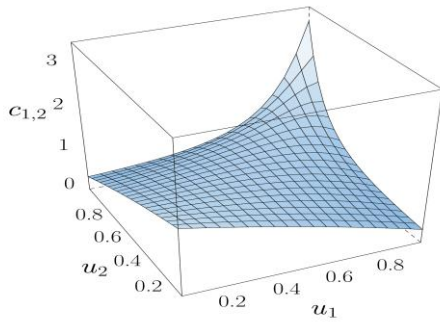
Influence of T Influence of ϕ
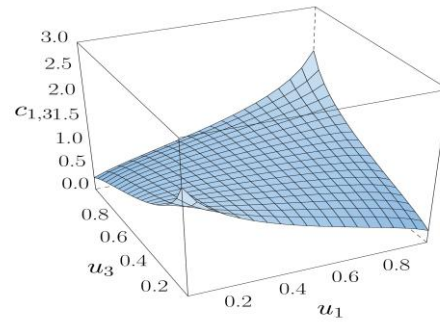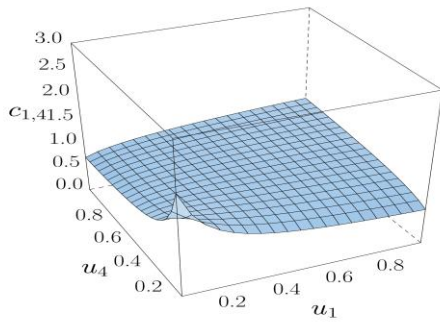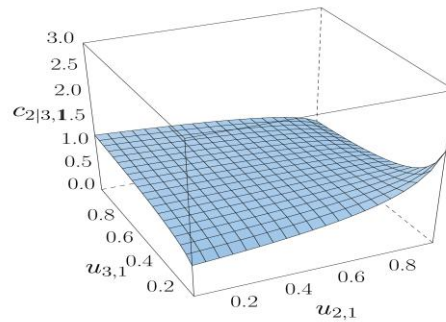
Influence of d_p Influence of T and ϕ
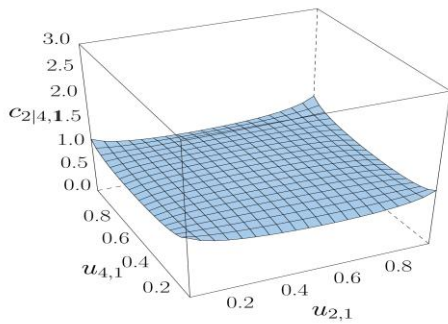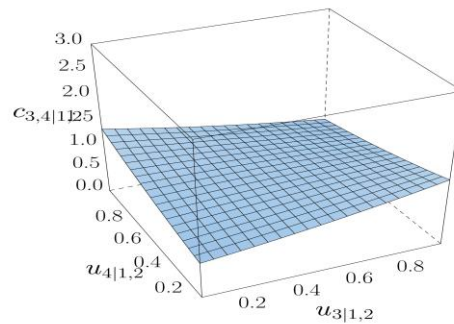
Influence of T and d_p Influence of ϕ and d_p with T

Figure 3-40 Visualization of bivariate copulas for constructing a thermal conductivity mathematical model with random variables $k_{nf} = x_1$, $T = x_2$, $\phi = x_3$ and $d_p = x_4$ using a four-dimensional conventional C-vine copula mathematical model

156
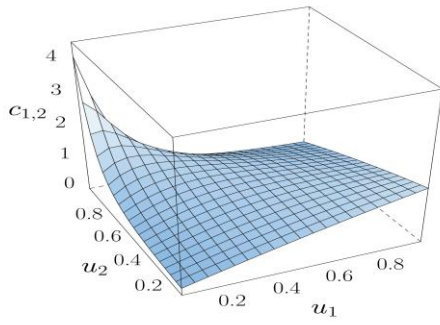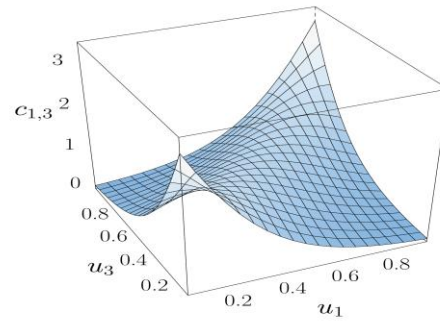
Influence of T Influence of ϕ
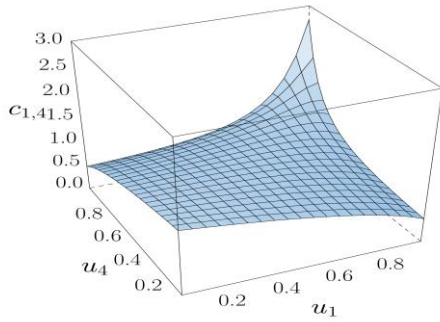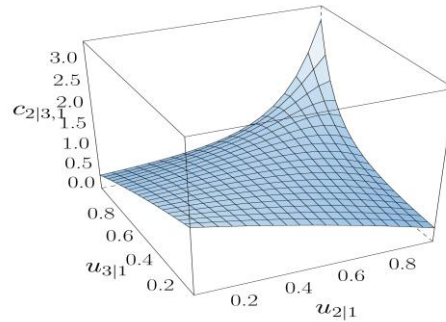
Influence of d_p Influence of T and ϕ
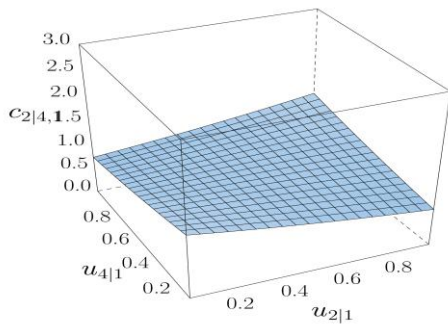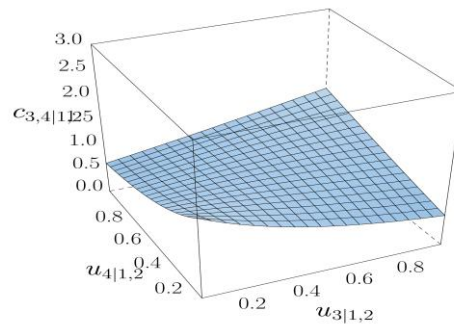
Influence of T and d_p Influence of ϕ and d_p with T

Figure 3-41 Summarized illustration of bivariate copulas for constructing a viscosity mathematical model with random variables $\mu_{nf} = x_1,\ T = x_2,\ \phi = x_3\ and\ d_p = x_4$ *using a four-dimensional conventional C-vine copula mathematical model*

4 Mathematical Predictions Using Copulas

4.1 Validity of Model Based Inputs in Mathematical Predictions

In the previous chapter the marginal probability density functions $u_i = F(x_i), i = 1,2,3,4$ for the thermal conductivity were determined and the associated bivariate copulas for a conventional C-vine copula construction scheme using Monte Carlo numerical simulations. In order to utilize the joint PDF $f(x_1, x_2, x_3, x_4)$ for engineering work a convenient means to evaluate quantities and make predictions with this mathematical model is necessary. Due to the fact that the model was constructed with actual physical experimental data reported in the open literature for various operating conditions the distribution function data is "messy" even with almost $N = 5000$ Monte Carlo simulation events mainly due to particular choices of available experimental data for the volume concentrations ϕ and nanoparticle diameter sizes d_p when constructing the database of thermal conductivity data. Although it is well known that a higher number of Monte Carlo simulation events increases the accuracy of solutions which converges as $N \to \infty$ this is in many practical cases less important as convergence is usually obtained in many practical laboratory situations for simulation events in the range between $N = 2500$ to $N = 7500$, and as a result the accuracy of predictions is essentially based on the underlying quality of the data that is used to perform the simulations. One approach to mitigate against poor quality experimental data is to increase the uncertainties of the data-points from for example standard uncertainties of $\pm 2.5\%$ for the x_i data to for example standard uncertainties of $\pm 10\%$, however this approach could then in turn produce artificial discrepancies in the predictions used with the developed mathematical models. In the field of nanofluids the central challenge is a lack of consistency in many of the experimental research performed in the literature as discussed by Aybar [121] who reached this conclusion based on a very wide review of the available data and also observed that in some cases the inconsistencies of observations could in certain cases lead to contradictory predictions. This observation is composed of two aspects from a mathematical modelling context with regards to the validity of the model inputs which is applicable to both our present focus in this dissertation of copula models and to alternative mathematical modelling schemes such as artificial intelligence (AI) and radial basis function (RBF) approaches amongst others, namely that the degree of confidence in any constructed mathematical model depends on both the quality of the measurements x_i as well as the quality of the associated uncertainties of the measurements $u(x_i)$. It has already been established that there are occasionally inconsistencies in measurement data x_i however the simplest conceptual solution to this problem of increasing the associated uncertainties until the measurement data is statistically consistent is based on the assumption that the data are inconsistent as opposed to being contradictory. Specialist measurement techniques using the well known metrological based mathematical concepts of degrees-of-equivalence in for example the computation of Key Comparison Reference Values (KCRV's) are available to address this issue as discussed by Cox [112] who developed a concept known as the largest consistent subset (LCS) if the x_i data has an element of reliability and there is a high degree of confidence in its associated uncertainty $u(x_i)$, however these two criteria are not necessarily always adequately satisfied in nanofluid measurements. There are technically four general scenarios in describing the state of knowledge of the combination of x_i and $u(x_i)$ in terms of a high confidence (H) and a low confidence (L) namely (i) x_i/H & $u(x_i)$/L, (ii) x_i/L & $u(x_i)$/H, (iii) x_i/H & $u(x_i)$/H, and (iv)

x_i/L & $u(x_i)$/L respectively.

Examples of a lower level of confidence in the quality of the x_i data is present due for example through the use of different experimental procedures in manufacturing the nanofluids as not all of the data sources consulted in the open literature adequately or consistently document the relevant methods and procedures. The use of different operating procedures in laboratories is manifested in for example different qualities of nanoparticles, sonification times, and physical procedures used by the respective laboratory staff for the mixing of the base fluid and nanoparticles for obtaining the required nanoparticle volume concentrations. It is therefore technically possible to have a low uncertainty $u(x_i)$ for a certain measurement by very strictly adhering to a particular laboratory's measurement protocol using for example many repeat measurements but a low confidence in the value of x_i since the measurement procedure was undertaken use different or non-standard equipment/instrumentation when compared to another different laboratory measurement x_j. A practical example of how this occurs is in for example the quantification of the nanoparticle diameter size d_p where some researchers use different equipment and techniques such as SEM, TEM and DLS approaches amongst others where both the measurement operating principles as well as the physical differences between equipment/instrument by different manufacturers/suppliers differs, and there is an additional complicating issue of how the measurement data is post-processed using different mathematical/software routines in order to arrive at the final estimates of x_i.

A related difficulty in nanofluid studies is in terms of the quantification of the estimated uncertainty $u(x_i)$ for a measurement. From the earlier literature review conducted it has been established that very few investigators perform an uncertainty analysis in a mathematically rigorous and statistically consistent manner. This lack of rigorous statistical uncertainty analysis is partly addressed through the introduction of assumed accuracy levels however these assumptions are difficult to independently assess for appropriateness since physical and mathematical aspects of the uncertainty analysis process are not widely or consistently reported in the various data sources in the open literature. Examples of some physical aspects include the type of thermo-couples or RTD's used to measure temperatures, the submerged lengths of the temperature devices, and the spatial and temporal homogeneity of the liquid baths in which the measurements were performed amongst other relevant physical information that is necessary to adequately construct a reasonable "uncertainty budget" since in many practical cases the manufacturer/supplier specified accuracy may be larger or even smaller than the uncertainty of the physical system measurement that is used to estimate the relevant meta-parameter. Two examples of how this could affect some measurement uncertainties is in the effective nanofluid temperature which may differ in different paths of a liquid bath away from the temperature sensor, and in for example the estimates of the nanoparticle mass densities which are usually assumed used in the volume concentration calculation based on separate estimates of the mass values used in the mixtures which have different statistical assumptions such as covariance estimates and slight differences between conventional and apparent mass values which different laboratories occasionally calculate in different measurement operating procedures as discussed in more technical detail by Palencar [204].

Based on these observations the overall reliability of the experimental data both in terms of the estimates of the quantities x_i and $u(x_i)$ of which there are four different possibilities of high

reliability (H) or low reliability (L) that is used to construct mathematical models for nanofluid thermophysical properties is difficult to independently verify and assess. As a result a practical consequence of this limitation is that any mathematical models that are constructed are at a fundamental level only as good as the underlying experimental data that was used to build them.

4.2 Numerical Techniques for Performing Predictions Using Copulas

In the available data from the previous chapter, it was observed that the distribution functions for the thermal conductivity $k_{nf} = x_1$ and base fluid temperature $T = x_2$ from the available data may be conveniently modelled in terms of extended lambda distributions, but that the distribution functions for the volume fraction $\phi = x_3$ and nanoparticle diameter $x_4 = d_p$ were "messy" due to the quality of the physical experimental data in the database constructed from the available open literature sources. Although it is technically possible to also "smooth" the distribution function data for $\phi = x_3$ and $d_p = x_4$ this approach is not considered appropriate since there will then be a "mismatch" between the marginal distributions and the copulas. In order to preserve mathematical consistency, we have therefore opted to retain the original distribution function data.

The joint PDF is formally specified as

$$
\begin{aligned}
f(x_1, x_2, x_3, x_4) = f_1(x_1) &\times f_2(x_2) \times f_3(x_3) \times f_4(x_4) \\
&\times \; c_{1,2}(u_1, u_2) \times c_{1,3}(u_1, u_3) \times c_{1,4}(u_1, u_4) \\
&\times \; c_{2,3;1}(u_{2|1}, u_{3|1}) \times c_{2,4;1}(u_{2|1}, u_{4|1}) \\
&\times \; c_{3,4;1,2}(u_{3|1,2}, u_{4|1,2})
\end{aligned}
\tag{4.1}
$$

To numerically evaluate the above expression numerical values for the various arguments of each of the six bivariate copulas are necessary. For a specified meta-parameter value x_i the corresponding copula data value u_i may be conveniently calculated using a univariate spline approach for sampled/specified known values of the copula values $u_j^*, j = 1,2,3,4$ from the earlier Monte Carlo simulations with a simple spline interpolation of the form

$$
u_j^* = spline(xjdata, ujdata, xjstar)
\tag{4.2}
$$

As a result of specified values of x_1, x_2, x_3, x_4 the corresponding copula data values u_1, u_2, u_3, u_4 in tree T_1 of the copula are relatively easy to directly calculate, however the calculation of the remaining four copula data values $u_{2|1}, u_{3|1}, u_{4|1}, u_{3|1,2}, u_{4|1,2}$ which are also required must be calculated indirectly.

In tree T_2 the values are calculated using the results from tree T_1 and the definition of a conditional distribution as

$$
u_{2|1} = \frac{\partial C_{1,2}(u_1, u_2)}{\partial u_1}
\tag{4.3}
$$

$$u_{3|1} = \frac{\partial C_{1,3}(u_1, u_3)}{\partial u_1} \tag{4.4}$$

$$u_{4|1} = \frac{\partial C_{1,4}(u_1, u_4)}{\partial u_1} \tag{4.5}$$

Following a similar approach, it may be shown that the copula data values in tree T_3 may then in turn be calculated as

$$u_{3|1,2} = \frac{\partial C_{2,3|1}(u_{3|1}, u_{2|1})}{\partial u_{2|1}} \tag{4.6}$$

$$u_{4|1,2} = \frac{\partial C_{2,4|1}(u_{4|1}, u_{2|1})}{\partial u_{2|1}} \tag{4.7}$$

As a result, the general algorithm to evaluate the joint PDF $f(x_1, x_2, x_3, x_4)$ may then be summarized as indicated in Table 4.1 where the final numerical predictions for the selected test points when compared to model predictions are reported in Table 4.1 for the thermal conductivity only since a similar numerical procedure will also apply for predictions using the viscosity copula model.

Step	Procedure
0	Specify values of the physical data inputs x_1, x_2, x_3, x_4
1	Calculate the corresponding copula data inputs
	$u_i = F(x_i), i = 1,2,3,4$ using the univariate spline
	interpolation routines or equivalent extended lamba distributions if available
2	In tree T_1 use the previously calculated values of u_1, u_2, u_3, u_4 to work out the values
	of the bivariate copulas $c_{12}(u_1, u_2)$, $c_{13}(u_1, u_3)$ and $c_{14}(u_1, u_4)$
3	In tree T_2 first work out the values of the conditional distributions as
	$u_{2|1} = \frac{\partial C(u_1, u_2)}{\partial u_1}$, $u_{3|1} = \frac{\partial C(u_1, u_3)}{\partial u_1}$ and $u_{4|1} = \frac{\partial C(u_1, u_4)}{\partial u_1}$, then use these values in turn to
	work out copula densities $c_{23|1}(u_{2|1}, u_{3|1})$ and $c_{24|1}(u_{2|1}, u_{4|1})$
4	In tree T_3 first work the conditional distributions as $u_{3|12} = \frac{\partial C_{23|1}(u_{3|1}, u_{2|1})}{\partial u_{2|1}}$ and
	$u_{4|12} = \frac{\partial C_{24|1}(u_{4|1}, u_{2|1})}{\partial u_{2|1}}$, and then inn turn use these values to work out the
	copula density as $c_{34|12}(u_{3|12}, u_{4|12})$
5	Use the above copula densities to work out the overall copula density
	as $c(u_1, u_2, u_3, u_4) = c_{12}c_{13}c_{14}c_{23|1}c_{24|1}c_{34|12}$
6	Evaluate the marginal probability density functions as
	$f(x_1), f(x_2), f(x_3), f(x_4)$ using the specified values
	of x_1, x_2, x_3, x_4
7	Calculate the overall joint PDF as
	$f(x_1, x_2, x_3, x_4) = f(x_1)f(x_2)f(x_3)f(x_4)c(u_1, u_2, u_3, u_4)$

Table 4. 1 Algorithm to evaluate joint probability density function $f(x_1, x_2, x_3, x_4)$ for specified values of x_1, x_2, x_3, x_4

Whilst the joint PDF is technically a function of all of the random variables as model inputs x_1, x_2, x_3, x_4 that when evaluating the joint PDF in the special case of conditional distributions where x_2, x_3, x_4 are fixed it logically follows that the marginal distribution PDF's $f(x_2), f(x_3), f(x_4)$ are also by definition fixed constants. In practical terms this then means that the behaviour of the PDF of for example a thermal conductivity $f(x_1|x_2, x_3, x_4)$ may be

approximated as

$$f(x_1|x_2, x_3, x_4) \approx f(x_1) \times c(u_1, u_2, u_3, u_4))$$ (4.8)

where $f(x_1)$ is the marginal distribution and $c(u_1, u_2, u_3, u_4)$ the corresponding copula density from our choice of C-vine tree construction after suitable scaling and normalization post-processing for statistical consistency. Selected technical aspects of how the above mathematical equations are numerically implemented using the **R** computer libraries however we elaborate on a few pertinent issues with the numerical implementation of a copula nanofluid model for performing predictions.

The first issue is the requirement of a good quality univariate interpolation routine particularly when the marginal distributions are "messy" as in our particular database for both the nanofluid effective thermal conductivity and effective viscosity. Unfortunately due to the wide variety of experimental results that have been reported in the open literature when the marginal distributions are constructed it becomes problematic to obtain smoothly varying marginal distributions mainly due to the choice of experimental data-points that are used to construct a nanofluid thermophysical database. Examples of these effects referring to the marginal PDF's reported in the previous chapter include the presence of "double-peaks" in the PDF's of the nanoparticle volume concentrations ϕ due to the preference of performing experimental measurements at selected choices of volume fractions and "spikes" in the PDF for the nanoparticle diameter d_p mainly due to the supply of nanoparticles from suppliers for fixed nanoparticle sizes.

Final illustrative results are shown for the data-point $u_1 = 0.57918$, $u_2 = 0.77553$, $u_3 = 0.36755$ are shown in Figure 4.1, Figure = 4.2 and Figure 4.3 respectively corresponding to the prediction of the nanofluid thermal conductivity for a meta-parameter specification of $x_2/[K] = 305.599555$, $x_3 = 0.06$ and $x_4/[nm] = 36$ to demonstrate the general principle. The general steps to work out a predicted value of the thermal conductivity is to first work out the respective marginal PDF's and then the copula density term $c(u_1, u_2, u_3, u_4)$ as previously discussed. When these two terms are multiplied by keeping the random variable x_1 free an equivalent probability density function will result. In our particular case we then use this PDF to calculate the expected value for the thermal conductivity and the associated standard deviation. For simplicity it has been assumed that the expanded uncertainty for the thermal conductivity predictions from our copula model at a 95% confidence level may be approximated by taking a coverage factor of $k_p = 2$. This procedure is repeated for each of the test points and the final results reported in Table 4.2.

The results in Table 4.2 after further analysis to determine the quality and consistency of predictions with the copula model is shown in Figure 4.4. Referring to this figure it is observed that model predictions are consistent with independent test points from the original database which were not used in the model construction. When these results are further analysed it is found that the corresponding E_n normalized error values are all less than unity i.e. $E_n \leq 1$ for all of the tested points and as a result it may be concluded that the developed model is able to provide statistically consistent predictions within the specified uncertainties of the database points that were used to build the mathematical model. Due to the fact that the database from the previous chapter incorporated extensive data from a variety of data sources in the literature with large experimental variances in measurement data a more restricted benchmarking is necessary in order

to compare the accuracy of the predictions with the copula model. This benchmarking for restricted experimental datasets is considered necessary due to the fact that nanofluids may exhibit complex and/or inconsistent behaviour even for low dimensional multivariate experimental data.
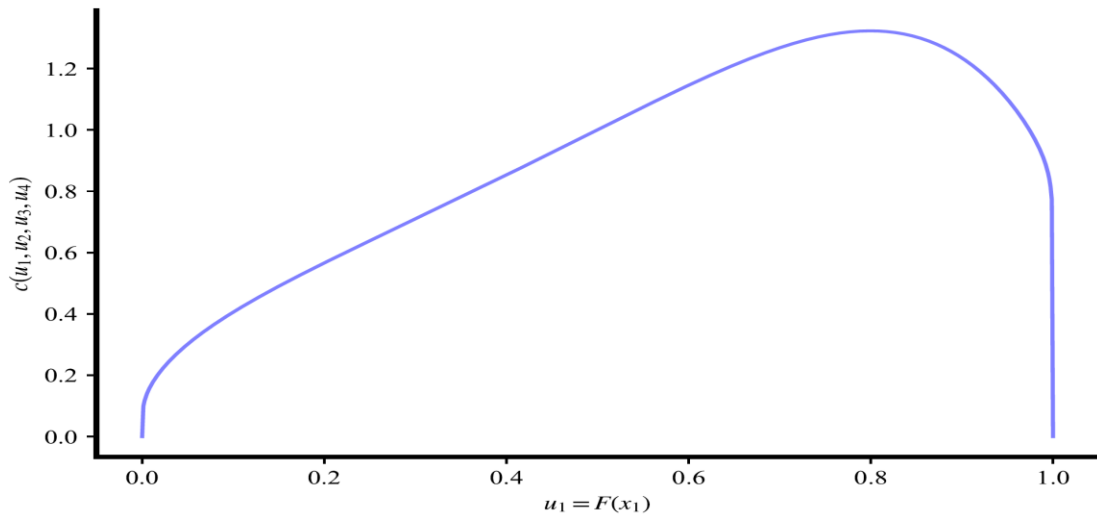
Figure 4-1 Illustrative example of the copula density $c(u_1, u_2, u_3, u_4)$ variation with the copula input u_1 for a nanofluid thermal conductivity model
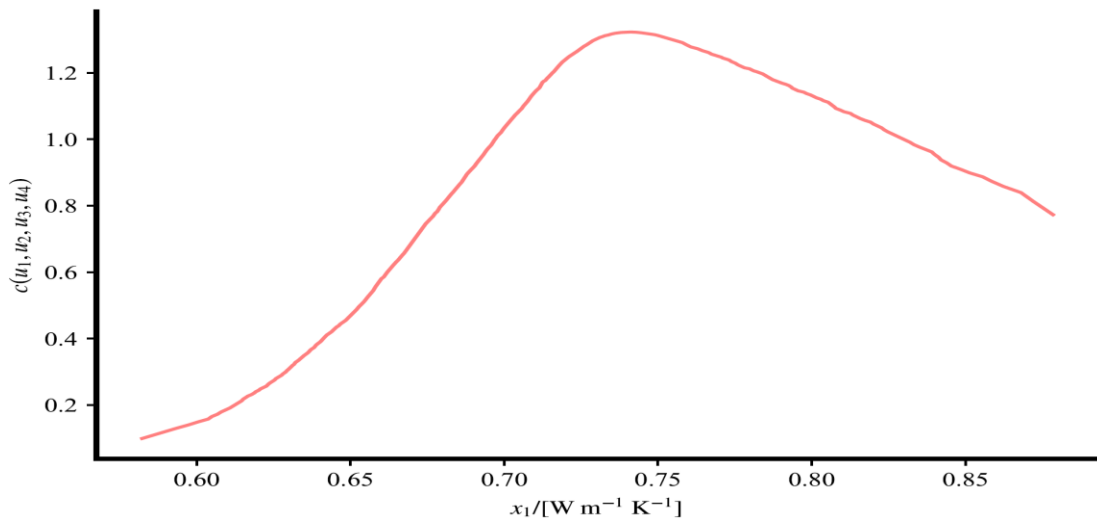
Figure 4-2 Illustrative example of the copula density $c(u_1, u_2, u_3, u_4)$ variation with the physical input for a nanofluid thermal conductivity model
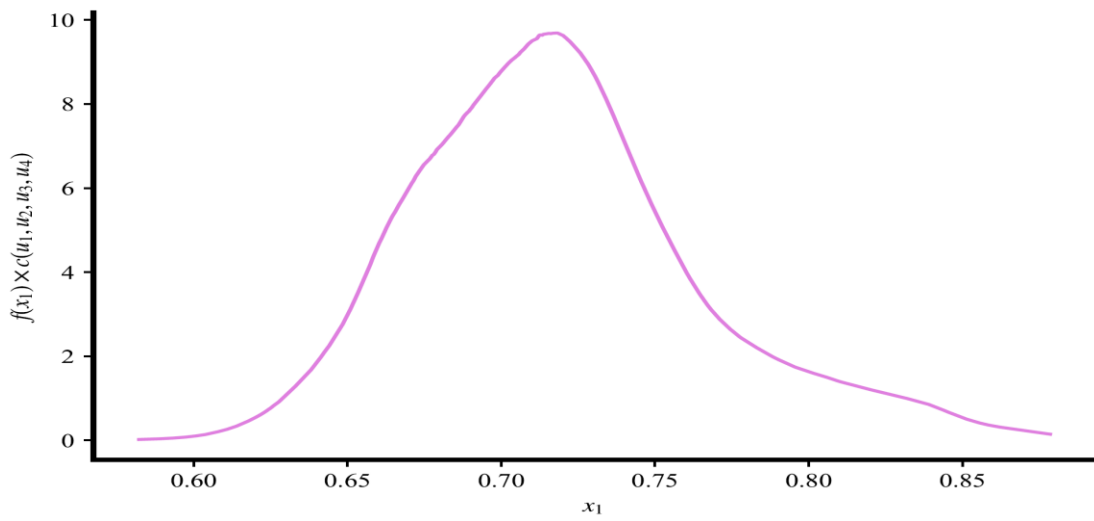
163

Figure 4-3 Illustrative example of the final probability density function $f(x_1)$ variation with the physical input x_1 for a nanofluid thermal conductivity model
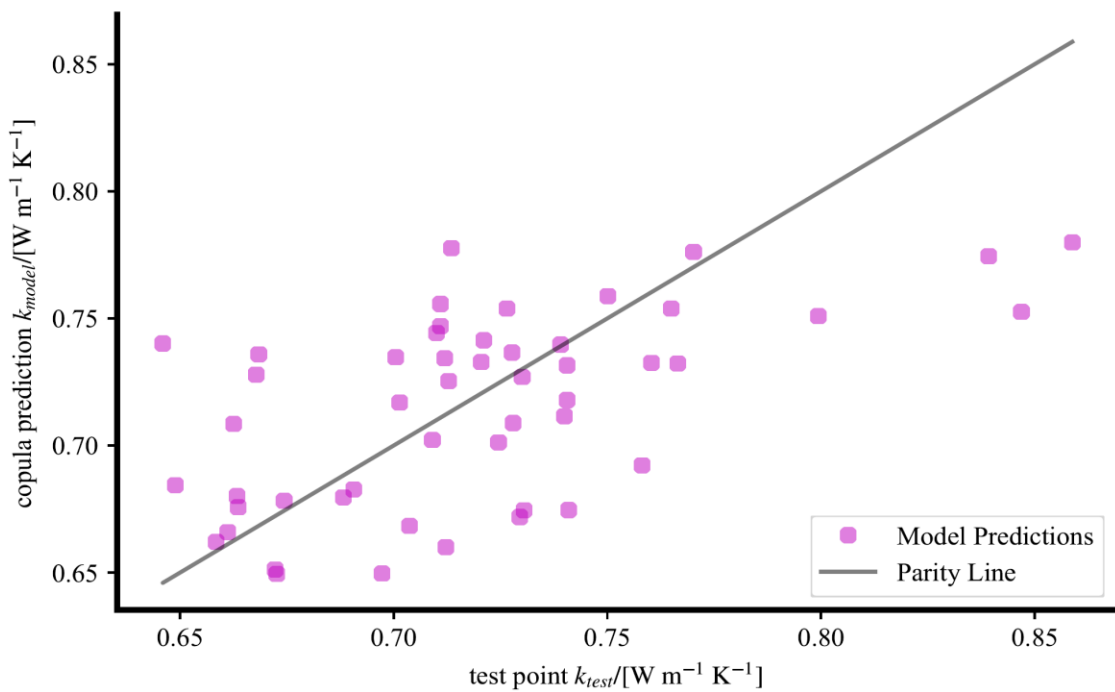

Figure 4-4 Illustration of copula model validity results for nanofluid effective thermal conductivity predictions for testing subset data

Point	ktest	Ttest	phitest	dtest	u(ktest)	kpredict	u(kpredict)
1	0.688234952	304.164808	0.013	0.000000013	0.017205874	0.679633101	0.038517106
2	0.760329577	320.091948	0.028	0.000000013	0.019008239	0.732535324	0.044141292
3	0.766457489	319.949177	0.028	0.000000013	0.019161437	0.732268843	0.044089676
4	0.690650783	304.15	0.019842554	3.84E-08	0.01726627	0.682754411	0.035667364
5	0.727949482	309.15	0.020093098	3.84E-08	0.018198737	0.708830513	0.038624785
6	0.764962513	324.15	0.020216968	3.84E-08	0.019124063	0.753856301	0.045826654
7	0.703720523	301.014985	0.02	0.000000036	0.017593013	0.66835484	0.034370844
8	0.758132165	305.970475	0.02	0.000000036	0.018953304	0.69223035	0.036812208
9	0.846877546	308.952671	0.06	0.000000036	0.021171939	0.752538147	0.046583394
10	0.727698418	301.193027	0.1	0.000000036	0.01819246	0.736561903	0.052920656
11	0.72953329	301.92547	0.02	0.000000036	0.018238332	0.671882624	0.03472664
12	0.672275293	298.15	0.018244267	6.04E-08	0.016806882	0.651280007	0.033551211
13	0.730530525	298.15	0.050299287	6.04E-08	0.018263263	0.674587532	0.03917312
14	0.740935918	298.15	0.050417003	6.04E-08	0.018523398	0.6746375	0.039188447
15	0.713540368	323.436779	0.059844075	0.00000002	0.017838509	0.777633318	0.050835229
16	0.6633478	303.565954	0.02	0.000000036	0.016583695	0.680117498	0.035552348
17	0.6684483	309.495093	0.04	0.000000036	0.016711208	0.735887319	0.042891013
18	0.6612167	301.376604	0.02	0.000000047	0.016530418	0.665992729	0.034294675
19	0.6678423	308.728297	0.04	0.000000047	0.016696058	0.727883069	0.042719429
20	0.6625398	302.717875	0.06	0.000000047	0.016563495	0.708470635	0.043356561
21	0.83922898	323.990198	0.04	3.84E-08	0.020980725	0.774438778	0.048454826
22	0.697310707	303.194863	0.01	0.00000008	0.017432768	0.649660619	0.034817664
23	0.663657038	299.860139	0.04	0.000000047	0.016591426	0.6756976	0.036586023
24	0.674384939	300.291163	0.04	0.000000047	0.016859623	0.678264786	0.036902743
25	0.739085227	311.731105	0.04	0.000000047	0.018477131	0.739692977	0.044172117
26	0.799357148	314.531188	0.04	0.000000047	0.019983929	0.750893107	0.045650719
27	0.658472554	298.389502	0.031	0.000000036	0.016461814	0.662070535	0.033984206
28	0.709069212	305.709376	0.031	0.000000036	0.01772673	0.702171674	0.038054956
29	0.740572792	308.595097	0.031	0.000000036	0.01851432	0.717880137	0.03992551
30	0.730071599	310.720277	0.031	0.000000036	0.01825179	0.726937361	0.041091797
31	0.740572792	312.054556	0.031	0.000000036	0.01851432	0.731538772	0.041713692
32	0.648926014	298.712966	0.06	0.000000036	0.01622315	0.684414222	0.039340411
33	0.701431981	303.366345	0.06	0.000000036	0.0175358	0.716892548	0.043202488
34	0.700477327	306.104998	0.06	0.000000036	0.017511933	0.734693679	0.045041709
35	0.71097852	309.60144	0.06	0.000000036	0.017774463	0.75567624	0.046823185
36	0.750119332	310.505867	0.06	0.000000036	0.018752983	0.758775145	0.047052643
37	0.712887828	302.394404	0.09	0.000000036	0.017822196	0.725370902	0.047447707
38	0.72052506	303.368065	0.09	0.000000036	0.018013127	0.732813164	0.048036263
39	0.711933174	303.547471	0.09	0.000000036	0.017798329	0.734318369	0.048141921
40	0.710023866	304.772525	0.09	0.000000036	0.017750597	0.744266398	0.048722208
41	0.71097852	305.313151	0.09	0.000000036	0.017774463	0.746958983	0.048842916

42	0.770167064	311.949114	0.09	0.000000036	0.019254177	0.776143953	0.049136472
43	0.712209152	303.15	0.005238963	0.00000002	0.017805229	0.660026002	0.037267935
44	0.724540175	323.15	0.005227967	0.00000002	0.018113504	0.701262445	0.042340361
45	0.646	322.3	0.0297	0.000000012	0.01615	0.740114558	0.045831724
46	0.67267581	300	0.007525926	0.000000043	0.016816895	0.64947018	0.032872754
47	0.726486371	313.15	0.049921997	0.000000055	0.018162159	0.753868026	0.048191212
48	0.721067929	312.824757	0.043185	0.000000075	0.018026698	0.741399238	0.049417284
49	0.739987937	303.146293	0.060432	0.000000075	0.018499698	0.711545744	0.04863721
50	0.858775803	312.96387	0.098778	0.000000075	0.021469395	0.779862818	0.053454852

Table 4. 2 Numerical predictions of nanofluid effective thermal conductivity using developed copula mathematical model

An example of how complex nanofluid multivariate data may be is that of measurements recently reported by Bouguerra *et al.*[205] for the simultaneous measurements of effective thermal conductivity k_{eff} and effective viscosity μ_{eff}. This work was performed in order to investigate agglomeration/clustering and nanoparticle dispersion effects as summarized in Figure 4.5 and Figure 4.6 which illustrates the contrasting behaviour for the k_{eff} and μ_{eff} enhancement ratios relative to the base fluid values for varying pH and volume concentrations at a constant temperature of $t = 25$ °C.
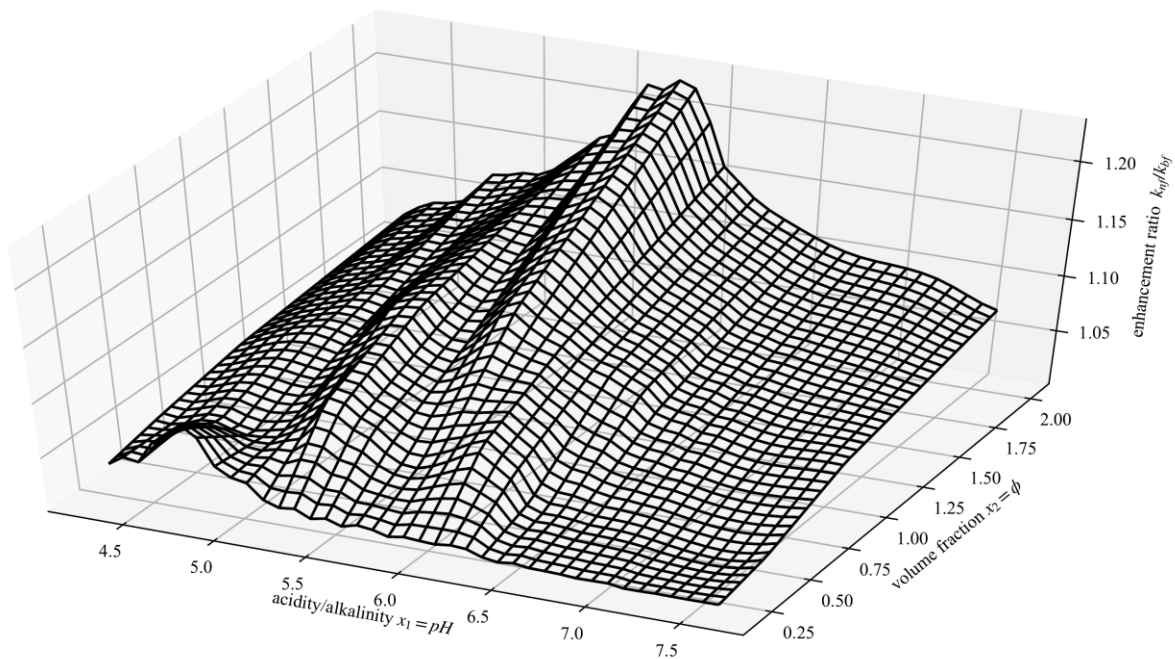
Figure 4-5 Illustration of water/alumina effective thermal conductivity enhancement ratio behaviour for a low dimensional mathematical model from data reported by Bouguerra et al.[205]
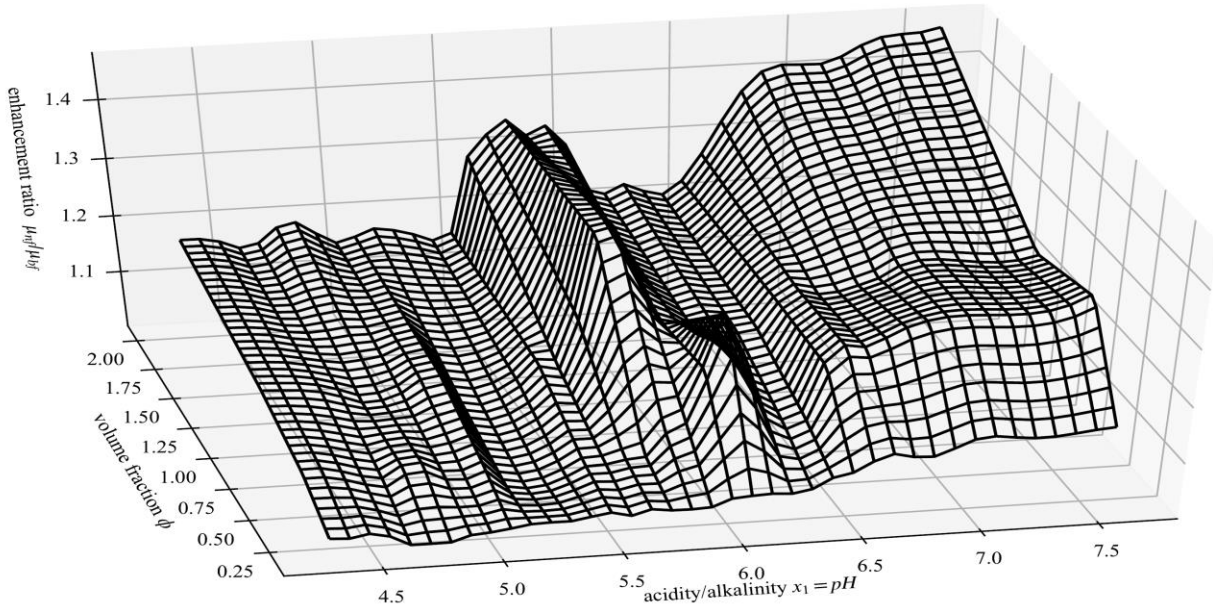
Figure 4-6 Illustration of water/alumina effective viscosity enhancement ratio behaviour for a low dimensional mathematical model from data reported by Bouguerra et al.[205]

4.3 Numerical Techniques for Neural Network Predictions

In order to perform predictions such as that for a nanofluid effective thermal conductivity k_{nf} with a standard neural network model assume that there are d inputs $x_1, x_2, \ldots, x_d$ for a single output y_1, and that there are ℓ hidden layers $h_1, h_2, \ldots, h_\ell$. For simplicity we assume a sigmoid activation function

$$f(x) = \frac{1}{1+e^{-x}} \tag{4.9}$$

for the input/hidden layers as per conventional nanofluid neural network modelling practise. If the throughputs to the hidden layer is ξ with a bias b, and the throughput to the outer layer is η then using vector/matrix notation we have that the input/hidden layer are then specified as

$$\boldsymbol{\xi} = \mathbf{W}\mathbf{x} + \mathbf{b} \tag{4.10}$$
$$\mathbf{h} = \mathbf{f}(\boldsymbol{\xi}) \tag{4.11}$$

and similarly

$$y = \mathbf{V}V\mathbf{h} \tag{4.12}$$
$$\mathbf{V} = [1, \ldots, 1]^{\mathrm{T}} \tag{4.13}$$

where $\mathbf{V}$ is a $1 \times L$ unit vector.

167
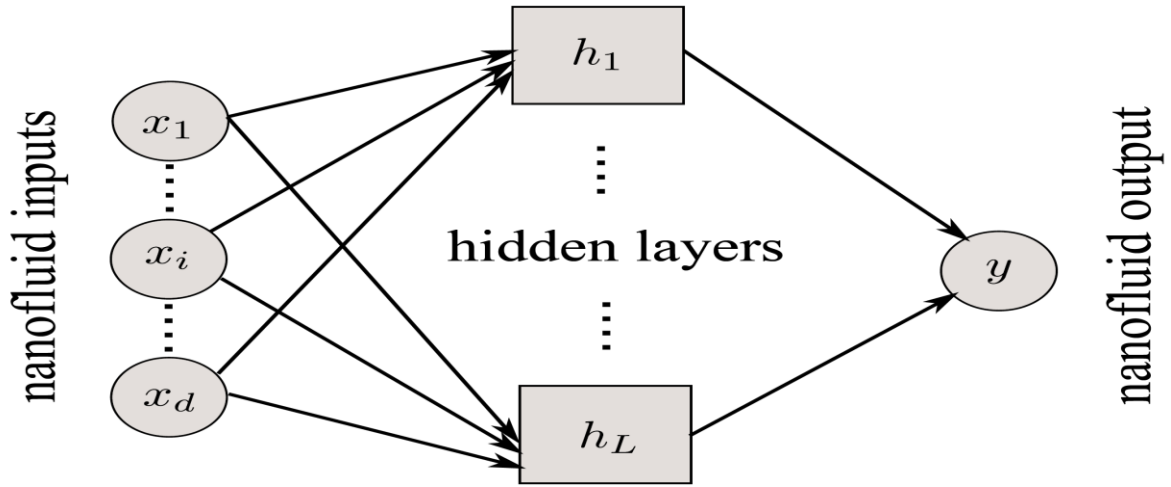
Figure 4-7 Illustration of conventional multiple layer perceptron neural network single layer scheme for modelling nanofluid thermophysical properties

The topology for this particular neural network configuration with the hidden/output layer is conceptually illustrated in Figure 4.7. For this particular configuration it follows that the vector/matrix dimensions are $\mathbf{W} = L \times d$, $\mathbf{b} = L \times 1$ and $\mathbf{V} = 1 \times L$ which is the standard MLP-NN configuration in nanofluid mathematical modelling studies. Due to the fact that there are formally two different weighting parameters our approach to optimize these parameters will be to use the standard trick of writing a vector/matrix variable in column-vector notation and then concatenating the various terms to create a new single parameter

$$\mathbf{a} = \{\mathbf{W}, \mathbf{b}\} \tag{4.14}$$

which has a dimension of $\dim(\mathbf{a}) = Ld + L = (d + 1)L$. When this scheme is used then the χ^2-merit function takes the familiar form

$$\chi^2(\mathbf{a}) = \sum_{i=1}^{M} [y_i - y_{model}(x_i)]^2 \tag{4.15}$$

This particular optimization may then be performed using a Levenberg-Marquardt or Nelder-Mead minimization technique and the with the technical implementation details that are outlined in the open literature utilizing the standard conventional neural network mathematical modelling approach for nanofluids. A limitation of this approach is that it does not explicitly consider the uncertainties of the model inputs such as $u(T)$, $u(\phi)$ and $u(d_p)$ respectively, and similarly also the uncertainties of the measured nanofluid properties such as $u(k_{nf})$ or $u(\mu_{nf})$. Considering a maximum likelihood argument presented by Saunders [145] it is known that for the univariate model

$$y = y(x; x_1, x_2, \ldots, x_M, y_1, y_2, \ldots, y_M) \tag{4.16}$$

168

with M experimental data points that the chi-squared function is constructed as

$$\chi^2 = \sum_{i=1}^M \left[\frac{y_i - y_{\text{model}}(x_i; \mathbf{a})}{\sigma_i}\right]^2 \tag{4.17}$$

In the above approach the weighting factor is specified as

$$\sigma_i^2 = u^2(y_i) + \left(\frac{\partial y}{\partial x}\Big|_{x=x_i} \cdot u(x_i)\right)^2 \tag{4.18}$$

Utilizing a similar line of statistical reasoning with the aid of the Guide to the Uncertainty of Measurement (GUM) the corresponding variance for the multidimensional model $y = f(x_1, x_2, \ldots, x_d)$ may then be specified as

$$\sigma_i^2 = u^2(y_i) + \sum_{j=1}^d \left(\frac{\partial f}{\partial x_j} u(x_j)\right)^2 \tag{4.19}$$

The chief difficulty with the application of the above formula which explicitly incorporates the measurement uncertainties is that there is no *a priori* means of correctly estimating the weighting factors σ_i in the absence of knowledge of the mathematical function $f(x_1, \ldots, x_d)$ which is used to specify the sensitivity coefficient $\frac{\partial f}{\partial x_j}$ terms. This is currently one of the major limitations of neural network modelling schemes as physical experimental measurement uncertainties cannot be incorporated into the mathematical modelling process. One practical implication of this limitation is that measures of the accuracy of the fit are usually restricted to AARD/MSE estimates, however these measures always attach equal weight to predictions everywhere in the d-dimensional domain $\mathbb{R}^d$ for a model input $\mathbf{x} = [x_1, \ldots, x_d]^{\mathrm{T}} \subset \mathbb{R}^d$. Consequently contributing terms to the underlying χ^2-merit function always carry equal values even for poor quality measurements or measurements with low accuracies although these deviations when calculating the AARD/MSE estimates may not be physically meaningful since the deviations are statistically consistent with the underlying measurement experimental uncertainties. As a result if for example high AARD/MSE values occur in some localized region i.e. for a restricted ranges of temperature, volume fraction and nanoparticle diameter whilst relatively low AARD/MSE values occur in the rest of the domain due to the equal weight attached to all the data points the localized discrepancies may adversely influence the global accuracy of the model since in practical terms the neural network topology is usually determined by a minimization of the AARD/MSE value from a Levenberg-Marquardt optimization. Nevertheless due to the fact that the use of the AARD and MSE statistics are widespread in nanofluid modelling studies we will for consistency utilize an AARD statistic in order to quantitatively benchmark our numerical simulation results.

As a result, the assumption of equal weighting factors reduces to the special case of the conventional neural network nanofluid mathematical modelling approach where the variance is implicitly specified as $\sigma_i = 1$ for $i = 1, 2, \ldots, M$. The sensitivity coefficient may nevertheless be formally estimated using finite differences as

$$\frac{\partial f(x_1, \ldots, x_i, \ldots, x_d)}{\partial x_i} \approx \frac{f(x_1, \ldots, x_i + \delta_i, \ldots, x_d) - f(x_1, \ldots, x_i, \ldots, x_d)}{\delta_i} \tag{4.20}$$

169

for inclusion in the χ^2-optimization in order estimate the corresponding value of the weighting factor σ_i. This direct non-instrusive numerical discretization approach whilst algebraically complex nevertheless introduces a conceptual simplicity for incorporating input/output but has not to date been utilized in any of the reported open literature sources that were consulted in the course of this research investigation. This approach may thus potentially offer a computationally cheaper alternative to the Kullback-Leibler (KL) divergence approach discussed by Levasseur *et al.*[87] for incorporating input/output uncertainties in order to estimate variances in the neural network parameters.

Due to these complexities in this chapter, it is considered advantageous to perform nanofluid predictions with a conventional neural network scheme for benchmarking for simplicity purposes by performing an unweighted χ^2-optimization for consistency. This approach is implemented through sequentially testing a range of possible numbers of hidden layers. From the earlier literature review variation of the number of hidden layers from $L = 5$ through to $L = 25$ hidden layers was considered as per the general guidelines reported by other researchers in order to reduce the AARD statistic as an indicator of the model accuracy. The results of this investigation are summarized in Figure 4.8 from which it was concluded that a value of $L = 8$ was able to produce the minimum $AARD$ accuracy level for the underlying thermal conductivity database information.
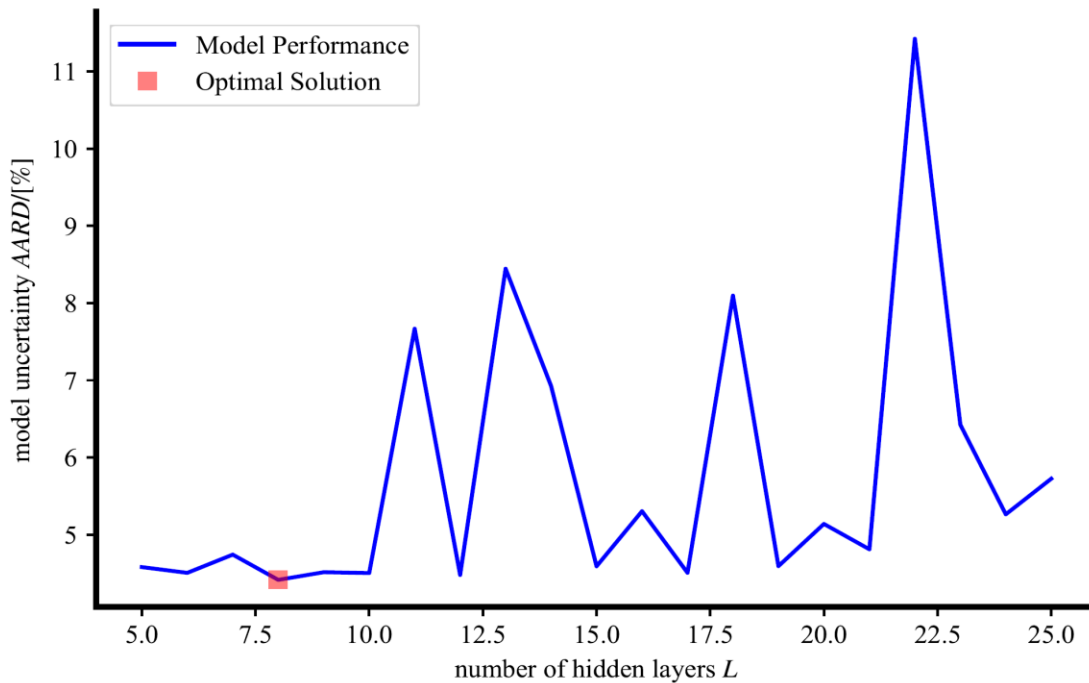
Figure 4-8 Summary of influence of variation of the number of hidden layers on MLP-NN nanofluid thermal conductivity model accuracy level
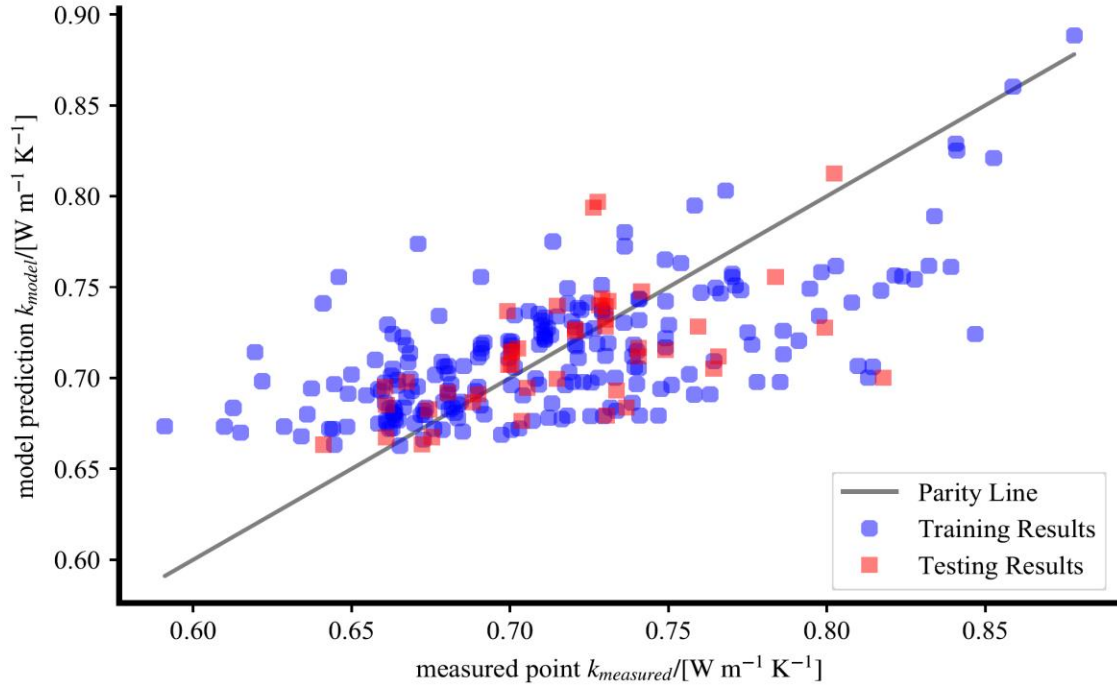
Figure 4-9 Graphical summary of MLP-NN nanofluid effective thermal conductivity mathematical model fit

From the numerical experiments that were performed using computer codes written in GNU Octave it was observed that convergence of the Levenberg-Marquardt optimization algorithm was not possible for all of the hidden layers that were tested due to the choice of multivariate starting solution for the scaled model parameter $\mathbf{a} = \{\mathbf{W}, \mathbf{b}\}$, where the termination criteria for the optimization was set as either a relative scalar tolerance of 0.001×10^{-3} or alternately a maximum number of iterations of $N_{\max} = 100$. This observation is consistent with the discussion by Press *et al.*[132] who remark that the optimization routine convergence is dependant on the relative closeness of the starting solution estimate to the final converged value and can fail to converge or diverge depending on the underlying data. For the MLP-NN model implementation both the input as well as the output data were normalized from the database limits such that

$$X_i = \left[\frac{T - T_{\min}}{T_{\max} - T_{\min}}, \frac{\phi - \phi_{\min}}{\phi_{\max} - \phi_{\min}}, \frac{(d_p)_{\max} - (d_p)_{\min}}{(d_p)_{\max} - (d_p)_{\min}} \right]^{\mathrm{T}} \tag{4.21}$$

$$Y_i = \frac{k_{nf} - (k_{nf})_{\min}}{(k_{nf})_{\max} - (k_{nf})_{\min}} \tag{4.22}$$

were row vectors that were used to construct a corresponding matrix input $\mathbf{X}$ and vector output $\mathbf{Y}$. These nanofluid input/output data from the thermal conductivity database were then utilized to construct the χ^2-merit function which was optimized with the Levenberg-Marquardt algorithm for a subset of nanofluid thermal conductivity information from the previously constructed database with model input ranges such that

$$25 \leq t/[°C] \leq 65 \tag{4.23}$$
$$0.5 \leq \phi/[\%] \leq 10 \tag{4.24}$$
$$10 \leq d_p/[\text{nm}] \leq 100 \tag{4.25}$$

The neural network fitting process using the above information and specifications is graphically summarized in Figure 4.10. For this modelling process, the final accuracies for the nanofluid effective thermal conductivity MLP-NN mathematical model were found to be

$$\text{Training Subset}(N_{train} = 219): \ AARD_{train} = 4.4144\% \tag{4.26}$$
$$\text{Test Subset}(N_{test} = 45): \ AARD_{test} = 4.2376\% \tag{4.27}$$

4.4 Comparison of Copula and Neural Network Model Predictions

The previous sections have outlined the technical numerical implementation approaches that are applicable for performing predictions with the neural network and copula mathematical models. To benchmark these approaches, it is necessary to compare them against the same dataset, however, due to the fact that a neural network cannot technically formally perform a statistical probability prediction of nanofluid thermophysical properties with conventional methods it is beneficial to to compare the conventional AARD% test statistics previously defined as

$$AARD\% = \frac{100}{N} \sum_{i=1}^{N} \left(\left| \frac{k_i^{exp} - k_i^{calc}}{k_i^{exp}} \right| \right) \tag{4.28}$$

The results of this comparison are shown in Figure 4.10 for the same test set that was constructed from the thermal conductivity database where 80% of the points were used to build the respective models and the comparison was done for the remaining 20% of the data points. When both sets of data are analysed is was concluded that the conventional single layer MLP-NN model can produce an AARD accuracy of 4.2376% for the test set whilst the copula model can produce an AARD accuracy of 3.0953% for the same test set. As a result, it was concluded that the proposed copula model can offer an AARD accuracy improvement of $3.0953\% - 4.2376\% = 1.1423\%$ in absolute terms when benchmarked against the existing standard nanofluid neural network modelling approach.

Although a dual layer MLP-NN scheme was also investigated as documented in the Appendix where the two-layer topology and mathematical scheme technical details are presented it was found that this was only able to achieve an AARD accuracy of 5.9048% with variation of the number of hidden neurons where the chief difficulty encountered was a lack of convergence for the more complex merit function which occasionally failed convergence criteria when an Levenberg-Marquardt optimization scheme was used. Although a dual layer MLP-NN may offer increased accuracies it was concluded that this comes at the potential cost of longer and more challenging optimization computational costs if inadequate computer codes are utilized. This observation is consistent with the earlier conclusions of Ariana et al [66] who reported a MLP network with only one hidden layer can in principal approximate any multivariate function to any desired accuracy, and as a result a trade off may be necessary in deciding on the appropriate number of hidden layers in a MLP-NN modelling scheme. This potential issue is largely avoided

in a copula modelling approach if conventional star-shaped topology schemes are utilized for simplicity.

Due to these observations, it can reasonably be concluded that a copula mathematical modelling technique has the research potential to offer improved accuracy predictive capabilities in the field of nanofluid studies. A fundamental key strength of the developed approach from this research investigation is that the use of copulas allows for the incorporation of physical experimental statistical uncertainties in the mathematical modelling construction process which is presently not considered computationally feasible with existing neural network modelling approaches that are coupled and incorporated into for example Markov Chain Monte Carlo (MCMC) based simulations as discussed by Levasseur *et al.*[177] .
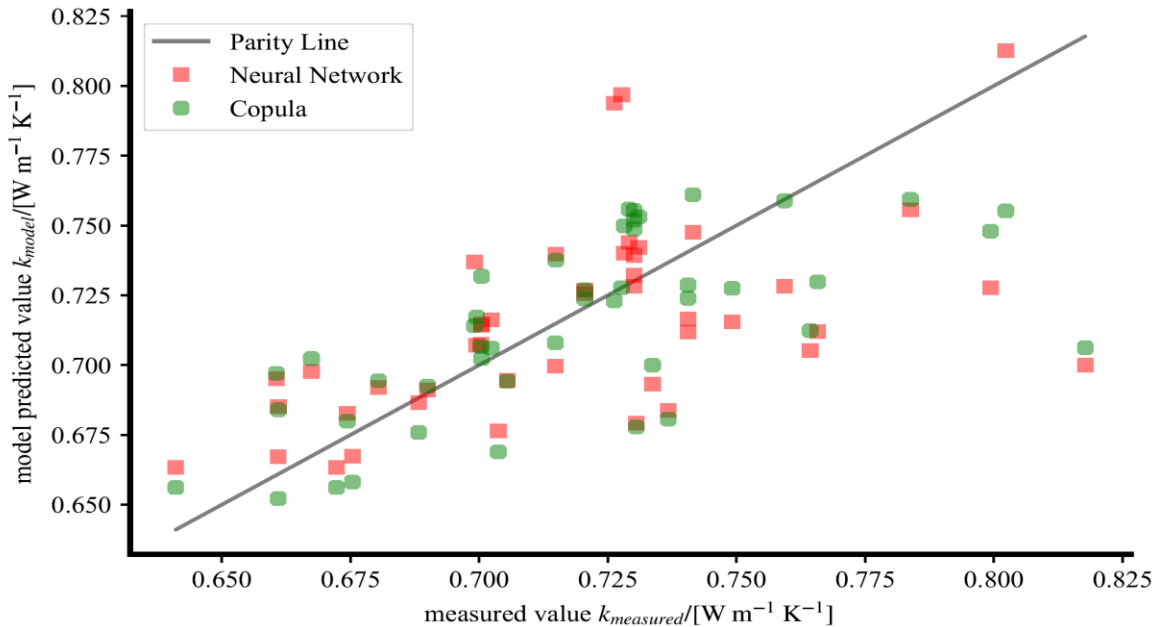
Figure 4-10 Comparison between prediction of neural network and copula nanofluid effective thermal conductivity mathematical models

4.5 Conclusions

In this chapter, a demonstration of how to perform numerical predictions of nanofluid effective thermal conductivities properties from the previously constructed database by utilizing univariate marginal distributions and the developed four-dimensional copula mathematical model has been presented. In the model physical units were utilized for the base fluid temperature T, nanoparticle volume fraction ϕ and nanoparticle diameter d_p as input meta-parameters along the physically measured nanofluid effective thermal conductivity k_{nf} so that joint PDF was constructed in terms of four random variables. As a result, the model was mathematically closed with just a set of six bivariate copula families where each family has a set of two parameters. The results of these

simulations for the thermal conductivity model were analysed and bench-marked against independent test data-points obtained in the earlier literature review and it was concluded that a copula based mathematical model can indeed perform reasonably well even with the presence of "messy" statistical data due to the Monte Carlo simulation process which is used to generate additional statistically consistent synthetic data-points using the input meta-parameter uncertainties such that the copula model construction automatically accounts for the natural aleatoric statistical variations that are present in the underlying physical experimental measurements. When the results between the current copula model were analysed it was concluded that the copula model predictions produced an average absolute relative deviation of $\text{AARD} = 3.0953\%$ whilst the standard neural network model for the same dataset produced a corresponding value of $\text{AARD} = 4.2376\%$. As a result it is concluded that the developed copula modelling approach has the potential to offer improved accuracy predictions of 1.1423% for the AARD in absolute terms when compared to the standard neural network approach. When both techniques were further investigated it was also determined that the developed copula approach has the competitive advantage of being able to incorporate predicted physical experimental statistical probability density function distributions i.e. PDF's at specified input conditions. This information may be used to quantitatively predict the model predicted expected values and variances, which is presently not considered computationally feasible with existing neural network modelling approaches.

Based on an analysis of the associated copula densities $c(\mathbf{u})$ for the various test points in the numerical simulations it was discovered that copula density function's behaviour varied from a conventional Gaussian type of PDF behaviour for certain values of the specified meta-parameters to a log-normal type of PDF behaviour for other ranges of the meta-parameters. Consequently whilst the variation in copula density $c(\mathbf{u})$ is slight in certain regions of the copula $\mathbf{u}$ coordinates it was observed that $c(\mathbf{u})$ may vary significantly in other regions. As a result due to the fact that the joint PDF is composed as a product of the marginal distributions and the copula density it is concluded that higher accuracy nanofluid thermophysical predictions may be possible for either smaller ranges of the meta-parameters or in corresponding regions of the meta-parameters where the copula density terms have less variation. This physical observation may therefore offer a potential future research advantage in nanofluid modelling studies by building models composed of unions of copulas of smaller domains so that instead of a single global model the nanofluid properties are specified in terms of sets of copulas for smaller regions of the meta-parameters. An example of this phenomenon is illustrated in Figure 4.11 which shows a visualization of a nanofluid effective viscosity model construction for our viscosity database. In this graph it is observed that there are a finite number of statistical outlier data-points in the region Ω_4 for the nanofluid effective viscosity μ_{nf} which are considered to be physically inconsistent with the underlying experimental data. The level of inconsistency is qualitatively indicated by the "distance" from the parity line for which points regardless of the magnitude of the corresponding physical uncertainties are at least in a certain sense "too far away" from the parity line. Our proposed solution for this issue is through the utilization of smaller domains such as for example Ω_1, Ω_2 and Ω_3 for illustrative purposes as shown in Figure 4.11.
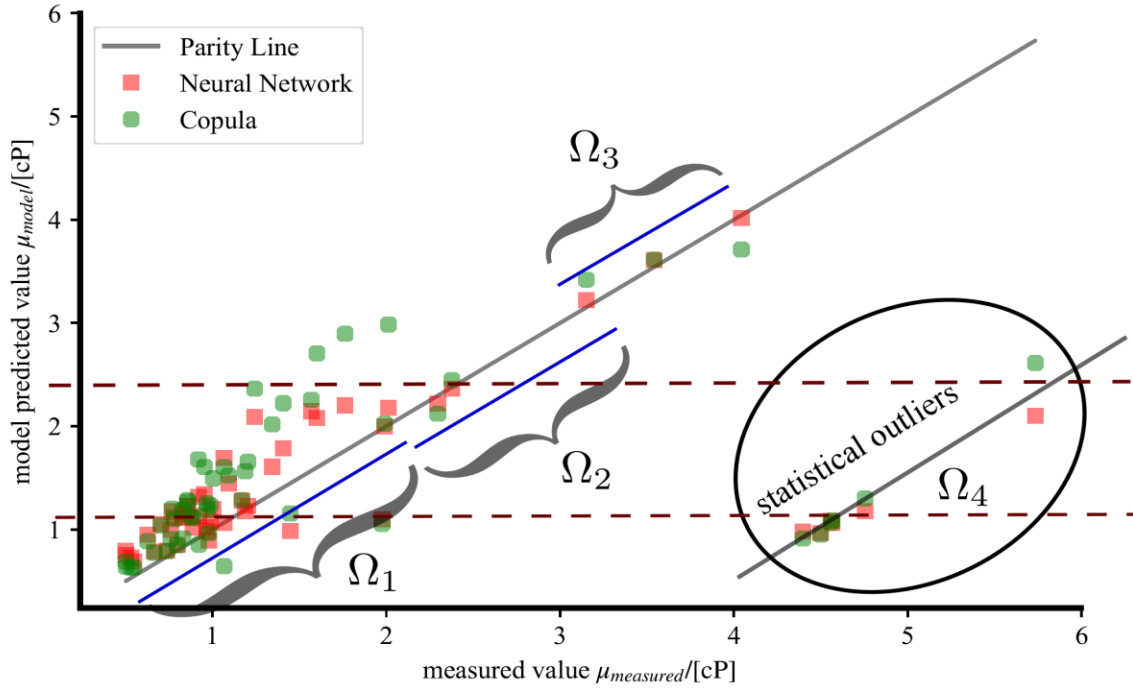
Figure 4-11 Illustration of statistical outliers for viscosity database model construction

In this approach the construction of the nanofluid model is subdivided into smaller domains Ω_i where

$$\Omega_i = [T_{min}^{(i)}, T_{max}^{(i)}]^T \times [\phi_{min}^{(i)}, \phi_{max}^{(i)}]^T \times [(d_p)_{min}^{(i)}, (d_p)_{max}^{(i)}]^T, i \in [1,2,3] \qquad (4.29)$$

consists of a region of the model input meta-parameters $T^{(i)}$, $\phi^{(i)}$ and $d_p^{(i)}$ for smaller restricted regions. Consequently, a set of nanofluid models for each of the smaller sub-domains may be constructed instead of attempting to fit a single nanofluid for a global domain. Methods for the identification of statistical outlier data-points to refine the model input data-points are also necessary and this has recently been investigated by Hemmati-Sarapardeh *et al.*[106] who elaborate on the mathematical implementation details of using William's plots for detecting probable statistical outliers and which is a recommended future refinement that may be used to pre-process the measurement data before implementing the copula mathematical model to achieve more consistent and better accuracy model predictions.

Potential areas of future research investigation include the exploration of different C-, D- and R-vine schemes as previously discussed for parametrized copulas in order to refine the interaction effects between the meta-parameter model inputs so that the accuracy of the numerical predictions may be increased, and in the utilization of the copula based nanofluid fluid property probability density functions in reliability engineering studies for mainly nanofluid thermal conductivity measurements as this exhibits relatively consistent statistical characteristics. Additional areas of

future research include the use of non-parametrized empirical copulas such as the Bernstein polynomial based empirical copulas recently reported by Segers *et al.*[191] with numerical schemes to efficiently calculate the corresponding copula density in order to directly compute the coupling interactions between the inputs for nanofluid viscosity measurements without any limiting parameter based restrictions due to the presence of noisy input statistical data.

5 Summary and Conclusions

5.1 Summary

This research study investigated the possibility of using copulas as mathematical objects to model nanofluid thermophysical properties such as either the effective thermal conductivity or alternately the effective viscosity. A detailed comprehensive literature study was first performed to establish the current state of knowledge both in terms of the available experimental data as well regarding the available mathematical techniques. The outcome of the literature review was that at present, there does not exist a complete physical or mathematical theory that adequately encompasses all of the features, properties and characteristics of nanofluids. Based on the literature review a database of a water/alumina nanofluid effective thermal conductivity and effective viscosity properties in terms of the temperature, nanoparticle volume concentration and nanoparticle diameter was constructed.

In the course of investigating the underlying database information, we developed two complementary mathematical techniques to construct nanofluid models of the respective thermophysical properties. The first approach is a variation on the GUM Supplement 1 Monte Carlo technique that utilizes a modified merit function optimization to estimate the probability density function distributions of algebraic models of nanofluids so that the algebraic model is then able to incorporate the aleatory statistical uncertainties of the physical experimental measurements. A novel research outcome of this first mathematical approach is that we developed a technique to either construct an uncoupled algebraic model of a nanofluid's properties such as just for the effective thermal conductivity or alternatively just for the effective viscosity, and in addition we developed the mathematical formalism to construct coupled algebraic models for the nanofluid's properties. Building on these earlier outcomes, we then proceeded to investigate the mechanism of utilizing copulas to model a nanofluid's properties, and this was also based on a Monte Carlo simulation technique, however, the key difference was that we did not make any *a priori* assumptions on the algebraic form of the nanofluid model. We considered analytical, empirical and vine copula schemes and determined that star-shaped C-vine tree-based schemes of copulas offered the most immediate functionality and generality to account for the wide variance in reported experimental results.

The second mathematical approach, therefore, developed and constructed a four-dimensional joint probability density function for the respective nanofluid thermophysical property and the three meta-parameters, and this was performed for both the effective thermal conductivity as well as for the effective viscosity. Results for the corresponding copulas were reported regarding the types of bivariate copulas as building blocks for the higher dimensional copula and their respective parameters. As a result, the copula density function is completely analytically specified however a difficulty that we encountered was that the associated marginal distributions for the meta-parameters is not easily amenable to a simple analytical expression such as an extended lambda distribution. This difficulty was determined as being primarily due to a finite number of nanoparticle size and volume concentration experimental measurements in the literature and was addressed through the adoption of univariate spline interpolations for the respective marginal distributions.

Once the copulas were mathematically characterized, we then developed statistical sampling techniques to utilize the copula models for the prediction of expected values and variances of the nanofluid thermophysical properties. The outcome of this investigation was that the developed copula mathematical models are considered to be statistically consistent and can offer moderate accuracy improvements on nanofluid model predictions compared to conventional algebraic and neural network modelling schemes. A unique powerful feature of our novel mathematical approach is the complete generality and ease of use of copulas for building, characterising and extending existing models for both model predictions as well as model uncertainty quantification analysis with relative ease as new data and meta-parameters become available.

5.2 Conclusions

Based on the outcomes of the present research investigation, the following conclusions were reached:

- Alternative tree based copula structures using either regular R-vines or dependence D-vines should be investigated as potential copula structures to incorporate existing experimental know-how and observations due to the wide variety of construction schemes for higher dimensional copulas;

- Higher dimensional copula models that incorporate the effect of the nanofluid pH and shear strain rate as additional meta-parameters should be investigated where experimentally feasible to generalize and extend the utility of existing models;

- The application of non-equilibrium molecular dynamics simulations for *ab initio* numerical predictions of nanofluid properties should be considered as a potential PhD study as the availability of high-performance computing (HPC) clusters starts to become more widely available within South Africa in order to independently address some of the inconsistencies and ambiguities such as nanoparticle sizes and agglomeration effects in the experimental results reported in the literature particularly for the nanofluid effective viscosity measurements;

- Existing parameter based algebraic nanofluid models may be refined using the developed mathematical approach in order to generate probability density functions of the parameters so that the existing formulae may be conveniently utilized in uncertainty analysis calculations within industry;

- The application of copula-based statistical models of nanofluid thermophysical properties may be utilized in heat exchanger reliability designs and associated equipment and instruments within the nuclear engineering sector that require estimates of probability density functions of fluid properties.

6 Appendix

6.1 Dual Layer Multi-Level Perceptron Neural Network

In neural network theory a common modelling approach is the Multi-Level Perceptron Neural Network (MLP-NN) approach. One particular topology approach for this scheme is shown below.
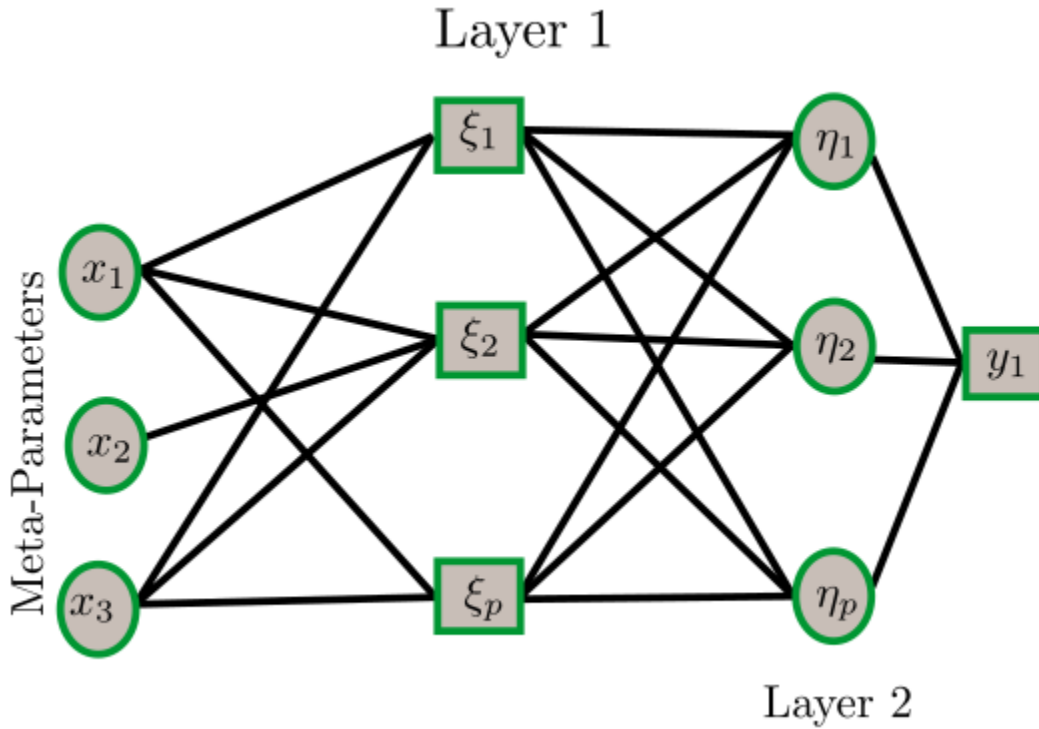
In the above topology x_1, x_2 and x_3 are the model inputs and y_1 the model output. Two hidden layers are present in the system and using a vector/matrix notation the intermediate neuron signals may be calculated as

$$\boldsymbol{\xi} = \boldsymbol{f}(\boldsymbol{U}\boldsymbol{x} + \boldsymbol{a}) \tag{A1}$$
$$\boldsymbol{\eta} = \boldsymbol{f}(\boldsymbol{V}\boldsymbol{\xi} + \boldsymbol{b}) \tag{A2}$$
$$y_1 = \sum_{i=1}^{p} \eta_i \tag{A3}$$

If both layers have p neurons then the vector/matrix parameters have dimensions such that

$$\dim(\boldsymbol{U}) = [p, 3] \tag{A4}$$
$$\dim(\boldsymbol{a}) = [p, 1] \tag{A5}$$
$$\dim(\boldsymbol{V}) = [p, p] \tag{A6}$$
$$dim(\boldsymbol{b}) = [p, 1] \tag{A7}$$

Although each hidden layer can technically have a different number of neurons if the largest number of neurons are used then by the judicious selection of non-zero and zero weighting factors

179

refinements can still be accomodated. When this model is implemented using $n = 25$ iterations as a convergence limit for a Levenberg-Marquardt optimization in a GNU Octave simulation then the following results are obtained as shown below for the thermal conductivity test data utilized from the earlier single layer MLP-NN and copula simulations from Chapter 4.

p	$AARD\%$
3	10.4325
4	17.5509
5	8.2756
6	5.9048
7	17.5507
8	17.5509

It was observed that the main challenge with the implementation of a dual layer MLP-NN scheme for the in-house computer code that was developed was with the specification of the starting values for the optimization search. This is an area of future research to refine the code to achieve better results.

6.2 Representive Computer Codes

The following m-files were developed in GNU Octave to test the feasibility of a dual layer MLP-NN approach but unfortuantely it was not considered feasible to utilize a two layer scheme, and a single layer MLP-NN approach was utilized as per the recommendations of Ariana et al [66].

Main Program

```
clear all
clc

pkg load optim

global X Y p

disp('Dual Layer MLP-NN')
ktrain = load('kmodel.txt');
Ttrain = load('Tmodel.txt');
phitrain = 1E2*load('phimodel.txt');
dtrain = 1E9*load('dmodel.txt');

ktest = load('ktest.txt');
Ttest = load('Ttest.txt');
phitest = 1E2*load('phitest.txt');
dtest = 1E9*load('dtest.txt');
```

```matlab
kmin = min(ktrain);
kmax = max(ktrain);
Tmin = min(Ttrain);
Tmax = max(Ttrain);

phimin = min(phitrain);
phimax = max(phitrain);

dmin = min(dtrain);
dmax = max(dtrain);

N = length(ktrain);

% x = [ T phi d ]

deltaT = (Tmax - Tmin);
deltaphi = (phimax - phimin);
deltad = (dmax - dmin);

deltak = (kmax - kmin);

for i = 1:N
    Xtrain(i, 1) = (Ttrain(i) - Tmin)/deltaT;
    Xtrain(i, 2) = (phitrain(i) - phimin)/deltaphi;
    Xtrain(i, 3) = (dtrain(i) - dmin)/deltad;
    Ytrain(i, 1) = (ktrain(i) - kmin)/deltak;
end

X = Xtrain;
Y = Ytrain;


p = 3; % number of hidden neurons

U0 = abs( randn(p, 3) ); % random matrix all components   between 0 and 1

a0 = abs( randn(p, 1) ); % random vector all components between 0 and 1

V0 = abs( randn(p, p) ); % random vector all components between 0 and 1

b0 = abs( randn(p, 1) ); % random vector all components between 0 and 1


Ucolumn = U0(:);
acolumn = a0(:);
Vcolumn = V0(:);
```

```matlab
bcolumn = b0(:);

A0 = [Ucolumn; acolumn; Vcolumn; bcolumn];

% U = p x 3
% a = p x 1
% V = p x p
% b = p x 1

optimizeLevenbergMarquardt = 1;

if optimizeLevenbergMarquardt == 1
    [f1, p1, cvg1, iter1, corp1, covp1, covr1, stdresid1, Z1, r21] = leasqr(X, Y, A0,
'modelDualLayerMLPNN', 0.0001, 25);
    % Set the converged Levenberg-Marquardt optimization solution to the optimal parameter in
column
    % format using standard Matlab/Fortran matrix-column notation
    aopt = p1;
    % Extract the coefficients from the optimal parameter and reconstruct the vector/matrix
terms
    % U = p x 3
    I1 = 1;
    I2 = 3*p;
    % a = p x 1
    I3 = I2 + 1;
    I4 = I2 + p;
    % V = p x p
    I5 = I4 + 1;
    I6 = I4 + (p*p);
    % b = p x 1
    I7 = I6 + 1;
    I8 = I6 + p;
    % reshape and reconstruct
    colU = aopt(I1:I2);
    U = reshape(colU, [p, 3]);
    cola = aopt(I3:I4);
    a = cola;
    colV = aopt(I5:I6);
    V = reshape(colV, [p, p]);
    colb = aopt(I7:I8);
    b = reshape(colb, [p, 1]);
end


M = length(ktest);
```

```matlab
for i = 1:M
    Xtest(i, 1) = (Ttest(i) - Tmin)/deltaT;
    Xtest(i, 2) = (phitest(i) - phimin)/deltaphi;
    Xtest(i, 3) = (dtest(i) - dmin)/deltad;
    Ytest(i, 1) = (ktest(i) - kmin)/deltak;
end

for j = 1:M
    x = Xtest(i, :);
        x = x';
        xi = factivation(U*x + a);
        eta = factivation(V*xi + b);
        y = gactivation(eta);
        ypredict(j, 1) = y;
end

% Reconstruct the physical values from the normalized coordinates

ktestdata = (kmax - kmin)*Ytest + kmin;
kpredictdata = (kmax - kmin)*ypredict + kmin;

y1 = ktestdata;
y2 = kpredictdata;

AARDtest = (100/M)*sum( abs( (y1 - y2)./y1 ) );

figure(1)
clf
plot(y1, y2, '-sk')
grid on
xlabel('ktest')
ylabel('kpredict')
titlestr = ['AARD% = ', num2str(AARDtest)];
title(titlestr);
```

Associated Model Implementation

```matlab
function fval = modelDualLayerMLPNN(X, amodel)

global p

% U = p x 3
I1 = 1;
I2 = 3*p;
% a = p x 1
I3 = I2 + 1;
```

183

```
I4 = I2 + p;

% V = p x p
I5 = I4 + 1;
I6 = I4 + (p*p);

% b = p x 1
I7 = I6 + 1;
I8 = I6 + p;

% reshape and reconstruct
colU = amodel(I1:I2);
U = reshape(colU, [p, 3]);

cola = amodel(I3:I4);
a = cola;
colV = amodel(I5:I6);
V = reshape(colV, [p, p]);

colb = amodel(I7:I8);
b = reshape(colb, [p, 1]);

dimX = size(X);
rowX = dimX(1, 1);
colX = dimX(1, 2);

M = rowX;

for i = 1:M
    x = X(i, :)';
        xi = factivation(U*x + a);
        eta = factivation(V*xi + b);
        ymodel(i, 1) = gactivation(eta);
end

fval = ymodel;
```

Activation Function for Both Input/Intermediate Layers

```
function fval = factivation(x)
fval = ( 1 + exp(-x) ).^(-1);
```

Activation Function for Output Layer

```
function gval = gactivation(x)
gval = sum(x);
```

7 References

[1] F. P. Incropera and D. P. DeWitt, Fundamentals of Heat and Mass Transfer. John Wiley & Sons, 4th ed., 1996. ISBN 0-471-30460-3.

[2] N. W. Ashcroft and N. D. Mermin, Solid State Physics. Cengage Learning, 1st ed., 1976. ISBN 0-03-083993-9.

[3] R. Siegel and J. R. Howell, Thermal Radiation Heat Transfer. Taylor & Francis, 4th ed., 2002. ISBN 1-56032-839-8.

[4] J. I. Castor, Radiation Hydrodynamics. Cambridge University Press, 1st ed., 2004. ISBN 0-521-83309-4.

[5] A. F. Mills, Basic Heat and Mass Transfer. Prentice Hall, 2nd ed., 1999. ISBN 0-13-096247-3.

[6] S. U. S. Choi, "Enhancing Thermal Conductivity of Fluids with Nanoparticles," in Developments and Applications of Non-Newtonian Flows – Proceedings of the 1995 ASME International Mechanical Engineering Congress and Exposition (D. A. Siginer and H. P. Wang, eds.), vol. 231, pp. 99–105, American Society of Mechanical Engineers Fluids Engineering Division, November 1995.

[7] Department of Trade and Industry, "Industrial Policy Action Plan (IPAP) Part 1: 2017/18–2019/20," tech. rep., Government of the Republic of South Africa, May 2017. https://www.gov.za/sites/default/files/IPAP1718_1920.pdf, ISBN 978-0-621-453669-0.

[8] D. Mihalas and B. Weibel-Mihalas, Foundations of Radiation Hydrodynamics. Dover Publications, 1999. ISBN 0-486-40925-2.

[9] E. W. Lemmon and R. T. Jacobsen, "Viscosity and Thermal Conductivity Equations for Nitro- gen, Oxygen, Argon, and Air," International Journal of Thermophysics, vol. 25, no. 1, pp. 21–69, 2004. DOI: 10.1023/B:IJOT.0000022327.04529.f3.

[10] F. Reif, Fundamentals of Statistical and Thermal Physics. McGraw-Hill Book Company, 1965. ISBN 0-07-085615-X.

[11] S. Chapman and T. G. Cowling, The Mathematical Theory of Non-Uniform Gases: An Account of the Kinetic Theory of Viscosity, Thermal Conduction, and Diffusion in Gases. Cambridge University Press, 2nd ed., 1953. ISBN 052140844X.

[12] J. N. Reddy, Principle of Continuum Mechanics: A Study of Conservation Principles with Applications. Cambridge University Press, 2010. ISBN 978-0-521-51369-2.

[13] L. S. Garc´ıa-Col´ın, R. M. Velasco, and F. J. Uribe, "Beyond the Navier-Stokes Equations: Burnett Hydrodynamics," Physics Reports, vol. 465, pp. 149–189, 2008. DOI: 10.1016/j.physrep.2008.04.010.

[14] F. M. White, Viscous Fluid Flow. McGraw-Hill, 2nd ed., 1991. ISBN 0070697132.

[15] J. C. Tannehill, D. A. Anderson, and R. H. Pletcher, Computational Fluid Mechanics and Heat Transfer. Taylor & Francis, 2nd ed., 1997. ISBN 1-56032-046-X.

[16] V. Y. Rudyak, "Viscosity of Nanofluids – Why It Is Not Described by the Classical Theories," Advances in Nanoparticles, vol. 2, pp. 266–279, 2013. DOI: 10.4236/anp.2013.23037.

[17] J. B. Young, "Calculation of Knudsen Layers and Jump Conditions Using the Linearised G13 and R13 Moment Methods," International Journal of Heat and Mass Transfer, vol. 54, pp. 2902–2912, 2011. DOI: 10.1016/j.ijheatmasstransfer.2011.03.009.

[18] Y. Y. Yan, Y. Q. Zu, and B. Dong, "LBM, A Useful Tool for Mesoscale Modelling of Single- Phase and Multiphase Flow," Applied Thermal Engineering, vol. 31, pp. 649–655, 2011. DOI: 10.1016/j.applthermaleng.2010.10.010.

[19] M. Sheikholeslami, M. Gorji-Bandpy, S. M. Seyyedi, D. D. Ganji, H. B. Rokni, and S. Soleimani, "Application of LBM in Simulation of Natural Convection in a Nanofluid Filled Square Cavity with Curve Boundaries," Powder Technology, vol. 247, pp. 87–94, 2013. DOI: 10.1016/j.powtec.2013.06.008.

[20] T. J. Scanlon, E. Roohi, C. White, M. Darbandi, and J. M. Reese, "An Open Source, Parallel DSMC Code for Rarefied Gas Flows in Arbitary Geometries," Computers & Fluids, vol. 39, pp. 2078–2089, 2010. DOI: 10.1016/j.compfluid.2010.07.014.

[21] G. A. Bird, "The Q-K Model for Gas-Phase Chemical Reaction Rates," Physics of Fluids, vol. 23, p. 106101, 2011. DOI: 10.1063/1.3650424.

[22] G. E. Karniadakis, A. Beskok, and N. Aluru, Microflows: Fundamentals and Simulation.

Springer, 1st ed., 2002. ISBN 978-0-387-95324-3.

[23] F. Sharipov and J. L. Strapasson, "Direct Simulation Monte Carlo Method for Arbitrary Intermolecular Potential," Physics of Fluids, vol. 24, p. 011703, 2012. DOI: 10.1063/1.3676060.

[24] C. Canuto, M. Y. Hussaini, A. Quarteroni, and T. A. Zang, Spectral Methods – Evolution to Complex Geometries and Applications to Fluid Dynamics. Springer-Verlag, 2007. ISBN 978-3-540-30727-3.

[25] X.-Q. Wang and A. S. Mujumdar, "Heat Transfer Characteristics of Nanofluids: A Review," International Journal of Thermal Sciences, vol. 46, pp. 1–19, 2007. DOI: 10.1016/j.ijthermalsci.2006.06.010.

[26] H. Bruus, Theoretical Microfluidics. Oxford University Press, 2008. ISBN 978-0-19-923508-7.

[27] D.-W. Oh, A. Jain, J. K. Eaton, K. E. Goodson, and J. S. Lee, "Thermal Conductivity Measurement and Sedimentation Detection of Aluminium Oxide Nanofluids by Using the 3ω Method," International Journal of Heat and Fluid Flow, vol. 29, pp. 1456–1461, 2008. DOI: 10.1016/j.ijheatfluidflow.2008.04.007.

[28] A. Turgut, I. Tavman, M. Chirtoc, H. P. Schuchmann, C. Sauter, and S. Tavman, "Thermal Conductivity and Viscosity Measurements of Water-Based TiO2 Nanofluids," International Journal of Thermophysics, vol. 30, pp. 1213–1226, 2009. DOI: 10.1007/s10765-009-0594-2.

[29] C. H. Li and G. P. Peterson, "Experimental Investigation of Temperature and Volume Fraction Variations on the Effective Thermal Conductivity of Nanoparticle Suspensions (Nanofluids)," Journal of Applied Physics, vol. 99, p. 084314, 2007. DOI: 10.1063/1.2191571.

[30] B. Ravisankar and V. T. Chand, "Influence of Nanoparticle Volume Fraction, Particle Size and Temperature on Thermal Conductivity and Viscosity of Nanofluids – A Review," International Journal of Automotive and Mechanical Engineering, vol. 8, pp. 1316–1338, 2013. DOI: 10.15282/ijame.8.2013.20.0108.

[31] X.-Q. Wang and A. S. Mujumdar, "A Review of Nanofluids – Part I: Theoretical and Numerical Investigations," Brazilian Journal of Chemical Engineering, vol. 25, pp. 613–630, 2008. DOI: 10.1590/S0104-66322008000400001.

[32] R. S. Vajjha, D. K. Das, and B. M. Mahagaonkar, "Density Measurement of Different Nanofluids and Their Comparison with Theory," Petroleum Science and Technology, vol. 27, pp. 612–624, 2009. DOI: 10.1080/10916460701857714.

[33] T.-P. Teng and Y.-H. Hung, "Estimation and Experimental Study of the Density and Specific Heat for Alumina Nanofluid," Journal of Experimental Nanoscience, vol. 9, no. 7, pp. 707–718, 2014. DOI: 10.1080/17458080.2012.696219.

[34] T.-P. Teng, Y.-H. Hung, T.-C. Teng, H.-E. Mo, and H.-G. Hsu, "The Effect of Alumina/Water Nanofluid Particle Size on Thermal Conductivity," Applied Thermal Engineering, vol. 30, pp. 2213–2218, 2010. DOI: 10.1016/j.applthermaleng.2010.05.036.

[35] M. Sharifpur, S. Yousefi, and J. P. Meyer, "A New Model for Density of Nanofluids Including Nanolayer," International Communications in Heat and Mass Transfer, vol. 78, pp. 168–174, 2016. DOI: 10.1016/j.powtec.2016.11.032.

[36] M. Sharifpur and J. P. Meyer, "The Effect of Uncertainty of Conductivity and Viscosity of Nanofluids on Heat Transfer," in 1st International Conference on Nanostructures and Nanomaterial: Science and Application (Nanotech2012) (P. Molaei, ed.), pp. 1–7, Iran University of Science and Technology (IUST), February 2012. URL: https://www.researchgate.net/publication/280611155.

[37] M. Mehrabi, M. Sharifpur, and J. P. Meyer, "Modelling and Multi-Objective Optimisation of the Convective Heat Transfer Characteristics and Pressure Drop of Low Concentration TiO2-Water Nanofluids in the Turbulent Flow Regime," International Journal of Heat and Mass Transfer, vol. 67, pp. 646–653, 2013. DOI: 10.1016/j.ijheatmasstransfer.2013.08.013.

[38] M. Mehrabi, M. Sharifpur, and J. P. Meyer, "Viscosity of Nanofluids Based On An Artificial Intelligence Model," International Communications in Heat and Mass Transfer, vol. 43, pp. 16–21, 2013. DOI: 10.1016/j.icheatmasstransfer.2013.02.008.

[39] C. T. Nguyen, F. Desgranges, G. Roy, N. Galanis, T. Mar´e, S. Boucher, and H. A. Mintsa, "Temperature and Particle-Size Dependent Viscosity Data for Water-Based Nanofluids – Hysteresis Phenomenon," International Journal of Heat and Fluid Flow, vol. 28, pp. 1492–1506, 2007. DOI: 10.1016/j.ijheatfluidflow.2007.02.004.

[40] I. Tavman, A. Turgut, M. Chirtoc, H. P. Schuchmann, and S. Tavman, "Experimental Investigation of Viscosity and Thermal Conductivity of Suspensions Containing Nanosized Ceramic Particles,"

Archives of Material Science and Engineering, vol. 34, no. 2, pp. 99–104, 2008.

[41] J.-H. Lee, K. S. Hwang, S. P. Jang, B. H. Lee, J. H. Kim, S. U. S. Choi, and C. J. Choi, "Effective Viscosities and Thermal Conductivities of Aqueous Nanofluids Containing Low Volume Concentrations of Al2O3 Nanoparticles," International Journal of Heat and Mass Transfer, vol. 51, pp. 2651–2656, 2008. DOI: 10.1016/j.ijheatmasstransfer.2007.10.026.

[42] K. B. Anoop, S. Kabelac, T. Sundararajan, and S. K. Das, "Rheological and Flow Characteristics of Nanofluids: Influence of Electroviscous Effects and Particle Agglomeration," Journal of Applied Physics, vol. 106, pp. 034909–1–034909–7, 2009. DOI: 10.1063/1.3182807.

[43] M. J. Pastoriza-Gallego, C. Casanova, R. Paramo, B. Barbes, J. L. Legido, and M. M. P. Neiro, "A Study on Stability and Thermophysical Properties (Density and Viscosity) of Al2O3 in Water Nanofluid," Journal of Applied Physics, vol. 106, pp. 064301–1–064301–8, 2009. DOI: 10.1063/1.3187732.

[44] D. Kwek, A. Crivoi, and F. Duan, "Effects of Temperature and Particle Size on the Thermal Property Measurements of Al2O3-Water Nanofluids," Journal Chemical Engineering Data, vol. 55, pp. 5690–5695, 2010. DOI: 10.1021/je1006407.

[45] S. A. Adio, M. Sharifpur, and J. P. Meyer, "Investigation Into Effective Viscosity, Electrical Conductivity, and pH of γ-Al2O3-Glycerol Nanofluids in Einstein Concentration Regime," Heat Transfer Engineering, vol. 36, no. 14–15, pp. 1241–1251, 2015. DOI: 10.1080/01457632.2015.994971.

[46] M. Sharifpur, S. A. Adio, and J. P. Meyer, "Experimental Investigation and Model Development for Effective Viscosity of Al2O3-Glycerol Nanofluids By Using Dimensional Analysis and GMDH- NN Methods," International Communications in Heat and Mass Transfer, vol. 68, pp. 208–219, 2015. DOI: 10.1016/j.icheatmasstransfer.2015.09.002.

[47] J. A. R. Babu, K. K. Kumar, and S. S. Rao, "State-of-Art Review on Hybrid Nanofluids," Renewable and Sustainable Energy Reviews, vol. 77, pp. 551–565, 2017. DOI: 10.1016/j.rser.2017.04.040.

[48] S. Kumar, S. K. Prasad, and J. Banerjee, "Analysis of Flow and Thermal Field in Nanofluid Using a Single Phase Thermal Dispersion Model," Applied Mathematical Modelling, vol. 34, pp. 573–592, 2010. DOI: 10.1016/j.apm.2009.06.026.

[49] M. K. Moraveji and R. M. Ardehali, "CFD Modeling (Comparing Single and Two-Phase Ap- proaches) on Thermal Performance of Al2O3/Water Nanofluid in Mini-Channel Heat Sink," International Communications in Heat and Mass Transfer, vol. 44, pp. 157–164, 2013. DOI: 10.1016/j.icheatmasstransfer.2013.02.012.

[50] R. Davarnejad, S. Barati, and M. Kooshki, "CFD Simulation of the Effect of Particle Size on the Nanofluids Convective Heat Transfer in the Developed Region in a Circular Tube," SpringerPlus, vol. 2, pp. 1–6, 2013. URL: http://www.springerplus.com/content/2/1/192.

[51] K. Khanafer and K. Vafai, "A Critical Sythesis of Thermophysical Characteristis of Nanofluids," International Journal of Heat and Mass Transfer, vol. 54, pp. 4410–4428, 2011. DOI: 10.1016/j.ijheatmasstransfer.2011.04.048.

[52] C. T. Nguyen, F. Desgranges, N. Galanis, G. Roy, T. Mar´e, S. Boucher, and H. A. Mintsa, "Viscosity Data for Al2O3-Water Nanofluid – Hysteris: Is Heat Transfer Enhancement Using Nanofluids Reliable?," International Journal of Thermal Sciences, vol. 47, pp. 103–111, 2008. DOI: 10.1016/j.ijthermalsci.2007.01.033.

[53] BIPM, IEC, IFCC, ILAC, ISO, IUPAC, IUPAP, and OILM, "Guide to the Expression of Un- certainty in Measurement," tech. rep., Bureau International de Poids et Mesures (BIPM), 2008. www.bipm.org/utils/common/documents/jcgm/JCGM_100_2008_E.pdf.

[54] M. Chandrasekar, S. Suresh, and A. C. Bose, "Experimental Investigations and Theoretical Determination of Thermal Conductivity and Viscosity of Al2O3/Water Nanofluid," Experimental and Thermal Science, vol. 29, pp. 210–216, 2010. DOI: 10.1016/j.expthermflusci.2009.10.022.

[55] M. Hosseini and S. Ghader, "A Model for Temperature and Particle Volume Fraction Effect on Nanofluid Viscosity," Journal of Molecular Liquids, vol. 153, pp. 139–145, 2010. DOI: 10.1016/j.molliq.2010.02.003.

[56] M. Corcione, E. Habib, and A. Quintino, "A Two Phase Numerical Study of Buoyancy Driven Convection of Alumina-Water Nanofluids in Differentially-Heated Horizontal Annuli," International Journal of Heat and Mass Transfer, vol. 65, pp. 327–338, 2013. DOI: 10.1016/j.ijheatmasstransfer.2013.06.014.

[57]   J. Albard, S. Tayal, and M. Alasadi, "Heat Transfer Through Heat Exchanger Using Al2O3 Nanofluid at Different Concentrations," Case Studies in Thermal Engineering, vol. 1, pp. 38–44, 2013. DOI: 10.1016/j.csite.2013.08.004.

[58]   M. R. Safaei, A. H. Jahanbin, A. Kianifar, S. Gharehkhani, A. S. Kherbeet, M. Goodarzi, and M. Dahari, "Modeling and Simulation in Engineering Sciences," in Mathematical Modeling for Nanofluids Simulation: A Review of the Latest Works (N. S. Akbar and O. A. Beg, eds.), ch. 9, pp. 189–220, InTechOpen, 2016. ISBN 978-953-51-2608-09 DOI: 10.5772/64154.

[59]   H. K. Versteeg and W. Malalasekera, An Introduction to Computational Fluid Dynamics – The Finite Volume Method. Pearson/Prentice Hall, 1st ed., 1995. ISBN 0-582-21884-5.

[60]   N. A. C. Sidik, M. N. A. W. M. Yazid, and S. Samion, "Latest Development on Computational Approaches for Nanofluid Flow Modeling: Navier-Stokes Based Multiphase Models," International Communications in Heat and Mass Transfer, vol. 74, pp. 114–124, 2016. DOI: 10.1016/j.icheatmasstransfer.2016.03.007.

[61]   M. Ghanbarpour, E. B. Haghigi, and R. Khodabandeh, "Thermal Properties and Rheological Behavior of Water Based Al2O3 Nanofluid as a Heat Transfer Fluid," Experimental Thermal and Fluid Science, vol. 53, pp. 227–235, 2014. DOI: 10.1016/j.expthermflusci.2013.12.013.

[62]   E. Abu-Nada, "Effects of Variable Viscosity and Thermal Conductivity of Al2O3-Water Nanofluid on Heat Transfer Enhancement in Natural Convection," International Journal of Heat and Fluid Flow, vol. 30, pp. 679–690, 2009. DOI: 10.1016/j.ijheatfluidflow.2009.02.003.

[63]   P. N. Nwosu, J. Meyer, and M. Sharifpur, "Nanofluid Viscosity: A Simple Model Selection Algorithm and Parametric Evaluation," Computers and Fluids, vol. 101, pp. 241–249, 2014. DOI: 10.1016/j.compfluid.2014.04.001.

[64]   E. A. Baltz, E. Trask, M. Binderbauer, M. Dikovsky, H. Gota, R. Mendoza, J. C. Platt, and P. F. Riley, "Achievement of Sustained Net Plasma Heating in a Fusion Experiment with the Optometrist Algorithm," Scientific Reports, vol. 7, p. 6425, 2017. DOI: 10.1038/s41598-017-06645-7.

[65]   N. Zhao, X. Wen, J. Yang, S. Li, and Z. Wang, "Modeling and Prediction of Viscosity of Water- Based Nanofluids by Radial Basis Function Neural Networks," Powder Technology, vol. 281, pp. 173–183, 2015. DOI: 10.1016/j.powtec.2015.04.058.

[66]   M. A. Ariana, B. Vaferi, and G. Karimi, "Prediction of Thermal Conductivity of Alumina Water-Based Nanofluids by Artificial Neural Networks," Powder Technology, vol. 278, pp. 1–10, 2015. DOI: 10.1016/j.powtec.2015.03.005.

[67]   M. K. Meybodi, S. Naseri, A. Shokrollahi, and A. Daryasafar, "Prediction of Viscosity of Water- Based Al2O3, TiO2, SiO2, and CuO Nanofluids Using a Reliable Approach," Chemometrics and Intelligent Laboratory Systems, vol. 149, pp. 60–69, 2015. DOI: 10.1016/j.chemolab.2015.10.001.

[68]   E. V. Timofeeva, A. N. Gavrilov, J. M. McCloskey, and Y. V. Tolmachev, "Thermal Conductivity and Particle Agglomeration in Alumina Nanofluids: Experiment and Theory," Physical Review E, vol. 76, pp. 061203–1–061203–16, 2007. DOI: 10.1103/PhysRevE.76.061203.

[69]   J. Meyer, S. Adio, M. Sharifpur, and P. Nwosu, "The Viscosity of Nanofluids: A Review of the Theoretical, Empirical and Numerical Models," Heat Transfer Engineering, vol. 37, no. 5, pp. 387–421, 2015. DOI: 10.1080/01457632.2015.1057447.

[70]   N. Masoumi, N. Sohrabi, and A. Behzadmehr, "A New Model for Calculating the Effective Viscosity of Nanofluids," Journal of Physics D: Applied Physics, vol. 42, pp. 055501–1–055501–6, 2009. DOI: 10.1088/0022-3727/42/5/055501.

[71]   S. M. Hosseini, A. R. Moghadassi, and D. E. Henneke, "A New Dimensionless Group Model for Determing the Viscosity of Nanofluids," Journal of Thermal Analysis and Calorimetry, vol. 100, pp. 873–877, 2010. DOI: 10.1007/s10973-010-0721-0.

[72]   M. F. Zawrah, R. M. Khattab, L. G. Girgis, H. E. Daidamony, and R. e. Abdel Aziz, "Sta- bility and Electrical Conductivity pf Water-Base Al2O3 Nanofluids for Different Applications," Housing and Building National Research Center Journal, vol. 12, pp. 227–234, 2016. DOI: 10.1016/j.hbrcj.2014.12.001.

[73]   H. Konakanchi, R. S. Vajjha, G. Chukwu, and D. K. Das, "Measurements of pH of Three Nanofluids and Development of New Correlations," Heat Transfer Engineering, vol. 36, no. 1, pp. 81–90, 2015. DOI: 10.1080/01457632.2014.906286.

[74]   M. Gupta, V. Singh, R. Kumar, and Z. Said, "A Review of Thermophysical Properties of Nanofluids and Heat Transfer Applications," Renewable and Sustainable Energy Reviews, vol. 74, pp. 638–670, 2017. DOI: 10.1016/j.rser.2017.02.073.

[75] S. M. S. Murshed and P. Estelle, "A State of the Art Review on Viscosity of Nanofluids," Renewable and Sustainable Energy Reviews, vol. 76, pp. 1134–1152, 2017. DOI: 10.1016/j.rser.2017.03.113.

[76] M. Mehrabi, M. Sharifpur, and J. P. Meyer, "Application of the FCM-Based Neuro-Fuzzy Inference System and Genetic Algorithm-Polynomial Neural Network Approaches to Modelling the Thermal Conductivity of Alumina-Water Nanofluids," International Communications in Heat and Mass Transfer, vol. 39, pp. 971–977, 2012. DOI: 10.1016/j.icheatmasstransfer.2012.05.017.

[77] H. Masuda, A. Ebata, K. Teramae, and N. Hishinuma, "Alteration of Thermal Conductivity and Viscosity of Liquid by Dispersing Ultra-Fine Particles (Dispersion of c-Al2O3, SiO2 and TiO2 Ultra-Fine Particles)," Netsu Bussei, vol. 4, pp. 227–233, 1993. DOI: 10.2963/jjtp.7.227 (In Japanese).

[78] S. Lee, S. U. S. Choi, S. Li, and J. A. Eastman, "Measuring Thermal Conductivity of Fluids Containing Oxide Nanoparticles," Journal of Heat Transfer, vol. 121, no. 2, pp. 280–289, 1999. DOI: 10.1115/1.2825978.

[79] S. K. Das, N. Putra, P. Thiesen, and W. Roetzel, "Temperature Dependence of Thermal Conductivity Enhancement for Nanofluids," Journal of Heat Transfer, vol. 125, pp. 567–574, 2004. DOI: 10.1115/1.1571080.

[80] N. Putra, W. Roetzel, and S. Das, "Natural Convection of Nano-Fluids," Heat and Mass Transfer, vol. 39, pp. 775–784, 2003. URL: DOI: 10.1007/s00231-002-0382-z.

[81] C. H. Chon, K. D. Kihm, S. P. Lee, and S. U. S. Choi, "Empirical Correlation Finding the Role of Temperature and Particle Size for Nanofluid (Al2O3) Thermal Conductivity Enhancement," Applied Physics Letters, vol. 87, pp. 153107–1–153107–3, 2007. DOI: 10.1063/1.2093936.

[82] C. H. Li and G. P. Peterson, "The Effect of Particle Size on the Effective Thermal Conductiv- ity of Al2O3-Water Nanofluids," Journal of Applied Physics, vol. 101, p. 044312, 2007. DOI: 10.1063/1.2436472.

[83] S. H. Kim, S. R. Choi, and D. Kim, "Thermal Conductivity of Metal-Oxide Nanofluids: Particle Size Dependence and Effect of Laser Irradiation," Journal of Heat Transfer, vol. 129, no. 3, pp. 298–307, 2006. DOI: 10.1115/1.2427071.

[84] X. Zhang, H. Gu, and M. Fujii, "Effective Thermal Conductivity and Thermal Diffusivity of Nanofluids Containing Spherical and Cylindrical Nanoparticles," Experimental Thermal and Fluid Science, vol. 31, pp. 593–599, 2007. DOI: 10.1016/j.expthermflusci.2006.06.009.

[85] Y. S. Ju, J. Kim, and M.-T. Hung, "Experimental Study of Heat Conduction in Aqueous Sus- pensions of Aluminium Oxide Nanoparticles," Journal of Heat Transfer, vol. 130, pp. 092403–1–092403–6, 2008. DOI: 10.1115/1.2945886.

[86] S. M. S. Murshed, K. C. Leong, and C. Yang, "Investigations of Thermal Conductivity and Viscosity of Nanofluids," International Journal of Thermal Sciences, vol. 47, pp. 560–568, 2008. DOI: 10.1016/j.ijthermalsci.2007.05.004.

[87] H. E. Patel, T. Sundararajan, and S. K. Das, "An Experimental Investigation Into The Ther- mal Conductivity Enhancement on Oxide and Metallic Nanofluids," Journal of Nanoparticle Research, vol. 12, pp. 1015–1031, 2010. DOI: 10.1007/s11051-009-9658-2.

[88] J. P. Meyer, P. N. Nwosu, M. Sharifpur, and T. Ntumba, "Parametric Analysis of Effective Viscosity Models for Nanofluids," in ASME 2012 International Mechanical Engineering Congress and Exposition – Volume 7: Fluids and Heat Transfer, Parts A, B, C and D (S. A. Sherif, F. Battaglia, and S. Neti, eds.), pp. 1149–1157, American Society of Mechanical Engineers (ASME), November 2012. ISBN 978-0-7918-4523-3 / DOI: 10.1115/IMECE2012-93200.

[89] A. Rohatgi, "WebPlotDigitizer." http://arohatgi.info/WebPlotDigitizer/app/. Version 3.12 (Gnu Affero GPL v3).

[90] M. G. Cox and P. M. Harris, "Validating the Applicability of the GUM Procedure," Metrologia, vol. 51, pp. S167–S175, 2014. DOI: 10.1088/0026-1394/51/4/S167.

[91] M. G. Cox and S. K, "Informative Bayesian TypeA Uncertainty Evaluation, Especially Applicable to a Small Number of Observations," Metrologia, vol. 54, pp. 642–652, 2017. DOI: 10.1088/1681-7575/aa787f.

[92] V. Ramnath, "Application of Quantile Functions for the Analysis and Comparison of Gas Pressure Balance Uncertainties," International Journal of Metrology and Quality Engineering, vol. 8, no. 4, pp. 1–18, 2017. DOI: 10.1051/ijmqe/2016020.

[93] R. Willink, "A Generalization of the Welch-Satterthwaite Formula for Use with Correlated Uncertainty Components," Metrologia, vol. 44, pp. 340–349, 2007. DOI: 10.1088/0026-1394/44/5/010.

[94] M. G. Cox and B. R. L. Siebert, "The Use of a Monte Carlo Method for Evaluating Uncertainty and Expanded Uncertainty," Metrologia, vol. 43, pp. S178–S188, 2006. DOI: 10.1088/0026-1394/43/4/S03.

[95] L. M. Lye, "Design of Experiments in Civil Engineering: Are We Still in the 1920's," in Annual Conference of the Canadian Society for Civil Engineering, Canadian Society for Civil Engineering, 2002.

[96] U. Army Materiel Command, "Experimental Design Handbook: Experimental Statistics Section 3 – Planning and Analysis of Comparative Experiments," tech. rep., U. S. Army, 1965. AMC Pamphlet No. 706-112.

[97] J. K. Telford, "A Brief Introduction to Design of Experiments," APL Technical Digest, vol. 27, no. 3, pp. 224–232, 2007.

[98] H. Spliid, "Design and Analysis of Experiments with k Factors Having p Levels," 2002. Lecture Notes in the Design and Analysis of Experiments.

[99] D. C. Montgomery, Design and Analysis of Experiments. John Wiley & Sons, 5th ed., 2001. ISBN 0-471-31649-0.

[100] M. A. Bezerra, R. E. Santelli, E. P. Oliveira, L. S. Villar, and l. A. Escaleira, "Response Surface Methodology (RSM) as a Tool for Optimization in Analytical Chemistry," Talanta, vol. 76, pp. 965–977, 2008. DOI: 10.1016/j.talanta.2008.05.019.

[101] NIST, "NIST/SEMATECH e-Handbook of Statistical Methods," tech. rep., Statistical Methods Group, 2012. http://www.itl.nist.gov/div898/handbook/index.htm.

[102] A. I. Khuri and S. Mukhopadhyay, "Response Surface Methodology," WIREs Computational Statistics, vol. 2, pp. 128–149, March/April 2010. DOI: 10.1002/wics.73.

[103] R. V. Lenth, "Response-Surface Analysis." https://cran.r-project.org. Version 2.8.

[104] H. Safikhani, A. Abbassi, A. Khalkhali, and M. Kaltech, "Multi-Objective Optimization of Nanofluid Flow in Flat Tubes Using CFD, Artificial Neural Networks and Genetic Algorithms," Advanced Powder Technology, vol. 25, no. 5, pp. 1608–1617, 2014. DOI: 10.1016/j.apt.2014.05.014.

[105] E. Ahmadloo and S. Azizi, "Prediction of Thermal Conductivity of Various Nanofluids Using Artificial Neural Network," International Communications in Heat and Mass Transfer, vol. 74, pp. 69–75, 2016. DOI: 10.1016/j.icheatmasstransfer.2016.03.008.

[106] A. Hemmati-Sarapardeh, A. Varamesh, M. M. Husein, and K. Karan, "On the Evaluation of the Viscosity of Nanofluid Systems: Modeling and Data Assessment," Renewable and Sustainable Energy Reviews, vol. 81, pp. 313–329, 2018. DOI: 10.1016/j.rser.2017.07.049.

[107] MetGen, "Calculation of the Density of Water." http://metgen.pagesperso-orange.fr/metrologieen19.htm, 2017.

[108] M. L. V. Ramires, C. A. N. de Castro, Y. Nagasaka, A. Nagashima, M. J. Assael, and W. A. Wakeham, "Standard Reference Data for the Thermal Conductivity of Water," Journal of Physical and Chemical Reference Data, vol. 24, pp. 1377–1381, 1995. DOI: 10.1063/1.555963.

[109] C. J. Seeton, "Viscosity–Temperature Correlation for Liquids," Tribology Letters, vol. 22, no. 1, pp. 67–78, 2006. DOI: 10.1007/s11249-006-9071-2.

[110] M. L. Huber, R. A. Perkins, A. laesecke, D. G. Friend, J. V. Sengers, M. J. Assael, I. N. Metaxa, E. Vogel, R. Mares, and K. Miyagawa, "New International Formulation for the Viscosity of H2O," Journal of Physical and Chemical Reference Data, vol. 38, no. 2, pp. 101–125, 2009. DOI: 10.1063/1.3088050.

[111] V. Ramnath, "Deterministic Numerical Simulation of a Non-Isothermal Blackbody Effective Emissivity Using a Coupled Fredholm Integral Equation System," in 6th IASTED International Conference of Modelling and Simulation (AfricaMS2016) (G. Mmopelwa, N. M. Seboni, J. Prakash, and G. O. Anderson, eds.), pp. 246–253, Acta Press, September 2016. ISBN 978-0-88986-984-4 / DOI: 10.2316/P.2016.838-012.

[112] M. G. Cox, "The Evaluation of Key Comparison Data: Determing the Largest Consistent Subset," Metrologia, vol. 44, pp. 187–200, 2007. DOI: 10.1088/0026-1394/44/3/005.

[113] X. Wang, X. Xu, and S. U. S. Choi, "Thermal conductivity of nanoparticle - fluid mixture," Jour- nal of Thermophysics and Heat Transfer, vol. 13, no. 4, pp. 474–480, 1999. DOI: 10.2514/2.6486.

[114]   J. Li and C. Kleinstreuer, "Thermal Performance of Nanofluid Flow in Microchannels," International Journal of Heat and Fluid Flow, vol. 29, pp. 1221–1232, 2008. DOI: 10.1016/j.ijheatfluidflow.2008.01.005.

[115] M. P. Beck, Y. Yuan, P. Warrier, and A. S. Teja, "The Effect of Particle Size on the Thermal Conductivity of Alumina Nanofluids," Journal of Nanoparticle Research, vol. 11, pp. 1129–1136, 2009. DOI: 10.1007/s11051-008-9500-2.

[116] H. A. Mintsa, G. Roy, C. T. Nguyen, and D. Doucet, "New Temperature Dependent Thermal Conductivity Data for Water-Based Nanofluids," International Journal of Thermal Sciences, vol. 48, pp. 363–371, 2009. DOI: 10.1016/j.ijthermalsci.2008.03.009.

[117] M. P. Beck, Y. Yuan, P. Warrier, and A. S. Teja, "The Thermal Conductivity of Alumina Nanofluids in Water, Ethylene Glycol, and Ethylene Glycol + Water Mixtures," Journal of Nanoparticle Research, vol. 12, pp. 1469–1477, 2010. DOI: 10.1007/s11051-009-9716-9.

[118] G. A. Longo and C. Zilio, "Experimemtal Measurement of Thermophysical Properties of Oxide- Water Nano-Fluids Down to Ice-Point," Experimental Thermal and Fluid Science, vol. 35, pp. 1313–1324, 2011. DOI: 10.1016/j.expthermflusci.2011.04.019.

[119] T. Yiamsawasd, A. S. Dalkilic, and S. Wongwises, "Measurement of the Thermal Conductivity of Titania and Alumina Nanofluids," Thermochimica Acta, vol. 545, pp. 48–56, 2012. DOI: 10.1016/j.tca.2012.06.026.

[120] M. H. Buschmann, "Thermal Conductivity and Heat Transfer of Ceramic Nanofluids," International Journal of Thermal Sciences, vol. 62, pp. 19–28, 2012. DOI: 10.1016/j.ijthermalsci.2011.09.019.

[121] H. S. Aybar, M. Sharifpur, M. R. Azizian, M. Mehrabi, and J. P. Meyer, "A Review of Thermal Conductivity Models for Nanofluids," Heat Transfer Engineering, vol. 36, no. 13, pp. 1085–1110, 2014. DOI: 10.1080/01457632.2015.987586.

[122] C. J. Ho, W. K. Liu, Y. S. Chang, and C. C. Lin, "Natural Convection Heat Transfer of Alumina- Water Nanofluid in Vertical Square Enclosures: An Experimental Study," International Journal of Thermal Sciences, vol. 49, pp. 1345–1353, 2017. DOI: 10.1016/j.ijthermalsci.2010.02.013.

[123] X. Wang, X. Xu, and S. U. S. Choi, "Thermal Conductivity of Nanoparticle-Fluid Mixture," Journal of Thermophyiscs and Heat Transfer, vol. 13, no. 4, pp. 474–480, 1999. DOI: 10.2514/2.6486.

[124] B. C. Pak and Y. I. Cho, "Hydrodynamic and Heat Transfer Study of Dispersed Fluids with Submicron Metallic Oxide Particles," Experimental Heat Transfer, vol. 11, no. 2, pp. 151–170, 2007. DOI: 10.1080/08916159808946559.

[125] Y. He, Y. Jin, H. Chen, Y. Ding, D. Cang, and H. Lu, "Heat Transfer and Flow Behaviour of Aqueous Suspensions of TiO2 Nanoparticles (Nanofluids) Flowing Upward Through a Vertical Pipe," International Journal of Heat and Mass Transfer, vol. 50, pp. 2272–2281, 2007. DOI: 10.1016/j.ijheatmasstransfer.2006.10.024.

[126] W. Duangthongsuk and S. Wongwises, "Measurement of Temperature-Dependent Thermal Conductivity and Viscosity of TiO2-Water Nanofluids," Experimental Thermal and Fluid Science, vol. 33, pp. 706–714, 2009. DOI: 10.1016/j.expthermflusci.2009.01.005.

[127] W. Duangthongsuk and S. Wongwises, "An Experimental Study on the Heat Transfer Performance and Pressure Drop of TiO2-Water Nanofluids Flowing Under a Turbulent Flow Regime," International Journal of Heat and Mass Transfer, vol. 53, pp. 334–344, 2010. DOI: 10.1016/j.ijheatmasstransfer.2009.09.024.

[128] J. Lee, P. E. Gharagozloo, B. Kolade, J. K. Eaton, and K. E. Goodson, "Nanofluid Convection in Microtubes," Journal of Heat Transfer, vol. 132, pp. 092401–1–092401–5, 2010. DOI: 10.1115/1.4001637.

[129] M. J. Pastoriza-Gallego, C. Casanova, J. L. Legido, and M. M. P. neiro, "CuO in Water Nanofluid: Influence of Particle Size and Polydispersity on Volumetric Behavior and Viscos- ity," Fluid Phase Equilibria, vol. 300, pp. 188–196, 2011. DOI: 10.1016/j.fluid.2010.10.015.

[130] I. M. Mahbubul, R. Saidur, and M. A. Amalina, "Latest Developments on the Viscosity of Nanofluids," International Journal on Heat and Mass Transfer, vol. 55, pp. 874–885, 2012. DOI: 10.1016/j.ijheatmasstransfer.2011.10.021.

[131] L. Fedele, L. Colla, and S. Bobbo, "Viscosity and Thermal Conductivity Measurements of Water- Based Nanofluids Containing Titanium Oxide Nanoparticles," International Journal of Refrig- eration, vol. 35, pp. 1359–1366, 2012. DOI: 10.1016/j.ijrefrig.2012.03.012.

[132] W. H. Press, S. A. Teukolsky, W. T. Vetterling, and B. P. Flannery, Numerical Recipes – The Art of Scientific Computing. Cambridge University Press, 3rd ed., 2007. ISBN 978-0-521-88068-8.

[133] R. L. Burden and J. D. Faires, Numerical Analysis. Brookes/Cole, 7th ed., 2001. ISBN 0-534-38216-9.

[134] D. P. Bertsekas, Constrained Optimization and Lagrange Multiplier Methods. Anthena Scientific, 1996.

ISBN 1-886529-04-3.

[135] P. M. Harris and M. G. Cox, "On a Monte Carlo Method for Measurement Uncertainty Evaluation and Its Implementation," Metrologia, vol. 51, pp. S176–S182, 2014. DOI: 10.1088/0026-1394/51/4/S176.

[136] R. Willink, "Representing Monte Carlo Output Distributions for Transferability in Uncertainty Analysis: Modelling with Quantile Functions," Metrologia, vol. 46, pp. 154–166, 2009. DOI: 10.1088/0026-1394/46/3/002.

[137] G. Anastasiades and P. McSharry, "Quantile Forecasting of Wind Power Using Variability Indices," Energies, vol. 6, pp. 662–695, 2013. DOI: 10.3390/en6020662.

[138] L. Yang, J. Xu, K. Du, and X. Zhang, "Recent Developments on Viscosity and Thermal Conductivity of Nanofluids," Powder Technology, vol. 317, pp. 348–369, 2017. DOI: 10.1016/j.powtec.2017.04.061.

[139] M. Kole and T. K. Dey, "Viscosity of Alumina Nanoparticles Dispersed in Car Engine Coolant," Exp. Thermal Fluid Sci., vol. 34, no. 6, pp. 677–683, 2010. DOI: 10.1016/j.expthermflusci.2009.12.009.

[140] P. K. Nambura, D. P. Kulkarni, D. Misra, and D. K. Das, "Viscosity of Copper Oxide Nanoparticles Dispersed in Ethylene Glycol and Water Mixture," Exp. Thermal Fluid Sci., vol. 32, no. 2, pp. 397–402, 2007. DOI: 10.1016/j.expthermflusci.2007.05.001.

[141] K. Sharma, P. K. Sarm, W. H. Azmi, R. Mamat, and K. Kadirgama, "Correlations to Predict Friction and Forced Convection Heat Transfer Coefficients of Water Based Nanofluids for Turbulent Flow in a Tube," Int. J. Microscale Nanoscale Therm. Fluid Transp. Phenom., vol. 3, no. 4, pp. 283–307, 2012. ISSN 1949-4955.

[142] P. K. Nambura, D. P. Kulkarni, A. Dandekar, and D. K. Das, "Experimental Investigation of Viscosity and Specific Heat of Silicon Dioxide Nanofluids," Micro Nano Letter Iet, vol. 2, no. 3, pp. 67–71, 2007. DOI: 10.1049/mnl:20070037.

[143] Y. Xuan, Q. Li, and W. Hu, "Aggregation Structure and Thermal Conductivity of Nanofluids," AICHE Journal, vol. 49, no. 4, pp. 1038–1043, 2003. DOI: 10.1002/aic.690490420.

[144] J. Koo and C. Kleinstreuer, "A New Thermal Conductivity Model for Nanofluids," Journal of Nanoparticle Research, vol. 6, no. 6, pp. 577–588, 2004. DOI: 10.1007/s11051-004-3170-5.

[145] P. Saunders, "Propagation of Uncertainty for Non-Linear Calibration Equations with An Application in Radiation Thermometry," Metrologia, vol. 40, pp. 93–101, 2003. URL: http://stacks.iop.org/Met/40/93.

[146] BIPM, IEC, IFCC, ILAC, ISO, IUPAC, IUPAP, and OILM, "Evaluation of Measurement Data – Supplement 2 to the "Guide to the Expression of Uncertainty in Measurement" – Extension to Any Number of Output Quantities," tech. rep., Bureau International de Poids et Mesures (BIPM), 2011. http://www.bipm.org/utils/common/documents/jcgm/JCGM_102_2011_E.pdf.

[147] A. H. Harvey, R. Span, K. Fujii, M. Tanaka, and R. S. Davies, "Density of Water: Roles of the CIPM and IAPWS Standards," Metrologia, vol. 46, no. 3, pp. 196–198, 2009. DOI: 10.1088/0026-1394/46/3/006.

[148] D. Hussain, K. Ahmad, J. Song, and H. Xie, "Advancess in the Atomic Force Microscopy for Critical Dimension Metrology," Measuremnt Science Technology, vol. 28, p. 012001, 2017. DOI: 10.1088/0957-0233/28/1/012001.

[149] C. B. McDonald, "OctSymPy – An Implementation Of A Symbolic Toolbox Using SymPy." https://octave.sourceforge.io/symbolic/index.html. Version 2.6.0.

[150] R. Johansson, Numerical Python: A Practical Techniques Approach for Industry. Apress, 1st ed., 2015. ISBN 978-1-4842-0553-2 / DOI: 10.1007/978-1-4842-0553-2.

[151] V. Ramnath, "Numerical Analysis of the Accuracy of Bivariate Quantile Distributions Utilizing Copulas Compared to the GUM Supplement 2 for Oil Pressure Balance Uncertainties," International Journal of Metrology and Quality Engineering, vol. 8, no. 4, 2017. DOI: 10.1051/ijmqe/2017018.

[152] H. Ghodsinezhad, "Experimental Investigation on Natural Convection of Al2O3-Water Nanofluids in Cavity Flow," Master's thesis, Department of Mechanical and Aeronautical Engineering, Faculty of Engineering, Built Environment and Information Technology, University of Pretoria, Gauteng Province, Republic of South Africa, 2016.

[153] M. Liu, C. Ding, and J. Wang, "Modeling of Thermal Conductivity of Nanofluids Considering Aggregation and Interfacial Thermal Resistance," Royal Society of Chemistry Advances, vol. 6, p. 3571, 2016. DOI: 10.1039/c5ra16327g.

[154] M. Mahdavi, Study of Flow and Heat Transfer Features of Nanofluids Using Multiphase Models: Eulerian Multiphase and Discrete Lagrangian Approaches. PhD thesis, Department of Mechanical and Aeronautical Engineering, Faculty of Engineering, Built Environment and Information Technology, University of Pretoria, Gauteng Province, Republic of South Africa, 2016.

[155] M. J. Uddin, K. S. A. Kalbani, M. M. Rahman, M. S. Alam, N. Al-Salti, and I. A. Eltayeb, "Fundamentals of Nanofluids: Evolution, Applications and New Theory," International Journal of Biomathematics and Systems Biology, vol. 2, no. 1, pp. 1–32, 2016. ISSN 2394-7772, URL: http://biomathsociety.in/issue2/paper4.pdf.

[156] N. G. Hadjiconstantinou, "Comment on Cercignani's Second-Order Slip Coefficient," Physics of Fluids, vol. 15, no. 8, p. 2352, 2003. DOI: 10.1063/1.1587155.

[157] V. Ramnath, "Computational Solution of the Extended Navier-Stokes PDE's: Incorporating Nonlinear Fluid-Solid Boundary Conditions for Microfluidic Simulations," in 4th International Conference of Metrology in Africa (CAFMET 2012) (A. Charki, ed.), pp. 78–88, Curran Associates, April 2012. ISBN 978-1-62276-063-3.

[158] N. Singh, R. S. Jadhav, and A. Agrawal, "Derivation of Stable Burnett Equations for Rarefied Gas Flows," Physical Review E, vol. 96, p. 013106, 2017. DOI: 10.1103/PhsRevE.96.013106.

[159] O. A. Rogozin, "Slow Nonisothermal Flows: Numerical and Asymptotic Analysis of the Boltzmann Equation," Computational Mathematics and Mathematical Physics, vol. 57, no. 7, pp. 1201–1224, 2017. DOI: 10.1134/S0965542517060112.

[160] F. Sharipov and V. Seleznev, "Data on Internal Rarefied Gas Flows," Journal of Physical and Chemical Reference Data, vol. 27, pp. 657–706, 1998. DOI: 10.1063/1.556019.

[161] F. H. Stillinger, "Theory and Molecular Models for Water," in Advances in Chemical Physics: Non-Simple Liquids (I. Prigogine and S. A. Rice, eds.), vol. 31, ch. 1, pp. 1–101, Wiley, 1975. DOI: 10.1002/9780470143834.

[162] J. Mrazek and J. V. Burda, "Can the pH of Water Solutions be Estimated by Quantum Chemical Calculations of Small Water Clusters?," The Journal of Chemical Physics, vol. 125, pp. 194518–1–194518–15, 2006. DOI: 10.1063/1.2363383.

[163] W.-Q. Lu and Q.-M. Fan, "Study for the Particle's Scale Effect on Some Thermophysical Properties of Nanofluids by a Simplified Molecular Dynamics Method," Engineering Analysis with Boundary Elements, vol. 32, pp. 282–289, 2008. DOI: 10.1016/j.enganabound.2007.10.006.

[164] L. Li, Y. Zhang, H. ma, and M. Yang, "An Investigation of Molecular Layering at the Liquid- Solid Interface in Nanofluids by Molecular Dynamics Simulation," Physics Letters A, vol. 372, pp. 4541–4544, 2008. DOI: 10.1016/j.phsleta.2008.04.046.

[165] N. Sankar, N. Mathew, and C. B. Sobhan, "Molecular Dynamics Modeling of Thermal Conductivity Enhancement in Metal Nanoparticle Suspensions," International Communications in Heat and Mass Transfer, vol. 35, pp. 867–872, 2008. DOI: 10.1016/j.icheatmasstransfer.2008.03.006.

[166] P. Sachdeva, Molecular Dynamics Study of Thermal Conductivity Enhancement of Water Based Nanofluids. PhD thesis, University of Central Florida, College of Engineering and Computer Science, Orlando, Florida, United States of America, 2009.

[167] C. Sun, W.-Q. Lu, J. Liu, and B. Bai, "Molecular Dynamics Simulation of Nanofluid's Effective Thermal Conductivity in High-Shear-Rate Couette Flow," International Journal of Heat and Mass Transfer, vol. 54, pp. 2560–2567, 2011. DOI: 10.1016/j.ijheatmasstransfer.2011.02.005.

[168] Z. Lou and M. Yang, "Molecular Dynamics Simulations on the Shear Viscosity of Al2O3 Nanofluids," Computers & Fluids, vol. 117, pp. 17–23, 2015. DOI: 10.1016/j.compfluid.2015.05.006.

[169] W. Cui, Z. Shen, J. Yang, and S. Wu, "Effect of Chatic Movements of Nanoparticles for Nanofluid Heat Transfer Augmentation by Molecular Dynamics Simulation," Applied Thermal Engineering, vol. 76, pp. 261–271, 2015. DOI: 10.1016/j.applthermaleng.2014.11.030.

[170] D. Frenkel and B. Smit, Understanding Molecular Simulation – From Algorithms to Applications. Academic Press, 2nd ed., 2002. ISBN 978-0-12-267351-1.

[171] S. Pirhadi, J. Sunseri, and D. R. Koes, "Open Source Molecular Modeling," Journal of Molecular Graphics and Modelling, vol. 69, pp. 127–143, 2016. DOI: 10.1016/j.jmgm.2016.07.008.

[172] M. E. Fortunato and C. M. Colina, "pysimm : A Python Package for Simulation of Molecular Systems," SoftwareX, vol. 7–12, pp. 1–6, 2016. DOI: 10.1016/j.softx.2016.12.002.

[173] P. N. Nwosu, J. P. Meyer, and M. Sharifpur, "A Review and Parametric Investigation Into Nanofluid Viscosity Models," Journal of Nanotechnology in Engineering and Medicine, vol. 5, pp. 031008–1–031008–11, 2014. DOI: 10.1115/1.4029079.

[174] M. Mehrabi, M. Sharifpur, and J. P. Meyer, "Adaptive Neuro-Fuzzy Modeling of the Thermal Conductivity of Alumina-Water Nanofluids," in ASME 2012 3rd Micro/Nanoscale Heat & Mass Transfer International Conference (MNHMT2012) (P. Cheng, Y. Bayazitoglu, G. Chen, S. Choi, Y. Jaluria, D. Li, P. Norris, B. Peterson, and B. Tzou, eds.), pp. 155–161, American Society of Mechanical Engineers (ASME), March 2012. ISBN 978-0-7918-5477-8 / DOI: 10.1115/MNHMT2012-75023.

[175] S. Raschka, Python Machine Learning. PACKT Publishing, 1st ed., 2015. ISBN 978-1-78355-513-0 / www.packtpub.com.

[176] A. Tarantola, Inverse Problem Theory and Methods for Model Parameter Estimation. Society for Industrial and Applied Mathematics (SIAM), 2005. ISBN 0-89871-572-5.

[177] L. P. Levasseur, Y. D. Hezaveh, and R. H. Wechsler, "Uncertainties in Parame- ters with Neural Networks: Application to Strong Gravitational Lensing." arXiv: https://arxiv.org/abs/1708.08843, Preprint Version 1 – 29 August 2017.

[178] A. B. Forbes, "Approaches to Evaluating Measurement Uncertainty," International Journal of Metrology and Quality Engineering, vol. 3, pp. 71–77, 2012. DOI: 10.1051/ijmqe/2012017.

[179] S. Scardapane and D. Wang, "Randomness in Neural Networks: An Overview," Wiley Inter-disciplinary Reviews: Data Mining and Knowledge Discovery, vol. X, p. Y, 2017. To Appear: January 2017 – Preprint https://www.researchgate.net/publication/312057617.

[180] G. E. Fasshauer, Meshfree Approximation Methods with MATLAB. World Scientific, 2007. ISBN 978-981-270-633-1.

[181] W. Li, G. Song, and G. Yao, "Piece-Wise Moving Least Squares Approximation," Applied Numerical Mathematics, vol. 115, pp. 68–81, 2017. DOI: 10.1016/j.apnum.2017.01.001.

[182] V. Skala, "RBF Interpolation with CSRBF of Large Data Sets," Procedia Computer Science, vol. 108C, pp. 2433–2437, 2017. DOI: 10.1016/j.procs.2017.05.081.

[183] S. A. Sarra and S. Cogar, "An Examination of Evaluation Algorithms for the RBF Method," Engineering Analysis with Boundary Elements, vol. 75, pp. 36–45, 2017. DOI: 10.1016/j.enganabound.2016.11.006.

[184] N. Kolev, U. dos Anjos, and B. V. de M. Mendes, "Copulas: A Review and Recent Develop- ments," Stochastic Models, vol. 22, pp. 617–660, 2005. DOI: 10.1080/15326340600878206.

[185] P. M. Harris, C. E. Matthews, M. G. Cox, and A. B. Forbes, "Summarizing the Output of a Monte Carlo Method for Uncertainty Evaluation," Metrologia, vol. 51, pp. 243–252, 2014. DOI: 10.1088/0026-1394/51/3/243.

[186] M. Fischer, "Multivariate Copula Models at Work." http://www.statistik.wiso. uni-erlangen.de University of Erlangen-Nuremberg, Germany, 2009.

[187] K. Aas, C. Czado, A. Frigessi, and H. Bakken, "Pair-Copula Constructions of Multiple De- pendence," Insurance: Mathematics and Economics, vol. 44, no. 2, pp. 182–198, 2009. DOI: 10.1016/j.insmatheco.2007.02.001.

[188] E. C. Brechmann and U. Schepsmeier, "Modeling Dependence with C- and D-Vine Copulas: The R Package CDVine," Journal of Statistical Software, vol. 52, no. 3, pp. 1–27, 2013. URL: http://www.jstatsoftware.org/.

[189] U. Schepsmeier, "A Goodness-of-Fit Test for Regular Vine Copula Models," Econometric Reviews, pp. 1–22, 2016. DOI: 10.1080/07474938.2016.1222231.

[190] CRAN, "The R Project for Statistical Computing." http://www.r-project.org/. The Comprehensive R Archive Network Version 3.3.3 (Another Canoe).

[191] J. Segers, M. Sibuya, and H. Tsukahara, "The Empirical Beta Copula," Journal of Multivariate Analysis, vol. 155, pp. 35–51, 2017. DOI: 10.1016/j.jmva.2016.11.010.

[192] W. Asquith, "The Comprehensive R Archive Network – General Bivariate Copula Theory and Many Utility Functions." https://cran.r-project.org. Version 2.0.4.

[193] L. D. Capitani, F. Nicolussi, and A. Zini, "Trivariate Burr-III Copula With Applications to Income Data," METRON, vol. 7–12, pp. 1–16, 2016. DOI: 10.1007/s40300-016-0104-9.

[194] S. S. Dhar, B. Chakraborty, and P. Chaudhuri, "Comparison of Multivariate Distributions Using Quantile-Quantile Plots and Related Tests," Bernoulli, pp. 1484–1506, 2014. DOI: 10.3150/13-BEJ530.

[195] BIPM, IEC, IFCC, ILAC, ISO, IUPAC, IUPAP, and OILM, "Evaluation of Measurement Data – Supplement 1 to the "Guide to the Expression of Uncertainty in Measurement" – Propaga- tion of Distributions using a Monte Carlo Method," tech. rep., Bureau International de Poids et Mesures

(BIPM), 2008. http://www.bipm.org/utils/common/documents/jcgm/JCGM_101_2008_E.pdf.

[196] T. Nagler, C. Schellhase, and C. Czado, "Nonparametric Estimation of Simplified Vine Cop- ula Models: Comparison of Methods," Dependence Modeling, vol. 5, pp. 99–120, 2017. DOI: 10.1515/demo-2017-0007.

[197] N. Barthel, C. Geerdens, M. Killiches, P. Janssen, and C. Czado, "Vine Copula Based Likelihood Estimation of Dependence Patterns in Multivariate Event Time Data." https://arxiv.org/abs/1603.01476. Version 2.

[198] S. Jiang and L. S. Luo, "Analysis and Accurate Numerical Solutions of the Integral Equation Derived from the Linearized BGKW Equation for the Steady Couette Flow," Journal of Com- putational Physics, vol. 316, pp. 416–434, 2016. DOI: 10.1016/j.jcp.2016.04.011.

[199] A. Maripia, M. Sharifpur, and J. P. Meyer, "Investigation into Cavity Flow Natural Convection for Al2O3-Water Nanofluids Numerically," in 10th International Conference on Heat Transfer, Fluid Mechanics and Thermodynamics (HEFAT2014) (J. P. Meyer, ed.), pp. 1–7, International Centre for Heat and Mass Transfer (ICHMT), July 2014. ISBN 978-1-77592-068-7.

[200] M. Mahdavi, M. Sharifpur, and J. P. Meyer, "Implementation of Diffusion and Electrostatic Forces to Produce a New Slip Velocity in the Multiphase Approach to Nanofluids," Powder Technology, vol. 307, pp. 153–162, 2016. DOI: 10.1016/j.powtec.2016.11.032.

[201] M. Mahdavi, M. Sharifpur, and J. P. Meyer, "A Novel Model of Discrete and Mixture Phases for Nanoparticles in Convective Turbulent Flow," Physics of Fluids, vol. 29, no. 8, p. 082005, 2017. DOI: 10.1063/1.4998181.

[202] A. Belopolsky, B. Chapman, P. Cock, D. Eddelbuettel, T. Kluyver, W. Moreira, L. Oget, J. Owens, N. Rapin, G. Slodkowicz, N. Smith, and G. Warnes, "rpy2 – R in Python." https://rpy2.bitbucket.io/. Version 2.9.1.

[203] D. Eddelbuettel, R. Francois, J. J. Allaire, K. Ushey, Q. Kou, N. Russell, D. Bates, and J. Chambers, "Rcpp: Seamless R and C++ Integration." https://cran.r-project.org/web/packages/Rcpp/index.html. Version 0.12.13.

[204] R. Palencar, G. Wimmer, and M. Halaj, "Determination of the Uncertainties and Covariances in the Calibration of the Set of Weights," Measurement Science Review, vol. 2, no. 1, pp. 9–20, 2002. http://www.measurement.sk/2002/S1/Palencar1.pdf.

[205] N. Bouguerra, S. Poncet, and S. Elkoun, "Dispersion of Regimes in Alumina/Water-Based Nanofluids: Simultaneous Measurements of Thermal Conductivity and Dynamic Viscosity," International Communications in Heat and Mass Transfer, vol. 92, pp. 51–55, 2018. DOI: 10.1016/j.icheatmasstransfer.2018.02.015.